Development of S-nitrosoglutathione loaded particles adapted to oral administration for preventing Inflammatory Bowel Disease relapses

Hui Ming

UNIVERSITÉ DE LORRAINE

Ecole Doctorale BioSE (Biologie-Santé-Environnement)

Thèse

Présentée et soutenue publiquement pour l'obtention du titre de

DOCTEUR DE l'UNIVERSITE DE LORRAINE

Mention : « Sciences de la Vie et de la Santé » par

Hui MING

Développement de formulations polymériques de *S*-nitrosoglutathion comme traitement *per os* pour prévenir les maladies inflammatoires chroniques de l'intestin

07 Décembre 2017

Membres du jury :

Rapporteurs :	**Gilles Ponchel**	**PR, UMR 8612, CNRS, Université Paris-Sud, Paris**
	Aurélie Malzert-Fréon	**PR, EA 4258, CNRS, Université de Caen Normandie, Caen**
Examinateurs :	**Anne Sapin-Minet**	**HDR, EA 3452, Université de lorraine, Nancy directeur de thèse**
	Franck Hansmannel	**MCU, UMR 954, INSERM, Université de lorraine, Nancy co-directeur de thèse**
Membre invité :	**David Moulin**	**DR, UMR 7365, CNRS, Université de lorraine, Nancy**

EA 3452 CITHEFOR : Cibles Thérapeutiques, Formulation et Expertise Préclinique du Médicament
5, rue Albert Lebrun, BP 80403, 54001 Nancy Cedex, France

ACKNOWLEDGEMENTS

I would like to express my gratitude to all those who helped me to survive from these 3 years of PhD study here.

I am sincerely grateful to Pr. Ponchel (Université Paris-Sud), Pr. Malzert-Fréon (Université de Caen Normandie) and Dr. Moulin (Université de lorraine): Pr. Ponchel and Pr. Malzert-Fréon for accepting to be my reviewers of this work; Pr. Ponchel and Dr. Moulin for their participation in my thesis committee and helpful suggestions.

I gratefully acknowledge Pr. Hu (my supervisor during master study in Wuhan University) and Pr. Maincent (Université de lorraine) for giving me the opportunity to start my PhD study here. Pr. Hu provided the research platform for me during the two years of master study in the lab, which helped me improve the experimental skills and inspired my research enthusiasm. Pr. Maincent gave me some really useful suggestions of the formulation part. The conversation with him was always relaxed and lively. His smile comforted me a lot when I did the presentation during the formulation meeting. He looks always optimistic. His friendly encouragement made me stronger when I lost my confidence.

I feel grateful to Pr. Leroy (the director of EA3452 CITHEFOR) for his critical opinions. His strong sense of responsibility, serious and detailed attitude of work influenced me a lot.

My deepest gratitude goes to my supervisors, Anne and Franck, for their instructive and valuable advices on my thesis. Anne helped me a lot not only in the guidance of thesis but also in the manipulation of experiment part. She is always nice and patient in analyzing and solving experimental problems with me. Besides the life in the lab, Anne also helped me to make my casual life easier in France. I learned a lot from Franck's profound knowledge in physiology part and analysis of data. He was very patient in explaining basic knowledge to me, such as western blot, statistic study, intestine physiology and pathology. Without their patient instruction, insightful criticism and expert guidance, the completion of this thesis would not have been possible.

I would like to express my gratitude to Caroline G. and Isabelle F. for their useful suggestion and helpful manipulation in Caco-2 experiment part. Caroline's smart mind and efficient work capacity impressed me a lot.

Great thanks shall be transported to Philippe G. for his work on GSNO preparation, apparatus setting and validation. His easygoing character and warm introduction helped me get used to this lab more easily and quickly.

My grateful words should go to Marianne as well for her sharing of interesting and useful literatures. She is very efficient in literature searching, analyzing and summarizing, which inspired me a lot.

I also own a truthful gratitude to Romain whose thesis is crossed with mine under the same supervisor of Anne. We shared a lot of happy moments together. He helped me a lot also in computer technical part. He is very good at communication which I can learn a lot from him.

Heartful gratitude is sent to Pascale, Nathalie and Ghizlane for their friendly smile every time and help in administrative things. Even though the language barrier exists, we still make us understandable to each other.

Special gratitude should go to my dear friends Haiyan and Yi, who accompanied me, comforted me and encouraged me a lot.

I also own my sincere gratitude to all my colleges for their help at any time for any cases.

At last, my thanks would go to my beloved family for their loving consideration and great support in me for all these years.

Hui MING
In Nancy

TABLE OF CONTENTS

SCIENTIFIC WORKS

Publications:

Polymer nanocomposites enhance *S*-nitrosoglutathione intestinal absorption and promote the formation of releasable nitric oxide stores in rat aorta. Wen Wu, Caroline Perrin-Sarrado, **Hui Ming**, Isabelle Lartaud, Philippe Maincent, Xian-Ming Hu, Anne Sapin-Minet, Caroline Gaucher. *Nanomedicine: Nanotechnology, Biology and Medicine* (2016), volume 12, issue 7, page 1795-1803.

Single step alginate nanocomposite formulation for GSNO intestine delivery: an *in vitro* and *in cellulo* characterization. **Hui Ming**, Franck Hansmannel, Wen Wu, Romain Schmitt, Caroline Gaucher, Philippe Maincent, Xian-Ming Hu, Pierre Leroy, Anne Sapin-Minet. *Journal of microencapsulation* (submitted)

Luminal *S*-nitrosoglutathione impacts intestinal barrier permeability by dose-dependent way in an *ex vivo* model of Ussing Chamber. Romain Schmitt, **Hui Ming** (same contribution), Franck Hansmannel, Caroline Gaucher, Pierre Leroy, Isabelle Lartaud, Anne Sapin-minet. *Journal of Gastroenterology*. (in progress)

Booker chapter: Polymer nanocomposites for drug oral delivery: development strategies and potentialities. **Hui Ming**, Wen Wu, Philippe Maincent, Marianne Parent, Caroline Gaucher, Anne Sapin-Minet. Volume 9: Organic particles, Composites in Biomedical Engineering: Particles (Series C) – ELSEVIER, Edited by Alexandru Mihai GRUMEZESCU (in progress)

Oral communications:

NutriOx 2015, November 19th - 20th 2015 in Luxembourg: Formulations of Nitric Oxide Donors Adapted to Oral Delivery: Perspectives for Preventing Inflammatory Bowel Disease Relapses. **Hui Ming,** Wen Wu, Franck Hansmannel, Caroline Gaucher, Philippe Maincent, Xian-Ming Hu, Pierre Leroy, Anne Sapin-Minet.

Journée scientifique de l'école doctorale BioSE, December 11th 2015 in Nancy (France): Formulation of *S*-nitrosoglutathione(GSNO) Adapted to Oral Delivery: Perspectives for Inflammatory Bowel Disease Relapses Prevention. **Hui Ming,** Franck Hansmannel, Wen Wu, Caroline Gaucher, Philippe Maincent, Xian-Ming Hu, Jean-Louis Guéant, Laurent Peyrin-Biroulet, Pierre Leroy, Anne Sapin-Minet.

The 4th edition of the conference DocSciLor, June 15th, 2017 in Nancy (France): *S*-nitrosoglutathione and intestine barrier integrity on an *ex vivo* rat model of LPS-induced inflammation. Romain Schmitt, **Hui Ming,** Franck Hansmannel, Caroline Gaucher, Isabelle Lartaud, Pierre Leroy, Anne Sapin-Minet.

Poster communications:

BioBarriers 2016, March 07th – 09th, 2016 in Saarbruecken (Germany): Formulations of nitric oxide donors adapted to oral delivery: perspectives for intestinal bowel disease relapses prevention. **Hui Ming**, Wen Wu, Franck Hansmannel, Caroline Gaucher, Philippe Maincent, Xian-Ming Hu, Pierre Leroy, Anne Sapin-Minet.

DocLor – Doctorial de Lorraine 2016, April 17th – 22th, 2016 in La Bolle Saint-Dié (France): Development of *S*-Nitrosoglutathione Formulation for the Prevention of Inflammatory Bowel Disease Relapses. **Hui Ming**.

OCC World Congress 2017 and Annual SFRR-E Conference, June 21th-23th, 2017 in Berlin (German): Intestine permeability of *S*-nitrosoglutathione as a potential nitric oxide donor via oral administration. Justinea Bonetti, Haiyan Yu, **Hui Ming**, Anne Sapin-Minet, Isabelle Fries, Igor Clarot, Patrick Chaimbault, Pierre Leroy, Caroline Gaucher.

LIST OF TABLES

LIST OF FIGURES

LIST OF ABBRIEVIATIONS

Abbreviation	Full name
6MP	6-mercaptopurine
aeNCP	alginate/Eudragit®E 100 nanocomposite particles
AJ	adherens junction
AMP	antimicrobial proteins
aNCP	alginate nanocomposite particles
Arm	armadillo
ASA	Aminosalicylates
AZA	azathioprine
BP	blood pressure
BUC(NO)2	*S,S'*-dinitrosobucillamine
CAR	coxsackie virus and adenovirus receptor
CD	Crohn's disease
Cgmp	cyclic guanosine monophosphate
CR1	carbonyl reductase 1
CysGlyNO	*S*-nitrosocysteinylglycine
DCM	dichloromethane
DCs	dendritic cells
EDRF	endothelial derived relaxing factor
EE	encapsulation efficiency
EGCs	enteric glia cells
EGFR	epithelial growth factor receptor
ELISA	enzyme-linked immunosorbent assay
eNOS	endothelial nitric oxide synthases
FAE	follicle-associated epithelium
GGT	γ-glutamyltranspeptidase
GI	gastrointestinal
GSH	glutathione
GSNO	*S*-nitrosoglutathion
GSNOR	*S*-nitrosoglutathion reductase
GSSG	oxidized glutathione
GTN	nitroglycerin
GTP	guanosine-5'-triphosphate
HPLC-MS	high-performance liquid chromatography coupled with mass spectrometry
HRP	horseradish peroxidase
IBD	inflammatory bowel diseases
IBS	irritable bowel syndrome
IC50	half maximal inhibitory concentration
IECs	intestinal epithelial cells
IFN	interferons

Ig	immunoglobulin
IL	interleukin
ILFs	isolated lymphoid follicles
iNOS	inducible nitric oxide synthases
ISDN	isosorbide dinitrate
ISMN	isosorbide mononitrate
JAM	junctional adhesion molecule
L-AT	L-amino acid transporter system
L-CysNO	*S*-nitroso-L-cysteine
L-NAME	L-NG-nitroarginine methyl ester
LP	lamina propria
LPS	lipopolysaccharide
M Cells	microfolds cells
MAMPs	microbial-associated molecular patterns
MDCK	Madin-Darby canine kidney
MLC	myosin light chain
MLCK	myosin light chain kinase
mLNs	mesenteric lymph nodes
MTX	methotrexate
NACNO	*S*-nitroso-N-acetylcysteine
NADPH	nicotine adenine disphosphonucleotide
NCP	nanocomposite particles
NF	nuclear factor
NH2OH	hydroxylamine
NK	natural killer
NLRs	nucleotide-binding oligomerization domain-like receptors
nNOS	neuronal nitric oxide synthases
NO	nitric oxide
NOD	nucleotide-binding oligomerization domain
NP	nanoparticles
Papp	apparent permeability coefficient
PDI	protein disulfide isomerase
PETN	pentaerythrityl nitrate
PKC	protein kinase C
PKCs	protein kinase Cs
P-MLC	phosphorylation of myosin light chain
PPs	Peyer's patches
PRR	pattern recognition receptor
RELMβ	resistin-like molecule-β
RNOS	reactive nitrogen oxide species
RSNO	*S*-nitrosothiols
SCFA	short chain fatty acids

Ser	serine
sGC	soluble guanylate cyclase
SNAP	*S*-nitroso-N-acetylpenicillamine
SNOPCs	*S*-nitrosophytochelatins
SNP	Sodium nitroprusside
SPIONs	superparamagnetic iron oxide nanoparticles
sprr2A	small proline-rich protein 2A
TEER	transepithelial electrical resistance
TFF3	trefoil factor 3
Thr	threonine
TJ	tight junction
TLRs	toll-like receptors
TNF	tumor necrosis factor
TPP	sodium tripolyphosphate
TrxR	thioredoxin reductase
UC	ulcerative colitis
ZO	zonula occludens

Résumé francophone du manuscrit

Les maladies inflammatoires chroniques de l'intestin (MICI) sont un groupe d'affections idiopathiques incluant la rectocolite hémorragique (RCH) et la maladie de Crohn (MC) qui affectent 200.000 personnes en France et 2,2 millions de personnes en Europe. La prévalence des MICI a augmenté principalement dans les pays occidentaux dans les 50 dernières années jusqu'à 200 / 100.000 pour les RCH et 200 / 100.000 pour la MC (Cosnes *et al.*, 2011). Elles apparaissent chez des sujets jeunes (15-35 ans) et sont incurables actuellement.

Elles représentent un véritable problème de santé publique compte tenu de leurs fréquences, de leurs pronostics à court et à long termes, du coût de leurs prises en charge ainsi que de leurs répercussions sur la qualité de vie des malades. Elles se caractérisent par des épisodes inflammatoires (poussées) répétés et invalidants pour le patient au cours desquels il ressent toutes les manifestations cliniques de la maladie. Actuellement la prise en charge des patients MICI se limite à la prise en charge de ces poussées inflammatoires. A plus ou moins long terme, les MICI conduisent fréquemment à des chirurgies visant à éliminer la zone enflammée (Cosnes *et al.*, 2011). De plus, l'inflammation chronique de la muqueuse du colon (colite) du patient MICI peut conduire à la mise en place d'un cancer colorectal (CCR) (Jess *et al.*, 2012).

Leurs étiologies sont inconnues, mais la pathogénie des MICI reposerait sur une activation inappropriée du système immunitaire intestinal, dirigé contre la flore intestinale de l'hôte chez des patients prédisposés (génétiquement ou épigénétiquement), dans un contexte de dysbiose. Cette dérégulation dans les interactions hôte-microbiote conduit à l'inflammation intestinale.

Des approches chirurgicales lourdes permettent de réaliser l'ablation de la zone lésée chez les malades lorsque le traitement médical n'est plus efficace, ou en cas de complications graves liées à la sévérité de la lésion. Ces interventions ne peuvent être envisagées qu'en seconde instance car elles sont d'une part très traumatisantes et d'autre part elles n'ont pas d'effet curatif réel puisque les récidives sont nombreuses après la chirurgie. Le développement de nouveaux axes de recherche et de nouveaux traitements chroniques permettant de prévenir les récidives inflammatoires améliorerait la qualité de vie des patients atteints de ces maladies et de diminuer le risque de

développement de cancer. Les traitements conventionnels des MICI visent à limiter l'inflammation de la muqueuse des patients et incluent les aminosalicylates, les corticostéroïdes, les antibiotiques et les agents immunosuppresseurs, qui sont nécessairement administrés pendant de longues périodes et par conséquent, entraînent des effets secondaires (Meissner and Lamprecht, 2008). De plus, les dernières innovations thérapeutiques proposées comme l'utilisation d'agent anti-Tumor Necrosis Factor (anti-TNF) ont de puissants effets anti-inflammatoires mais une perte de réponse est observée lors d'un traitement au long cours et seulement un tiers des patients présente une rémission clinique totale après un an. L'identification de nouvelles cibles, de nouveaux agents, produits naturellement par l'organisme sain, pourrait ouvrir de nouvelles perspectives thérapeutiques pour ces pathologies.

Lors d'une inflammation, l'oxyde nitrique (NO) joue un rôle pivot et paradoxal, discuté de façon récurrente dans de nombreuses études. Ainsi, le NO intervient à la fois dans des processus physiologiques se déroulant dans des tissus sains et dans des processus physiopathologiques. C'est particulièrement le cas au niveau du tractus gastro-intestinal, où le NO intervient à la fois comme médiateur important dans la préservation et la réparation de la muqueuse (Figure 1) mais contribue également directement aux dommages constatés dans les pathologies digestives, par une action pro-inflammatoire. Compte tenu de cette dualité, le développement de principes actifs pouvant moduler la synthèse ou l'action du NO constitue évidemment un véritable challenge et le rôle pivot du NO justifie les recherches de nouvelles stratégies thérapeutiques autour de ce composé. Le rôle bénéfique du NO dans ce contexte pathologique implique une action préventive en délivrant de faibles concentrations en NO (nM à µM) dans un environnement peu engagé dans l'inflammation (la balance redox doit être peu perturbée) afin qu'il exerce son action anti-inflammatoires.

L'apport de NO à l'état gazeux est particulièrement délicat pour remplir ces conditions, en raison d'une demi-vie très courte (de l'ordre de la seconde) et de sa très grande réactivité qui l'amène à interagir très rapidement avec les éléments de son environnement, de façon non contrôlable. Toutefois, différentes molécules libérant le NO ou des espèces apparentées, appelées « donneurs de NO », sont décrites voire même utilisées en thérapeutique (dans un contexte cardiovasculaire notamment) (Parent *et al.*, 2013c). Certains donneurs de NO ont ainsi été étudiés dès les années 90, dans le contexte des MICI pour promouvoir les actions bénéfiques du NO au niveau intestinal

(tableau 1).

Tableau 1 Exemples d'actions protectrices des donneurs de NO observée au niveau intestinal

Donneur de NO	Nature de l'étude	Auteur, date	Action protectrice
NO-mesalamine (Composés nitrosés)	Préclinique	(Wallace *et al*., 1999)	Diminue les dommages de la muqueuse intestinale : • Diminution infiltration des leucocytes • Augmentation de la sécrétion de mucus • Maintien du flux sanguin local
Glyceryltrinitrate	Clinique	(Lund and Scholefield, 1997)	Améliore la cicatrisation de fissures anales associées à la maladie de Crohn
NO-NSAIDS	Préclinique	(Muscará *et al.*, 1998, Wallace *et al.,* 1999)	Potentialise action du NSAIDS
SNAP	Préclinique	(Lefer and Lefer, 1999)	• Evite augmentation de la P-Sélectine sur la membrane des neutrophiles • Inhibe le dysfonctionnement de l'endothélium
NO gaz et NaNO2 acidifié	Préclinique	(Aoki *et al.,* 1990)	Diminue l'adhérence des neutrophiles au niveau de l'endothélium mésentérique

Parmi les donneurs de NO évoqués, les *S*-nitrosothiols (RSNO) représentent une classe de composés particulièrement intéressante pour un traitement de différentes pathologies inflammatoires chroniques (cérébrovasculaires, pulmonaires et intestinales) en jouant sur l'intégrité des barrières physiologiques.

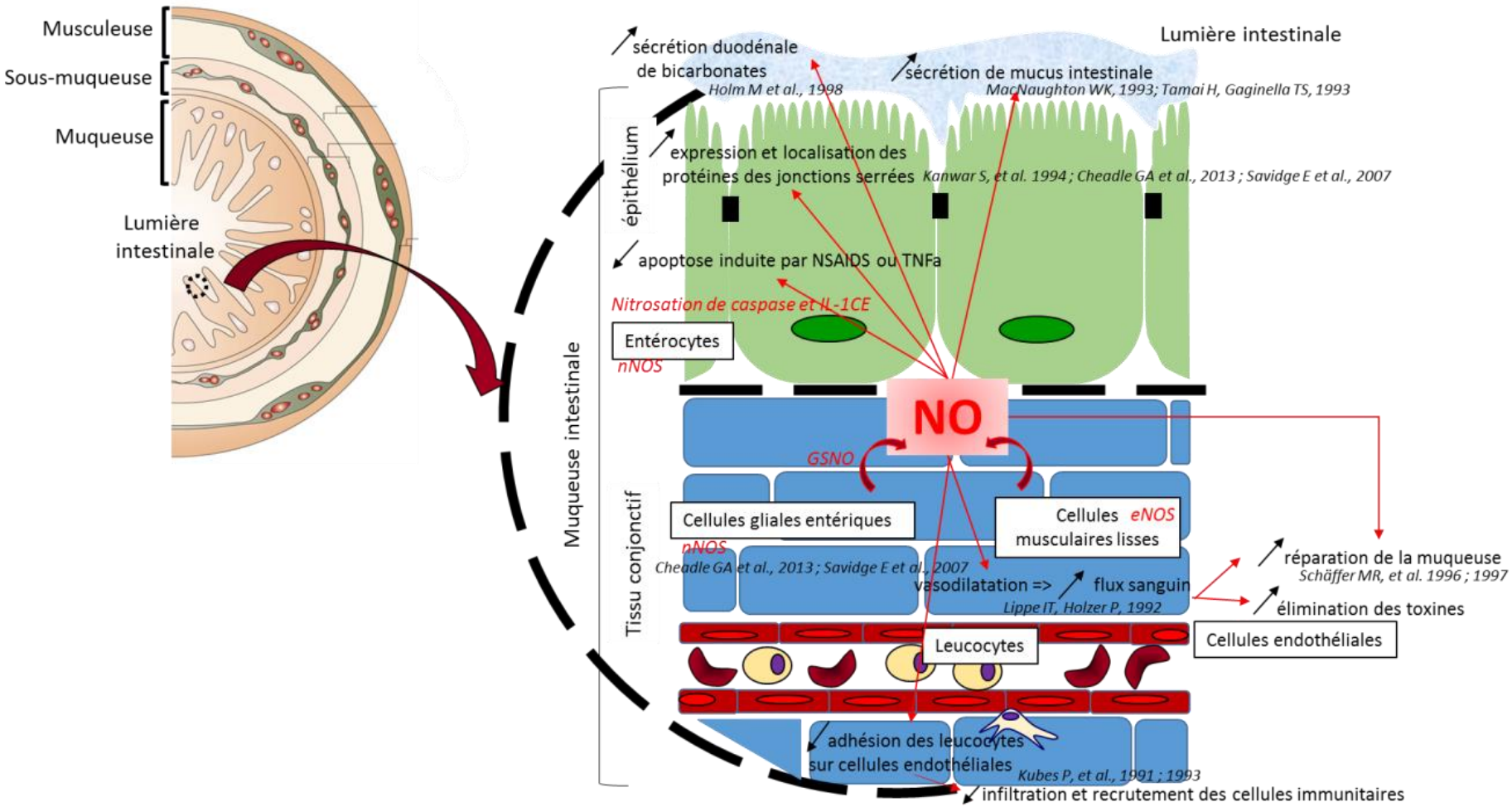

Figure 1 Rôles protecteurs de l'oxyde nitrique dans les conditions physiologiques : le maintien de l'intégrité de la barrière intestinale (Wallace and Miller, 2000, Heanue and Pachnis, 2007)

En effet, quand le NO est combiné avec un donneur (R) au niveau d'un groupement thiol pour former un RSNO, la demi-vie du NO se trouve augmentée (plusieurs heures) et le NO est alors délivré aux cellules et aux tissus de façon plus contrôlée que sous la forme d'anion peroxynitrite. Ceci est d'autant plus intéressant dans un contexte inflammatoire lorsque le donneur (R) est une molécule antioxydante naturellement produite par l'organisme, par exemple le glutathion formant ainsi le *S*-nitrosoglutathion (GSNO). Il a d'ailleurs été démontré que le GSNO sécrété par les cellules gliales entériques à la suite d'une stimulation du nerf vague permet de prévenir un épisode inflammatoire au niveau intestinal et de préserver l'intégrité de la barrière (Savidge *et al.*, 2007, Cheadle *et al.*, 2013). **La mise en place d'un traitement chronique préventif, basé sur l'administration orale de *S*-nitrosoglutathion (GSNO) représente une nouvelle stratégie pour limiter les récidives inflammatoires et les dommages au niveau de la barrière intestinale chez des patients atteints de MICI.**

Cependant, le développement d'un traitement chronique préventif des MICI, par voie orale, à base de GSNO représente un véritable challenge. Il s'agit de proposer une forme pharmaceutique stable adaptée à la voie orale, administrée à distance d'un épisode inflammatoire aigu, contrôlant la concentration de NO délivré au niveau intestinal pour assurer une action locale bénéfique.

Ce projet de thèse répond à une réelle attente des patients pour améliorer leur confort mais répond aussi à un réel besoin économique, proposant une solution pour diminuer le taux de récidives des MICI après un épisode aigu et pour réduire la période et le coût des traitements chroniques actuels. Le traitement préventif des MICI tel qu'il a été envisagé ci-dessus requiert donc la vérification de plusieurs points autour desquels s'articule cette thèse.

La première étape de cette thèse consiste à vérifier que le GSNO apporté dans la lumière intestinale (donc administré par voie orale) maintient l'intégrité de la barrière intestinale au même titre que le GSNO produit de manière endogène par les cellules gliales

entériques présentes dans la muqueuse intestinale (Savidge *et al.*, 2007, Cheadle *et al.*, 2013). Pour ce faire, une méthode expérimentale *ex vivo* a été utilisée pour suivre la capacité du GSNO à préserver l'intégrité de la barrière intestinale. Nous avons utilisé la chambre de Ussing qui est un dispositif permettant l'étude de la diffusion, du transport de molécules à travers une membrane. Dans ce dispositif, du tissu intestinal peut-être positionné de façon à séparer deux compartiments : un compartiment donneur (mimant la lumière intestinale) et un compartiment accepteur (mimant le tissu conjonctif sous-jacent voire le compartiment sanguin). Cette étude a été réalisée sur des tissus intestinaux prélevés chez des rats Wistar sains. Pour ce faire, différentes concentrations en GSNO ont été déposées (de 0,1 µM à 100 µM) dans le compartiment donneur de la chambre de Ussing et nous avons évalué plusieurs critères :

- la perméabilité d'une molécule fluorescente « de référence » (la fluorescéine sodique) au cours du temps,
- la mesure de la résistance transépithéliale (TEER),
- le niveau d'expression des protéines de jonctions serrées et de cytokines pro-inflammatoires (par Western Blot).

Nos études, conduites pendant 2 h, ont montré pour la première fois, que la perméabilité de la fluorescéine sodique (marqueur du passage entre les cellules intestinales, au travers des jonctions cellulaires) est significativement diminuée, en présence d'une faible concentration en GSNO (0,1 µM), par rapport aux plus fortes concentrations testées (10 et 100 µM). En revanche, aucune modification significative de la résistance transépithéliale (TEER) et de la quantité des protéines de jonction étudiées n'a été observée. Seule une diminution de 50 % de la quantité d'occludine (protéine constitutive des jonctions serrées) a été constatée en présence de 100 µM de GSNO. Ainsi, nos résultats indiquent qu'une faible concentration en GSNO (0,1 µM) retarderait la perte d'intégrité de la muqueuse intestinale dans ce système *ex vivo*, alors que les fortes concentrations en GSNO (100 µM) accélèreraient cette perte d'intégrité et altèreraient les jonctions cellulaires responsables de cette intégrité.

Une étude plus précise de l'expression des protéines de jonction (par la technique de Western Blot sur extraits membranaires uniquement, et non sur lysats tissulaires totaux ou par ELISA) pourrait affiner ces résultats. Pour compléter ces travaux, l'internalisation des protéines des jonctions cellulaires pourrait également être étudiée par immunofluorescence en microscopie confocale. Le TEER et l'expression des protéines de jonction à la membrane sont finalement des marqueurs tardifs des effets précoces du GSNO. Dans un tissu sain présentant une balance RedOx contrôlée, la capacité de la cellule à lutter contre le stress pourrait masquer ces effets précoces du NO. A l'inverse, dans un tissu inflammatoire, cette capacité de la cellule est altérée et l'effet du NO pourrait être observé plus aisément car ils pourraient résulter d'une nitrosation modérée de protéines impliquées dans l'intégrité de la barrière. Ce résultat constitue la première « preuve de concept », la première étude de faisabilité quant à l'utilisation de GSNO comme traitement préventif des MICI.

L'administration orale requiert une mise en forme adaptée du GSNO et constitue une seconde partie majeure de ce manuscrit. Si le NO voit sa demi-vie augmentée sous la forme GSNO (de quelques minutes à plusieurs heures), ces donneurs de NO n'en demeurent pas moins fragiles et très réactifs vis-à-vis de leur environnement. Sensible à différents facteurs environnementaux comme par exemple la lumière, les variations de température ou la présence d'ions métalliques divalents, la liaison S-NO est maintenue dans le temps très difficilement (Gaucher *et al.*, 2013). L'établissement d'un traitement chronique avec ce type de molécules nécessite une mise en forme galénique adaptée afin de protéger le NO jusqu'à son lieu d'action. De plus, cette forme galénique doit permettre un contrôle des doses de NO libéré. Les systèmes particulaires à libération contrôlée, tel que des nano- ou microparticules polymériques, peuvent tout à fait répondre à ces contraintes puisqu'elles sont basées sur l'utilisation de polymères biocompatibles, approuvés par les autorités de santé, et que les particules développées offrent une surface d'échange avec leur environnement particulièrement adaptée à la muqueuse intestinale.

L'encapsulation directe de GSNO est un véritable challenge, liée notamment à la difficulté de préserver la liaison S-NO durant le procédé de formulation des systèmes particulaires. Cette stratégie offre la possibilité d'obtenir des charges en NO très intéressantes pour minimiser les quantités de particules à administrer, pour protéger le GSNO véhiculé et pour proposer des libérations et des actions plus prolongées dans le temps. Pour une application orale et un effet au contact de l'intestin, une libération sur 24 h serait plus adaptée. **Ce travail de thèse fait suite à différents travaux entrepris au sein de l'équipe CITHEFOR** ayant démontré la faisabilité de cette encapsulation directe du GSNO par différentes techniques de formulation (Parent *et al.*, 2013c, Wu *et al.*, 2015a, Diab *et al.*, 2016) par exemple démontré une encapsulation efficace du GSNO (54% d'encapsulation de GSNO, soit 40 mmol de GSNO/L de suspension) dans des nanoparticules d'Eudragit® RL (un polymère polycationique de type méthacrylique utilisé couramment dans de très nombreuses formes orales sous forme de film de pelliculage et actuellement sur le marché), libérant un GSNO actif de façon plus prolongée dans le temps et limitant sa dégradation en ions nitrite et nitrate (Wu *et al.*, 2015a). Afin d'augmenter la stabilité et de prolonger la libération du GSNO au cours du temps, l'incorporation des nanoparticules dans une matrice polymérique pour former les systèmes particulaires composites (Wu *et al.*, 2015b) a été proposée (Figure 2).

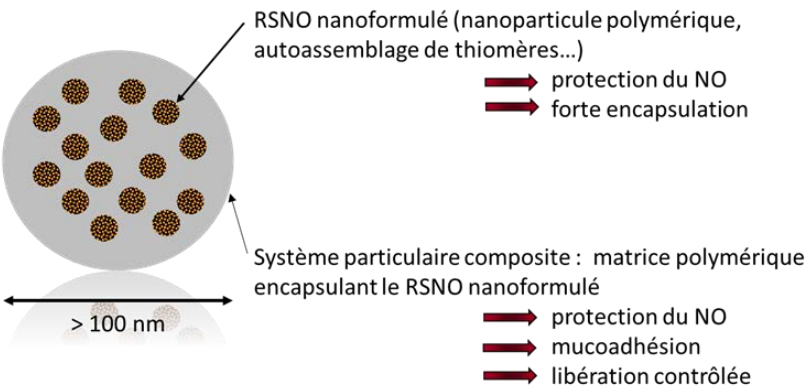

Figure 2 Description d'un système particulaire composite délivrant un RSNO.

Ce type de système est recommandé dans la littérature pour réduire la libération initiale massive de principe actif (Hassan *et al.*, 2009). Des systèmes particulaires pouvant mesurer jusqu'à plusieurs dizaines de micromètre ont été préparés par un procédé de gélification ionique, menant à des particules de chitosane ou d'alginate de calcium (Nasti *et al.*, 2009, Koukaras *et al.*, 2012). Ces systèmes particulaires composites ont été caractérisés en termes de taille, de taux d'encapsulation du GSNO, de cinétique de libération à pH 7,4 dans un milieu tamponné mais aussi de toxicité cellulaire par établissement de tests MTT sur une lignée d'adénocarcinome colique humaine (Caco-2).

Au cours de cette thèse, de **nouveaux systèmes composites** ont été formulés et caractérisés pour renforcer la protection du GSNO tout au long du tractus gastro-intestinal et contrôler davantage la libération de ce dernier : les nanoparticules d'Eudragit® RL préalablement développées au sein de l'équipe ont été elles-mêmes encapsulées dans une matrice polymérique à base d'alginate, polymère adapté à la voie orale et décrivant des propriétés favorisant la mucopénétration au niveau intestinal (Laffleur and Bernkop-Schnürch, 2013, Kumar *et al.*, 2014).

Pour ce faire, deux procédés de formulation de la matrice d'alginate ont été développés et comparés (article soumis dans *Journal of Microencapsulation*). Un procédé simple de complexation de polyélectrolytes (entre les nanoparticules d'Eudragit® RL chargées positivement et l'alginate de sodium chargé négativement) a été comparé à un procédé plus classique de gélification ionotropique, utilisant le chlorure de calcium comme agent structurant des chaines d'alginate (« cross-linker »). Le procédé simple de complexation de polyélectrolytes a conduit à l'obtention de particules composites avec une charge en GSNO plus importante mais une libération *in vitro* plus rapide que celles formulées par gélification ionotropique (tableau 2).

Tableau 2 : Charge et libération du GSNO dans les particules composites formulées par complexation de polyélectrolytes et par gélification ionotropique.

Procédés de formulation	Charge en GSNO (mg/g de polymère)	Libération du GSNO à 3h (%)
Complexation de polyélectrolytes	4,4 ± 0,4	27,9 ± 4,7
Gélification ionotropique	2,7 ± 0,2	97,8 ± 7,9

Cette différence de libération du GSNO observée *in vitro*, est minimisée au contact des cellules (cellules Caco-2 cultivées en système de Transwell®) : la perméabilité du GSNO et de ses produits de dégradation (ions nitrite et nitrate) est retardée de la même façon quelle que soit la formulation choisie. **Le procédé de complexation de polyelectrolytes, plus simple et plus facilement industrialisable que le procédé de gélification ionotropique, est adapté à la libération du GSNO. Ces deux procédés répondent donc au cahier des charges mentionné plus haut, en termes d'encapsulation, de libération et de délivrance locale au niveau intestinal.** Il sera néanmoins nécessaire de confirmer ces caractéristiques par des essais chez l'animal, sur un tissu intestinal.

Un autre type de formulation a été proposé en parallèle de cette étude. Il s'agissait de proposer une **nouvelle association de polymères**, non décrite dans la littérature et répondant au même cahier des charges, **pour constituer la matrice des particules composites** par un procédé de gélification ionotropique (Wu *et al.*, 2016). Le chitosan a été remplacé par un autre polymère polycationique (l'Eudragit®E) pour constituer la matrice en association avec l'alginate. Contrairement au chitosan qui est connu pour ouvrir les jonctions serrées, donc inadapté à notre problématique, (Thanou *et al.*, 2001, Wu *et al.*, 2016), l'Eudragit® E pourrait limiter la libération du GSNO au niveau intestinal. L'encapsulation de GSNO dans ces systèmes particulaires est efficace (2,5±0,6 mg de GSNO/g de polymère) et équivalente à celles des particules composites à base d'alginate seul ou associé avec le chitosan. La caractérisation physico-chimique de ces particules composites doit être complétée par des études *in vitro* et *in cellulo* de

libération du GSNO.

En conclusion, ce travail s'attache donc au développement et à la caractérisation, limitée à la détermination des paramètres physico-chimiques des particules, à l'évaluation de leur cytotoxicité et à l'étude de la perméabilité du GSNO délivré sur un modèle de barrière intestinale en culture. A l'issue de ces travaux de thèse, trois formulations adaptées à la délivrance orale de GSNO sont proposées. La démarche entreprise devra être poursuivie par :

- des études de stabilité des formulations proposées
- des études *in vivo* (modèles animaux de MICI) évaluant la capacité des systèmes particulaires composites de GSNO les plus efficaces à prévenir le développement et à limiter l'apparition d'épisodes inflammatoires aigus. Il s'agira d'administrer oralement (par gavage) les formulations (sous la forme de suspensions) de manière préalable à l'induction de l'inflammation induite par des composés chimiques (sulfate de dextran sodique par exemple) (Tran CD et al., 2012) (Figure 3).

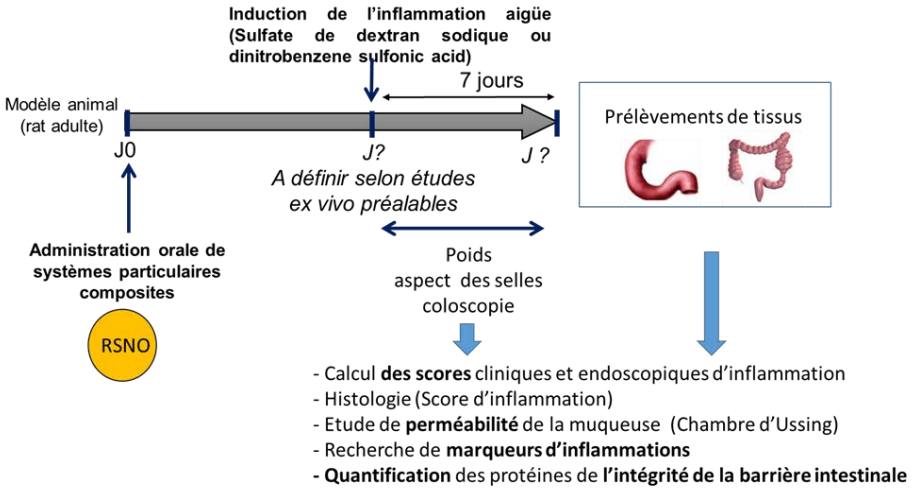

Figure 3 : Schéma expérimental des expériences qui pourront être menées *in vivo*.

Pour présenter ces travaux de thèse, le manuscrit s'articule de la manière suivante :

Dans une première partie, les pathologies MICI, les traitements de références actuels

et les traitements innovants sont présentés. Parmi ces derniers, le choix du GSNO et de l'oxyde nitrique est argumenté en décrivant les actions bénéfiques de ce dernier au niveau intestinal. La mise en forme du GSNO pour proposer cette molécule comme candidat à un traitement oral chronique est ensuite évoquée. L'intérêt des formulations appelées « nanoparticules composites » pour la délivrance de principe actif par voie orale est alors documentée au travers d'une revue bibliographique *(Polymer nanocomposites for drug oral delivery: development strategies and potentialities. Hui Ming, Wen Wu, Philippe Maincent, Marianne Parent, Caroline Gaucher, Anne Sapin-Minet. Volume 9: Organic particles, Composites in Biomedical Engineering: Particles (Series C) – ELSEVIER, Edited by Alexandru Mihai GRUMEZESCU (in progress)).*

La seconde partie rapporte l'étude du maintien, du renforcement de la barrière intestinale par le GSNO (non formulé) apporté dans la lumière intestinale : cette étude originale constitue la preuve de concept, l'étude de faisabilité de ce projet. Elle s'articule autour d'un article devant être prochainement soumis dans *Journal of gastroenterology*.

La formulation de GSNO constitue la **troisième partie du manuscrit**. Un article soumis dans *Journal of Microencapsulation* décrit et compare deux systèmes particulaires composites. Un troisième système est ensuite décrit en données complémentaires.

A ce stade du travail, nous avons proposé, caractérisé et évalué plusieurs méthodologies de formulation dont les avantages et les limites sont discutées dans une dernière partie du manuscrit. L'étude de ces formulations peut maintenant être poursuivie *in vivo* par l'évaluation de leur capacité à prévenir les récidives inflammatoires au niveau intestinal.

Chapter 1.
Introduction

1.1 Inflammation bowel disease

Inflammatory bowel diseases (IBD) are chronic and relapsing disorders affecting gastrointestinal (GI) tract and associated with intestinal mucosa lesions and inflammation. The most known subtypes are Crohn's disease (CD) and ulcerative colitis (UC). While both subtypes can lead to symptoms such as abdominal pain, cramping, diarrhea or weight loss, there are differences between them. It is important to note that CD can occur all over the digestion tract, from the mouth to the anus, but most often affects the large and small intestines, whereas UC primarily affects only the colon and rectum. As chronic disease, IBD are disabling, lead to significant health care costs and cause patients to suffer a lot in life quality and work capacity (Bannaga and Selinger, 2015).

1.1.1 IBD epidemiology

IBD has become a worldwide disease. Incidence and prevalence of IBD are higher in developed countries than in developing countries, and in urban areas than in rural areas (Molodecky *et al.*, 2012). Currently, the highest annual incidence of CD is in Canada (20.2 per 100 000), New Zealand (16.5 per 100 000), northern Europe (10.6 per 100 000), and Australia (29.3 per 100 000) (Torres *et al.*, 2016). Meanwhile the highest incidences of UC have been reported in northern Europe (24.3 per 100 000), Canada (19.2 per 100 000), and Australia (17.4 per 100 000) (Ungaro *et al.*, 2016b). The prevalence of both UC and CD are highest in Europe (505 and 322, per 100,000 respectively), Canada (319 and 248 per 100 000 respectively), and the USA (214 per 100 000 for both) (Molodecky *et al.*, 2012, Ponder and Long, 2013, Torres *et al.*, 2016, Ungaro *et al.*, 2016b). A significant increasing trend of IBD incidence was observed with developing countries, such as Asian, Middle East, South America and Africa while a plateaued of incidence was achieved for the western areas (Ng *et al.*, 2013, Ng *et al.*, 2016, Torres *et al.*, 2016, Ungaro *et al.*, 2016b). IBD has become more common in Asia over the past few decades. The rate of increase in prevalence of the disease varies

greatly in Asia, with several countries in East Asia experiencing a more than doubled increase in IBD prevalence over the past decade (Ng *et al.*, 2016).

1.1.2 IBD physiopathology

Till now, the exact physiopathology remains unknown. Genetic susceptibility, environment factors, intestinal microbial flora dysbiosis and immune dysfunction are all correlated with the pathogenesis.

1.1.2.1 Genetic susceptibility

About 12% of patients have a family history of CD while the ratio for UC is 8–14% of patients (Moller *et al.*, 2015, Torres *et al.*, 2016, Ungaro *et al.*, 2016b). Ashkenazi Jews have higher rates of IBD than in non-Jewish populations, and African-American and Asian ancestries are associated with the lowest risk (Ananthakrishnan, 2015, Huang *et al.*, 2015). Genome-wide association studies have identified more than 200 alleles associated with IBD, of which most genes contributing to both ulcerative colitis and Crohn's disease phenotypes (Jostins *et al.*, 2012, Liu *et al.*, 2015b). The discovery of genes associated with bacterial sensing, innate immunity, Th17-cell function (NOD2, ATG16L1, LRRK2, IRGM, Il23R, HLA, STAT3, JAK2, and Th17 pathways) and an altered mucus layer (MUC2), human leukocyte antigen, barrier function, such as HNF4A and CDH1 brought major insights into disease pathogenesis (Barrett *et al.*, 2009, Jostins *et al.*, 2012, McGovern *et al.*, 2015). However, only 13.1% of CD and 7.5% of UC heritability is explained by genetic variation (Torres *et al.*, 2016, Ungaro *et al.*, 2016b). The importance of epigenetic and other nongenetic environmental factors are highlighted (Huang *et al.*, 2015). Therefore, genetics alone has little predictive capacity for phenotype, and currently are of limited clinical use.

1.1.2.2 Environment factors

The increasing incidence of IBD worldwide suggests the importance of environmental factors in its development. Smoking is one of the well-studied factor and strongest

environmental risk for CD and UC. The protective effect of current smoking on the development of UC was confirmed. The active smokers are less likely to develop UC compared with former and non-smokers and have a milder disease course (Birrenbach and Böcker, 2004, Cosnes, 2004). Contrary to its effect on UC, smoking is associated an increasing risk of developing CD by two-fold (Mahid *et al.*, 2006). However, the mechanism how smoking impacts IBD remains unclear as does the reason for its protective effect in UC but deleterious impact on CD (Cosnes *et al.*, 2011). The medications such as aspirin, non-steroidal anti-inflammatory drugs, oral contraceptives and antibiotics are potentially associated with increased risk (Ananthakrishnan, 2013), whereas statins have been related with a decreased risk, especially in older people (Ungaro *et al.*, 2016a). Stress is another environment factor that plays a role in the pathogenesis of CD (Mawdsley and Rampton, 2007). Mood components of perceived stress including depression and anxiety exacerbated the disease related to stress (Cámara *et al.*, 2011) while individuals with lower levels of stress and better coping mechanisms had a reduced risk of disease flare (Bitton *et al.*, 2008). Micronutrients (zinc and iron) and vitamin D has also been proposed for a role of environmental role (Ananthakrishnan, 2015). Diet has been implicated with an important factor of IBD pathology. An increasing risk of UC and CD was observed with reduction in dietary fiber and increase in saturated fat intake (Ananthakrishnan *et al.*, 2014). Many environmental factors need to be proven in the further study.

1.1.2.3 Intestinal microbial flora dysbiosis

The involvement of the intestinal microbial flora alteration in the pathophysiology of IBD has recently been highlighted (Matsuoka and Kanai, 2015). The altered balance of the gut microbiota is referred to dysbiosis. Dysbiosis of IBD patient includes reduced diversity of the gut microbiota (Tong *et al.*, 2013), a decrease in Bacteroides and Firmicutes bacteria and an increase in Gammaproteobacteria, Actinobacteria, Enterobacteriaceae and Proteobacteria (Matsuoka and Kanai, 2015, Torres *et al.*, 2016,

Ungaro *et al.*, 2016b). The reduced diversity of the gut microbiota observed in IBD patients is largely owing to a reduction in the diversity of Firmicutes. An increase abundance of Escherichia coli which is mucosa associated adherent-invasive bacteria were observed in about one third CD patient (Darfeuille-Michaud *et al.*, 2004, Lapaquette *et al.*, 2010, Torres *et al.*, 2016). These strains trigger high amount of tumor necrosis factor-α (TNF-α) secretion. The mechanism is that Escherichia coli goes through the intestinal mucosal barrier, adhere to and invade intestinal epithelial cells, then survive and replicate within macrophages (Torres *et al.*, 2016). Although the alternation of intestinal microbial flora is a highly active research area, it has not yet applied to practices, because of the difficulties in microbiota manipulation (Torres *et al.*, 2016).

1.1.2.4 Immune dysfunction

Immunity is one of physiological functions in humans, which can be divided into innate and adaptive immunity (Huang and Chen, 2016). Two major processes of the innate immunity are usage of a large set of different pattern recognition receptors (PRRs) and a system for random and nonselective generation of antigen specific receptors. The adaptive immunity has been considered as a complement to the innate immunity and a definitive solution to pathogen recognition (Huang and Chen, 2016). The differences between innate immunity and adaptive immunity are presented in Table 1.

Table 1 The differences between the innate and adaptive immunity (Huang and Chen, 2016)

Item	**Innate immunity**	**Adaptive immunity**
Acquired form	Inherent (or congenital)	Acquired
	Do not need to contact the antigens	Need to contact with the antigens
Time to play roles	Early, rapid (minutes-4 days)	4-5 days
Immune recognition receptors	Pattern recognition receptor	Specific antigen recognition receptors
Immune memory	Nothing	Generation of memory cells
Examples	Antibacterial substances, bactericidal substances, inflammatory cytokines, phagocytic cells, NK cells, NK T cells	T cells (cell immunity) B cells (humoral immunity)

Inflammation happens when the immune system dysfunction occurs. The Figure 1 showed the link of IBD and immune dysfunction. The innate immune abnormalities of inflammatory bowel disease result in adaptive immune disorders (Th1/Th2 regulation imbalance and Th17/Treg transformation imbalance). The inflammatory cytokines in turn increase the innate immune damages (apoptosis of intestinal epithelial cells, reduction of connection protein expression, decrease of antibacterial peptides secreted by Paneth cells, etc.), abate the intestinal barrier function, and aggravate inflammation.

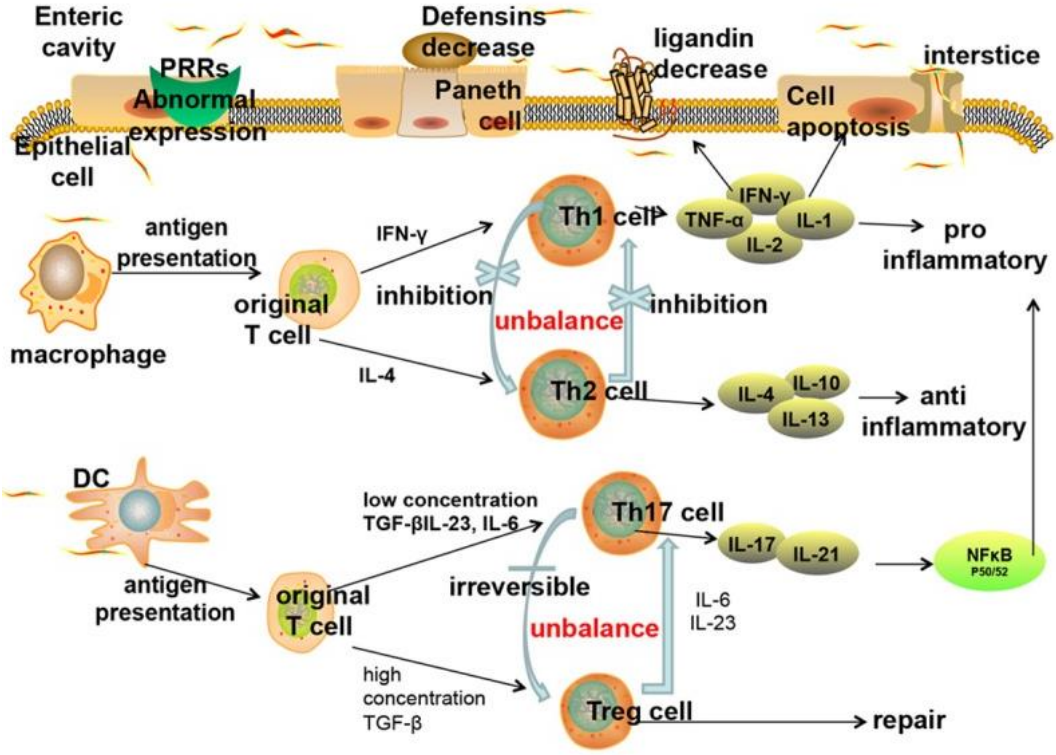

Figure 1 IBD and immune dysfunction (Huang and Chen, 2016).

1.1.2.4.1 Innate immunity defects in IBD

The innate intestinal immune system is constituted of intestinal mucosal barrier (see paragraph 1.2.1), innate immune cells, innate immune molecules… Innate immunity defects in IBD are associated with intestinal barrier by apoptosis of intestinal epithelial cells and increasing intestinal permeability.

Immune cells in inflammatory intestinal mucosa of IBD patients induce expression of

epithelial cell apoptosis related proteins, such as Caspase-1 by producing inflammation factors, such as tumor necrosis factor-α (TNF-α) and interferons-γ (IFN-γ), which, and inhibit expression of anti-apoptotic proteins, such as Bcl-2, which lead to induced epithelial cell apoptosis, weakened function of epithelial cells resisting pathogens and increased permeability of intestinal mucosa (Bouma and Strober, 2003). During an active stage of IBD, junction protein and its corresponding mRNA in intestinal tissue decrease significantly, resulting in the disruption of intestinal barrier integrity (Gassler *et al.*, 2001). Innate immune cells include Macrophages, Dendritic cells (DCs) and Natural killer (NK) cells. Macrophages can decompose engulfed pathogens into specific antigenic determinants, such as peptides and lipopolysaccharide, using proteases and oxygen free radicals (Huang and Chen, 2016). During the acute phase of IBD, quantity of macrophages in intestinal mucosa dramatically increases, leading to secretion of macrophage pro-inflammatory factors (Baj-Krzyworzeka *et al.*, 2006). Mature DCs are antigens presenting cells. In colonic mucosa of IBD patients, interactions between DCs and T cells increase the secretion of inflammatory cytokines and cause inflammation (Drakes *et al.*, 2005). NK cells can control viral and bacterial infections, produce cytokines, kill tumor cells, and build a relationship between innate immunity and acquired immunity (Colucci *et al.*, 2003). NK cells that express interleukin 22 (IL-22) have a protective effect on initiation of IBD (Zenewicz *et al.*, 2008).

Innate immune molecules contain defensins and PRRs. Defensins, which contain two types: α and β, have lots of functions. They play an important role in cell immunity by serving as a bridge between innate immunity and adaptive immunity. Thus, a decline of defensins not only weakens innate immunity, but also influences initiation and regulation of adaptive immunity (Huang and Chen, 2016). More bacteria invasion of intestinal mucosa was observed with a loss of mucosal defensins, which resulted in inflammation (Wehkamp *et al.*, 2005). PRRs contain Toll-like receptors (TLRs) and nucleotide-binding oligomerization domain like receptors (NLRs) (Huang and Chen,

2016). PRRs also act as a bridge between innate immunity and adaptive immunity. They can activate innate immunity by secreting cytokines to fight against pathogens(Huang and Chen, 2016).

1.1.2.4.2 Adapted immune response in IBD

Adapted immunity works as a complementary immune response of innate immunity against the invasion of pathogenic microorganisms. After antigens stimulating, the original T cells amplify and are differentiated into different subsets such as Th1, Th2, Th17 and Treg cells (Huang and Chen, 2016). Th1 cells eliminate pathogens inside cells; Th2 cells protect human body from harmful parasites and adjust allergic reactions; Th17 cells remove extracellular bacteria and fungi; Treg cells help tissue repairs(Huang and Chen, 2016). However, disorders of T cell responses and imbalance of Th1/Th2 cells and Th17/Treg cells promote excessive secretion of cytokines and chemokines, resulting inflammation (Huang and Chen, 2016). Thl and Th2 cells are in dynamic equilibrium under normal conditions, and are regulated and inhibited by cytokines produced by each other (Huang and Chen, 2016). Imbalance of Th1/Th2 cells is associated with pathogenesis of IBD (Kanai *et al.*, 2006). Th1 cells release pro-inflammatory cytokines, such as IL-1, IL-2, IL-6 and IL-8 which involved in cellular immune response, while Th2 cells secret anti-inflammatory cytokines, such as IL-4, IL-10 and IL-13 which is correlated with humoral immune responses (Huang and Chen, 2016). Thus, balance of Thl and Th2 cells decides balance of pro-inflammatory and anti-inflammatory cytokines, which then leads to whether and which kinds of immune reactions occur (Huang and Chen, 2016). Under normal condition, balance of Th17 cells and Treg cells exist in dynamic way. If the balance was broken, intestinal mucosa damages occur. In IBD patients, the balance is disrupted with over-increases of Th17 cells, over-enhancements of immunogenicity and decreases or abnormal functions of Treg cells (Huang and Chen, 2016).

The disruption of intestinal barrier has been implicated in the pathology of IBD as well. The intestinal barrier plays a crucial role in observed in the preventing microbiota

invasion. This barrier defect was observed in IBD patients (Söderholm et al., 1999), which caused by decreased expression and redistribution of tight junction proteins, including occludin, claudin-3, -5, -8, and JAM-1, and increased expression of pore-forming claudin-2, and cytoskeletal dysregulation caused by alternation of MLCK expression and MLC phosphorylation (Zeissig et al., 2007, Vetrano et al., 2008, Blair et al., 2006). Therefore, the improvement of intestinal mucosal barrier represents a potential therapeutic target of IBD.

1.2 Intestine physiology

The intestine is a remarkable organ. It is filled with 10^{13}–10^{14} bacteria and also with digestive enzymes, which has two important function for human health: digestion and protection from external environment. For these functions, intestine covers a surface of about 400 m^2 and requires approximately 40% of the body's energy expenditure (Bischoff *et al.*, 2014). The body has two types of intestine: small intestine which begins at the pyloric sphincter of the stomach and extends to the cecum with a length of approximately 6.7 meters; large intestine which is also called colon with a length of 1.8 meters. The small intestine is divided in three major segments: the duodenum, the jejunum, and the ileum. The large intestine is composed of four parts: the ascending colon, the transverse colon, the descending colon and the sigmoid colon.

The intestine tissue is composed of four concentric layers: the serosa, muscularis, submucosa, and mucosa (Figure 2) (Rubin and Langer, 2009). The **serosa** (the outmost layer) is a smooth membrane that is also a thin layer of connective tissue. It is constituted of a thin layer of cells (epithelium) that produce serous fluid. Serous fluid is a lubricating fluid which decrease friction from the muscularis movement. The **muscularis** is in charge of the movement or peristalsis of the intestine. It normally has two obvious layers of smooth muscle: circular and longitudinal. The **submucosa** is the dense layer of irregular connective tissue that supports the mucosa, as well as joins the mucosa to the bulk of underlying smooth muscle. The **mucosa** is a mucous membrane,

which is the innermost tissue layer of the small intestine It includes digestive enzymes and hormones. The intestinal villi are part of the mucosa, which has bigger surface that can enhance the nutrients absorption. The mucosal layer of the gut consists of epithelium overlying the lamina propria, and resting on a narrow layer of smooth muscle, the muscularis mucosae. It represents the obvious physical boundary between the external and internal environment to constitute an important defense barrier of human body.

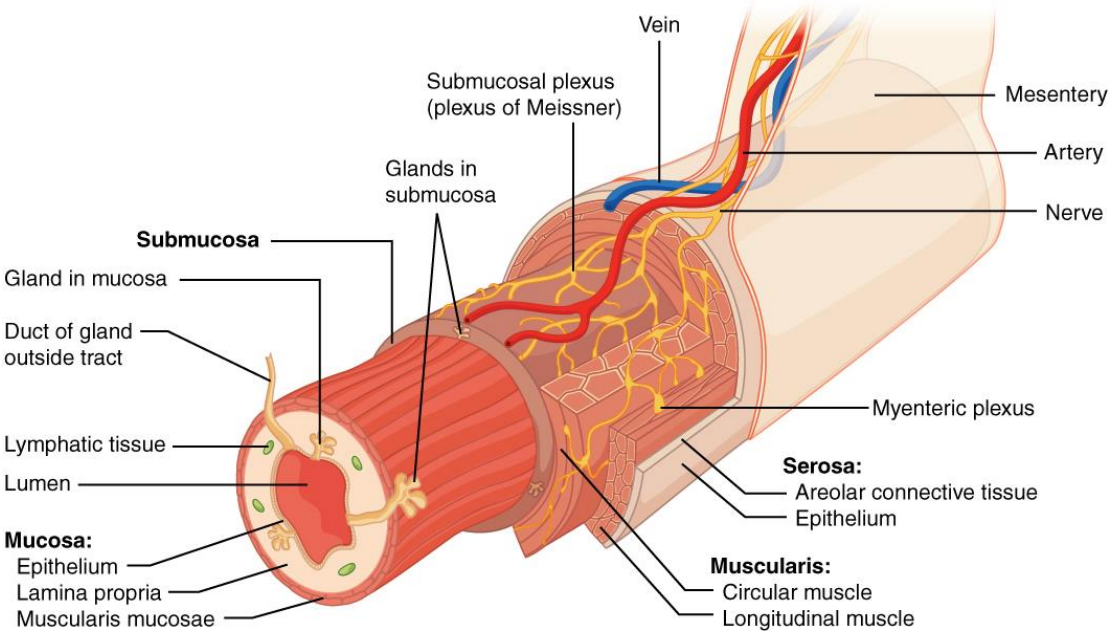

Figure 2 Anatomy of intestine

In direct contact with external environment, intestinal mucosa plays a critical role in the maintenance of the intestinal homeostasis. It has two critical functions. Firstly, it helps the absorption of nutrients, electrolytes and water into vascular, followed by circulation in the whole body. Secondly, the intestinal mucosa plays a crucial role of barrier as it prevents the uncontrolled translocation of luminal contents such as microorganisms or toxins into the intestinal tissue circulatory system and in the end in the whole organism (Groschwitz and Hogan, 2009). This barrier function is particularly important in the defense against the invasion by microorganisms of the gut microbiota and to avoid septic shock. The intestinal barrier is a complex biological system including several components with two main functions: the prevention of the mucosa

invasion and the elimination of the microorganism who succeeded in the invasion.

1.2.1 Intestinal barrier components

Intestinal barrier is a complex multilayer system, consisting in an external "physical" barrier and an inner "functional" immunological barrier. The tight interaction of these two barriers maintains an equilibrated permeability to nutrients, electrolytes and avoids the entry of pathogens, toxins, antigens (Bischoff *et al.*, 2014). To understand this complex barrier, the functions of its components is very crucial to be described. Several components are assembled to form a functional intestinal barrier (Figure 3).

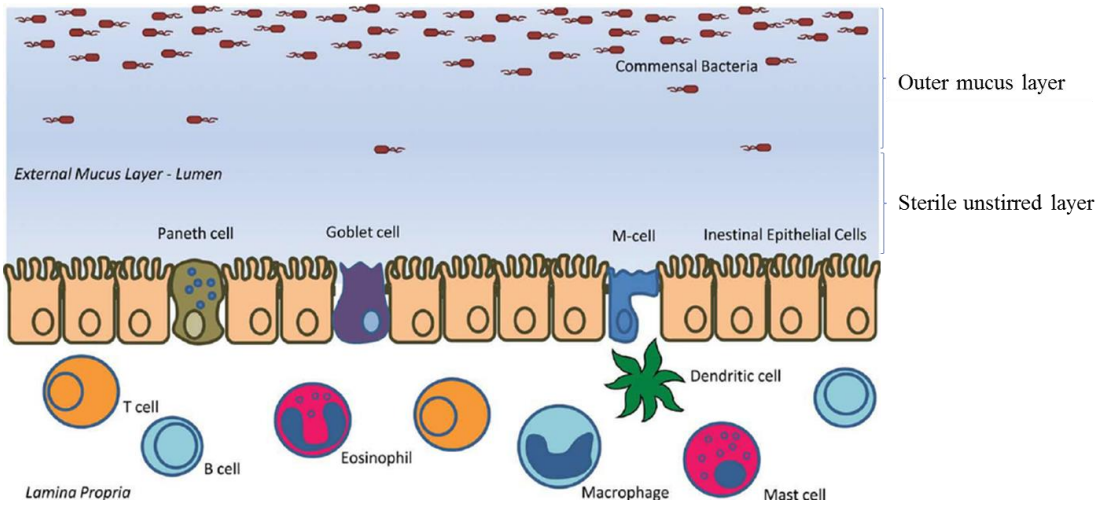

Figure 3 Elements comprising the intestinal mucosal barrier(Salim and Soderholm, 2011).

First, the endothelial cell layer is covered with two mucus layers, a thick, unstirred and relatively sterile mucus layer and an outer layer in direct contact with the cell which forms a protective area. The single layer of epithelial cells interspersed with mucus producing goblet cells, anti-microbial peptide producing Paneth cells, and specialized luminal sampling enterocytes M-cells forms the main barrier between the outside world and the internal body proper. In the lamina propria, innate and adaptive immune cells such as T cells, B cells, eosinophils, mast cells, dendritic cells, and macrophages, comprise the mucosal immune system that responds with “active” eradication or “toleragenic-reaction” towards foreign antigens. In addition, the degradative properties of gastric acids, pancreatic and biliary juices, and the intestinal propulsive motility have

also been recognized to be important factors in intestinal barrier function. It is imperative to keep in mind that although these components might be presented individually, they are inextricably linked and can affect the functional responses of each other (Salim and Soderholm, 2011).

1.2.1.1 The role of the commensal microbiota

More than 500 different microbial species constituting up to 100 trillion (10^{14}) microorganisms per human colonize the intestinal tract (Figure 4) (Konturek *et al.*, 2015). The gut microbiota maintains a symbiotic relationship with the gut mucosa and imparts substantial metabolic, immunological and gut protective functions in the healthy individual (Jandhyala *et al.*, 2015). The normal human gut microbiota comprises of two major phyla, namely *Bacteroidetes* and *Firmicutes* (Jandhyala *et al.*, 2015).

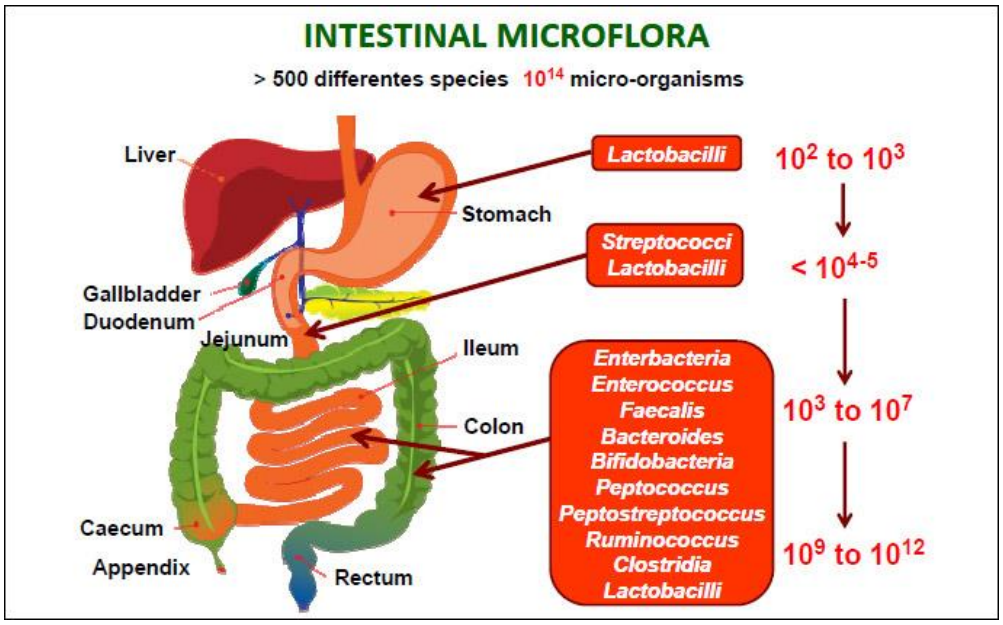

Figure 4 Spatial and longitudinal variations in microbial numbers and composition across the length of the gastrointestinal tract (Konturek et al., 2015). The number of bacterial cells present in the mammalian gut shows a continuum that goes from 102 to 103 bacteria per gram of contents in the stomach and duodenum, progressing to 104 to 107 bacteria per gram in the jejunum and ileum and culminating in 109 to 1012 cells per gram in the colon.

The composition of the gut microbiota remains relatively unchanged from late childhood to old age, the changes occur when aging process starts (Petschow *et al.*,

2013, Sun and Chang, 2014). Gut microbiota plays a crucial role in host health through different aspects.

- It can impact on host nutrient, xenobiotic and drug metabolism (Jandhyala *et al.*, 2015). For example, the gut microbiota ferment non-digestible dietary carbohydrates into short chain fatty acids (SCFA) such as butyrate, propionate and acetate, which are rich sources of energy for the host epithelial cells (Macfarlane and Macfarlane, 2003, Sartor, 2008). Microbiome induced drug metabolism function is reflect by an interesting example: the microbial β-glucoronidase induced deconjugation of the anticancer drug irinotecan that can contribute to its toxic adverse effects, such as diarrhea, inflammation and anorexia (Wallace *et al.*, 2010).
- Gut microbiota is furthermore implied in maintenance of structural integrity of the gut mucosal barrier, immunomodulation, and protection against pathogens. For example, the gut microbiota, via its structural components and metabolites, has been shown to promote the mucosal barrier function via a pattern recognition receptor (PRR) mediated mechanism, which results in activation of several signaling pathways that are essential for the production of antimicrobial proteins (AMP) such as cathelicidins, C-type lectins, and (pro)defensins by the host Paneth cells, mucin glycoproteins and IgA (Salzman *et al.*, 2007, Hooper, 2009). *Bacteroides thetaiotaomicron* is reported to induce expression of the small proline-rich protein 2A (sprr2A), which is required for maintenance of desmosomes at the epithelial villus (Lutgendorff *et al.*, 2008). Furthermore, the *Lactobacillus rhamnosus GG strain* produces two soluble proteins namely p40 and p75 that can prevent cytokine induced apoptosis of the intestinal epithelial cells in an epithelial growth factor receptor (EGFR) and protein kinase C (PKC) pathway dependent manner (Yan *et al.*, 2011). Finally, the gut microbiota contributes to the structural development of the gut mucosa by inducing the transcription factor angiogenin-3, which has been implicated in the

development of intestinal microvasculature (Stappenbeck *et al.*, 2002).

The dysbiosis of gut microbiota is caused by different factors, such as aging, diet changing and utilization of antibiotics… This can result in exposure the host intestine to luminal contents, including toxins, pathogens, antigens… Therefore, microbial dysbiosis can be trigged, which contributes to intestinal disorders and extra-intestinal disorders. Intestinal disorders include inflammatory bowel disease (IBD), irritable bowel syndrome (IBS), and coeliac disease, while extra-intestinal disorders include allergy, asthma, arthritis, metabolic syndrome, cardiovascular disease, and obesity (Carding *et al.*, 2015).

1.2.1.2 Role of mucus layer

The production of a thick mucus layer that overlies the entire intestinal epithelium prevents large particles, including most bacteria, from direct contact with the epithelial cell layer. Goblet cells secrete large amounts of mucin glycoprotein, via the expression of the MUC2 gene. Mucin forms into a protective gel-like layer that can extend up to as much as 800 μm thick in the colon (Atuma *et al.*, 2001). As mentioned previously, the majority of microorganisms in the lumen can be found in the outer mucus layer, there is an inner, protected, and unstirred layer that is directly adjacent to the epithelial surface and is relatively sterile (Figure 3). The sterility of this layer contributes to the retention of a high concentration of antimicrobial proteins (such as cathelicidiens, defensins) produced by various intestinal epithelial lineages, including enterocytes and Paneth cells (see paragraph 1.2.1.3). The existence of unstirred layer can slow down the diffusion of small molecule (ions and small solutes…) which can pass through the heavily outer layer with relative ease (Turner, 2009). The crucial role of the mucus layer in maintaining the intestinal barrier has been illustrated in MUC2 knockout mice, where bacteria were found to be in direct contact with the epithelial cells (Van der Sluis *et al.*, 2006, Johansson *et al.*, 2008). This subsequently led to the exacerbation of intestinal inflammation. Defective mucus layers resulting from the lack of MUC2 mucin, mutated

MUC2 mucin Willebrand factor domains, or from deletion of core mucin glycosyltransferase enzymes in mice increased bacterial adhesion to the epithelium surface, intestinal permeability, and enhanced susceptibility to colitis caused by dextran sodium sulfate (Kim and Ho, 2010).

1.2.1.3 Role of the intestinal epithelial cells

The intestinal epithelial cells (IECs) are by far the most integral part of the mucosal barrier. Epithelial cells form a continuous, polarized monolayer that is linked together by a series of dynamic junctional complexes. The pluripotent intestinal epithelial stem cells that are located at the crypt region of the intestine include enterocytes, Paneth cells, the mucus-secreting Goblet cells and enteroendocrine cells (Barker *et al.*, 2008). **Enterocytes** are columnar cells, primarily functioning as absorptive cells, regulating nutrients and ions absorption (Salim and Soderholm, 2011). At the apical surface, these epithelial cells possess an extensive network of microvillar extensions that form the brush border and contain many of the digestive enzymes and transporter receptors that are essential in metabolism and uptake of dietary antigens. The enterocytes have also developed intricate transport mechanisms (Passage Routes, described in paragraph 1.2.2) while maintaining an effective barrier to harmful macromolecules and microorganisms. The enterocytes take up and process antigen via two function pathways. In the major pathway, the antigens are degraded by enzymes in the lysosomes. In the other pathway, antigens are released into the interstitial space without degradation. Moreover, the enterocytes are often directly involved in immune processes by presenting processed antigens directly to T cells (Snoeck *et al.*, 2005). In addition to constitute a physical barrier, epithelial cells maintain a mucosal defense system through the expression of a wide range of pattern recognition receptors (PRRs), such as Toll-like receptors (TLRs) and intracellular nucleotide-binding oligomerization domain (NOD)-like receptors (NLRs). These PRRs form the backbone of the innate immune system through the rapid response and recognition of the unique and conserved

microbial components, the microbial-associated molecular patterns (MAMPs) (Kumar *et al.*, 2011, Chu and Mazmanian, 2013) In general, the detection of bacteria or its components results in the ligands binding of TLRs and/or NLRs. And triggers a cascade of events that activates signaling molecules such as nuclear factor-κB (NF-κB), resulting in the expression of proinflammatory cytokines, chemokines, and antimicrobial peptides. The result is the eradication of any invading microbes. The enormous bacterial populations and proximity of epithelial PRRs presents the paradox of how gut epithelia avoid continuous activation of inflammatory responses to resident symbiotic bacteria. ‘‘Physiological inflammation’’ where the intestine is at a constant state of low-grade inflammation has been identified to constitute part of the intestine mucosal barrier (Fiocchi, 2008). However, aberrant commensal-mediated signaling of PRRs can lead to the stimulation of diverse inflammatory responses that may result in “pathological inflammation” (Fiocchi, 2008).

Paneth cells also participate to this response by sensing luminal bacteria release a host of AMPs, including defensins, cryptidines, and lysozymes, forming a biochemical barrier that limit bacterial access to and penetration into the gut epithelial surfaces (Gersemann *et al.*, 2008, Duerkop *et al.*, 2009). These AMPs disrupt highly conserved and essential features of bacterial biology, such as surface membranes, which are targeted by pore-forming defensins and cathelicidins, and Gram-positive cell wall peptidoglycans, which are targeted by C-type lectins (Gallo and Hooper, 2012, Mukherjee *et al.*, 2014). Paneth cells deficient mice exhibit an enhanced translocation of bacteria into the host tissues (Vaishnava *et al.*, 2008). It also illustrates the ability of epithelial cells to monitor the total bacterial census, thereby activating antimicrobial responses that are density-dependent. This in turn allows epithelial cells to directly control ‘‘surface-associated’’ bacterial populations without disrupting the luminal microbiota that are crucial for host metabolic health.

Goblet cells can not only produce the mucin glycoproteins to form a physical barrier, but also producing factors like trefoil factor 3 (TFF3) and the resistin-like molecule-β

(RELMβ) that can further stabilize and regulate this physical barrier of intestine. TFF3 stabilizes structural integrity to mucus through mucin crosslinking and act as a signal that promotes epithelial repair, migration of IECs and resistance to apoptosis (Dignass *et al.*, 1994, Taupin *et al.*, 2000). RELMβ works by promoting MUC2 secretion, regulate macrophage and adaptive T cell responses during inflammation and, in the case of nematode infection, directly inhibit parasite chemotaxis (Artis *et al.*, 2004, Nair *et al.*, 2008). Study showed that goblet cells dysfunction is an epithelial-autonomous defect in the cystic fibrosis intestine that could be responsible of intestinal manifestations of obstruction and inflammation (Liu *et al.*, 2015a).

Enteroendocrine cells help the linkage between the central and enteric neuroendocrine systems by secreting numerous hormones and other signal molecules of digestive function (Peterson and Artis, 2014). The cells are involved in the efficient absorption of food and participate in sensing hunger and thirst.

The epithelial cells are tightly joined with junctional complexes. The perfect communication between cells to assume role of barrier is essential and possible by establishment of many junctional complexes.

1.2.1.4 Junctional complexes between epithelial cells

Junctional complexes are symmetrical structures between the epithelial cells. There are three different junctional complexes: from the luminal side to the basolateral side of the epithelial cell layer, there is firstly, tight junction (TJ) where claudin, occludin, zonula occluden (ZO), junctional adhesion molecule (JAM) and F-actin interact; secondly, adherens junction (AJ) where E-cadherin, α-catenin 1 and β-catenin interact; and thirdly, desmosomes where the interaction is between desmoglein, desmocollin, desmoplakin and keratin filaments (Figure 5) (Turner, 2009, Pavelka *et al.*, 2010).

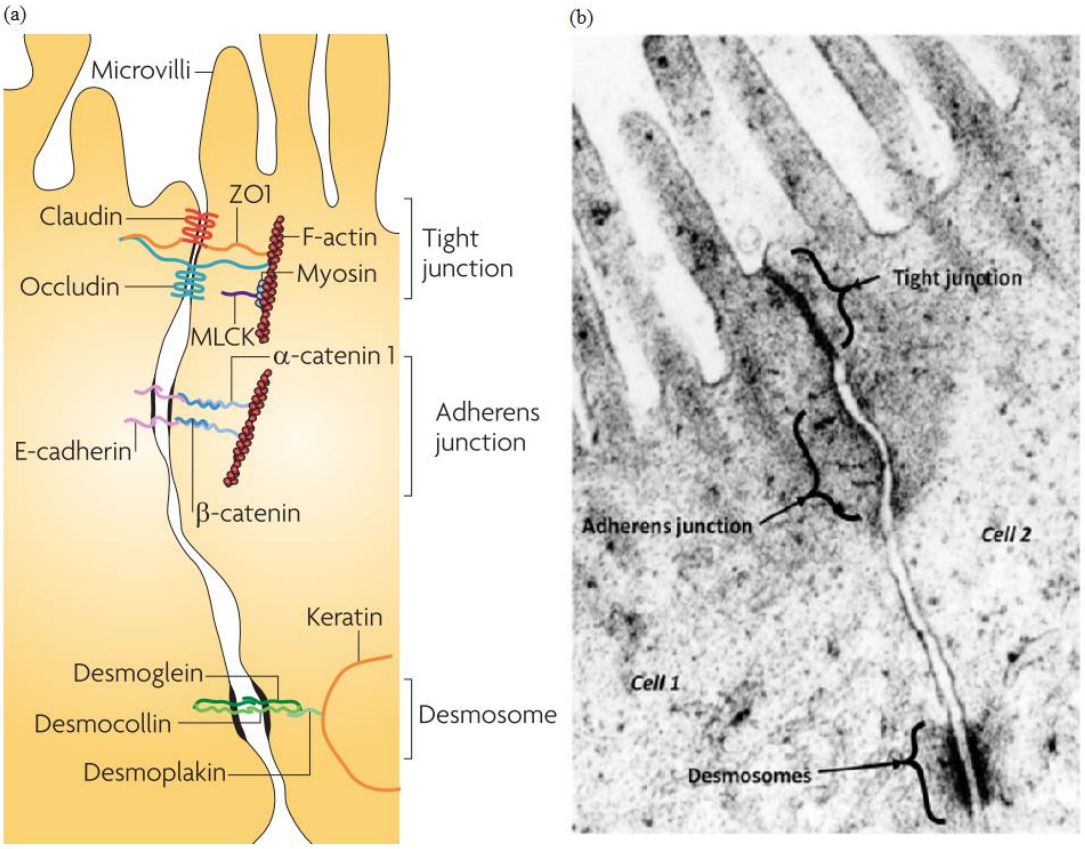

Figure 5 The junctional complexes (a)The junctional complexes, comprised of tight junctions, adherens junctions, gap junctions, and desmosomes.(Turner, 2009) (b) Electron micrograph of apical junctional complex between two intestinal epithelial cells of human ileal mucosa.(Salim and Soderholm, 2011)

1.2.1.4.1 Tight junction: the first line of defense

As the apical member of the junctional complexes, the TJ forms a continuous, circumferential, belt-like structure at the luminal end of the intercellular space (Schneeberger and Lynch, 2004). Thanks to the development of electron microscopy in the 1960's, the TJ biology evolution emerged. In the morphology study, these so-called "kissing point" in TJ are different from AJ and desmosomes, where the adjacent cell membranes remain 15-20 nm apart (Tsukita *et al.*, 2001). TJ is a multiple protein complex which consist of three integral transmembrane proteins (occludins, claudins, junctional adhesion molecules (JAM)) associated with the cytoplasmic proteins (Groschwitz and Hogan, 2009). The intracellular domains of these transmembrane proteins interact with cytosolic scaffold proteins, such as ZO proteins, which in turn

anchor the transmembrane proteins to the actin (F-actin) cytoskeleton (Figure 6).

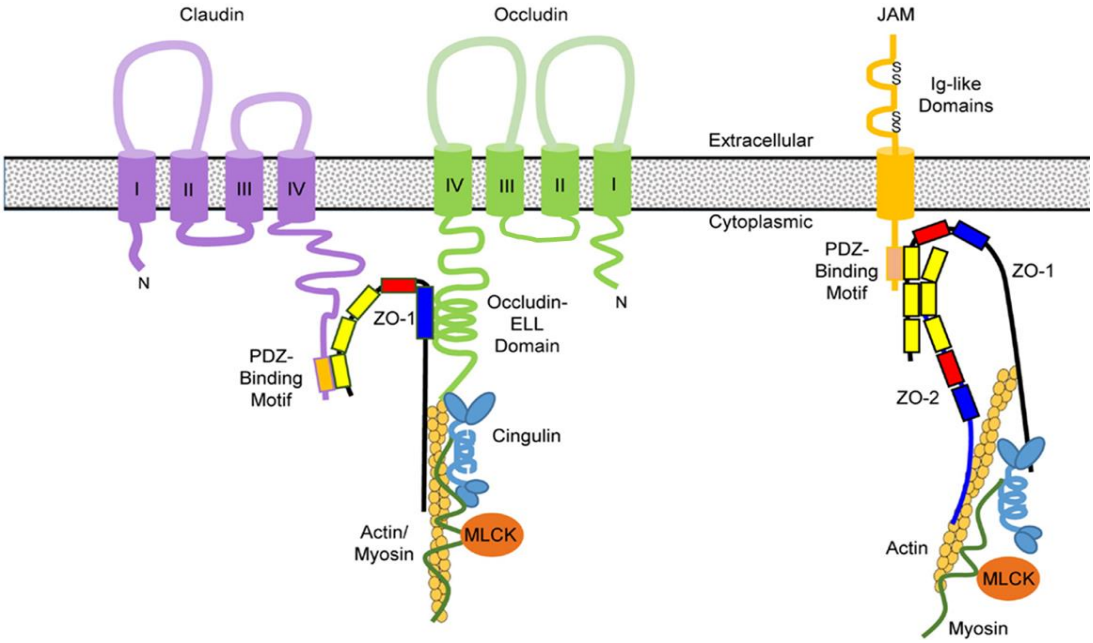

Figure 6 Molecular structures of TJ proteins and their interaction (Robinson et al., 2014).

1.2.1.4.1.1 Occludin

Occludin is a tetraspan membrane protein with a molecule weight around 60~82 kDa. It forms two extracellular loops, one intracellular loop, a short cytoplasmic N-terminus and a long cytoplasmic C-terminus project into the intracellular compartment (Figure 6) (Harhaj and Antonetti, 2004, Hartsock and Nelson, 2008). The long C-terminal domain of occludin interacts with several intracellular TJ proteins, such as ZO proteins, which are requested to link occludin to the actin cytoskelet (Figure 5) (Furuse *et al.*, 1994, Li *et al.*, 2005a). Investigations have also confirmed roles for the extracellular loops and at least one transmembrane domain in occludin localization and TJ stability by expressing mutant and chimeric occludin that exert a dominant negative effect on paracellular permeability. (Balda *et al.*, 2000). Numerous studies showed that occludin has crucial roles in the maintenance and assembly of TJ structure (Al-Sadi *et al.*, 2011). Study showed that knockdown of occludin in *in vitro* (filter-grown Caco-2 monolayers) and *in vivo* (recycling perfusion of mouse intestine) intestinal epithelial models induces an increase in paracellular permeability to macromolecules (Al-Sadi *et al.*, 2011). In the intact epithelium, occludin is highly phosphorylated on the serine (Ser) and

threonine (Thr) residues (Sakakibara *et al.*, 1997). Dynamic phosphorylation of occludin seems to play an important role in the assembly and disassembly of tight junctions. The phosphorylation rate of occludin depends of Protein kinase Cs (PKCs) and Ser/Thr phosphatase. (Seth *et al.*, 2007, Jain *et al.*, 2011). PKCη plays an important role in occludin phosphorylation and assembly of tight junctions (Suzuki *et al.*, 2009). PKCζ directly interacts with the C-terminal domain of occludin and phosphorylates it on specific Thr residues, which help assembly into tight junctions (Jain *et al.*, 2011). Disruption of tight junctions by calcium depletion (Seth *et al.*, 2007), phorbol ester (Clarke *et al.*, 2000) and pathogens (Simonovic *et al.*, 2001) results in dephosphorylation of occludin on Ser/Thr residues. Protein Ser/Thr phosphatases, PP2A and PP1, are involved in occludin dephosphorylation and destabilization of tight junctions (Seth *et al.*, 2007).

1.2.1.4.1.2 Claudins

Claudins, similar with occcludin, are tetraspan integral membrane proteins with a molecular weight 20~27 kDa. They have four hydrophobic transmembrane domains, two extracellular loops, a short intracellular loop and N- and C-terminal cytoplasmic domains (Figure 6) (Turksen and Troy, 2004, Van Itallie and Anderson, 2006, Lee, 2015). The extracellular loops are critical for TJ protein-protein interactions and the formation of ion-selective channels (Van Itallie and Anderson, 2006). The intracellular C-terminal domain is involved in anchoring claudin to the cytoskeleton via interactions with cytosolic scaffold proteins, including ZO-1, and ZO-2 and -3 (less investigated) (Itoh *et al.*, 1999, Morita *et al.*, 1999). Twenty four members of claudin family have been identified (Mitic and Van Itallie, 2001, Tsukita *et al.*, 2001). As occludin, some claudin isoforms are phosphorylated in the cells, which is associated with localization and paracellular permeability (D'Souza *et al.*, 2005, D'souza *et al.*, 2007). Claudin-1 knockout mice die within 24 hours of birth because of a dramatic loss of fluid and electrolytes through the impaired epidermal barrier. Therefore, Claudins play a very important role in the barrier formation and paracellular permeable selectivity in various

tissues (Tamura *et al.*, 2011).

1.2.1.4.1.3 Junctional Adhesion Molecules

The junctional adhesion molecules (JAMs) family is integral membrane protein which belongs to the immunoglobulin (Ig) superfamily and is characterized by 2 extracellular Ig-like domains, one transmembrane domain, and one intracellular C-terminal domain (Figure 6) (Cunningham *et al.*, 2000). They are subdivided in two classes based on the expression of Type I or II binding motifs in the intracellular C-terminus, which suggests that the two types interact with specific scaffolding and cytoplasmic proteins (Ebnet *et al.*, 2004). JAM-1, -2 and -3 have Type II binding motifs, while the atypical JAMs, including JAM-4, coxsackie and adenovirus receptor (CAR) and endothelial selective adhesion molecule (ESAM) contain Type I binding motifs (Ebnet *et al.*, 2004, Ebnet, 2008). Homophilic JAM-1 or -2 interactions regulate the formation of functional TJs and cell-cell border formation (Bazzoni *et al.*, 2000, Babinska *et al.*, 2002), while heterophilic JAM interactions play a role in leukocyte-endothelial cell adhesion (Bazzoni, 2003). The extracellular N-terminal domains of the JAM family members bind to multiple ligands through homophilic and heterophilic interactions which are proposed to regulate the cellular functions and paracellular permeability of JAMs (Bazzoni, 2003, Ebnet *et al.*, 2004).

In intestinal epithelial cells, JAM-1 and JAM-4 are expressed and associated with TJ regulation. *In vitro* and *in vivo* studies indicate that JAM-1 is important in the maintenance of the TJ barrier. Treatment of intestinal epithelial cells with monoclonal JAM-1 antibodies inhibited the resealing of the TJs, as indicated by delays in transepithelial electrical resistance (TEER) recovery and occludin assembly (Liu *et al.*, 2000). JAM-1 knockout mice show a higher permeability to dextran and an increase of myeloperoxidase activity (an inflammation marker) in the colon compared to wild type mice. In addition, the colonic injury and inflammation induced by dextran sodium sulfate are more severe in the JAM-1 knockout mice than in wild type mice (Laukoetter *et al.*, 2007). Furthermore, the colonic mucosa of JAM-1 deficient mice shows

increased paracellular permeability, leukocyte infiltration and lymphoid aggregates, and, consequently, these mice are more susceptible to experimentally induced colitis (Luissint *et al.*, 2014)

1.2.1.4.1.4 Zonula Occludens

ZO proteins contain multiple domains that bind a diverse set of junction proteins. To date, three ZO proteins, ZO-1, -2, and -3, have been identified (Haskins *et al.*, 1998). These multi-domain proteins carry three post-synaptic density 95/Drosophila disc large/zona-occludens (PDZ) domains, a Src homology-3 (SH-3) domain and a region of homology to guanylate kinase (GUK) from the side of the N-terminus (Figure 7) (Lee, 2015). Unlike occludins and claudins which are integral membrane proteins that form inter cellular homophilic and heterophilic adhesions, ZO proteins are cytoplasmic proteins that form a scaffold between the transmembrane proteins and the actin cytoskeleton (McNeil *et al.*, 2006).

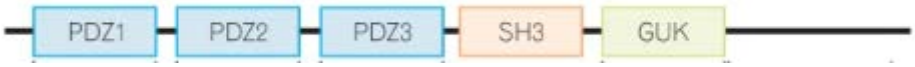

Figure 7. The multiple domains of ZO proteins. PDZ: large/zona-occludens domains, SH-3:a Src homology-3 domain; GUK: a region of homology to guanylate kinase.

Interestingly, many TJ proteins bind to the N-terminal half region of ZO proteins, while the C-terminal region interacts with the actin cytoskeleton and cytoskeleton-associated proteins (Fanning *et al.*, 2002). Among the ZO protein, the functions of ZO-1 was better investigated compared with ZO-2 and -3. Investigators demonstrate that gene silencing of ZO-1 causes a delay of ~3 h in tight junction formation in Madin-Darby canine kidney (MDCK) epithelial cells, but mature junctions seem functionally normal even in the continuing absence of ZO-1 (McNeil *et al.*, 2006). Therefore, ZO-1 plays a vital role in the regulation of TJ assembly.

ZO-2 was demonstrated to serve as a simple structural component of the "cytoplasmic plaque" which is involved in TJ assembly and function (Traweger *et al.*, 2013). Protein kinases, signaling molecules and other regulatory proteins including cytokines which directly or indirectly target ZO-2 complete the dynamic network of the ZO-2 scaffold.

These lead to phosphorylation of ZO-1 and ZO-2 resulting in disruption of TJs and an increase in paracellular permeability (Sabath *et al.*, 2008). ZO-1 and ZO-2 play pivotal roles in the final establishment of the TJs with paracellular barrier function, thereby providing the general basis for selective paracellular permeability in epithelial and endothelial cells (Tsukita *et al.*, 2009).

The importance of ZO-1 and ZO-2 was proved by respective knockout mice embryonic lethality (Katsuno *et al.*, 2008, Xu *et al.*, 2008). In contrast, ZO-3 seems to be not as important as them. Although ZO-3 exhibited a prominent localization and was specifically expressed in epithelial-type cells ZO-3 knockout mice showed no phenotypes, suggesting that ZO-3 was not essential *in vivo* (Adachi *et al.*, 2006, Xu *et al.*, 2008). In addition, ZO-3 could not target junctional areas by itself and required the preexistence of ZO-1 and/or ZO-2 (Tsukita *et al.*, 2009).

1.2.1.4.2 Adherens junction and desmosomes

AJ is immediately subjacent to the TJ and consists of the transmembrane protein E-cadherin, and intracellular components, include β-catenin and α-catenin (Figure 5 and 8). It occurs at points of cell-cell contact in a belt-like way and formed by cadherin-catenin interactions which is called cadherin-catenin complex (Figure 8) (Hoffman and Yap, 2015). Localisation of cadherins to the plasma membrane is regulated by p120-catenin. Mechanical linkages between cadherin and actin are mediated by α-and β-catenin(Hoffman and Yap, 2015). AJ provides a strong mechanical attachment between adjacent cells. Classical cadherins, such as E-cadherin, are the major transmembrane protein of the AJ and initiate intercellular contacts through trans-pairing between cadherins on opposing cells (Mehta *et al.*, 2015). One of the main function of AJ is to provide the dynamic adhesive connection between epithelial cells. Classical cadherins bind directly and indirectly to many cytoplasmic proteins. particularly members of the catenin family (α-catenin and β-catenin). This binding locally regulates the organization of the actin cytoskeleton, cadherin stability. Another function is involved in intracellular signaling pathways that control gene transcription (Perez-Moreno and Fuchs, 2006). AJ

is necessary for the TJ assembly. Cadherin-catenin complexes are important not only for linking adjacent cells, but also for maintaining cell polarity, regulating epithelial migration and proliferation and the formation of other adhesive complexes such as desmosomes (Perez-Moreno *et al.*, 2003, Ebnet, 2008). As a consequence, loss of AJ results in disruption of cell–cell and cell-matrix contacts, ineffective epithelial cell polarization and differentiation, and premature apoptosis (Hermiston and Gordon, 1995).

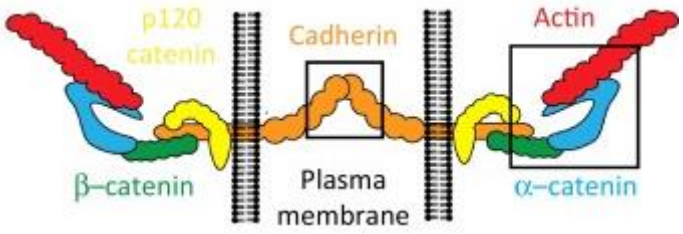

Figure 8 AJ belt-like connection structure formed by cadherin-catenin complex (Hoffman and Yap, 2015)

Desmosome is an adhesive junction that holds two adjacent epithelial cells together. Desmosome has similar structure with AJ but is like a button instead of a belt (Figure 9) (Alberts *et al.*, 2002). It consists of transmembrane linker glycoproteins (e.g. demosgleins and desmocollins - which are cadherin proteins) attached to desmosomal plaque linked by desmoplakin with the intermediate filaments (called keratin in epithelial cells) cytoskeleton (Figure 5 and 9). There are three major gene families encoding desmosomal proteins. The first one is desmosomal cadherins, comprising two subtypes called desmogleins and desmocollins. They are a subfamily of the cadherin superfamily that mediate calcium-dependent cell–cell adhesion (Thomason *et al.*, 2010, Saito *et al.*, 2012). Emerging evidence suggests important roles of desmosomal cadherins for these expression patterns in driving epithelial patterning and differentiation (Thomason *et al.*, 2010, Saito *et al.*, 2012). The second major gene family is armadillo family proteins which represent cadherin binding partners. They play important roles in tissue integrity and cell signaling. Two types of armadillo proteins are present in desmosomal plaque represent cadherin binding partners

(Hatzfeld, 2007, Carnahan *et al.*, 2010). They are plakoglobin and plakophilins which play important roles in tissue integrity and cell signaling(Kowalczyk and Green, 2013). The third major gene family encoding desmosomal proteins is the plakin family (Sonnenberg and Liem, 2007). Among its members, desmoplakin is an obligate desmosomal protein that couples intermediate filaments to the desmosomal plaque (Bornslaeger *et al.*, 1996, Gallicano *et al.*, 1998).

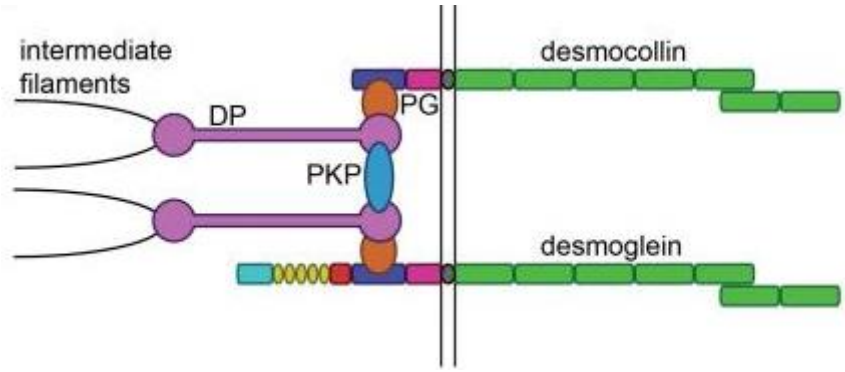

Figure 9 Molecular components and model of desmosomal protein organization (Kowalczyk and Green, 2013); DP: desmoplakin, PG: plakoglobin, PKP: plakophilins.

AJ, along with desmosome, provide the strong adhesive bonds that maintain cellular proximity and are also a site of intercellular communication.

1.2.1.5 Subepithelial immune cells

Intrinsic immune system which exists in intestinal tract is to ensure the selective absorption of nutrients and fluids, the prevention of commensals translocation and pathogenic microorganisms across this barrier. Figure 10 showed the different role of immune cells in intestine. Most scattered intestinal immune cells and tissue-specific organized lymphoid structures, such as Peyer's patches (PPs), cryptopatches and isolated lymphoid follicles (ILFs), are located just below the epithelial layer in the lamina propria (LP). The intestinal immune system also consist of intraepithelial effector lymphocytes interspersed in the epithelial lining and extra-intestinal outposts, such as the mesenteric lymph nodes (mLNs) (Tomasello and Bedoui, 2013). Although effector T and B lymphocytes provide the host with potent, adaptive immune responses against the vast numbers of antigens that are continuously encountered (Maynard *et al.*,

2012), the intestinal immune system relies to mainly on innate immune cells and their rapid effector functions to maintain intestinal homeostasis.

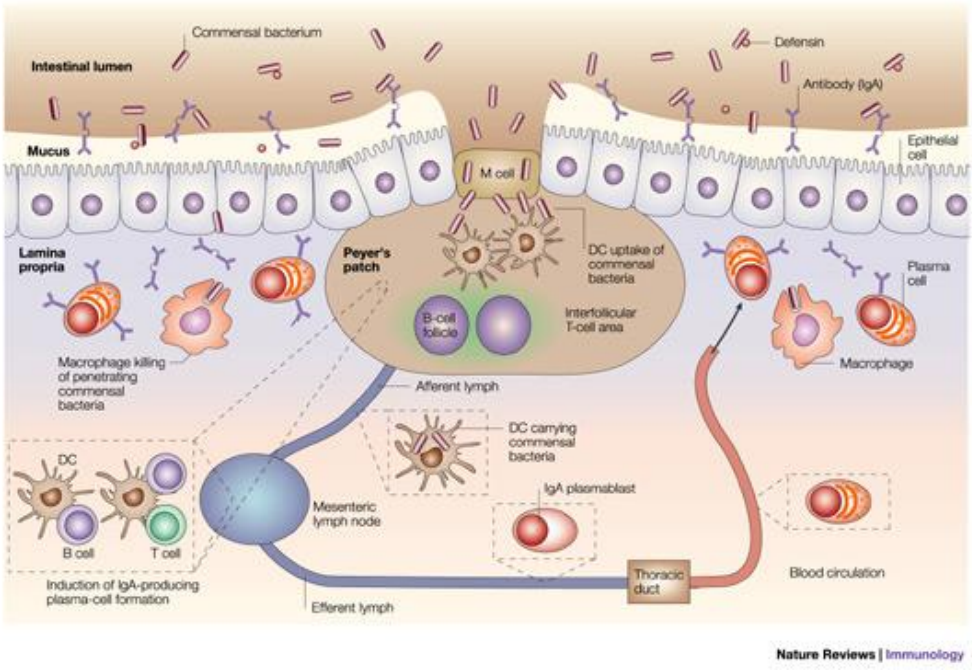

Figure 10 Key feature of intestinal immune system (Macpherson and Harris, 2004)

Bacteria that cross the enterocyte epithelial layer and invade the intestinal mucosa are rapidly killed by the macrophages in the LP (Macpherson and Harris, 2004). The others which penetrate through the PPs are not only rapidly killed by macrophages, but also transported to underlying immune cells. The PPs are the major immune inductive sites for the intestinal mucosal immune responses (Salim and Soderholm, 2011). PPs, found mostly at the distal ileum, consist of aggregated lymphoid follicles. PPs can be considered as the immune sensors of the intestine because of their ability to detect process and present luminal antigens to other immune cells. **Microfolds cells (M Cells)** in the FAE firstly transport macromolecules and microorganisms through endocytosis, and delivers them to underlying immune cells. Antigen-presenting cells and lymphocyte continuously pick up them. Among the subsets of antigen-presenting cells, **dendritic cells (DCs)** serve as the key sentinels that can mount appropriate responses, determining whether to ignore or react to the transported foreign antigens (Salim and Soderholm, 2011). The presence of either pathogenic bacteria or disruption of the

epithelial-cell barrier results in activation and migration of DCs to the mesenteric lymph nodes, where they activate naive T cells. Finally, the T cells undergo differentiation under the influence of factors released by DCs and other stromal elements (Cho, 2008). The only aim of the subepithelial immune system is to maintain intestinal homeostasis. The net effect is to eradicate the unwanted foreign antigens by releasing corresponding cytokines, chemokines and the recruitment of innate immune cells.

1.2.2 Epithelial passage routes

Molecules pass through the intestinal epithelial monolayer either through the cells via the transcellular pathway, or between the cells through the paracellular pathway (Figure 11). The transcellular pathway is active or passive movement across cell membranes, usually involves in specific transport channels. The paracellular pathway is a passive movement through the space between adjacent cells. Low molecular weight molecules (≤ 600 Da *in vivo*; ≤ 10 kDa *in vitro* in the cell lines), such as small ions and water pass TJ in the paracellular route, while larger macromolecules such as protein pass through the epithelial cells via the transcellular route (Watson *et al.*, 2001, Krug *et al.*, 2009).

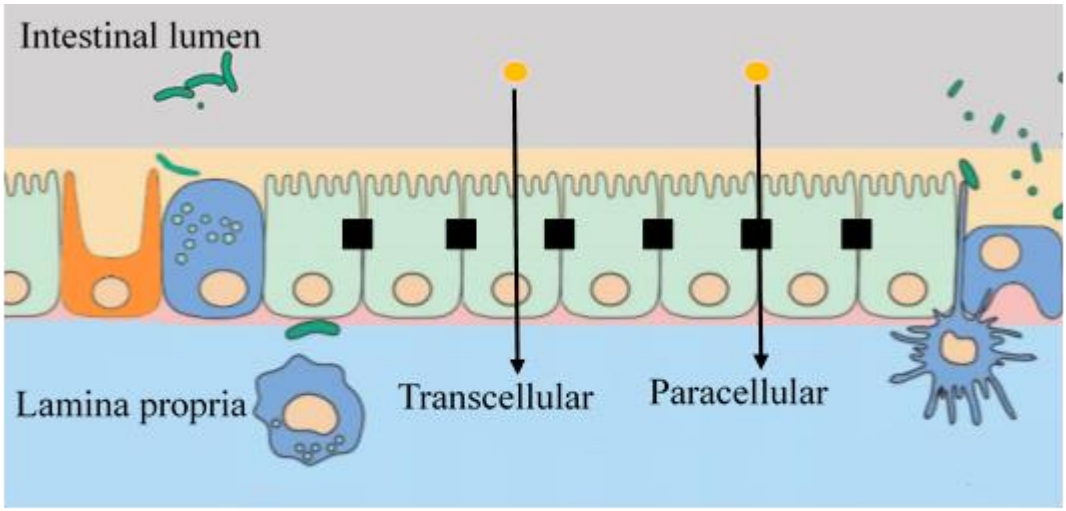

Figure 11 Epithelial pathway route: transcellular pathway and paracellular pathway.

1.2.2.1 Transcellular pathway

Transcellular pathway allows macromolecules transporting from intestinal lumen into subepithelial compartment. Epithelial cells take up luminal contents non-selectively

through phagocytosis or pinocytosis, or selectively through receptor-mediated endocytosis (Figure 12). Non-selective phagocytosis, mostly utilized by M cells, transport luminal contents such as bacterial antigens to the underlying basement membrane. (Owen *et al.*, 1986, Conner and Schmid, 2003). The initial process of both pinocytosis and receptor-mediated endocytosis involves the formation of clathrin-coated pits. Most of the contents in the vesicles of nonselective pinocytosis fuse with lysosomes and undergo degradation, although low amounts of intact proteins escape degradation and are transcytosed to the basolateral compartment (Hewlett *et al.*, 1994). Fluid-phase macromolecular transport normally mediates the uptake of nutrients and soluble protein antigens. Receptor-mediated endocytosis is a highly specific process that involves the binding of ligands to their specific receptor. Internalized antigens bound to receptors either undergo the degradation or are directed to the underlying basement membrane and into the lamina propria (Schwartz, 1995, Mukherjee *et al.*, 1997).

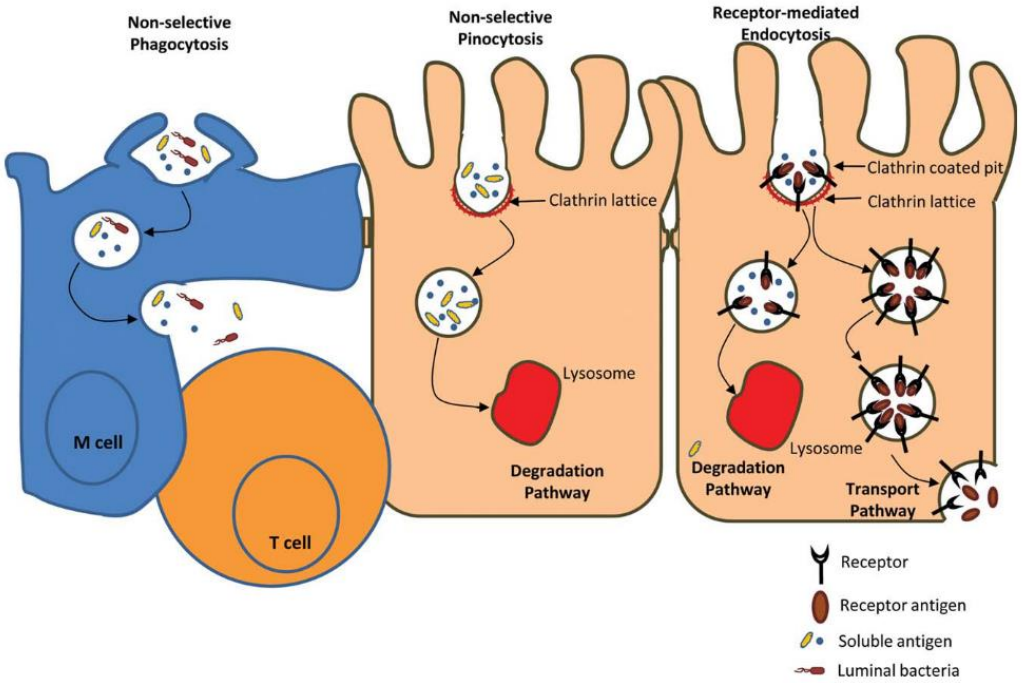

Figure 12 Transcellular pathway: non-selective phagocytosis, non-selective pinocytosis and receptor-mediated endocytosis (Salim and Soderholm, 2011)

1.2.2.2 Paracellular pathway

Paracellular route across the epithelial barrier is highly regulated and allow the access not only to small molecules such as Ca^{2+} and Mg^{2+} through the "pore pathway" but also to larger molecules, including small peptides and bacterial lipopolysaccharides through the "leak pathway" in an intact intestinal barrier.

Pore pathway is a high-capacity, size- and charge-selective paracellular route that permeable to molecules with radii of ~4 Å or less (Shen *et al.*, 2011). Claudins expression change is responsible for the ion selectivity and modulation of pore pathway permeability. This pathway can be regulated by interactions among claudin proteins to form pores, interactions between specific claudins and other tight junction proteins, which finally regulate pore opening and closing events (Shen *et al.*, 2011). IL-4, IL-6, IL-9 and IL-13 have been reported to activate pore pathway by inducing increases in claudin-2 expression, which finally enhance the intestinal permeability (Shen *et al.*, 2011, Odenwald and Turner, 2017). Some bacterial pathogens, such as *Clostridium perfringens* enterotoxin, binding to specific claudins (claudins-3 and -4, here) can also lead to a disruption of intestinal barrier (Saitoh *et al.*, 2015).

Leak pathway is a low-capacity, paracellular route that does not discriminate between solutes and allows limited flux of large molecules. Leak pathway is regulated by ZO-1, occludin and myosin light chain kinase (MLCK) (Shen *et al.*, 2011, Odenwald and Turner, 2017). The width of the lateral space below the TJ is around 75 Å, being wider in comparison to 4–9 Å for the TJ pores in villi or 50–60 Å for the TJ pores in crypts (Ćirković Veličković and Gavrović-Jankulović, 2014). The main rate-limiting factor for paracellular transport pathway is the junctional complex between epithelial cells as mentioned above. Leak pathway flux of Madin-Darby canine kidney (MDCK) cells monolayer was increased after ZO-1 knockdown (Van Itallie *et al.*, 2009). MDCK cells lacking ZO-1 also showed increased sensitivity to barrier disruption induced by actin depolymerization, extracellular Ca^{2+} chelation, or myosin II motor inhibition (Van Itallie *et al.*, 2009). Occluding internalization induced by TNF diminished intestinal

barrier function trough activate leak pathway (Marchiando *et al.*, 2010). ZO-1 and occludin, but not claudins, are redistributed following MLCK activation in cultured monolayers as well as after immune activation *in vivo* (Van Itallie *et al.*, 2009).

Although the leak and pore pathways are separable across the paracellular barrier, the two pathways are often affected in parallel. For example, MLCK-dependent increases in intestinal epithelial leak pathway permeability are also able to induce mucosal IL-13 production, which, in turn, increases claudin-2 expression and pore pathway permeability (Weber *et al.*, 2010). During homeostasis and less active inflammatory disease, the intestinal barrier is generally intact and barrier function primarily reflects flux across the paracellular pore and leak pathways (Odenwald and Turner, 2017).

At sites of intestinal mucosa damage in active diseases, such as erosions and ulcers, luminal contents cross the intestinal barrier through a third pathway, named as **"unrestricted pathway"** (Odenwald and Turner, 2017). In these cases, tight junctions are lost and therefore cannot contribute to local barrier function. Therefore, the unrestricted pathway is high-capacity and nonselective with respect to solute size and charge (Odenwald and Turner, 2017). Large proteins and even whole bacteria can cross the unrestricted pathway, which partially explains the severe disease initiated by intestinal mucosa damage. Nonsteroidal anti-inflammatory drug (NSAID) treatment lead to epithelial damage by increasing flux across the unrestricted pathway, which probably provokes colitis in IL10$^{-/-}$ mice (Berg *et al.*, 2002).

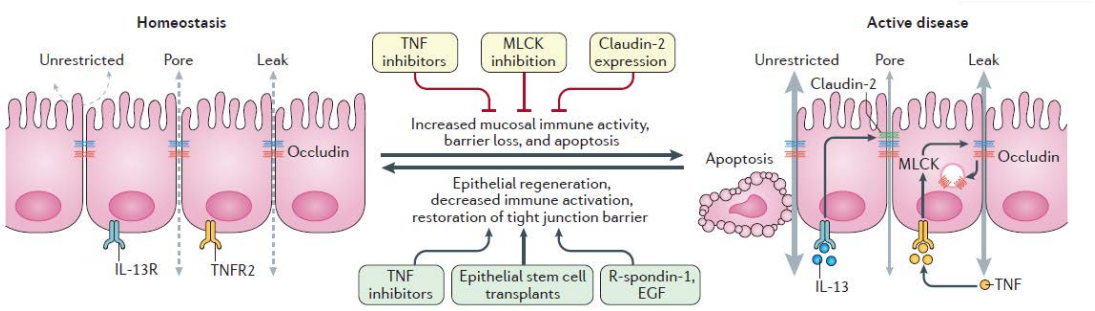

Figure 13. Three distinct paracellular epithelial permeability pathways in homeostasis and active disease state (Odenwald and Turner, 2017). EGF: epidermal growth factor; IL-13R:

IL-13 receptor; TNFR2: TNF receptor 2

During homeostasis (Figure 13, left) there is little underlying mucosal immune activity and the leak and pore pathways, modulated by tight junctions (such as ZO-1, occludin and claudin-2), define intestinal permeability. Cellular membranes seal the 'unrestricted' pathway in an intact intestinal barrier, which is independent of tight junctions. During disease pathogenesis (Figure 13, right), increased mucosal immune activation leads to TNF and IL-13 production, which can result in enhanced permeability across the leak and pore pathways, respectively. TNF increases leak pathway permeability by both increasing myosin light chain kinase (MLCK) transcription and activity at the tight junction and leading to occluding internalization. IL-13-dependent claudin-2 upregulation increased pore pathway permeability. As inflammatory disease progresses, epithelial cells apoptosis occurs and causes unrestricted pathway permeability across the high-capacity, charge and size-nonselective molecules. But this pathway is reversible. After removal of inflammatory stimuli, the unrestricted pathway can be sealed by epithelial cells regeneration and tight junctions between them (Odenwald and Turner, 2017). Multiple therapeutic strategies targeting the intestinal barrier have been proposed (Figure 13, center). These strategies aim to either inhibit initiation and progression of disease by immunosuppression or inhibition of barrier loss dependent on tight junctions, or by restoration of intestinal barriers after disease onset by inhibiting inflammation or promoting epithelial cells regeneration (Odenwald and Turner, 2017).

1.2.3 Intestinal permeability measurement

The concept of intestinal permeability is defined as a functional feature of the intestinal barrier at given sites, measurable by analyzing flux rates across the intestinal barrier as a whole or across barrier components of defined molecules that are largely inert during the process (Bischoff *et al.*, 2014). And it can be adequately measured in different settings (*in vitro*, *ex vivo* or *in vivo*). Intestinal permeability tests give researchers valuable information about the status of epithelial barrier integrity, the effectiveness of

barrier-targeting therapeutics, and the pathophysiology of diseases (Galipeau and Verdu, 2016).

1.2.3.1 *In vivo* functional test

The gold standard for functional measurements of intestinal permeability in humans is the test of urinary excretion of the two orally administered non-metabolized sugars (lactulose and mannitol) over a 6 h period. The intestinal permeability is expressed by lactulose/mannitol ratio. Both lactulose and mannitol are paracellular marker, whereas mannitol permeability is independent of intestinal barrier damage or dysfunction. By expressing lactulose excretion as a percentage of mannitol excretion, it is possible to correct for variables unrelated to intestinal permeability (Ziegler *et al.*, 1988). Apart from oral gavage of sugars, fluorescently labeled dextrans, PEG, or ^{51}Cr-EDTA followed by detection in the urine or blood are commonly used methods in animal studies.

In conclusion, both advantages and disadvantages exist in the *in vivo* functional test. The advantage of these tests is non-invasive real-life setting where the host-microbe interactions can be taken into account and it can be conducted in clinic permeability study. However, the drawbacks are time-consuming, existences of several confounding factors which can hamper interpretation of results, such as big individual differences in motility, intestinal cell surface, epithelial cell integrity, renal function, bacterial degradation, gastric dilution, and diet, and no standardized protocols (Quigley, 2016). Even though, the *in vivo* functional test is still very useful in the applications because it can reflect the reality and complexity of process which cannot be replaced by *ex vivo* and *in vitro* testes.

1.2.3.2 *Ex vivo* functional test

Ussing Chamber is usually used in *ex vivo* functional test of intestinal permeability. The system mimics the compartmentalization between the lumen of the intestine and the mucosal part of the intestine *in vivo*. It can be separated by intestine segment into two

compartments (equal volume): a donor compartment (also referred to as the apical, mucosal or luminal-side membrane) and an acceptor compartment (also referred to as the basolateral, serosal, nutrient, or mucosal-side membrane) (Figure 14).

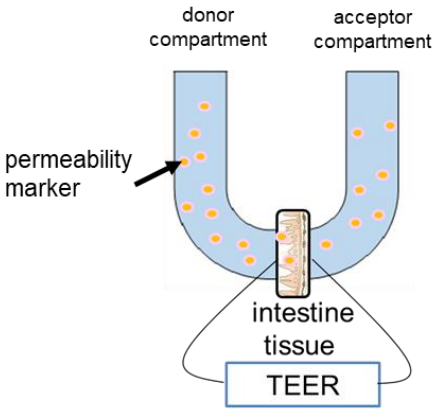

Figure 14 Ussing Chamber system

The permeability is assayed by the ability of markers to cross the intestine tissue and to accumulate in the acceptor compartment. Different permeability markers, such as ^{51}Cr-EDTA, mannitol, sodium fluorescein (paracellular), horseradish peroxidase (HRP) and propranolol (transcellular), can be deposited in donor compartment and harvested in acceptor compartment to measure the intestinal permeability. At the same time, electrodes are used to measure the potential difference across the membrane, and determine the short circuit current, which reflects active ion transport taking place across the membrane. From this, transepithelial electrical resistance (TEER) can be calculated or it can be immediately measured, which reflects the integrity of the tissue in relation to paracellular permeability (Clarke, 2009).

One of the advantage is the ability to measure the specific region of intestine. The main shortcoming is that the study is limited in time because the viability of *ex vivo* tissue limited in usually 2 h. Furthermore, it may not reflect the complexity of process that occurs *in vivo*.

1.2.3.3 *In vitro* functional test

For *in vitro* permeability study, cultured cells monolayer and parallel artificial membrane permeability assay (PAMPA) are wildly used.

Cultured cells monolayer offers a reductionist approach, where differentiated intestinal epithelial cells such as Caco-2, T-84, and HT-29 cells, are grown on semipermeable filter supports forming apical and basolateral compartments (Figure 15). This has been especially advantageous for assaying drug delivery systems (Wu *et al.*, 2016) and screening potential drug compounds. The *in vitro* model has been used to rapidly predict a drug candidate's physiochemical characteristics toward cellular permeability, the pathways utilized during transport, and identify potential toxic effect that could disrupt the epithelial barrier (Meunier *et al.*, 1995, Grès *et al.*, 1998, Press and Di Grandi, 2008). TEER and permeability of specific marker can also be measured in this system. It has longer experiment durations (up to 24 h) compared with Ussing Chamber. So it can be applied in the drug absorption in the particles (Wu *et al.*, 2016), which extended the application. But it has the same limitation with Ussing Chamber, which lacks the complexity of process that occurs *in vivo*. It takes longer time, because cells need to be grown on filters up to several weeks before they can be used. Furthermore differences in cell culture conditions can also cause significant differences of permeability results.

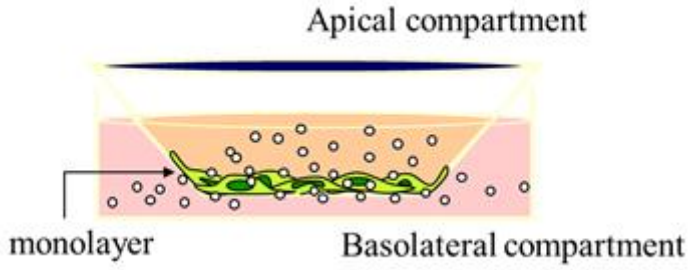

Figure 15 Transwell® system: cell culture monolayer

PAMPA is a static model used to study the passive permeability. This model consists in adding a mixture of phospholipids and organic solvent onto a porous hydrophobic filter support to form a lipid membrane. PAMPA is a high-throughput screening technique, the main limit is that it can study only passive permeability. There are different types of PAMPA models based on the nature of the filter, lipids and transport media used (Billat *et al.*, 2017). Several factors influence PAMPA permeability performance, such

as incubation temperature, pH conditions and lipid membrane composition. Indeed, the lipids in these PAMPA models are mainly commercially available lipids or extracted from natural tissues. Different lipid compositions are now available: PC-PAMPA (phosphatidylcholine-PAMPA), DS-PAMPA (a dodecane solution of lecithin mixture-PAMPA), DOPC-PAMPA [a dodecane solution of highly purified dioleyoylphosphatidylcholine (DOPC)-PAMPA], HDM PAMP (a hexadecane solution of DOPC-PAMPA) and BML-PAMP (a biomimetic lipid membrane based on a mixture of phosphatidylcholine, phosphatidylethanolamine, phosphatidylserine, phosphatidylinositol, cholesterol, 1,7-octadiene membrane-PAMPA (Yu *et al.*, 2015). Moreover, similar with cell models cultivated on the Transwell® system, a filter separates one side containing the test molecule (apical compartment) from a receiver side (initially free of the molecule) (basolateral compartment).

1.3 IBD therapy

As incurable disease, the major aim of the IBD therapy is to induce and maintenance of remission. Current clinical drugs for the treatment of IBD include aminosalicylates, corticosteroids, classic immunosuppressive drugs and anti-TNF agent (Neurath, 2017).

1.3.1 Aminosalicylates

Aminosalicylates (ASA) are a group of drugs containing the active ingredient "5-aminosalicylic acid (5-ASA)" (Sales-Campos *et al.*, 2015). They usually are the first medicines used to treat IBD within several decades. They are widely used to relieve symptoms and reduce inflammation in treatment of mild to moderate UC in active and remission period or mild active CD by oral or topical administration.

The beneficial effect of ASA is known as a scavenger of reactive oxygen metabolites (Ahnfelt-Rønne *et al.*, 1990), inhibition of microphage chemotaxis (Nielsen *et al.*, 1988) and decreasing of different inflammation molecules production such as tumor necrosis factor (TNF)-α effects, interleukin(IL)-1β and nuclear factor (NF)-κB (Mahida *et al.*, 1991, Kaiser *et al.*, 1999). They can also activate peroxisome proliferator activated

receptor-γ which is typically expressed in epithelial and immune cells in the colonic mucosa and is important in the regulation of IBD (Rousseaux *et al.*, 2005, Dubuquoy *et al.*, 2006).

The frequently used class of aminosalicylates as therapeutic agents for IBD are basolazide, mesalamine, olsalazine and sulfasalazine. Even though ASA are well tolerated and safe in most cases, some side effects were presented in different symptoms such as headache, nausea, abdominal pain and cramping, loss of appetite, vomiting, rash, fever, diarrhea and rare kidney injury. Another drawback of this treatment is that lack of responsive is also observed for some patient.

Therefore, ASA represent a good treatment of IBD but the present of significant side effects and poorly responsive patients limit this therapy application.

1.3.2 Corticosteroids

Corticosteroids are known as the most effective drugs at inducing remission in both ulcerative colitis and Crohn's disease but bot suitable in maintaining remission in IBD. They have been used for more than half a century. They are commonly prescribed for treatment of acute exacerbation of IBD. Corticosteroids profoundly work on both immunologic and inflammatory responses. As mentioned in the review (Sands, 2000), for the immunologic part, they can inhibit lots of leukocyte functions, including adherence, chemotaxis and phagocytosis, and interfere with metabolism of arachidonic acid and production of eicosanoids. For the inflammation response part, it can downregulate the production of proinflammation cytokines (e.g., IL-1and IL-6, the chemokine IL-8, the Th1 cytokines IL-2 and IFN-γ, and the Th2 cytokines IL-4 and IL-5).

However, this therapeutic class presents a well-known serious side effects when used daily and long-term or even low-dose. The adverse effects are mostly reported to be related with systemic administration, include sleep disturbance, mood disturbance, acne, striae, hirsutism, adrenal suppression, proximal myopathy, glucose intolerance,

hypertension, narrow angle glaucoma, cataracts, pseudotumor cerebri, infection, edema, impaired wound healing, growth retardation, osteoporosis, and aseptic necrosis (Sands, 2000). Therefore, topical administration is an alternative treatment for corticosteroids. Combined treatment with other agents such as ASA and immunosuppressive drugs are also effective strategy for UC or CD therapy (Mulder *et al.*, 1996, Markowitz *et al.*, 2000, Hartmann and Stein, 2010).

In summary, corticosteroid therapy is one of the best choice for acute exacerbation treatment. But the significant side effects by systemic administration limit the continuous use. To reduce the occurrence of side effects, topical administration and combined treatment present a promising method.

1.3.3 Immunosuppressive drugs

Immunosuppressive drugs are the mainstay in the long-tern treatment of steroid-dependent or steroid-refractory IBD. Several immunosuppressive agents have been successfully used for induction and maintenance treatment in IBD. These include The thiopurine immunosuppressants azathioprine (AZA) and 6-mercaptopurine (6MP), methotrexate (MTX), anti-alpha 4 integrins, and anti-IL-12/23 agent.

AZA and 6MP have been effectively used for induction and maintenance of IBD. The mechanisms of thiopurine are not completely clear. The action has been involved with nucleotide or protein synthesis and lymphocytes proliferation. Patients refractory to AZA treatment is occurred by the fact that half of the patients are intolerant to AZA (Hindorf *et al.*, 2009).

MTX may be prescribed for patients' refractory or intolerant to thiopurine therapy, and is generally preferred for induction and maintenance of remission in CD. The anti-inflammatory properties of MTX is associated with increasing of the extracellular level of adenosine which is caused by the inhibition of some enzymes related to the folate pathway and involved in purine and pyrimidine synthesis (Cronstein *et al.*, 1993). The limitation of MTX is low efficacy during long-term use (Suares *et al.*, 2012).

1.3.4 Anti-TNF agents

Anti-TNF therapy is prescribed as a new therapeutic class with high efficacy, rapid onset of action prolonged effect, and improved tolerance (Sandborn and Hanauer, 1999). A number of different anti-TNF antibodies are available, such as infliximab, adalimumab, certolizumab pegol, and golimumab (Sales-Campos *et al.*, 2015). Anti-TNF antibodies can suppress intestinal inflammation in IBD through several mechanisms (Neurath, 2017): inhibit macrophages to produce proinflammatory cytokines; prevent Paneth cell death from necroptosis; reduce intestinal epithelial cells apoptosis42; regulates T-cell apoptosis; and increase production of tissue inhibitor of matrix metalloproteinases (MMPs) by fibroblasts to mediate tissue injury via preventing activation of MMPs45.

Anti-TNF therapy have shown great efficacy, represent improvement and advance in management of IBD. However, loss of response and side-effects were appeared as well. Over the past 10 years, ~30–50% of patients with IBD do not respond to anti-TNF therapy (Neurath, 2017). These side effects include infection, other autoimmune phenomena, heart failure, malignancies such as non-melanoma skin cancers, melanoma, leukemia, and lymphoma, which have been previously reported to be associated with biologics (Mariette *et al.*, 2011, McLean and Cross, 2014).

1.3.5 Innovative therapy

As mentioned above, lots of limitations, such as significant side effects, low efficiency and loss of response, exist in current treatment, which indicates the need of new therapies. Modulations of intestinal barrier, gut microbiota, fibrosis and tissue remodeling, macrophage and lymphocyte activation, homing and retention, as well as angiogenesis, are emerging new targets for therapy in clinic trials (Neurath, 2017). Among all the molecules work on these different targets, nitric oxide (NO) is good candidate. Because it can work on several targets involving in new therapies of IBD (Magierowski *et al.*, 2015). Firstly, it can regulate the intestinal barrier integrity by

increasing mucus secretion, tight-junction proteins localization and expression. Secondly, it targets on different immune cells to reduce cytokines and mediators releasing. At last, NO can also target on angiogenesis to increase new vessels formation, which can finally help inflamed intestinal mucosa healing. In a word, NO is a promising candidate for the innovative treatment of IBD.

1.4 Nitric oxide

Nitric oxide (NO) is a free radical that has been involved in a wide range of biochemical reaction to evoke plenty of biological responses. It has been recognized as a powerful relaxing factor derived from the endothelial lining (endothelial derived relaxing factor: EDRF) of blood vessels in response to agonists such as acetylcholine and bradykinin at first place (Furchgott and Zawadzki, 1980, Palmer *et al.*, 1987). However this endogenous messenger molecules plays important roles not only in vascular system but also in neural and immune systems (Ignarro, 2000). NO generated by neurons acts as a neurotransmitter and is implicated with memory formation (Snyder, 1992). NO produced by immune system works as a immunomodulator and intracellular signaling molecule (Thomas *et al.*, 2008). Besides, NO generated by macrophages in response to invading microbes acts as an antimicrobial agent (Fang, 1997). Endogenous NO is synthesized by nitric oxide synthases (NOS) using L-arginine, oxygen and cofactors as substrates (Figure 16).

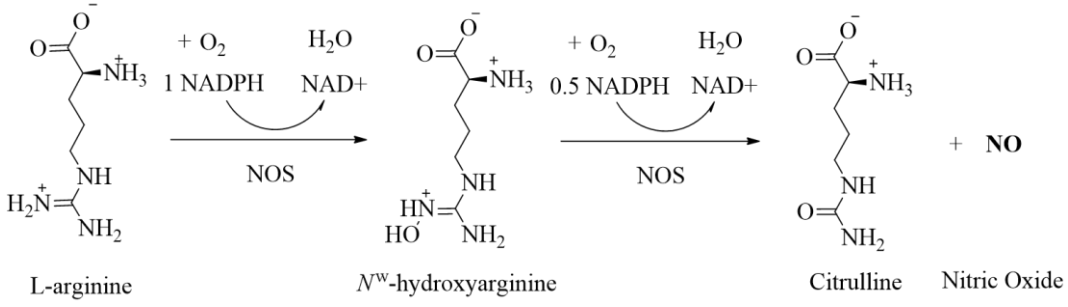

Figure 16 Endogenous synthesis of nitric oxide using L-arginine, oxygen and cofactors as the substrates.

Three isoforms of the enzymes are identified: endothelial (eNOS) and neuronal (nNOS) isozymes are constitutively expressed and regulated to generate relatively small

amounts of NO for signaling, while the inducible isoform (iNOS) is expressed in response to inflammatory mediators leading to high and cytotoxic local concentrations of NO (Knowles and Moncada, 1994). The primary target for low levels of endothelium derived NO is the soluble guanylate cyclase (sGC). Stimulation of sGC by NO coordination to the ferrous prosthetic group of the haem moiety induces the conversion of guanosine-5'-triphosphate (GTP) to cyclic guanosine monophosphate (cGMP), that activates the cGMP-dependent kinase: the protein kinase G (Francis et al., 2010). Over this traditional mechanism, NO is also involved in other cellular signaling pathways including the phospholipase C/calcium signaling systems (Sterin‐Borda et al., 1995), tyrosine kinase signaling pathways (Monteiro et al., 2005), G-protein linked receptors (Garthwaite, 2008), ion channels (Gonzalez et al., 2009), and the apoptotic pathway (Singh and Dikshit, 2007), often at multiple sites in the same pathway. NO presents both beneficial and detrimental biological effects, which tightly dependents on concentration and location (Figure 17).

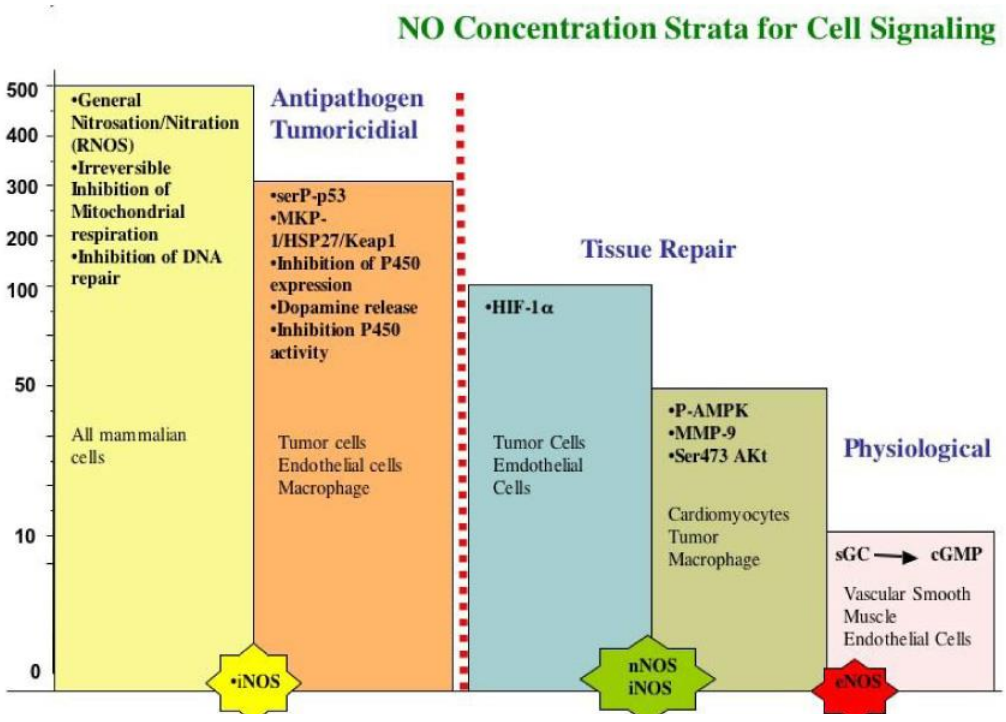

Figure 17 Concentration dependency of NO functions. (Thomas *et al.,* 2006, Thomas *et al.,* 2008)

A burst of research activity was focused on the action of NO in intestinal inflammation in the early 1990s. The paradox role of NO functions in intestinal inflammation became apparent. Inhibition of NO promoted the tissue dysfunction and injury in many inflammation models while NO production inhibition showed beneficial action in other inflammation model. The pathological actions of NO in the gut are always correlated with high expression of iNOS which then generates large amount of NO. The overproduction of NO may react with virous molecules such as oxygen (O_2) and superoxide ions (O_2^-) to produce reactive nitrogen oxide species (RNOS) such as $ONOO^-$ which is a potent cytotoxic oxidant. The physiological actions of NO in the gut normally occur at low concentration which are produced by eNOS and nNOS. The mechanism can be summarized by four parts: reduce inflammation and oxidative stress, increase intestinal barrier and help wound healing (Figure 18).

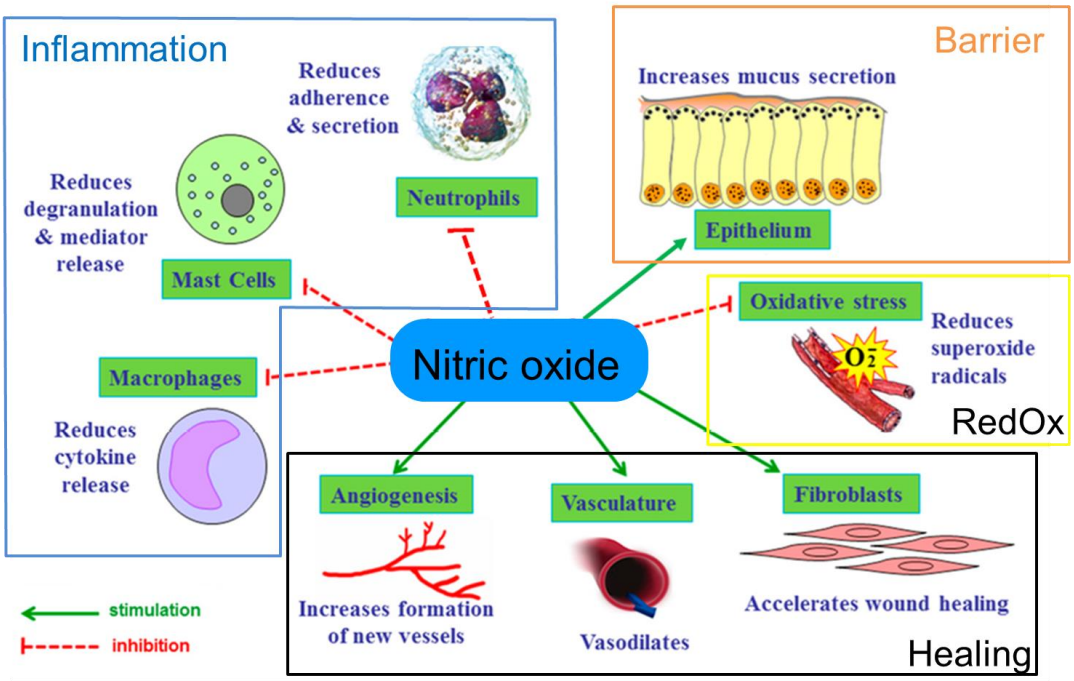

Figure 18 Major beneficial actions of NO in intestine (Magierowski et al., 2015)

1.4.1 Role of nitric oxide in intestinal mucosal defense

NO plays an important role in mucosal defense (Wallace and Miller, 2000) which is disordered in IBD patients. Firstly, NO which was produced by epithelial cells can

increase mucus (Price *et al.*, 1994) and fluid (Dow *et al.*, 1994) secretion in the gastrointestinal tract. The secretion of mucus and fluid can not only reduce bacterial adherence to the epithelial but also dilute and flush away any potentially noxious substance in the lumen. If microbes or antigens are able to penetrate through the mucus and fluid secreted, the next barrier they will encounter is the tight-junction between adjacent epithelial cells. NO secreted by enteric glia cells can also locally enhance this barrier by improving the expression and localization of occludin, zonula occludens-1 (ZO-1), and phosphorylation of myosin light chain (P-MLC) (Savidge *et al.*, 2007, Gerald A. Cheadle, 2012) which play important roles in tight-junction. If the mucosal barrier failed to prevent microbial invasion, NO still works on it from two systemic functions. The first one is that NO causes relaxation of the vascular smooth muscle (Ignarro *et al.*, 1981), and as a result of the dilation of submucosal arterioles, the increase of mucosal blood flow and the removal of any toxins that had across the epithelium. The other function is that NO inhibits expression of the β-2 adhesion molecules on neutrophils (Banick *et al.*, 1997) and P-selectin on the vascular endothelium (Davenpeck *et al.*, 1994). It also down-regulates neutrophil aggregation and secretion (May *et al.*, 1991). In this way, NO acts as a homeostatic regulatory molecule designed to attenuate leukocyte-endothelium interaction and thus attenuate local inflammation. In addition, NO is an important modulator of mucosal repair, because of vascular smooth muscle relaxation causing blood flow increasing, enhancement of collagen deposition by fibroblasts and angiogenesis stimulation (Schäffer *et al.*, 1996, Schäffer *et al.*, 1997, Jadeski and Lala, 1999). NO also has potent effects on immunocytes within the gastrointestinal lamina propria. NO secreted by mast cell appears to reduce the release of inflammatory mediators, including histamine, platelet-activating factor PAF, TNF (Salvemini *et al.*, 1990, Bissonnette *et al.*, 1991, Masini *et al.*, 1991, Hogaboam *et al.*, 1993, Van Overveld *et al.*, 1993). Macrophage function is modulated by NO, with important implications for mucosal defense. For example, the production of various immunomodulatory cytokines (e.g., IL-12 and IL-

1) can be inhibited by NO (Huang *et al.*, 1998, Obermeier *et al.*, 1999). Thus, the overall action of NO could be characterized as anti-inflammatory.

1.4.2 NO donors

NO, as a free radical, is very sensitive to the environment. It can react with a variety of atoms and radicals, such as oxygen superoxide anion, which leads to its very short half-life (within seconds). Due to its instability, treatment with drugs, which can deliver NO, has been used for more than a century (e.g. nitroglycerin (GTN)). In cardiovascular disease, for prevention and treatment of angina pectoris and hypertension, organic nitrates and sodium nitroprusside respectively have been used (Al-Sa'doni and Ferro, 2000; Ignarro, 2002). The most commonly used drugs in therapy of cardiovascular disease are organic nitrate and nitrate esters, including GTN, amyl nitrate, isosorbide dinitrate (ISDN), isosorbide mononitrate (ISMN) and pentaerythrityl nitrate (PETN) (Ignarro, 2002; Schade et al., 2010). Organic nitrates are indirect NO donors; for example GTN is used in acute *angina pectoris* is a prodrug, which needs enzymatic activation to generate bioactive NO (Ignarro, 2002). For the treatment of patients suffering from chronic stable angina, slower NO-releaser nitrate such as ISMN, ISDN or PETN are used, as well as retarded GTN in the form of transdermal patches. Isosorbide mononitrate and ISDN are useful for the treatment of chronic heart failure, especially for patient with concomitant coronary insufficiency. Disadvantages of conventional organic nitrates are their short therapeutic half-life, drug tolerance, hemodynamic effects, lack of selectivity, systemic absorption and limited bioavailability (Ignarro, 2002).

Among direct NO donors, only sodium nitroprusside (SNP) and NO gas have clinical relevance. Sodium nitroprusside is used in intensive care medicine to provide rapid lowering of high blood pressure crises (Al-Sa'doni and Ferro, 2000; Miller and Megson, 2007; Schade et al., 2010). In SN, NO is coordinated, as a nitrosyl group, to iron in a square bipyramidal complex (Ignarro, 2002). Side effects associated with toxic

metabolites, cyanide and thiocyanide appear with prolonged administration. Nitric oxide in gaseous phase can be used therapeutically only by inhalation in pulmonary hypertension (Creagh-Brown et al., 2009), and in neonates inhalation (Miller and Megson, 2007).

Novel NO donors including diazeniumdiolates and *S*-nitrosothiols have been widely investigated for biomedical applications. Diazeniumdiolates are synthesized by exposing nucleophiles to NO. These compounds are generally stable in solid form but decompose spontaneously in solution to generate up to two molar equivalents of NO (Megson and Webb, 2002). Diazeniumdiolates present the major bioactivities through activation of sGC and depend on the rate of NO generation (Megson and Webb, 2002). *S*-nitrosothiols (RSNO) such as *S*-nitrosoglutathion (GSNO), may be more effective than currently available NO donor drugs (Hogg, 2000, Richardson and Benjamin, 2002, Parent *et al.*, 2013a, Dahboul *et al.*, 2014). They have a number of potential advantages over other classes of NO donors. They do not appear to engender vascular tolerance (Miller and Megson, 2007) and are characterized by an *in vitro* half-life ranging from 10 to 38 h (Mancuso *et al.*, 2003). *S*-nitrosothiols do not induce oxidative stress and, in arteries with endothelial cells dysfunction, play a role in the storage and transport of NO (Sarr *et al.*, 2007). *S*-nitrosothiols have made a promise for the future as interesting tools as complementary therapy.

1.4.3 *S*-Nitrosoglutathione: a potent *S*-nitrosothiol

S-Nitrosoglutathione (GSNO, Figure 19) is the *S*-nitrosated derivative of the most abundant cellular thiol, glutathione (GSH), which is a tripeptide of gamma-glutamine, L-cysteine, and glycine. It is one of the physiological RSNO and an attractive therapeutic candidate:

a) It has been reported to be involved in the chemical biology and physiological functions of NO in intestine (mentioned above);
b) It has been discovered as endogeneously present in extracellular fluids and

tissues (Gaston *et al.*, 1993, Snyder *et al.*, 2002);

c) Compared to other NO donor such as organic nitrates, GSNO presents non reported tolerance (Sarr *et al.*, 2005).

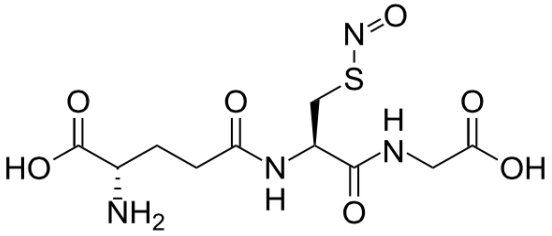

Figure 19 Chemical structure of *S*-nitrosoglutathione (GSNO)

1.4.3.1 Synthesis

Three strategies to synthesize GSNO were described in the literature: i) the most popular method to produce GSNO is reacting glutathione (GSH) with acidified sodium nitrite (Hogg, 2000, Heikal *et al.*, 2009), ii) GSNO can also be synthesized by reacting GSH with nitrous acid (HONO) (Kettenhofen *et al.*, 2007), iii) simply bubbling NO through GSH solution produces GSNO as well (Seabra *et al.*, 2004b).

Unlike most of other low-molecular-weight *S*-nitrosothiols, GSNO can be precipitated with acetone and purified as a solid (Hart, 1985), and this has promoted its use as an experimental tool. The molar extinction coefficient of GSNO has been variously reported, with a wide range of values. (Hart, 1985) gave an extinction coefficient of 922 M^{-1} cm^{-1} at 335 nm, with agreement to this result, we measured the value as 922 M^{-1} cm^{-1} at 334 nm (Parent *et al.*, 2013a).

1.4.3.2 *In vitro* stability

The limitation of GSNO application is its fast and often unpredictable rate of decomposition in aqueous solutions. In aqueous solutions, the stability of GSNO may be explained by the S-NO bond mesomerization (Eq. 1). The distribution of those mesomers depends on the electrophile and nucleophile groups in the S-NO bond environment.

$$GSN{=}O \longleftrightarrow GS^{+}{=}NO^{-} \qquad \text{(Eq. 1)}$$

Published half-lives of GSNO are not unified and are clearly condition-dependent. Basically, GSNO is subject to several mechanisms of decomposition, including S-NO bond homolysis (Eq. 2) metal ion-catalyzed (mainly Cu^{2+}) decomposition (Eq. 3), heterolysis (Eq. 4), and hydrolysis (Eq. 4).

$$GS{-}NO \xrightarrow{\triangle\ /\ h\nu} GS^{\cdot} + {}^{\cdot}NO \qquad \text{(Eq. 2)}$$

$$2GS{-}NO \xrightarrow{Cu^{2+}} GSSG + 2\,{}^{\cdot}NO \qquad \text{(Eq. 3)}$$

$$2GS{-}NO + H_2O + O_2 \longrightarrow GSSG + NO_2^- + NO_3^- + 2H^+ \qquad \text{(Eq. 4)}$$

Those reactions may explain why, despite the proven benefits of GSNO, this tripeptide is not yet present in any pharmaceutical composition. Hence it is important to develop dosage forms to protect GSNO from environmental decomposition for further applications, especially for chronic medical application.

1.4.3.3 *In vivo* metabolism

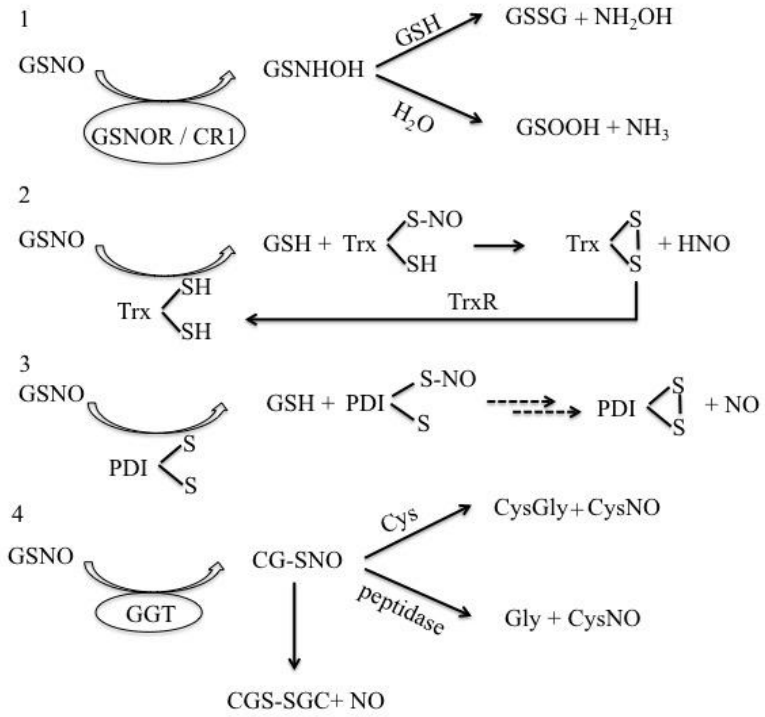

Figure 20 *In vivo* metabolism of GSNO by enzymes: 1. GSNO reductase (GSNOR) and carbonyl reductase 1 (CR1); 2. thioredoxin system (Trx); 3. protein disulfide isomerase (PDI); 4, γ-glutamyltranspeptidase (GGT).

As described above, GSNO is unstable *in vitro,* and it is susceptible to many enzymes

as well. In the literature, GSNO reductase (GSNOR), carbonyl reductase 1 (CR1), the thioredoxin (Trx) system, the protein disulfide isomerase (PDI) and γ-glutamyltranspeptidase (GGT) are the main enzymes reported to be involved in GSNO decomposition (Figure 20).

1.4.3.3.1 *S*-Nitrosoglutathione reductase and carbonyl reductase 1

The GSNOR reduces GSNO to an unstable intermediate, *S*-hydroxylaminoglutathione, which then rearranges to form glutathione sulfonamide, or in the presence of GSH, forms oxidized glutathione (GSSG) and hydroxylamine (NH_2OH) (Figure 20) (Koivusalo *et al.*, 1989, JENSEN *et al.*, 1998). Through this catabolic process, GSNOR regulates the cellular concentrations of GSNO and plays a central role in regulating the levels of endogenous *S*-nitrosothiols and controlling protein *S*-nitrosation-based signaling (Höög and Östberg, 2011). In fact, GSNOR-dependent oxidation of *S*-hydroxylaminoglutathione is increased 8-fold in the presence of GSNO *in vitro* and more than 20-fold in crude lung and liver lysates. These results highlight the potential impact of alternative GSNO reductase substrates on the biological activity and degradation of GSNO (Staab *et al.*, 2008).

Similar to GSNOR, CR1 metabolizes GSNO to an intermediate product which can then react with GSH to produce NH_2OH and GSSG, thus there is no NO liberation in its catalytic reaction as well (Staab *et al.*, 2011).

1.4.3.3.2 The thioredoxin system

The Thioredoxins (Trx) system comprises three main players, Trx, thioredoxin reductase (TrxR), and NADPH, and it plays a critical role in the control and maintenance of redox homeostasis (Nishiyama *et al.*, 2001). Thioredoxins, with a dithiol/disulfide active site are the major cellular protein disulfide reductases (Arnér and Holmgren, 2000). Two isoforms of Trx localize to subcellular compartments including the cytosol (Trx1), nucleus (Trx1), and mitochondria (Trx2) and they are responsible for reduction of protein disulfides *via* the active site vicinal dithiols. Reduced Trx (rTrx) reacts directly with a protein disulfide through a thiol-switching

mechanism to yield a reduced protein dithiol and oxidized Trx (oTrx) (Figure 20).

Although Trx has long been recognized as a target of *S*-nitrosation (Haendeler *et al.*, 2002), it has also been identified as a major player in the reduction of low-molecular weight and protein *S*-nitrosothiols where it participates in both denitrosation and transnitrosation reactions (Mitchell and Marletta, 2005, Sengupta *et al.*, 2007, Barglow *et al.*, 2011). Through denitrosation, rTrx reacts directly with either a low-molecular-weight or protein *S*-nitrosothiol (including GSNO) to liberate NO and thiols (Nikitovic and Holmgren, 1996). Through transnitrosation, the active-site thiol for Trx becomes *S*-nitrosated, leaving behind a low-molecular weight or protein thiol. The nitroso group now residing on Trx will then be turned over through unclear mechanism with release of nitroxyl (HNO) and oxidation of Trx (Figure 20). Oxidized Trx is then reduced by TrxR and nicotine adenine disphosphonucleotide (NADPH). Compared to GSNOR and CR1, the Trx system has ubiquitous expression, hence it has been proposed as the primary regulator of the *S*-nitroso proteome in most tissues (Sengupta and Holmgren, 2013).

1.4.3.3.3 Protein disulfide isomerase

Another enzyme involved in NO transfer is PDI, which catalyzes thio-disulfide exchange reactions, mechanistically similar to RSH-RSNO exchange reaction (Zai *et al.*, 1999). The protein disulfide isomerase catalyzes transnitrosation and denitrosation regulating intracellular transfer of NO (Figure 20). The protein disulfide isomerase has been reported to denitrosate GSNO and it is postulated that NO released *via* this reaction combines with dioxygen in the hydrophobic environment of either the cell membrane or the PDI protein structure, to form N_2O_3 (Sliskovic *et al.*, 2005) (Figure 20). This "NO-charged PDI" can perform intra- and intermolecular *S*-nitrosation reactions similar to that proposed for serum albumin. Reduced PDI was able to denitrosate *S*-nitrosated PDI (PDI-SNO) resulting in the release of NO.

1.4.3.3.4 γ-Glutamyl transpeptidase

γ-Glutamyltranspeptidase is an extracellular cell surface enzyme involved in the

catabolism of GSH adducts and the metabolism of thiol-based leukotrienes. The enzyme transfers the γ-glutamyl group of GSH through either hydrolysis or in the presence of co-substrates (an amino acid, a peptide) leaving behind cysteinyl–glycine (Figure 20) (Neil *et al.*, 1997). It was shown that GGT used GSNO as a substrate, generating *S*-nitrosocysteinylglycine to accelerate the decomposition of GSNO. GGT is membrane bound and appears to act during the translocation of GSH across cell membranes to deliver extracellular cysteine. Many substituted derivatives of GSH, and GSSG, are also substrates for GGT, and this enzyme acts to degrade and recycle both GSSG and the products of glutathione *S*-transferase activity (Abbott *et al.*, 1986).

1.4.3.4 Cell transport of *S*-nitrosoglutathione

The *S*-nitrosoglutathione itself is not directly taken up into cells because of molecular weight and its good hydrophily; however, GSNO treatment increases cell *S*-nitrosothiol levels in many conditions. Initially, it was hypothesized that GSNO decomposes in the extracellular space to release NO which is then able to diffuse across the cell membrane to *S*-nitrosate protein targets (Ramachandran *et al.*, 1999, Ramachandran *et al.*, 2001). Enzymes like GGT and PDI are involved in the transmembrane GSNO transportation. As previously described, GGT can use GSNO as a substrate to generate *S*-nitrosocysteinylglycine (CysGlyNO), which is not stable, further deliver NO spontaneously or transfer NO to L-cysteine, prior to uptake. In a similar way, PDI catalyzes transnitrosation and denitrosation of GSNO to release NO. Besides the NO dependent mechanism, the NO-independent mechanism was also involved in GSNO uptake into cells. This mechanism requires the transfer of the nitroso group from GSNO to another thiol containing amino acid, L-cysteine. This transnitrosation produces GSH and a new low-molecular weight *S*-nitrosothiol, *S*-nitroso-L-cysteine (L-CysNO) which is a good substrate for uptake through the L-amino acid transporter system (L-AT) (Rassaf *et al.*, 2003, Zhang and Hogg, 2004). L-CysNO is readily transported into cells and can either *S*-nitrosate cellular GSH to reform GSNO inside the cell or directly *S*-

nitrosate protein thiols to elicit cellular responses. It was observed that the presence of cystine in cell culture media was required for the cellular metabolism of GSNO (Zeng *et al.*, 2001). This is summarized in Figure 21.

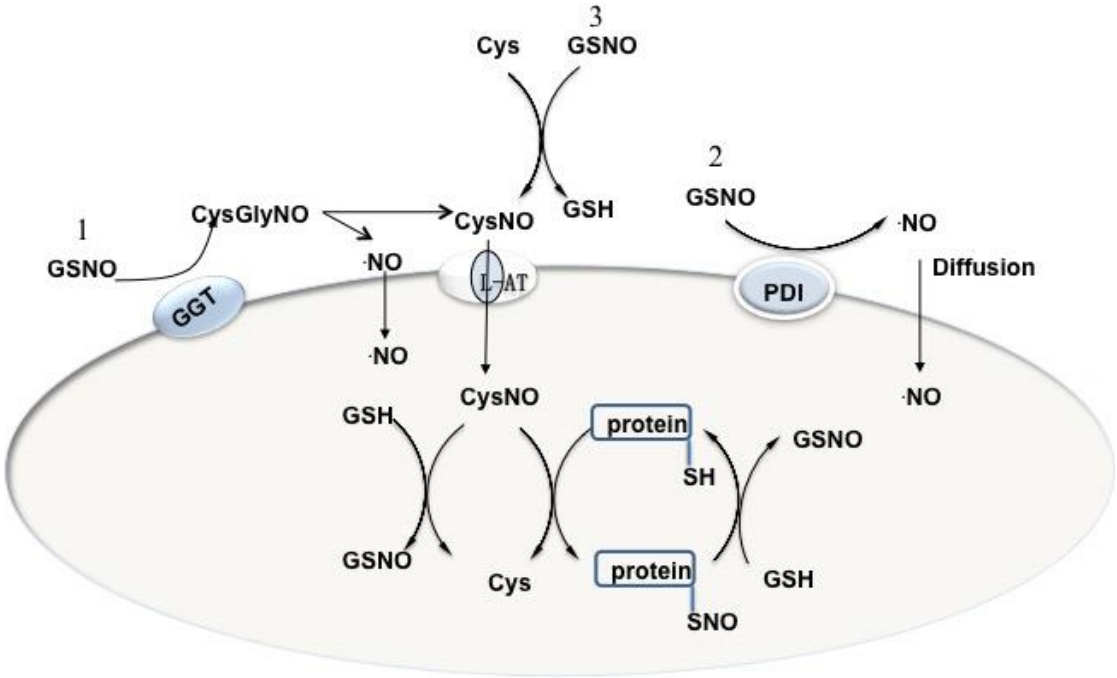

Figure 21 A model for cellular GSNO uptake (Broniowska et al., 2013, Gaucher et al., 2013). 1: GSNO was metabolised by GGT forming *S*-nitrosocysteinylglycine, which further deliver NO spontaneously and then diffused into cell, or transfer NO to L-cysteine. 2: PDI catalyzes transnitrosation and denitrosation of GSNO to release NO. 3: GSNO transfers NO to L-cysteine forming CysNO, which is transported into the cell through the L-amino acid transporter system (L-AT).

1.4.3.5 *S*-nitrosoglutathione and intestinal barrier integrity maintenance

GSNO which is secreted from enteric glia cells (EGCs) has been shown a protection and maintenance function in intestinal barrier (Savidge *et al.*, 2007, Cheadle *et al.*, 2013, Yu and Li, 2014). Savidge and co-workers showed that intraperitoneally administrated GSNO obviously attenuated the disruption of intestinal barrier induced by enteric glial cell ablation in transgenic mice. In their work, The Ussing Chamber result further confirmed the idea by GSNO significantly restored mucosal barrier function in colonic biopsy specimens from patients with Crohn's disease (Savidge *et al.*, 2007). The mechanism might be implicated with improving expression of peri-junctional F-actin and TJ proteins such as zonula occludens-1 (ZO-1) and occludin after GSNO treatment

(Savidge *et al.*, 2007). The same function of GSNO preventing intestinal barrier breakdown was observed by Cheadle. The *in vitro* model demonstrated that the maintenance of the intestinal barrier function by increasing the localization of the intestinal tight junction proteins, such as ZO-1, occudin and phosphorylated MLC (Cheadle *et al.*, 2013). Furthemore, GSNO can attenuate the intestine inflammatory response by redox-sensitive *S*-nitrosylation of nuclear factor κB (NF-κB) inflammatory signaling, inhibiting the transcription of proinflammatory mediators such as TNF-α (Reynaert *et al.*, 2004). Changing NF-κB inflammatory signaling also plays vital roles in the inhibition of endothelial cell adhesion molecules that accelerate leukocyte infiltration (Awad *et al.*, 2013). However, it is noteworthy that GSNO did not regulate the intestinal barrier integrity in a dose-dependent manner. It was reported that disruptive function of GSNO on the epithelial integrity was obtained at relatively higher concentrations (Savidge *et al.*, 2007). The *in vitro* study showed that GSNO promotes a significant increase in Caco-2 transepithelial electrical resistance (TEER) at 5-100 μmol/L. This TEER is reversed at concentrations ≥150 μmol/L. In addition, Tetramethylrhodamine isothiocyanate phalloidin-labeling of MDCK cells in the presence of different GSNO concentration (10 μmol/L, and 250 μmol/L) for 24 hours demonstrated that at low micromolar concentrations GSNO promotes tight-junction–associated proteins to associate with cytoskeletal components, whereas at higher and potentially pathogenic doses it directly disrupts this cytoskeletal F-actin network. However, the molecular mechanism remains unclear. It could be attributed to altered NO production. GSNO is a potent nitric oxide donor, which can function to *S*-nitrosylate proteins and play an important role in proper epithelial ion transport (Jaffrey *et al.*, 2001, Marshall *et al.*, 2004). GSNO works not only by releasing NO but also by the residual, reduced glutathione (GSH) which is known as an antioxidant cytoprotective molecule (Dringen *et al.*, 2000, Yap *et al.*, 2010). GSH reacts nonenzymatically with radicals (R·) and is the electron donor for the reduction of peroxides (ROOH) in the reaction catalyzed by GPx. GSH is regenerated from GSSG

by GR which uses NADPH as cofactor (Figure 22).

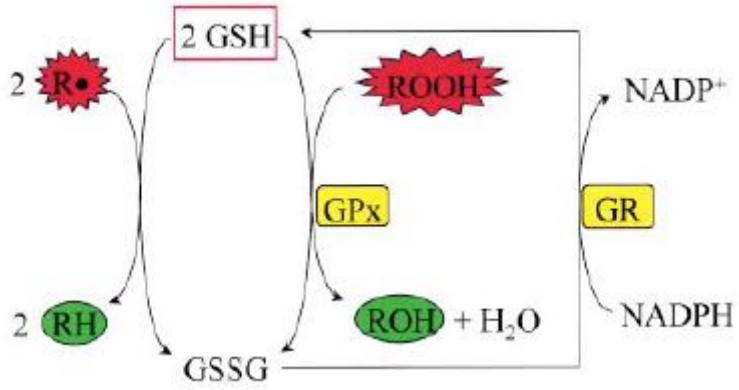

Figure 22 Function of GSH as an antioxidant (Dringen *et al*., 2000).

GSNO is not available as a prescription drug in any format till now. The apparent lack of drug testing and clinic application investigation may be due to its instability and thus a sufficiently stable drug formulation is difficult to be achieved. Compared with NO it has better stability. However it's still too unstable as they are susceptible to physical factor such as light, temperature, divalent cations and biochemical factors such as enzymes (Gaucher *et al.*, 2013). Therefore, if GSNO want to be used for oral administration, a delivery system is necessary to protect GSNO from the harsh environment of gastrointestinal tract (oxygen, enzyme...), which can also release effective amount of GSNO in a controlled way.

1.5 *S*-nitrosoglutathione related delivery system

The delivery of GSNO poses substantial challenges owing to its susceptibility to degradation and small size (easy to diffusion, which may cause low encapsulation efficiency and burst release). The aim of GSNO encapsulation is not only to protect GSNO from degradation but also to control GSNO release in effective concentration. The bioactivity of GSNO are also location dependent, so the encapsulation strategy can reveal targeting in functional site as well with another goal of minimum the systemic side effect. Because of the real challenges, there are not a lot of publications mentioned about GSNO formulations (Table 2). After a careful literature searching, all the approaches can be clarified into three strategies:

1) Development of GSNO conjugated formulation
2) Encapsulation of glutathione (precursor of GSNO), thereby constructing a thiol-loaded formulation, followed by *S*-nitrosation
3) Direct encapsulation of GSNO in delivery system such as liposomes, polymeric nanoparticles/microparticles, polymeric film/matrix/hydrogel and polymer nanocomposite particles…

Each strategy has merits and drawbacks. For illustration, the first one can extend the half-life of GSNO and easily overcome the disadvantage of small molecule, leading to GSNO diffusion limitation, resulting in higher GSNO loading capacity (depending on the *S*-nitrosation yield) and sustained release. However, the main issues are the potent toxicity induced by reagents or organic solvent used in synthesis, complicated synthesis and purification process. The second strategy provide the large opportunities to avoid S-NO bound cleavage during the preparation process with a *S*-nitrosation at the step. Nevertheless, GSNO encapsulation efficiency was limited by the poor presence of active and available thiol group. Unlike the two above strategies, the last one is independent from chemical reaction, which facilitates the manufacture process, avoids limited *S*-nitrosation yield. As a consequence, GSNO encapsulation efficiency is relatively higher. But it is challenging to preserve the S-NO bond integrity throughout the formulation process.

Table 2 GSNO related delivery system

polymer	formulation type	strategy	administration route	efficiency	application	reference
alginate	macromolecular	1	oral	improved GSNO stability and sustained release	crohn's disease	(Shah *et al.*, 2016)
chitosan	macromolecular	1	oral	improved GSNO stability and sustained release	crohn's disease	(Shah *et al.*, 2015)
oligopeptide analogues	macromolecular	1	-	enhanced intracellular NO delivery	cardiovascular disease	(Heikal *et al.*, 2009, Heikal *et al.*, 2011)
oligoethylene glycol-methacrylate/2-vinyl-4,4-dimethyl-5-oxazolone monomer	nanoparticle	1	intravenous injection	protection and sustained release	liver fibrosis and portal hypertension	(Duong *et al.*, 2013, Duong *et al.*, 2015)
poly(ethylene glycol) /Superparamagnetic iron oxide	inorganic nanoparticle	2	-	considerable NO loading capacity	cancer	(Santos *et al.*, 2016)
alginate/chitosan	nanoparticle	2	-	sustained release, decreased cytotoxic effect and protection of GSNO	-	(Marcato *et al.*, 2011, D. Marcato *et al.*, 2013, Pereira *et al.*, 2015)
poly(ethylene glycol)	matrix	2	topical	decrease the thermal and photochemical NO release from GSNO	percutaneous absorption enhancer (co-delivery)	(Seabra *et al.*, 2004b)

Poly(vinyl alcohol)/ poly(vinyl pyrrolidone)	films	3	topical	sustained release	enhancing wound healing in diabetes	(Seabra and De Oliveira, 2004, Seabra *et al.*, 2005)
Poly(vinyl alcohol)	films	3	topical	sustained diffusion of GSNO	dermal wound dressings or for promoting local vasodilation in ischemic tissues	(Simoes and de Oliveira, 2010)
chitosan	films	3	topical	sustained release	antibacterial activity and wound healing	(Kim *et al.*, 2015)
pluronic®F-127	hydrogel	3	topical	sustained and biologically effective release of NO	wound healing and pain treatment	(Shishido *et al.*, 2003, Seabra *et al.*, 2004a, Georgii *et al.*, 2011, Vercelino *et al.*, 2013)
Carbopol 934P/ hydroxypropyl methylcellulose/Polyethylene glycol	films	3	topical	improved stability and increased duration of GSNO action	Female sexual dysfunction	(Yoo *et al.*, 2009)
poly (lactic-co-glycolic acid)/ polyethylene glycol /polycaprolactone	polymeric stent	3	implantation	sustained release	reduce platelet adhesion -restenosis	(Acharya *et al.*, 2012)
poly(lactide-co-glycolide)/poly(ε-caprolactone)	scaffolds	3	-	intermediate cell anchorage, preserved cells redox balance	cardiovascular tissue engineering	(Parent *et al.*, 2015a)

poly(D,L-lactide-co-glycolide)	in situ microparticle	3	subcutaneous	sustained release	cerebral ischemic diseases	(Parent *et al.*, 2015b)
polyhedral oligomeric silsesquioxane/poly(carbonate-urea)urethane	polymer nanocomposite *in situ* implant	3	subcutaneous	sustained release	cardiovascular disease	(de Mel *et al.*, 2014)
phospholipids and cholesterol	liposome	3	pulmonary	sustained release and target to macrophages	antibacterial behavior	(Diab *et al.*, 2016)
Eudragit®RL	nanoparticle	3	oral	improved stability and delayed protein nitrosation, enhanced cellular uptake	vascular disease	(Wu *et al.*, 2015a)
Eudragit®RL/alginate/chitosan	nanocomposite particles	3	oral	improved stability and sustained release	vascular disease	(Wu *et al.*, 2015b, Wu *et al.*, 2016)

1.5.1 *S*-nitrosoglutathione conjugated delivery system

As mentioned previously, GSNO directly applicated as a therapy is limited because of the lack of stability mainly due to light, temperature, metal ions and enzymes… Thus, some researchers focused on the development of conjugation GSNO with macromolecular to aim at improving GSNO stability and achieving sustained release or increase biological activity. For example, binding chitosan to GSNO has been reported as a method to increase the storage and delivery of GSNO (Shah *et al.*, 2015). With this new macromolecular, up to 525.08 ± 151.35 µmol of GSNO per gram polymer was obtained. When contact with intestine tissue, 20% S-NO bond integrity was preserved for this new macromolecular while 100% GSNO was degraded during 6 h. In another study, GSNO was chemically linked to alginate, which leaded to a loading capacity of GSNO up to 468 ± 23 µmol/g polymer (Shah *et al.*, 2016). *S*-nitrosoglutathione-alginate finally showed better stability and sustained release of NO. *S*-nitrosophytochelatins(SNOPCs) are oligopeptide analogues of GSNO (Heikal *et al.*, 2009, Heikal *et al.*, 2011). with by increasing the NO "load" per mol compound, the SNOPCs exhibited more potent than GSNO in inhibiting platelet aggregation, stimulating vasorelaxation and targeting intracellular. However, the rate of NO release in buffer was greater for SNOPCs in comparison to GSNO. For further stability and sustained released improvement, the GSNO conjugated macromolecular can be assembled as nanostructures to present also a better site-specific delivery. Self-assembled polymeric nanoparticles by GSNO conjugated diblock copolymers which includes oligoethylene glycol-methacrylate and 2-vinyl-4,4-dimethyl-5-oxazolone monomer, resulted in an 5 times more enhanced stability compared with GSNO, which were also non-toxic and could efficiently release NO intracellularly (Duong *et al.*, 2013).

1.5.2 *S*-nitrosation of glutathione related delivery system

Encapsulation of GSH (precursor of GSNO) and further *S*-nitrosation to form GSNO

presented an option to delivery GSNO. As reported, GSH was encapsulated into mucoadhesive alginate/chitosan nanoparticles by polyelectrolyte complexation firstly, followed by thiol group *S*-nitrosation, leading to GSNO encapsulation (Marcato *et al.*, 2011, D. Marcato *et al.*, 2013, Pereira *et al.*, 2015). The rates of NO release from GSNO are greatly reduced due to GSNO encapsulation into biodegradable and non-toxic nanoparticles. Furthermore, the GSNO encapsulation decreased the cytotoxic effect of GSNO in fibroblast V79 cells. Thus, the better stability of encapsulated GSNO compared to free GSNO and the absence of cytotoxicity of alginate/chitosan/GSNO nanoparticles enables the use this new NO-nanocarrier in pharmaceutical applications, or other uses where the NO effects are required, without severe side effects. In another study, the surfaces of the superparamagnetic iron oxide nanoparticles (SPIONs) was coated with GSH firstly, followed by free thiol group *S*-nitrosation (Santos *et al.*, 2016). The amounts of NO released from GSNO-SPIONs were 124 ± 1.0 μmol of NO per gram of nanoparticles (NP), which is considered to have therapeutic effects in different biomedical applications, such as the inhibition of platelet adhesion, promotion of wound healing and increased blood flow (Ignarro, 2000, Georgii *et al.*, 2011, Molina *et al.*, 2013). Alternatively, in *in vitro*/*in vivo*, GSH-coated nanoparticles are reported to facilitate nanoparticle internalization, since cells intake of GSH is rapidly increasing during pathological conditions including inflammation and cancer. Therefore, the remaining un-nitrosated GSH residual may help the NP serve as targeted nano-vehicle and/or diagnostic tool in biomedical applications.

1.5.3 Direct *S*-nitrosoglutathione encapsulation

Through Table 2, it demonstrated that most studies concentrated on direct encapsulation of GSNO. Different formulation forms were developed to encapsulate GSNO, such as polymeric nanoparticles, *in situ* microparticles, liposomes, films, stents/scaffolds, hydrogels, and polymer nanocomposites…

For a topical wound healing treatment. GSNO incorporated into different polymeric films made of poly(vinyl alcohol), poly(vinyl pyrrolidone) (Seabra and De Oliveira,

2004, Seabra *et al.*, 2005, Simoes and de Oliveira, 2010) or chitosan (Kim *et al.*, 2015). These polymeric films imposed a great protection of GSNO from decomposition, stabilizing the storage and controlling local NO release. Pluronic®F-127 hydrogel incorporate GSNO with consistent, sustained and biologically effective release of NO was developed for different topical treatment application such as thermal and photochemical delivery of GSNO to target areas (Shishido *et al.*, 2003), inflammation pain and impaired dermal blood flow (Seabra *et al.*, 2004a, Vercelino *et al.*, 2013) and ischaemic wounds (Georgii *et al.*, 2011). For a female sexual dysfunction application of GSNO, it was encapsulated in a gel Carbopol 934P/HPMC/Polyethylene glycol films to achieve improved GSNO stability (at least 30 days) and increased duration of GSNO action (at least 6 h) (Yoo *et al.*, 2009). Respectable researched were focused on more complex GSNO delivery systems such as on poly(lactide-co-glycolide)/poly(ε-caprolactone) implants (Parent *et al.*, 2015a), poly(D,L-lactide-co-glycolide) *in situ* microparticles (Parent *et al.*, 2015b), polyhedral oligomeric silsesquioxane/poly(carbonate-urea) urethane nanocomposites (de Mel *et al.*, 2014) and poly (lactic-co-glycolic acid)/ polyethylene glycol /polycaprolactone stents (Acharya *et al.*, 2012) . All these scaffolds were developed for treatment of cardiovascular diseases and demonstrate a stable release trend of NO over al least 24 h, some even up to 28 days. Furthermore, innovative lipid and polymer particles using more complex formulation processes were also proposed. Phospholipids and cholesterol liposomes incorporating GSNO demonstrated sustained release (less than 30% of encapsulated GSNO was released within 8 h) and macrophage targeting behavior (Diab *et al.*, 2016). With GSNO loaded polymer Eudragit®RL nanoparticles, improved stability, delayed protein *S*-nitrosation and enhanced cellular uptake were observed compared with non-encapsulated GSNO (Wu *et al.*, 2015a). With a further incorporation of GSNO-Eudragit®RL nanoparticles within alginate or chitosan or the blend polymer matrix, a stronger protection and better sustained release were obtained, leading *in vivo* to enhanced GSNO intestinal absorption and promotion of a releasable NO store into the

rat aorta (Wu *et al.*, 2016). Nanocomposite formulations presents advantages, such as control of NO loading, spherical shape favor exchanges with environment *et al*. and disadvantages, such as difficulties to peptide encapsulation in lipophilic tools (limitation in loading), risk of degradation during process…it will be further investigated in the following part, focusing efficient GSNO oral delivery.

1.6 Polymer nanocomposites for drug oral delivery: development strategies and potentialities

Polymer nanocomposites are complex drug delivery systems, which combine nanoscale tool embedded into a polymer matrix. The following part (reviews proposed as a chapter book) clarifies the development and potentialities of polymer nanocomposites adapted to oral delivery. Advantages and inconvenient of these drug delivery systems for drug controlled release will be discussed.

Composites in Biomedical Engineering: Particles (Series C)

Volume 9: Organic particles

Polymer nanocomposites for drug oral delivery: development strategies and potentialities

Hui Ming, Wen Wu, Philippe Maincent, Marianne Parent, Caroline Gaucher, Anne Sapin-Minet *

Université de Lorraine, CITHEFOR EA3452, Faculté de Pharmacie, Nancy, France

Group's Website: *cithefor.univ-lorraine.fr*

* Corresponding author:

Anne SAPIN-MINET (H-index: 10; *Web of knowledge, 09 12 2016*)

anne.sapin@univ-lorraine.fr

LIST OF ABBREVIATIONS

Abbreviation	Full name
ASHF	Hydroxypropyl-methylcellulose acetate succinate based polymer
CD	Cyclodextrins
CMC	Critical micelle concentration
EC	Ethylcellulose
FITC-dex	Fluorescein isothiocyanate-dextran
GI	Gastrointestinal
HA	Hyaluronic acid
IA	Itaconic acid
IPM	Isopropyl myristate
MPEGMA	Poly(ethylene glycol) methyl ether methacrylate
NC	Polymer nanocomposites
PCEC	Poly(ε-caprolactone)-poly(ethylene glycol)-poly(ε-caprolactone) copolymer
PCL	Poly(ε-caprolactone)
PECA	Methoxyl poly(ethylene glycol)-poly(ε-caprolactone)-acryloyl chloride
PEG	Poly(ethylene glycol)
PEI	Polyethyleneimine
PLA	Poly(glycolic acid)
PLGA	Poly(lactide-co-glycolide)
PMVEMA	Poly(methyl vinyl ether-co-maleic acid)
PPI	Poly propylene
PSi	Porous silicon
RES	Reticuloendothelial system
SLNs	Solid lipid nanoparticles
TEL	Telmisartan

Abstract: The association of polymers and nanocarriers in one system (i.e. nanocomposites) has been designed to address the challenges in oral drug delivery, combining drug delivery nano-system advantages (improvement of bioavailability, targeting…) and polymer matrix benefits in improving safety and drug release efficiency. This chapter describes the development and potentialities of polymer nanocomposites in oral delivery. In particular, the improvement of therapeutic efficiency is highlighted, including drug protection, drug solubility improvement, release profile modification, target delivery to specific area in gastrointestinal tract. The application of nanocomposite made by incorporation of organic nanoplatforms (such as polymeric or solid lipid nanoparticles, liposomes, micelles, cyclodextrins, dendrimers …) into a polymer matrix (based on polyacrylate, polymethacrylate, poly(lactic-co-glycolic acid), chitosan, alginate…) for improved drug delivery will be described.

Keywords: polymer nanocomposites, drug protection, burst release, target delivery

Introduction

In the past two decades, the improvement and application of nanotechnology in the biomedical field has resulted in enormous work leading to hundreds of articles with new ideas, trends and methods for the development of a suitable drug delivery system. Polymer nanocomposites (NC) have been designed to combine the merits of both polymer matrix and nanoplatforms in one system, improving mechanical properties (such as tensile strength, elastic modulus or varying stiffness), permeability, crystallinity, thermal stability, biodegradability, and biocompatibility (Bhattacharya *et al.*, 2008). Not a mixture of two materials, the NC may be presented as a core-shell, a particle or a bulk (Figure 1). These carriers are composed of three main components: i) the drug to be released, ii) the core material or nanoplatform, iii) the shell material or polymer matrix. The properties of drug such as solubility, lipophilicity, surface charge and therapeutic index determine the core materials nature to form nanoplatforms. The drug can be encapsulated in the nanoplatforms, adsorbed on the surface of nanoplatforms or conjugated with polymer matrix. The unique location allows controlling the manner and rate of the release process. Organic nanoplatforms consist of polymeric nanoparticles, solid lipid nanoparticles, polymeric micelles, dendrimers or liposomes (Figure 1). The polymer matrix can be based on synthetic (controlled degradation and well-defined physicochemical properties) and natural polymers (low toxicity, biocompatibility and biodegradability).

This chapter will not attempt to cover all areas, including mixtures of two or more materials forming a homogeneous mixture (so not composites), neither the entrapment of nanocrystals composed of pure drug in polymer matrix. In this case, no nanocarriers were present and the nanocomposites were limited to only two components.

The main objective of this chapter is to describe the formulation strategies and potentialities of polymer NC made by the incorporation of nanoplatforms into a polymer matrix for improved delivery efficiency.

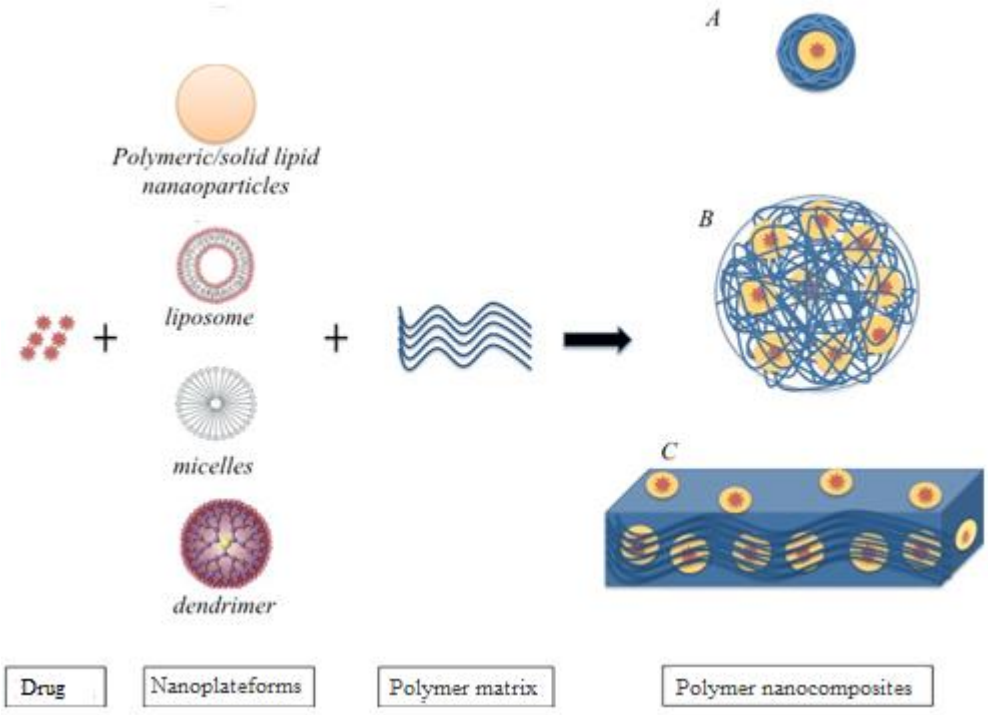

Figure 1 Representative scheme of polymer nanocomposites: drug, nanoplatforms and polymer matrix. They may present as A) core-shell structures, B) particles and C) bulk/film

Formulation strategies for polymer nanocomposites

The traditional drug delivery systems, including tablets and capsules for oral administration or solution for parenteral administration, may not represent the most efficient way to deliver the drugs. The delivery of drugs to active sites is challenging regarding to i) the physicochemical characteristic of the drug (low solubility, high sensitivity, poor bioavailability and potential toxic side effects because of distribution to non-target sites); ii) the multiple barriers to overcome, such as the varying and harsh acidic gastrointestinal (GI) environment, enzymes, the mucus layer, and the tight junctions in the epithelium for oral delivery; iii) the mononuclear phagocyte system, which may phagocytose the delivery system before arriving to the target site. In light of this, polymer NC would represent attractive devices to improve the delivery efficiency, because the nanoplatform possesses high loading capacity and protection drug from the aggressive environment. Meanwhile the polymer matrix provides further protection of nanoplatform and controlled delivery of drug.

Influence on drug properties

As previously described, polymer NC generally consist of three main components. The selection of the different materials and the fabrication methodology depend on the properties of drug that will be encapsulated, such as solubility, lipophilicity, surface charge and therapeutic index… Polymer NC have turned into a versatile platform especially for applications in the field of biomedicine thanks to their capacity to load different substances such as hydrophilic and hydrophobic drugs, peptides and proteins, and nucleic acids (Table 1).

With a careful selection of the nanoplatforms, the polymers and the methodology of production, polymer NC can be exploited to incorporate both hydrophilic and hydrophobic drugs. The hydrophobic drugs were often limited by their solubility, the application of hydrophilic polymeric encapsulation contributed to improve their solubility (Wang *et al.*, 2014, Kang and Ko, 2015, Delmar and Bianco-Peled, 2016, Mansuri *et al.*, 2016). Whereas hydrophilic drug delivery was often challenged by poor cellular permeability, the encapsulation in hydrophobic polymeric or lipidic nanoparticles was presented as promising strategies to improve the bioavailability (Garcıa-Fuentes *et al.*, 2003, Vrignaud *et al.*, 2011).

This strategy was also developed for peptides and proteins. The short half-life and fragility of peptides and proteins reveal the need to develop sustained delivery systems with very controlled burst effects. However, the challenge in protein drug delivery is to conserve its conformation, crucial for the bioactivity. Exposure of proteins to unfavorable conditions during the manufacturing process tended to attenuate their bioactivity(Yeo *et al.*, 2001). Two general approaches have been used to avoid protein denaturation during the production of polymer nanocomposites: i) incorporation of solid protein nanoparticles into hydrophobic polymeric microparticles (Leach *et al.*, 2005, Han *et al.*, 2009, Klingler *et al.*, 2009, Kakizawa *et al.*, 2010); ii) combination with hydrophilic polymers, which are biocompatible with peptide and protein drugs, and avoid direct contact with hydrophobic polymers, which might induce unfolding of

peptide or protein drugs(Sluzky *et al.*, 1991). Thus, peptides or proteins could be primarily encapsulated in nanoparticles made of hydrophilic polymers such as dextran or gelatin(Li *et al.*, 1997) or alginate (Schoubben *et al.*, 2009), for better encapsulation efficiency and preservation of bioactivities, and then microencapsulated in a hydrophobic polymer like poly(lactic-co-glycolic acid) (PLGA) to reach sustained release(Li *et al.*, 1997, Schoubben *et al.*, 2009).

Besides peptides and proteins, nucleic acid-based macromolecules such as siRNA or DNA-plasmids were also adapted to combine with NC for the protection of these substances from degradation in the GI tract. One of the most important advantages of using polymer NC is the ability to increase nucleic acid loading. Moreover, polymer NC might permit the specific delivery of the nucleic acid in the GI tract such as the intestine. Researchers have encapsulated plasmid DNA containing gelatin nanoparticles into poly(epsilon-caprolactone) (PCL) matrix to form polymer NC with a size less than 5 μm (Bhavsar *et al.*, 2006). In the presence of degrading enzymes, the PCL matrix provided protection for gelatin nanoparticles and supported the DNA specific delivery in intestines. In this way, the plasmid DNA survived from the harsh environment in the stomach and preserved its bioactivity (Bhavsar and Amiji, 2007). When radioactively labeled polymeric NC were administered orally to rats, there was preferential long-lasting accumulation in the small and large intestine. In contrast, simple gelatin nanoparticles travelled very quickly along the GI tract. The longer residence of polymer NC in intestine as compared to the unencapsulated gelatin nanoparticles may translate into enhanced transfection efficiency of the plasmid DNA (Bhavsar and Amiji, 2008).

Physicochemical characteristics of polymer matrix

As in traditional composite devices, the role of the matrix in nanocomposites is to support and protect their nanoplatforms. Matrix molecules can be anchored to the nanoplatforms surface by chemical reactions or adsorption, which determines the strength of interfacial adhesion. The polymer NC can be formulated with both synthetic and natural polymers. Synthetic polymers can be tailor-made for specific application,

having controlled degradation and well-defined physicochemical properties, such as poly(L-lactic acid) (PLA), PLGA, and PLA/ PLGA-b-poly(ethylene glycol) (PEG). Natural polymers including chitosan, gelatin, alginate, hyaluronic acid (HA), starch, and dextran present a low toxicity, biocompatibility and biodegradability. The choice of a matrix depends on several factors like application, compatibility with drug and nanoplatform, technique of processing, and costs. In the present section, we will overview the most popular polymers used for the production of polymer NC adapted for oral delivery (Table 1).

Table 1 Simplified summary of drugs, nanoplateforms, polymer matrix and their efficiencies.

Drugs	Nanoplatforms		Polymer matrices		Efficiency	References
	Material	Form	Material	Form		
Vitamin C	Phospholipid and cholesterol	Liposomes	Chitosan/ alginate	Microencapsules	Increased stability	(Liu *et al.*, 2016)
Amaranth red	Chitosan	Nanoparticles	Alginate	Microparticles	Protection in GI Tract	(Garrait *et al.*, 2014)
5(6)-carboxyfluorescein	Phospholipid	Liposomes	Chitosan	Biopolymer−liposome composite	Increased stability and preserved membrane permeability	(Tan *et al.*, 2015)
triptorelin acetate/ Ibuprofen	PCL	Nanoparticles	Ethylcellulose /Eudragit® RS 100	Microparticles	Sustained release and reduction of burst release	(Hasan *et al.*, 2007)
Ibuprofen	PCL	Nanoparticles	PLGA	Microparticles	Sustained release and reduction of burst release	(Sheikh Hassan *et al.*, 2009)
Nile red/Curcumin	IPM	Microemulsion	Chitosan	Hydrogel	Sustained release	(Delmar and Bianco-Peled, 2016)
Docetaxel	PCEC	Micelles	PECA/MPEG MA /IA	Hydrogel	Protected in stomach and specific delivery in intestine	(Wang *et al.*, 2014)
Albendazole	PPI	Dendrimers	Chitosan	Matrix tablet	Prolonged the retention in the GI tract	(Mansuri *et al.*, 2016)
Probucol	PEGylated poly(amidoamine)	Dendrimers	phospholipids	Solid lipids	Slower burst release rate and higher total release amount	(Qi *et al.*, 2015)
Bovine insulin	Alginate	Hydrogel particles	PLGA	Microparticles	Protected payload and sustained release	(Schoubben *et al.*, 2009)
Insulin	PLGA	Nanoparticles	Eudragit® FS 30D	Microcapsules	Protected in stomach and released in intestine	(Sun *et al.*, 2015)
Plasmid DNA	Gelatin	Nanoparticles	PCL	Microspheres	Protected in stomach and specific delivery in intestine	(Bhavsar and Amiji, 2007, Bhavsar and Amiji, 2008)

Processing technologies

Several methodologies have been developed to prepare polymer nanocomposites. Generally, this process involves two main steps: first, the production of the nanoplatforms by any of the available methods, it depends on the type of nanoplateform. In this review, five kinds of nanoplateform were introduced. Polymeric meric/solid lipid nanoparticles, liposome, micelles, dendrimer (Figure 1).

For polymeric nanoparticles, water in oil in water (W/O/W) double emulsion was widely used (Sheikh Hassan *et al.*, 2009, Sun *et al.*, 2015, Delmar and Bianco-Peled, 2016). The emulsions were formed by dispersing primary emulsion which was obtained by dispersing an aqueous phase into immiscible liquid into aqueous phase. The emulsification is rarely a spontaneous process. Therefore, the input of energy is necessary. Normally, the energy is provided by mechanical shear which comes from different kinds of mixers. The final size of the emulsion is caused not only the chemistry but also power of energy used. To stabilize the emulsion, the use of emulsifiers or emulsion stabilizers are also important. The emulsifiers and emulsion stabilizers are mostly amphiphilic molecules with a hydrophilic “head” attached to a hydrophobic “tail”. Nanoprecipitation method was also common applied in prepare the polymeric nanoparticle (Reis *et al.*, 2006, Joshi *et al.*, 2010, Garrait *et al.*, 2014). Nanoprecipitation is a facile, mild, and low energy input process for the preparation of polymeric nanoparticles. Generally, the method describes the precipitation of a dissolved material as nanoscale particle after exposure to a non-solvent that is miscible with the solvent(Schubert *et al.*, 2011). The polymeric nanoparticles whave the drawbacks of the lack of safe polymers with regulatory approval and high cost. Solid lipid nanoparticles (SLNs) were developed to overcome these limitation with advantage of improved drug absorption in the oral delivery system(Mukherjee *et al.*, 2009). They can enhance the mucosal adhesion because of small particles size and long gastrointestinal tract (GIT) resident time. Hydrophilic drugs were usually encapsulated in the solid lipid nanoparticles to acquire better controlled release profile and good

encapsulation efficiency. SLNs are consist of solid lipid, emulsifier and water/solvent(Mukherjee *et al.*, 2009). Different techniques were introduced in a review wrote by S. Mukherjee, Such as high shear homogenization, Hot homogenization, cold homogenization, ultrasonication or high speed homogenization, solvent emulsification/evaporation, micro emulsion, supercritical fluid, spray drying method and double emulsion method(Mukherjee *et al.*, 2009). Therefore, no more details will be explained in this chapter.

A liposome is a spherical vesicle consisting of a lipid bilayer surrounding an aqueous core (Liu *et al.*, 2016). The liposome was widely used as a delivery system of nutrients and pharmaceutical drugs. The preparation methods of liposome were described in a review in detail by A. Akbarzadeh. All the preparation methods involve four basic stages: 1). Drying down lipids from organic solvent; 2). Dispersing the lipid in aqueous media; 3). Purifying the resultant liposome; 4). Analyzing the final product(Akbarzadeh *et al.*, 2013). In the review, the preparation techniques include 3 different methods: mechanical dispersion method, solvenr dispersion method and detergent removal method (removal of non-encapsulated material). More details could be found in the review.

Polymeric micelles are formed by self-assembling of amphiphilic block copolymers containing hydrophilic “head” and hydrophobic “tail” in aqueous phase at or above the critical micelle concentration (CMC). Micelles are widely used in encapsulating scarcely water-soluble drugs owing to the core-shell structure. This effective drug delivery system has a lot of merits such as small particle size (<100 nm), targeting ability, prolonging blood circulation duration and easy preparation (Sezgin *et al.*, 2006). Due to the properties and interrelations of drug and polymer, drugs can be incorporated into micellar core by chemical conjugation or physical encapsulation trough dialysis or emulsification (Ahmad *et al.*, 2014). In chemical conjugation technique, the formation of covalent bond between the specific group of the drug and the hydrophobic core of the micelles cause incorporation of the hydrophobic drug inside the polymeric micelle

core. Such micelles can avoid renal clearance and Reticuloendothelial system (RES) phagocytosis. In comparison to the chemical method, physical method is more favorable for drug incorporation. Polyionic compounds can be incorporated through the formation of polyion complex micelles. Physical entrapment of drugs is generally done by dialysis or oil-in-water emulsion procedure. In dialysis, the drug and polymer are brought from the selective solvent to a solvent that is selective only for the hydrophilic part of the polymer. By the replacement of good solvent with selective one, the hydrophobic portion of the polymer associates to form the micellar core, thus, incorporating insoluble drug. Extending the dialysis over several days can ensure the complete removal of the organic solvent. The oil-in-water emulsion method consists of preparing an aqueous solution of the copolymer to which a solution of the drug in a water-insoluble volatile solvent is added in order to form an oil-in water emulsion. The micelle–drug conjugate is formed as the solvent evaporates. The main advantage of the dialysis procedure over the latter method is that the use of potentially toxic solvents can be avoided.

Dendrimers are nano-sized, radially symmetric molecules with well-defined, homogeneous, and monodisperse structure consisting of tree-like arms or branches (Abbasi *et al.,* 2014). Dendrimers are generally prepared using either a divergentapproach or a convergent one. In the divergent approach, used in early periods, the synthesis starts from the core of the dendrimer to which the arms are attached by adding building blocks in an exhaustive and step-wise manner (Abbasi *et al.,* 2014, Mansuri *et al.,* 2016). In the convergent approach, synthesis starts from the exterior, beginning with the molecular structure that ultimately becomes the outermost arm of the final dendrimer. In this strategy, the final generation number is pre-determined, necessitating the synthesis of branches of a variety of requisite sizes beforehand for each generation (Grayson and Frechet, 2001).

There second, the encapsulation of such nanoplatforms into polymer matrix is usually based on emulsification, gelation and polyelectrolyte complexation. The

Table 2 simple summary of proceeding methods to prepare polymer nanocomposites

nanoplatform			polymer matrics			References
material	form	method	material	form	method	
PCL	Nanoparticles	W/O/W solvent evaporation method	Ethylcellulose /Eudragit® RS 100	Microparticles	emulsification	(Sheikh Hassan et al., 2007)
Chitosan	Nanoparticles	precipitation/coaversion method	Alginate	Microparticles	ionotropic gelation	(Garrait et al., 2014)
PCL	Nanoparticles	W/O/W solvent evaporation method	PLGA	Microparticles	emulsification	(Sheikh Hassan et al., 2009)
PLGA	Nanoparticles	emulsion solvent diffusion method	Eudragit® FS 30D	Microcapsules	spray-drying	(Sun et al., 2015)
Gelatin	Nanoparticle	ethanol precipitation method	PCL	Microsphere	ionotropic gelation	(Bhavsar et al., ,2007,2008)
Phospholipid and cholesterol	Liposomes	film dispersion method	Chitosan/alginate	Microencapsules	polyelectrolyte complexation	(Liu et al., 2016)
Phospholipid	Liposomes	reverse evaporation	Chitosan	biopolymer−liposome composite	polyelectrolyte complexation	(Tan et al., 2015)
IPM	Microemulsion	microemulsion	Chitosan	Hydrogel	ionotropic gelation	(Delmar et al., 2016
PCEC	Micelles	thin-film hydration method	PECA/MPEGMA /IA	Hydrogel	heat-initiated free radical	(Wang et al., 2014)
PPI	Dendrimers	divergent approach	Chitosan	Matrix tablet	lyophilization and compression	(Mansuri et al., 2016)
PEGylated poly(amidoamine)	Dendrimers	condensation reaction	glycerin monostearate/stearic	Solid lipid	emulsion-evaporation and low temperature-	(Qi et al., 2015)
Alginate	Hydrogel particles	ionotropic gelation	PLGA	Microparticles	solvent diffusion evaporation method	(Schoubben et al., 2009)

microencapsulation step should neither destroy the nanoplateform nor lead the release of drug during the preparation.

Potentialities of polymer nanocomposites

Major goals of polymer NC application in drug delivery are the maximization of drug bioavailability and efficacy, the control of pharmacokinetics, pharmacodynamics, non-specific toxicity, immunogenicity as well as the overcoming of obstacles arising from low drug solubility, degradation, fast clearance rates, relatively short-lasting biological activity and inability to cross biological barriers.

Solubility improvement

Almost 40% of commercial drugs are poorly water-soluble. In particular, in the biopharmaceutical classification system, class II drugs (poorly soluble and highly permeable drugs) have limited oral absorption because of their inappropriate dissolution rates (Löbenberg and Amidon, 2000). Various methods to improve the dissolution behavior and bioavailability of drugs have been developed (Gulsun *et al.*, 2009, Singh *et al.*, 2011, Krishnaiah, 2012, Kesarwani *et al.*, 2014). One of the effective strategies improving drug solubility and drug dissolution rates is reducing the particles size to the nanoscale, either drug nanocrystals or the accociation with nanocarrier (Ozeki and Tagami, 2013; S.R. Krishnaiah, 2010). The surface area of drug particles increases with decreasing particle size and consequently, the large surface area increases the drug dissolution rate. In addition, decreasing the size of drug particles enhances the saturation solubility (Hu *et al.*, 2004, Keck and Müller, 2006). Cyclodextrins (CD) have been described as “an important tool in the formulator's armamentarium to improve drug solubility and dissolution rate for poorly water-soluble drug candidates” and efforts have been made to predict whether cyclodextrins will be of benefit in creating a dosage form for a particular drug candidate (Loftsson and Brewster, 2010).

The work of Sangwai and coworkers (Sangwai and Vavia, 2013), explored an innovative ternary beta-CD NC to deliver telmisartan (TEL) having exceedingly pH

dependent and poor solubility profile. In comparison with plain drug and marketed formulation, TEL NC exhibited remarkable improvement in *in vitro* dissolution characteristics in multimedia and biorelevant media. Beside CD, natural carriers like gelatin, acacia, cassia and ghatti gum with less swelling and low viscosity were also used to improve drug solubility thus improving the oral bioavailability (Kushare and Gattani, 2013).

Drug protection

The bioavailability of labile drugs such as peptides and proteins was limited by their poor stability, which was highlighted while encapsulating them in various devices (De Rosa *et al.*, 2000, Woo *et al.*, 2001, Yu *et al.*, 2002, Hinds *et al.*, 2005). The application of polymer NC is beneficial to protect the drug during fabrication procedure and also against enzymatic and hydrolytic degradation in the GI tract by preventing the direct contact between the drugs and the harsh, digestive environments. G. Garrait developed a polymer nanocomposite carrier to protect drug from gastric acid and pepsin, based on two natural polymers, namely chitosan and alginate (Garrait *et al.*, 2014). Chitosan nanoparticles were developed to protect a model molecule (amaranth red) from enzymatic attack in the small intestine. However, the glycosidic bonds of chitosan are rapidly hydrolyzed under gastric conditions(George and Abraham, 2006). Sodium alginate is more resistant, and since it is an anionic polysaccharide with charges opposed to those of chitosan, it was chosen as a natural polymer to protect chitosan nanoparticles from gastric hydrolysis. The intention was to ensure protection of the nanoparticles until they reach the lumen of the small intestine, where they may be released in order to deliver the entrapped active compound. As presented in their study, polymer dissolution and drug release into the gastric environment are slowed down. This polymer NC system allowed a pH-sensitive or polypeptidic drug to pass intact through the stomach (Garrait *et al.*, 2014). For more resistance to the acidic conditions in the stomach, PLGA was used as the polymer matrix. Schoubben developed polymer NC as the delivery vectors for bovine insulin (Schoubben *et al.*, 2009). They loaded

bovine insulin into alginate nanoparticles, a hydrophilic polymer to produce a friendly environment preventing denaturation by stress conditions. Then these nanoparticles were embedded into PLGA polymer matrix to avoid the degradation of alginate nanoplatform in acidic condition. Compared with the conventional PLGA microparticles, these polymer NC presented higher encapsulation efficiency and protection of the drug with improved stability during the *in vitro* release under acidic pH(Schoubben *et al.*, 2009).

Modification of drug release

In drug therapy, it is important to provide and maintain therapeutic levels of pharmaceutically active agents to the site of action throughout the treatment. Furthermore, it is necessary to minimize temporal variations in drug concentration that can lead to periods of over-dosing. As described previously, the main target of drug absorption for oral delivery is the intestine. However, in physiological conditions, the delivery system has to survive in extreme acidic condition of stomach before reaching the desired target. So when, where and how to release the drug from the delivery system is an important consideration in the design of formulations. To these considerations, modified release technologies are employed to deliver drugs in a controlled manner, providing some actual sustained therapeutic doses within the desired time frame and/or spatial control of drug release. In this respect, polymer NC could be potential carrier for controlled drug delivery due to their enhanced functionality and more complex structures, compared with single-component counterparts. Mainly, the release of drug from polymer NC depended on the diffusion alone or was accompanied with the erosion of polymer matrix. Different combination of nanoplatform and polymer matrix could achieve the reduction of burst release, sustained release, stimulate release and target release.

Table 3 Elimination of burst effect by polymer nanocomposites. Drug release (%): the mean cumulative release of drug from simple nanoplatforms and polymer nanocomposites at first 15 min. Burst effect reduction was calculated by drug release from nanoplatforms (%)/drug release from nanocomposites (%).

Drug	Nanoplatform	Polymer matrix	Drug release (%)	Burst effect reduction ratio	References
Ibuprofen	PCL	-	86 ± 7	1	Sheikh Hassan et al., 2009
	PCL	PLGA	9 ± 4	10	
	PCL	RS	33 ± 7	2	Hasan et al., 2007
	PCL	EC	28 ± 10	3	
	PCL	RS/EC	24 ± 4	3	
Triptorelin acetate	PCL	-	71 ± 11	1	Hasan et al., 2007
	PCL	RS	27 ± 2	3	
	PCL	EC	5 ± 8	20	
	PCL	RS/EC	27 ± 6	3	
Diclofenac sodium	PCL/EC	-	88±1	1	Jelvehgari et al., 2010
	PCL	EC	23.46±0.77	4	
Insulin	PLGA	-	pH1.2 (0-2h) 50±2; pH6.8 (0-6h) 59±4; pH7.4 (0-24 h) 90±4	1	Sun et al., 2015
	PLGA	Eudragit®FS 30D	22±1; 38±2; 90±4	2	

Reduction of burst release

One of the prominent merits of polymer NC as delivery system is the reduction of the burst effect, especially when the drug was previously encapsulated in lipidic or polymeric nanoparticles then incorporated into the polymer matrix. The association of polymer matrix in NC provides prolonged diffusion distance that slows down the release speed and achieves sustained delivery, because first the drug has to overcome the nanoparticle barrier, and then cross the polymer matrix. It was demonstrated by different researchers that the polymer matrix made with hydrophobic polymers such as PLA, PLGA, PCL, Eudragit® RS 100 or ethylcellulose (EC) diminished the burst effect more effectively than hydrophilic polymers such as gelatin, alginate, and chitosan.

These hydrophilic polymers used for nanoparticles might favor water uptake by the microparticles and consequently induce a faster release and/or a faster hydrolysis of the non-soluble polyester polymer, as it was shown in the case of the PCL microparticles. For instance, PCL encapsulated ibuprofen nanoparticles presented obvious burst effect *in vitro* release. The further incorporation of PCL nanoparticles into polymer matrix (PLGA, RS, EC or the blend of RS and EC) reduced the initial burst release efficiently. These systems were also adapted to triptorelin acetate, ibuprofen and insulin (Hasan *et al.*, 2007, Sun *et al.*, 2015) (Table 3).

Target delivery

Drug targeting is a useful tool for achieving selective and efficient delivery of drug at the anticipated site of action with minimized unwanted side effects. Different strategies based on physical environment leading to time or pH dependent delivery systems or based on biological environment such as microflora or enzymes (Prasad *et al.*, 2011) have been proposed.

The most investigated targeting system is pH-dependent polymer NC devoted to protect the drug in acidic environment (as described in protection of drug) and release in the intestine, the promising absorption site, or localized targeting to colonic region(Chourasia and Jain, 2003). The systems are suitable for oral administration leading systemic activities, and the treatment of colonic region diseases like colorectal cancer or inflammation bowel disease. As described by Huang, indomethacin polymer NC, constructed by incorporation of drug loaded micelles into alginate beads, presented modified release behavior when compared to indomethacin loaded simple micelles and indomethacin loaded simple alginate beads (Huang *et al.*, 2012). Specifically, indomethacin was released at neutral pH instead of acidic pH, thus, its side effect in stomach was diminished.

Conclusion:

This chapter summarized the formulation strategies and potentialities of polymer nanocomposites in oral delivery. According to the drug properties, different materials

and processing technologies will be selected. Compared with oral drug administration alone, the nanoplateform can provide good protection from the harsh gastrointestinal environment. With the further encapsulation of polymer matrix, oral administrated drug can have further protection, higher loading efficiency, better controlled release, reduced burst release and specific target delivery. Thus, the combination of nanoplateform and polymer matrix strengthened the drug therapeutic efficiency. In conclusion, polymer nanocomposites are promising candidates for oral delivery.

Acknowledgements:

The authors acknowledge the program of Chinese Scholarships Council and University of Lorraine for their financial support. The work was co-financed by the European Union with the “Fonds Européen de Développement Régional (FEDER)”.

References

A Santos, H., M Bimbo, L., Lehto, V.-P., J Airaksinen, A., Salonen, J. & Hirvonen, J., 2011. Multifunctional porous silicon for therapeutic drug delivery and imaging. *Current drug discovery technologies,* 8**,** 228-249.

Abbasi, E., Aval, S.F., Akbarzadeh, A., Milani, M., Nasrabadi, H.T., Joo, S.W., Hanifehpour, Y., Nejati-Koshki, K. & Pashaei-Asl, R., 2014. Dendrimers: synthesis, applications, and properties. *Nanoscale Research Letters,* 9**,** 247.

Ahmad, Z., Shah, A., Siddiq, M. & Kraatz, H.-B., 2014. Polymeric micelles as drug delivery vehicles. *RSC Advances,* 4**,** 17028.

Akbarzadeh, A., Rezaei-Sadabady, R., Davaran, S., Joo, S.W., Zarghami, N., Hanifehpour, Y., Samiei, M., Kouhi, M. & Nejati-Koshki, K., 2013. Liposome: classification, preparation, and applications. *Nanoscale research letters,* 8**,** 1.

Al-Qadi, S., Grenha, A. & Remuñán-López, C., 2011. Microspheres loaded with polysaccharide nanoparticles for pulmonary delivery: Preparation, structure and surface analysis. *Carbohydrate polymers,* 86**,** 25-34.

Bhattacharya, S., Gupta, R. & Kamal, M., 2008. *Polymeric nanocomposites theory and practice*: Carl Hanser Publishers.

Bhavsar, M.D. & Amiji, M.M., 2007. Gastrointestinal distribution and in vivo gene transfection studies with nanoparticles-in-microsphere oral system (NiMOS). *J Control Release,* 119**,** 339-48.

Bhavsar, M.D. & Amiji, M.M., 2008. Development of novel biodegradable polymeric nanoparticles-in-microsphere formulation for local plasmid DNA delivery in the gastrointestinal tract. *AAPS PharmSciTech,* 9**,** 288-94.

Bhavsar, M.D., Tiwari, S.B. & Amiji, M.M., 2006. Formulation optimization for the nanoparticles-in-microsphere hybrid oral delivery system using factorial design. *Journal of controlled release,* 110**,** 422-430.

Bimbo, L.M., Denisova, O.V., MäKilä, E., Kaasalainen, M., De Brabander, J.K., Hirvonen, J., Salonen, J., Kakkola, L., Kainov, D. & Santos, H.L.A., 2013. Inhibition of influenza a virus infection *in vitro* by saliphenylhalamide-loaded porous silicon nanoparticles. *ACS nano,* 7**,** 6884-6893.

Bimbo, L.M., Sarparanta, M., Mäkilä, E., Laaksonen, T., Laaksonen, P., Salonen, J., Linder, M.B., Hirvonen, J., Airaksinen, A.J. & Santos, H.A., 2012. Cellular interactions of surface modified nanoporous silicon particles. *Nanoscale,* 4**,** 3184-3192.

Chourasia, M. & Jain, S., 2003. Pharmaceutical approaches to colon targeted drug delivery systems. *J Pharm Pharm Sci,* 6**,** 33-66.

De Rosa, G., Iommelli, R., La Rotonda, M.I., Miro, A. & Quaglia, F., 2000. Influence of the co-encapsulation of different non-ionic surfactants on the properties of PLGA insulin-loaded microspheres. *Journal of Controlled Release,* 69**,** 283-295.

Delmar, K. & Bianco-Peled, H., 2016. Composite chitosan hydrogels for extended release of hydrophobic drugs. *Carbohydr Polym,* 136**,** 570-80.

Garcıa-Fuentes, M., Torres, D. & Alonso, M., 2003. Design of lipid nanoparticles for the oral delivery of hydrophilic macromolecules. *Colloids and Surfaces B: Biointerfaces,* 27**,** 159-168.

Garrait, G., Beyssac, E. & Subirade, M., 2014. Development of a novel drug delivery system: chitosan nanoparticles entrapped in alginate microparticles. *J Microencapsul,* 31**,** 363-72.

George, M. & Abraham, T.E., 2006. Polyionic hydrocolloids for the intestinal delivery of protein drugs: alginate and chitosan—a review. *Journal of controlled release,* 114**,** 1-14.

Grayson, S.M. & Frechet, J.M., 2001. Convergent dendrons and dendrimers: from synthesis to applications. *Chemical Reviews,* 101**,** 3819-3868.

Grenha, A., Seijo, B. & Remunán-López, C., 2005. Microencapsulated chitosan nanoparticles for lung protein delivery. *European journal of pharmaceutical sciences,* 25**,** 427-437.

Gulsun, T., Gursoy, R. & Levent, O., 2009. Nanocrystal technology for oral delivery of poorly water-soluble drugs. *FARAD Journal of Pharmaceutical Sciences,* 34**,** 55-65.

Han, Y., Tian, H., He, P., Chen, X. & Jing, X., 2009. Insulin nanoparticle preparation and encapsulation into poly (lactic-co-glycolic acid) microspheres by using an anhydrous system. *International journal of pharmaceutics,* 378**,** 159-166.

Hasan, A.S., Socha, M., Lamprecht, A., Ghazouani, F.E., Sapin, A., Hoffman, M., Maincent, P. & Ubrich, N., 2007. Effect of the microencapsulation of nanoparticles on the reduction of burst release. *Int J Pharm,* 344**,** 53-61.

Hinds, K.D., Campbell, K.M., Holland, K.M., Lewis, D.H., Piché, C.A. & Schmidt, P.G., 2005. PEGylated insulin in PLGA microparticles. In vivo and *in vitro* analysis. *Journal of controlled release,* 104**,** 447-460.

Hu, J., Johnston, K.P. & Williams Iii, R.O., 2004. Nanoparticle engineering processes for enhancing the dissolution rates of poorly water soluble drugs. *Drug development and industrial pharmacy,* 30**,** 233-245.

Huang, X., Xiao, Y. & Lang, M., 2012. Micelles/sodium-alginate composite gel beads: A new matrix for oral drug delivery of indomethacin. *Carbohydrate polymers,* 87**,** 790-798.

Joshi, A., Keerthiprasad, R., Jayant, R.D. & Srivastava, R., 2010. Nano-in-micro alginate based hybrid particles. *Carbohydrate Polymers,* 81**,** 790-798.

Kakizawa, Y., Nishio, R., Hirano, T., Koshi, Y., Nukiwa, M., Koiwa, M., Michizoe, J. & Ida, N., 2010. Controlled release of protein drugs from newly developed amphiphilic polymer-based microparticles composed of nanoparticles. *Journal of Controlled Release,* 142**,** 8-13.

Kang, J.H. & Ko, Y.T., 2015. Lipid-coated gold nanocomposites for enhanced cancer therapy. *Int J Nanomedicine,* 10 Spec Iss**,** 33-45.

Keck, C.M. & Müller, R.H., 2006. Drug nanocrystals of poorly soluble drugs produced by high pressure homogenisation. *European Journal of Pharmaceutics and*

Biopharmaceutics, 62**,** 3-16.

Kesarwani, P., Rastogi, S., Bhalla, V. & Arora, V., 2014. Solubility Enhancement of Poorly Water Soluble Drugs: A Review. *International Journal of Pharmaceutical Sciences and Research,* 5**,** 3123.

Klingler, C., Müller, B.W. & Steckel, H., 2009. Insulin-micro-and nanoparticles for pulmonary delivery. *International journal of pharmaceutics,* 377**,** 173-179.

Krishnaiah, Y.S., 2012. Pharmaceutical technologies for enhancing oral bioavailability of poorly soluble drugs. *Journal of Bioequivalence & Bioavailability,* 2010.

Kushare, S.S. & Gattani, S.G., 2013. Microwave‐generated bionanocomposites for solubility and dissolution enhancement of poorly water‐soluble drug glipizide: in‐vitro and in‐vivo studies. *Journal of pharmacy and pharmacology,* 65**,** 79-93.

Leach, W.T., Simpson, D.T., Val, T.N., Anuta, E.C., Yu, Z., Williams, R.O. & Johnston, K.P., 2005. Uniform encapsulation of stable protein nanoparticles produced by spray freezing for the reduction of burst release. *Journal of pharmaceutical sciences,* 94**,** 56-69.

Lee, Y.-S., Johnson, P.J., Robbins, P.T. & Bridson, R.H., 2013. Production of nanoparticles-in-microparticles by a double emulsion method: A comprehensive study. *European Journal of Pharmaceutics and Biopharmaceutics,* 83**,** 168-173.

Li, J.K., Wang, N. & Wu, X.S., 1997. A novel biodegradable system based on gelatin nanoparticles and poly (lactic‐co‐glycolic acid) microspheres for protein and peptide drug delivery. *Journal of pharmaceutical sciences,* 86**,** 891-895.

Liu, D., Bimbo, L.M., Mäkilä, E., Villanova, F., Kaasalainen, M., Herranz-Blanco, B., Caramella, C.M., Lehto, V.-P., Salonen, J. & Herzig, K.-H., 2013. Co-delivery of a hydrophobic small molecule and a hydrophilic peptide by porous silicon nanoparticles. *Journal of Controlled Release,* 170**,** 268-278.

Liu, W., Liu, W., Ye, A., Peng, S., Wei, F., Liu, C. & Han, J., 2016. Environmental stress stability of microencapsules based on liposomes decorated with chitosan and sodium alginate. *Food Chem,* 196**,** 396-404.

Löbenberg, R. & Amidon, G.L., 2000. Modern bioavailability, bioequivalence and biopharmaceutics classification system. New scientific approaches to international regulatory standards. *European Journal of Pharmaceutics and Biopharmaceutics,* 50**,** 3-12.

Loftsson, T. & Brewster, M.E., 2010. Pharmaceutical applications of cyclodextrins: basic science and product development. *Journal of pharmacy and pharmacology,* 62**,** 1607-1621.

Mansuri, S., Kesharwani, P., Tekade, R.K. & Jain, N.K., 2016. Lyophilized mucoadhesive-dendrimer enclosed matrix tablet for extended oral delivery of albendazole. *European Journal of Pharmaceutics and Biopharmaceutics,* 102**,** 202-213.

Mukherjee, S., Ray, S. & Thakur, R., 2009. Solid lipid nanoparticles: a modern formulation approach in drug delivery system. *Indian journal of pharmaceutical*

sciences, 71**,** 349.

Prasad, K., Badarinath, A., Anilkumar, P., Reddy, B.R., Naveen, N., Nirosha, M. & Hyndavi, M., 2011. Colon targeted drug delivery systems: A review. *Journal of Global Trends in Pharmaceutical Sciences,* 2**,** 459-475.

Reis, C.P., Neufeld, R.J., Ribeiro, A.J. & Veiga, F., 2006. Nanoencapsulation I. Methods for preparation of drug-loaded polymeric nanoparticles. *Nanomedicine: Nanotechnology, Biology and Medicine,* 2**,** 8-21.

Sangwai, M. & Vavia, P., 2013. Amorphous ternary cyclodextrin nanocomposites of telmisartan for oral drug delivery: Improved solubility and reduced pharmacokinetic variability. *International journal of pharmaceutics,* 453**,** 423-432.

Schoubben, A., Blasi, P., Giovagnoli, S., Perioli, L., Rossi, C. & Ricci, M., 2009. Novel composite microparticles for protein stabilization and delivery. *Eur J Pharm Sci,* 36**,** 226-34.

Schubert, S., Delaney, J.J.T. & Schubert, U.S., 2011. Nanoprecipitation and nanoformulation of polymers: from history to powerful possibilities beyond poly(lactic acid). *Soft Matter,* 7**,** 1581-1588.

Sezgin, Z., Yuksel, N. & Baykara, T., 2006. Preparation and characterization of polymeric micelles for solubilization of poorly soluble anticancer drugs. *Eur J Pharm Biopharm,* 64**,** 261-8.

Sham, J.O.-H., Zhang, Y., Finlay, W.H., Roa, W.H. & Löbenberg, R., 2004. Formulation and characterization of spray-dried powders containing nanoparticles for aerosol delivery to the lung. *International Journal of Pharmaceutics,* 269**,** 457-467.

Sheikh Hassan, A., Sapin, A., Lamprecht, A., Emond, E., El Ghazouani, F. & Maincent, P., 2009. Composite microparticles with in vivo reduction of the burst release effect. *Eur J Pharm Biopharm,* 73**,** 337-44.

Singh, A., Worku, Z.A. & Van Den Mooter, G., 2011. Oral formulation strategies to improve solubility of poorly water-soluble drugs. *Expert opinion on drug delivery,* 8**,** 1361-1378.

Sluzky, V., Tamada, J.A., Klibanov, A.M. & Langer, R., 1991. Kinetics of insulin aggregation in aqueous solutions upon agitation in the presence of hydrophobic surfaces. *Proceedings of the National Academy of Sciences,* 88**,** 9377-9381.

Sun, S., Liang, N., Yamamoto, H., Kawashima, Y., Cui, F. & Yan, P., 2015. pH-sensitive poly(lactide-co-glycolide) nanoparticle composite microcapsules for oral delivery of insulin. *Int J Nanomedicine,* 10**,** 3489-98.

Vrignaud, S., Benoit, J.-P. & Saulnier, P., 2011. Strategies for the nanoencapsulation of hydrophilic molecules in polymer-based nanoparticles. *Biomaterials,* 32**,** 8593-8604.

Wang, C.-F., Mäkilä, E.M., Kaasalainen, M.H., Liu, D., Sarparanta, M.P., Airaksinen, A.J., Salonen, J.J., Hirvonen, J.T. & Santos, H.A., 2014a. Copper-free azide–alkyne cycloaddition of targeting peptides to porous silicon nanoparticles for

intracellular drug uptake. *Biomaterials,* 35**,** 1257-1266.

Wang, Y., Chen, L., Tan, L., Zhao, Q., Luo, F., Wei, Y. & Qian, Z., 2014b. PEG-PCL based micelle hydrogels as oral docetaxel delivery systems for breast cancer therapy. *Biomaterials,* 35**,** 6972-85.

Woo, B.H., Jiang, G., Jo, Y.W. & Deluca, P.P., 2001. Preparation and characterization of a composite PLGA and poly (acryloyl hydroxyethyl starch) microsphere system for protein delivery. *Pharmaceutical research,* 18**,** 1600-1606.

Yeo, Y., Baek, N. & Park, K., 2001. Microencapsulation methods for delivery of protein drugs. *Biotechnology and Bioprocess Engineering,* 6**,** 213-230.

Yu, Z., Rogers, T.L., Hu, J., Johnston, K.P. & Williams, R.O., 2002. Preparation and characterization of microparticles containing peptide produced by a novel process: spray freezing into liquid. *European journal of pharmaceutics and biopharmaceutics,* 54**,** 221-228.

Zhang, H., Liu, D., Shahbazi, M.A., Makila, E., Herranz-Blanco, B., Salonen, J., Hirvonen, J. & Santos, H.A., 2014. Fabrication of a multifunctional nano-in-micro drug delivery platform by microfluidic templated encapsulation of porous silicon in polymer matrix. *Adv Mater,* 26**,** 4497-503.

Chapter 2.
Luminal GSNO effects on the intestinal barrier integrity

2.1 Introduction

In direct contact with external environment, intestinal mucosa plays the crucial role of barrier that can avoid the invasion of the mucosa by microbiota. As described in chapter 1 (paragraph 1.2.1). The functional intestine mucosal barrier consists of a mucus layer on the surface of epithelial cells, strong junctions between adjacent epithelial cells, and immune cells involved in the innate immune response. In healthy physiological conditions, this intestine barrier is efficient and keep intestine homeostasis. In contrast, this barrier is disrupted in IBD patients. The disruption of the intestinal barrier is an important cause of IBD because it allows pathogen and toxin penetration and triggers an excessive and uncontrolled inflammation. The disruption of tight junction structure is always followed with intestinal barrier defects, proinflammatory cytokines production (such as TNFa, IL-1β), activation of NF-κB signaling pathway, expression of MLCK expression, which subsequently increases the intestinal epithelial permeability by disrupting epithelial TJs in intestinal inflammation (Li *et al.*, 2016). Therefore, a potent therapeutic approach of preventing intestinal inflammation is to improve the intestinal mucosal barrier function by reducing intestinal permeability.

S-Nitrosoglutathione (GSNO) is the endogenous *S*-nitrosylated derivative of the major antioxidant glutathione (GSH). GSNO, which is secreted by Enteric Glia Cells (EGCs) from Enteric Nervous System (ENS), has been shown to maintain and protect intestinal mucosal barrier (Savidge *et al.*, 2007, Flamant *et al.*, 2011, Cheadle *et al.*, 2013). Savidge and co-workers showed that glial-derived GSNO was identified as a potent inducer of mucosal barrier function *in vitro* and *in vivo* and of attenuated tissue inflammation after ablation of enteric glia gene in mice. GSNO regulation of mucosal barrier function was associated directly with an increased expression of perijunctional F-actin and TJ associated proteins ZO-1 and occludin. GSNO also significantly restored mucosal barrier function in colonic biopsy specimens from patients with Crohn's disease in the *ex vivo* Ussing Chamber experiment. Flamant *et al* investigated that both EGCs and GSNO but not GSH significantly reduced barrier disruption and

inflammatory response induced by *shigella flexneri* infectious in Caco-2 monolayers. Cheadle *et al* further investigated the mechanism of GSNO secreted by EGCs prevent intestinal mucosal barrier disruption through an *in vitro* model. The result showed both GSNO and co-culture with EGCs prevented Cytomix-induced increases in permeability by improving expression and localization of occludin, ZO-1, and P-MLC (phosphorylated myosin light chain). Recently, Li *et al* tested the potential therapeutic effect and mechanism of femoral venous injected GSNO on lipopolysaccharide (LPS)-induced inflammatory response and intestinal mucosal barrier injury in a rat model of endotoxemia (Li *et al.*, 2016). GSNO (1mg/kg) was administered by femoral venous injection 15 mins after LPS injection. The result demonstrated that GSNO addition reduced the intestinal injury observed in histologic sections, decreased permeability to fluorescein isothiocyanate dextran, attenuated damage of the junction between epithelia, and protected against the LPS-induced expression decrease of ZO-1. Furthermore, addition of GSNO reduced plasma and intestinal TNF-α and IL-1β levels as well as inhibited the LPS-induced up-regulation of myosin light-chain kinase expression and NF-κB p65 level in the intestine.

GSNO effects on intestine exhibited a dose-dependent way in both *in vitro* and *in vivo* studies (Savidge *et al.*, 2007, Goncalves *et al.*, 2015). Different concentrations of GSNO (5 μM -250 μM) exposure to Caco-2 cells monolayer. Dose-response curves showed that GSNO promoted a significant increase in Caco-2 TEER at 5–100 μM. This TEER was reversed at concentrations >150 μM. At low micromolar concentrations GSNO promotes tight-junction–associated proteins to associate with cytoskeletal components, whereas at higher and potentially pathogenic doses it directly disrupts this cytoskeletal F-actin network. An *in vivo* study showed also dose effect (0.05 μM-5 μM) on intestine. Fetal treatment with lower concentration of GSNO (0.05 μM) resulted in significant better improvement of bowel morphology in gastroschisis (Goncalves *et al.*, 2015).

To summarize all these literatures, the source of GSNO is from the mucosal side of

intestine (secreted by EGCs and femoral venous injection…) However, no publication investigates GSNO which comes from the luminal side of intestine (after oral administration) to date. Therefore, the first aim of present study is to prove the concept that luminal GSNO can also has a protective effect on intestine as mucosal GSNO.

2.2 Study of the impact of the GSNO on the intestinal barrier permeability

To confirm our first hypothesis, GSNO impacts on the intestinal barrier permeability was investigated in Ussing chamber by following a paracellular marker permeability after different concentration GSNO treatment in luminal side of the chamber (donor compartement). And the mechanism was studied by measuring the junction protein expression with western blot. That constitute the article presented below (to be submitted in Journal of Gastroenterology).

Luminal *S*-nitrosoglutathione impacts intestinal barrier permeability by dose-dependent way in an *ex vivo* model of Ussing Chamber

Romain SCHMITT[a], Hui MING[a], Franck HANSMANNEL[b], Caroline GAUCHER[a], Pierre LEROY[a], Isabelle LARTAUD[a], Anne SAPIN-MINET[a*]

[a] *University of Lorraine, CITHEFOR EA 3452; Faculty of Pharmacy, BP 80403 Nancy Cedex, France.*

[b] *University of Lorraine, NGERE Inserm U954 and Department of Hepato-Gastroenterology, Vandoeuvre-lès-Nancy, France.*

Authors: Same contribution in both experimental part and writing part to this article

*Corresponding author: Anne SAPIN-MINET

CITHEFOR EA 3452

Faculté de Pharmacie

5, rue Albert Lebrun - BP 80403

F-54001 Nancy Cedex, France

Tel: +33 (0)3 83 64 73 30

Email: anne.sapin@univ-lorraine.fr

Conflicts of interest: none.

Acknowledgement: The authors acknowledge the program of Chinese Scholarships Council and University of Lorraine for their financial support. The work was co-financed by the European Union with the "Fonds Européen de Développement Régional (FEDER)". The funders had no role in study design, data collection and analysis, decision to publish, or preparation of the manuscript.

Abstract:

Backgrounds: Inflammatory bowel diseases (IBD) such as Crohn's Disease and Ulcerative Colitis, are disabling pathologies affecting young patients who undergo high relapses of acute inflammatory episodes all over their life. This may finally lead to colorectal cancer. All of these shortcomings are related to a failure of the intestinal barrier. Nitric oxide (secreted by enteric glial cells) plays a pivotal role to maintain integrity of the intestinal barrier. Therefore, an innovative chronic treatment of IBD may rely on supplementation of small amounts of nitric oxide to preserve the intestinal barrier integrity. As nitric oxide is an unstable radical, *S*-nitrosothiols, especially the endogenously produced *S*-nitrosoglutathione (GSNO), may be used as nitric oxide donors.

Methods: In this preliminary pre-clinical study, impacts of GSNO on epithelial cells junctions and barrier permeability were evaluated, using the Ussing Chamber model, an *ex vivo* model composed of an oriented rat intestine tissue (0.25 cm^2, ileum segment) separating two compartments (luminal and mucosal). Intestinal barrier integrity was evaluated by measuring the intestinal permeability of sodium fluorescein (NaFlu, medium permeability, paracellular transport) with incubation of different concentrations of GSNO (0.1, 10 and 100 μM). Cell junction proteins expression were examined by western blot after the permeability study in Ussing chamber.

Results: The result showed that GSNO can modulate intestinal barrier integrity in a dose-dependent manner.

Conclusion: In conclusion, low concentrations of GSNO may be a novel treatment to prevent barrier disruption and IBD relapses.

Keywords*:* GSNO, Ussing Chamber, intestinal barrier integrity

Introduction

Several actors ensure integrity and permeability of the intestinal barrier which both play a critical role in the defense of the body against external environmental aggressions. The intestine mucosa allows renewing of the epithelium through stem cells every 3 to 5 days (Potten *et al.*, 2002). Cell junctions – which are divided, from intraluminal to deeper parts of the intestinal wall, into tight junctions, adherent junctions and desmosomes – are the main elements involved in the maintenance of integrity (desmosomes) and function of the intestinal barrier: tight junctions and adherent junctions especially regulate intestinal permeability and absorption, as entry of luminal elements through conjunctive tissues to intestinal vessels (Turner, 2000). Under physiological conditions, intercellular crossing is limited to small molecules. A selective crossing through enterocytes is also possible using transporters. Mucus – composed of glycoproteins (mainly mucins) and forming a gel recovering the epithelium (Kim and Ho, 2010) – also contributes to intestine integrity. Immune cells, in Peyer's patches and in conjunctive tissue, reinforce the role and the maintenance of the barrier integrity by an innate immune response and a control of inflammation (Hooper and Macpherson, 2010). Finally, the intestine microbiota takes over food components that cannot be absorbed such as fibers and digestible polysaccharidic compounds and contribute to the renewing and contributes to maturation and renewing of the epithelium, and to cellular differentiation (Payros *et al.*, 2014).

Amongst the different models used to evaluate intestine permeability, the Ussing diffusion Chamber model developed by Hans Henriksen Ussing in 1946, allows *ex vivo* study of the transport of ions, nutrients or drugs through a donor to an acceptor compartments separated by an insert on which is fixed the intestinal tissue (Clarke, 2009). Both sides of the intestinal tissue are immersed in an osmotic solution maintained at 37°C. This technique permits to study absorption differences, by dosage of components in both compartments and inside the tissue, according to the different intestinal sections. This requires low amounts of molecules. In this model,

morphological and functional modifications can be observed during the experiment. Intestinal permeability is witnessed by measuring the crossing (flux) of a substance through the intestinal barrier, while intestinal integrity is reflected by the trans-epithelial electrical resistance (TEER). The later traduces the viability of the tissue and witnesses the open state of cell junctions (Srinivasan *et al.*, 2015). The effect of an active substance on the barrier itself can be evaluated using markers of intestinal permeability (sodium fluorescein, NaFlu, medium permeability, paracellular transport).

At the intestinal level, nitric oxide (NO) plays an important but paradoxical role: in one hand, NO has also beneficial effects: at smaller concentrations than above, it is the most important neurotransmitter at the gastro-intestinal level, allowing to control gastric motility. It also allows to control intestinal secretion of mucus and to improve absorption in physiological conditions (Kochar *et al.*, 2011). In the other hand, excessive production of NO has been correlated with sustained inflammation in the colon, particularly observed for epithelial cells near to the inflammation site (Kolios *et al.*, 2004). This is due to an increased production of peroxynitrites ions ($ONOO^-$). Therefore, new therapeutics of IBD, with the challenges to maintain low concentrations of NO during remission period of IBD (Kochar *et al.*, 2011) remain to be developed. Under its gaseous form, NO is unstable (half-life within seconds) and is easily and uncontrollably reacted in its environment (Dattilo and Makhoul, 1997). Thus, NO donors are necessary to avoid this drawback. NO donors show longer half-life and some of them are already used in therapeutic (*i.e*. cardiovascular context (Parent *et al.*, 2013b)). One family of NO donors is the *S*-nitrosothiols (RSNO) with the *S*-nitrosoglutathione (GSNO) as the leader molecule. GSNO is a very interesting molecule as it is naturally produced in the organism. This GSNO is derived from the most important intracellular thiol, glutathione (GSH, a tripeptide gamma-glutamyl-cysteinyl-glycine that intervenes in RedOx regulation by the glutathione/disulfide glutathione ratio). GSNO secreted by enteric glial cells after stimulation of the vagus nerve prevents inflammatory events and preserves barrier integrity (Savidge *et al.*, 2007,

Cheadle *et al.*, 2013). In this context, it becomes an evidence to consider supplementation with low concentrations of GSNO as a potential therapeutic candidate in IBD pathologies.

Before setting a prevention treatment of IBD using oral administration of GSNO, its ability to maintain or reinforce intestinal barrier integrity remains to be evaluated. This is the goal of the present study. Intestinal barrier permeability and integrity were evaluated by measuring, in the presence or not of GSNO, apparent permeability (Papp) of NaFlu, and TEER. The expression of cell junction proteins was also evaluated by Western Blot. Occludin and claudin-1 were chosen as markers of tight junction, beta-catenin and e-cadherin as markers of adherens junctions (Turner, 2009).

Material and Methods

Substances used and synthesis of GSNO

All reagents were of analytical grade and all solutions prepared with ultrapure deionized water (>18.2 mΩ.cm at 25°C). Sodium nitrite was purchased from Merck (Darmstadt, Germany), and all other reagents (including glutathione, sodium fluorescein) from Sigma-Aldrich (Saint-Quentin-Fallavier, France). Antibodies for occludin (71-1500) and claudin-1 (37-4900) were purchase from Invitrogen; antibody for E-cadherin (SC-7870) from Santa-Cruz; antibody for β-catenin (MA1-2001) from Thermo Fisher Scientific (Pierce Biotechnology, USA); antibody for β-actin loading control (HRP) (ab197277) from Abcam; antibody for HRP conjugated secondary goat-rabbit/mouse from Jackson ImmunoResearch Laboratories, Inc. *S*-nitrosoglutathione synthesis was performed in the laboratory according to a previously described method (Parent *et al.*, 2013a) and all experiments involving GSNO were conducted under conditions of subdued light and at 4 °C in order to minimize light- and temperature-induced GSNO degradation. The concentration of GSNO was assessed by UV spectrophotometry (UV-1800, Shimadzu, France) using the specific molar absorbance of the S-NO bond at 334 nm using the Beer-Lambert law (molar absorbance 922 $M^{-1}cm^{-1}$); the expected

concentration is of 10^{-2} M with a tolerance of ± 5 %.

Animals and ethical statement

Intestinal barrier integrity was evaluated on ileum isolated from 12-week-old, male, normotensive, Wistar rats (Janvier Laboratories, Le Genest-St-Isle, France; 400-500 g). All experiments were performed in accordance with the European Community guidelines (2010/63/EU) for the use of experimental animals in the respect of the 3 Rs' requirements for Animal Welfare. The project untitled "Nitro-Vivo" was positively evaluated by the regional ethical committee for animal experiments and approved by the French Ministry of Research (n°APAFIS#1614-2015090216575422v2). Animals were kept under standard conditions (temperature: 21 ± 1 °C, hygrometry 60 ± 10%, light on from 6 am to 6 pm) and had diet *ad libitum* (A04, Safe, Villemoisson-sur-Orge, France) and water (reverse osmosis system, Culligan, Brussells, Belgium).

Wistar rats were sacrificed by exsanguination after anesthesia (sodium pentobarbitone 60 mg/kg, intraperitoneal, Sanofi Santé Nutrition Animale®, Libourne, France). An ileum segment (around 12 cm) of the rat intestine was removed and immediately placed in cold Krebs-Henseleit buffer (NaCl 119, $NaHCO_3$ 24, KCl 4.7, $MgSO_4$ 1.2, KH_2PO_4 1.2, $CaCl_2$:$2H_2O$ 1.6 and glucose 10 mM; pH adjusted to 7.4 and equilibrated with 95 % O_2 / 5 % CO_2 for 30 minutes before use). Intestine pieces were cleaned from fat tissue and cut into 2-cm long segments (6 segments per rat). The segments were opened along the mesenteric vein, cleaned with cold Krebs-Henseleit buffer, pinned on insert and immediately placed in Ussing Chamber system. A 6-Ussing Chamber bench (P2404 Physiologic Instrument®, Easymount LVSYS, Harvard Apparatus) was used. In each chamber, compartments were filled with Krebs-Henseleit buffer (2.5 mL), temperature was maintained at 37°C in continuous circulation (using a water bath) and pH was maintained at 7.4 with gas infusion (12 mL/min using a peristaltic pump). A current electrode and a voltage electrode (multimeter, Millicell-ERS2, Millipore®; electrodes P2020, Physiologic Instrument®) were placed in each compartment for TEER

measurement. TEER (Ω×cm²) was determined by the $U = R \times I$ law after inducing a current from one compartment to the other, with U the potential gradient, I the induced current by the apparatus and R the resistance of the tissue (Ω) multiplied by the tissue area separating both compartments (cm²).

Permeability experiments

NaFlu (2.7 mM) permeability (from donor/luminal compartment to acceptor/mucosal compartment) were assessed by measuring changes in concentration of the compounds with time. Samples (250 µL of medium) were harvested in the acceptor compartment at different times (every 30 min, until 2 hours; each removed volume was replaced by an equal volume of 37°C pre-heated Krebs-Henselheit buffer) for the quantification of permeability markers flux. TEER measurement was performed at these same time intervals to follow intestine tissue integrity. [NaFlu] was evaluated with a spectro-fluorimeter (BioTek®, λ_{ex} = 460 nm; λ_{em} = 515 nm)

The flux (J) of compounds or their apparent permeability (Papp) through the intestine were calculated according to the following formulae:

$$J = \left(\frac{dQ}{A\,.dt}\right) \qquad P_{app} = \left(\frac{dQ}{dt}\right) \times \left(\frac{1}{AC_o}\right) = \frac{J}{C_0}$$

($\frac{dQ}{dt}$ is the the slope of the steady state portion of the amount of the drug permeated during time t, A the tissue area separating both compartments and C_0 the initial concentration in active molecule; units: J in µg·cm^{-2}·s^{-1}, *Papp* in cm·s^{-1}; Q in mg; t in s; A in cm², C_0 in mg·cm^{-3}).

Evaluation of the effects of GSNO on intestine permeability and integrity

First, stability of GSNO was evaluated by measuring its concentration all over the 2 hours under experimental conditions, without intestine (100 µM = 500 nmol added to the donor compartment at 37 °C, Krebs-Henselheit buffer with 95% O_2 / 5% CO_2 at 12 mL/min).

Then, a second series of intestinal segments was exposed to GSNO (0.1 µM – 100 µM,

donor compartment), with 10 min equilibrium before starting the experiment on 2 hours, in order to measure permeability marker and TEER. In parallel, for each series of 6 Ussing Chambers, one or two were dedicated to control conditions (therefore, the control group includes the highest number of experiments, see Figure 3), in order to evaluate quality and viability of the segments and allow comparison of results between each series of Ussing experiments. Quality criteria were fixed according to NaFlu flux at t = 2 h, and TEER values, on control condition, to have more reliable results. At the end of the experiment, intestinal tissues were taken out of the Ussing chambers and placed in plastic tubes, frozen in liquid nitrogen and conserved at -80°C until western blot analysis.

Cell junction proteins expression by Western blot

Intestinal piece was taken out from -80°C and mashed into powder, using mortar and pestle, in liquid nitrogen. Proteins were extracted from the tissue in RIPA buffer (NaCl 140; NaH_2PO_4 12; KH_2PO_4 2 mM; sodium deoxycholate 0.5%; nonidet P-40 1%, SDS 1%) with additional polymethylsulfonyl fluoride, sodium orthovanadate and protease inhibitor cocktail. Firstly, tissue powder was incubated with RIPA buffer (ice, 10 mins), then homogenized. Mixture was frozen and thawed, for 3 cycles, in liquid nitrogen and 37°C water bath. After centrifugation (12 000 × *g*, 4 ◦C, 30 mins), supernatant was used for proteins quantification by bicinchoninic acid (BCA) assay.

Protein samples were mixed with an equal volume of Laemmli 2X sample buffer and heated to 95°C for 5 mins. Total proteins (30 µg) were separated with sodium dodecyl sulfate–polyacrylamide gels and transferred to polyvinylidene difluoride membranes. The membranes were blocked with 5% bovine serum albumin or non-fat milk/TBST for 1 hour at room temperature and then incubated with primary antibodies (occludin,1:600; claudin-1, 1:600; E-cadherin, 1:800; β-catenin, 1:700) overnight at 4°C. After washing in TBST, the appropriate HRP-conjugated secondary antibody was added and the membrane was incubated for 1h at room temperature. After further

washing in TBST, the proteins were detected using an ECL or ECL PLUS kit (Amersham, Velizy-Villacoublay, France), and with the "fusion" software (Vilber®). Densitometric analysis was performed with "Image J" software.

β-actin was used as a reference protein, and so the relative amount was expressed with the ratio of protein /beta-actin expressions. Results were normalized from "wild type" group and expressed in percentage: "wild type" is a tissue harvested from animal and directly frozen; control+Ussing is a tissue that has been set in Ussing system and frozen after 2-hours experiment without treatment.

Statistical analysis

Results are expressed as mean ± standard error of the mean (sem). Statistical comparisons were performed using a one-way (groups: controls and GSNO at different concentrations) or two-way (groups and time) ANOVA, or a linear regression analysis for correlation test ($p < 0.05$). Statistical analyses were performed using the GraphPad Prism software (GraphPad Software version 5.0, San Diego, USA).

Results

Assessment of quality criteria

Before the real experiment starts, quality criteria of Ussing Chamber should be validated to obtain reliable result: in the present study, the *ex vivo* intestine viability is crucial. A preliminary study was performed for 3 h, following NaFlu flux and TEER values that significantly changed at t=3 h, indicating a loss of intestinal barrier integrity. Therefore, the Ussing Chamber duration was limited to 2 h, to have more reliable result: this drastic intestine tissue viability decreasing after 2 hours was also observed in the literature (Forsgård *et al.*, 2014).

The results of NaFlu permeability and TEER values of intestine tissue without any treatment in Ussing Chamber (control condition) were given in Figure 1. After calculation of NaFlu flux and statistical analysis, the cut-off was fixed for NaFlu and TEER, this leads to a cut-off values of 15 $\mu g \cdot cm^{-2} \cdot s^{-1}$ for NaFlu flux. Moreover, a lower

TEER value than 30 Ω·cm² at the beginning of the experiment (t = 0 h) and a loss of TEER more than 50% after 0.5 h during the experiment, witnessed too high extension or rupture of the tissue during setting. Those results were also in the range of other values from the literature (Srinivasan *et al.*, 2015). If NaFlu flux and TEER values were out of criteria that has been mentioned above, it means that the tissue has taken too much time to be set in the system, or that the tissue was too much extended and was broken during the setting. The correlation between markers of permeability and TEER values in this first series of tissues was confirmed by using a linear regression analysis ($p < 0.05$; Figure 2). Results of further study were analyzed according to these criteria.

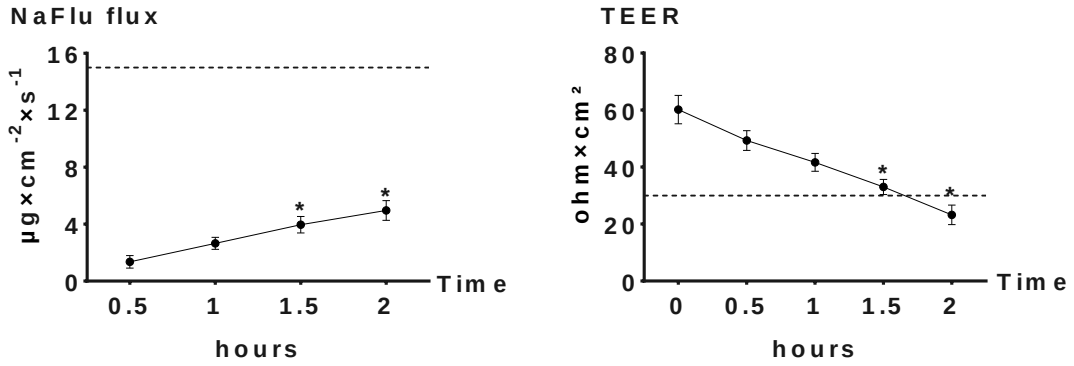

Figure 1 Criteria of NaFlu permeability and TEER result during 2 h in Ussing chamber (--- criteria: NaFlu flux at 15 µg×cm^{-2}×s^{-1} at t=2 h, and TEER at 30 Ω×cm² at t=0). *p < 0.05, statistic difference s 0 h and 0.5 h; one-way ANOVA

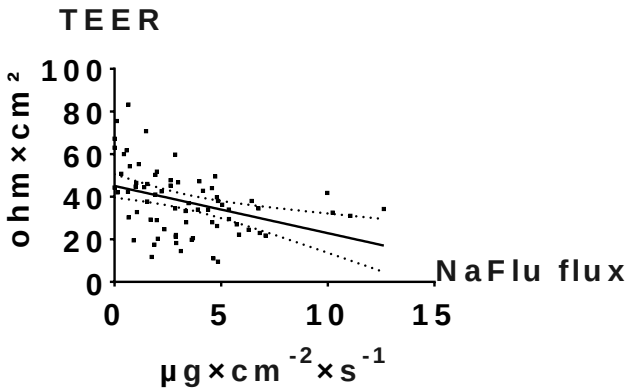

Figure 2 Correlation between NaFlu permeability and TEER result during 2 h in Ussing chamber (---confidence interval 95%, CI 95%). Linear regression test with CI 95%.

Evaluation of the effects of GSNO on intestine permeability and integrity

GSNO is a very fragile and sensitive molecule which can be degraded easily by light, temperature, oxygenation by bubbling during Ussing Chamber experiment. Thus, to start the experiment with the presence of GSNO in Ussing Chamber system. The stability in Ussing Chamber was tested. 100 μM GSNO was adding in the system without presence of intestine tissue. All the other conditions were exactly the same with permeability study. After 2 hours, GSNO concentration is not significantly affected. The result showed a stable state during our experiment with a condition of 37 ˚C and oxygenation with 95% O_2 / 5% CO_2 at 12 $mL \cdot min^{-1}$.

After the confirmation of GSNO stability in this experimental system. The GSNO effects on intestinal barrier integrity was evaluated by adding GSNO (0.1, 10, 100 μM) and permeability markers in the donor (luminal) compartment and the marker permeation to acceptor (mucosal) compartment was followed during 2 h. The flux of markers and TEER result was given in Figure 3 and Papp values were shown in Table 1. Through the NaFlu permeability result (Figure 3 and Table 1), dose-dependent effect was observed. On healthy tissue, high concentrations of GSNO (100 μM) showed a trend to increase the NaFlu flux (or Papp) compared to the Control group; while low concentration of GSNO (0.1 μM) showed a trend to decrease the NaFlu flux (or Papp, Table 1) compared to Control. A significant difference was observed between high concentration of GSNO (100 μM) and Control at t=2 h for both NaFlu flux and Papp value. There was observed a significant increase of this paracellular marker after a high-concentration treatment of GSNO (100 μM), in comparison to low-concentration GSNO (0.1 μM). NaFlu flux and apparent permeability coefficient showed similar results. The TEER values showed in Figure 3 showed no significant difference in different groups. At the beginning of the experiment, the intestine tissue was discarded if the TEER values were less than 30 $\Omega \times cm^2$ which indicated the intact intestine tissues. But with experiments going, the TEER decreased, which showed a decreased tissue integrity during experiments.

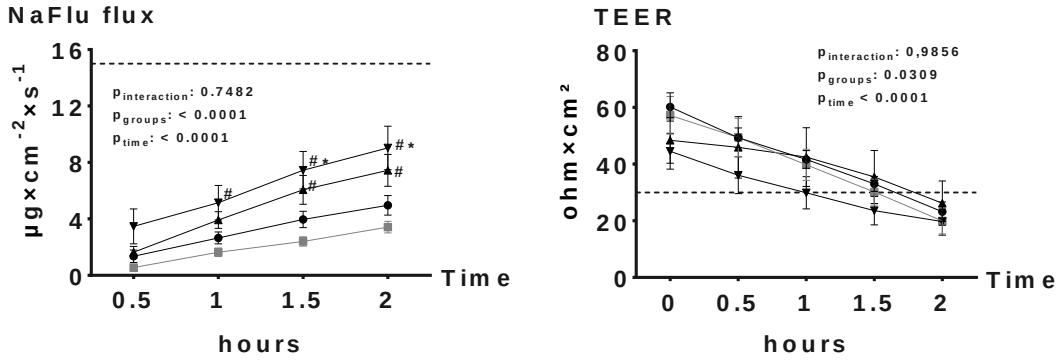

Figure 3 NaFlu flux: Evolution of sodium fluorescein (NaFlu, 1 mg/mL) flux, --- NaFlu flux criteria at 15 µg×cm^{-2}×s^{-1} at t=2 h; TEER: Evolution of trans-epithelial electrical resistance, --- TEER criteria at 30 Ω×cm² at t=0, in Ussing chamber during 2 h. ● Control (n = 19; N = 17), ■ 0.1 µM (n = 7; N = 5), ▲ 10 µM (n = 7; N = 5), ▼100 µM (n = 6; N = 5). *p < 0.05 *vs* control; # p < 0.05 *vs* 0.1 µM GSNO; two-way ANOVA (groups and time).

Table 1 Evolution of the apparent permeability coefficient (Papp) of sodium fluorescein (NaFlu, 1 mg/mL). *statistic difference *vs* Control; # statistic difference *vs* 100 µM; p<0.05; one-way ANOVA

GSNO(µM) / Time	0	0.1	10	100
0.5 h – 1 h	1.1±0.2	0.7±0.1#	1.7±0.2	1.9±0.5
1 h – 2 h	2.0±0.3	1.4±0.2#	3.0±0.6	3.6±0.6
0.5 h – 2 h	1.7±0.2	1.2±0.1#	2.6±0.4	3.1±0.5*

Cell junction proteins expression after GSNO treatment in Ussing Chamber

The result was shown in the Figure 4. The relative amount of Claudin-1 and Occludin did not significantly change in tissue during the experiment (Control) when compared with fresh tissue (WT). The similar result was observed with E-cadherin proteins. Unexpectedly, the apparent molecular weight of E-cadherin appears to be smaller in the control tissue compared with fresh tissue, which might be linked with protein degradation in this *ex vivo* model.

No significant changes in the amount of this cell junction proteins were observed with both low and high concentration of NO. Despite this lack of statistical significance, we noted that the amount of occludin is reduced by 50 % in the presence of 100 μM of GSNO.

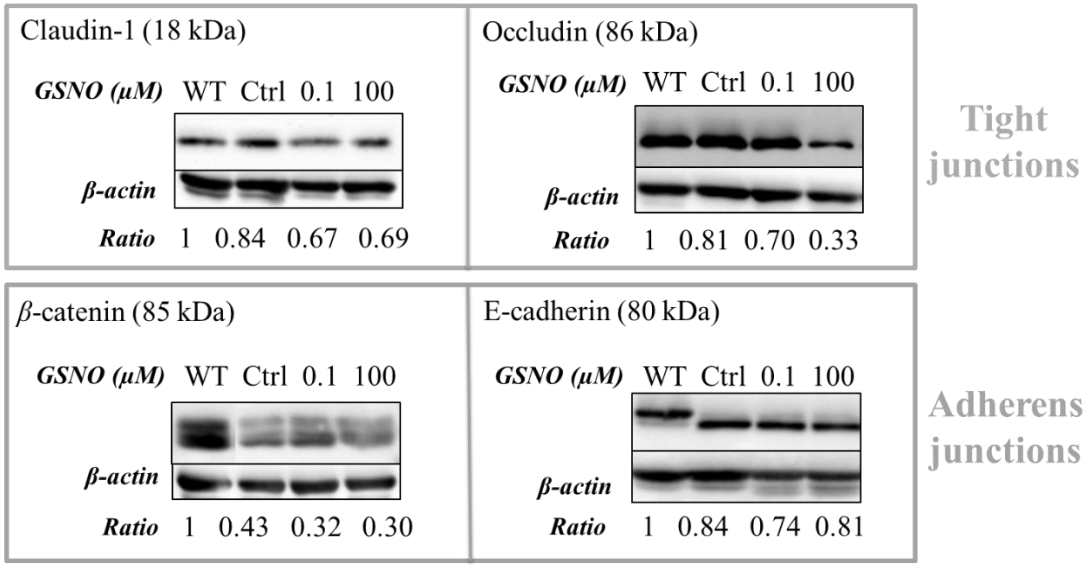

Figure 4 Expression of cell junction proteins by western blotting after different concentration of GSNO exposure in Ussing chamber for 2 h. The ratio value was normalized results from WT; two-way ANOVA (groups and proteins), n=5. WT: wild type, ctrl: control in Ussing chamber system.

Discussion and conclusion

The Ussing chamber system is a simple, but powerful technique to investigate the intestinal permeability. In the present study, Ussing Chamber system was chosen to investigate the GSNO effects on intestinal barrier integrity by following the intestinal permeability to a paracellular marker (NaFlu) because of its convenience, effectiveness (6 tissues in parallel) and better mimicking *in vivo* environment in compared with Caco-2 cells monolayer. Upon removal from the animal, an *ex vivo* intestinal preparation and incubation in Krebs-Henseleit buffer has limited viability (Clarke, 2009). Thus, the limitation of this system is the difficulties to ensure the tissue viability. There are not uniform quality criteria to control the tissue viability in the literatures. TEER and paracellular marker permeability is mostly used as the main indicators. For example,

TEER remaining within 15% of the starting value was considered as indicator of viable tissue, and tissues were excluded where TEER fell by more than this in some literatures (Stephens *et al.*, 2002, Fortuna *et al.*, 2012). Marker permeated less than 0.01% was indicated in the literature as tissue viability indicator (Woitiski *et al.*, 2011). There are not standard criteria. Thus, to ensure that we can obtain the reliable result with Ussing chamber system, the validation of quality criteria was performed by both TEER value and paracellular marker (NaFlu) permeability. The result indicated that the tissue with a TEER value lower than 30 $\Omega \cdot cm^2$ at the beginning of experiment or a decrease more than 50% of the initial TEER value after 0.5 h should be discarded because of destroyed barrier integrity during the preparation. To control the tissue viability during experiment, the NaFlu permeability in the control group at every experiment without any treatment was used as a reference. If the flux of NaFlu for control group at 2 h was less than 15 $\mu g \cdot cm^{-2} \cdot s^{-1}$, the data from the whole experiment was exclude. Therefore, all the experiments and data were performed under these quality criteria to get reliable and analyzable result.

The dynamic equilibrium between all the actors of the barrier and the interactions between mucus, epithelial cells, microbiota and immune defense, are essential for the maintenance of the barrier integrity and the intestinal homeostasis. The disruption of this homeostasis induced an increase of the permeability, and leads to an inflammation and strong damages of the mucosa which is not able anymore to ensure the vital function of protection and absorption. It is what happened in the context of Inflammatory Bowel Diseases (IBD).

Our study showed that a low concentration of GSNO in the luminal compartment of the using chamber tend to delay and limit the permeability of the intestinal mucosa while high concentration aggravates the permeability. GSNO protective action on intestinal barrier was published by different authors (Savidge *et al.*, 2007, Cheadle *et al.*, 2013, Li *et al.*, 2016). Enteric glia cells derived GSNO was identified by Savidge in 2007 as a potent inducer of intestinal barrier function *ex vivo* and *in vivo* and of attenuated tissue

inflammation by an increased expression of perijunctional F-actin and tight-junction–associated proteins zonula occludens-1 and occludin (Savidge *et al.*, 2007). Same idea was published by Cheadle and co-workers in 2013 with *in vitro* cells model. GSNO secreted by enteric glia cells prevented intestinal barrier failure after injury and improved expression and localization of tight junction proteins including ZO-1 and occludin (Cheadle *et al.*, 2013). Li and co-workers showed that exogeneous femoral venous injected GSNO protected intestinal barrier under endotoxin-induced inflammation by preserving tight junction protein ZO-1 expression and reducing inflammation marker releasing (IL-1β and TNF-α) through inhibiting NF-κB pathway (Li *et al.*, 2016). But all these GSNO can be identified as a source from mucosal side of intestine. Thus, the present work is the first one that mentioned about the GSNO derived from oral administration route (luminal side) effects on intestinal integrity. The permeability study and western blot results suggested that GSNO can affect intestinal barrier in a dose-dependent manner, which proved the same idea as mentioned by Savidge (Savidge *et al.*, 2007). This is in accordance with our hypothesis that the delivery of a low concentration of NO donor on the luminal side of the intestinal mucosa might be a good approach to prevent a disruption of the mucosal barrier integrity. The exact mechanism hasn't been investigated yet, but it could be associated with hypothetic action like post-translational modifications of proteins caused by addition of NO (Figure 5).

We speculate that different NO concentrations may cause different post-translational modifications of proteins according to the literatures. In the presence of low concentration of NO (0.1 μM), it might be a *S*-nitrosation caused by an interaction between NO and cystein residue of protein. The final product RSNO (*S*-nitrothione) could also act as a storage form of NO. In contrast, in the presence of high concentration of NO (100 μM) with oxidative stress condition, there might exist nitration of proteins on the tyrosine residue, which may provoke deleterious effect such as an increase of the intestinal permeability or a modulation of the activity of the immune response effectors

and finally trigger the pathological inflammation process. Through different literatures, different proteins could be the interesting targets of different post-translational modification way caused by NO, which may finally modulate the intestinal barrier integrity.

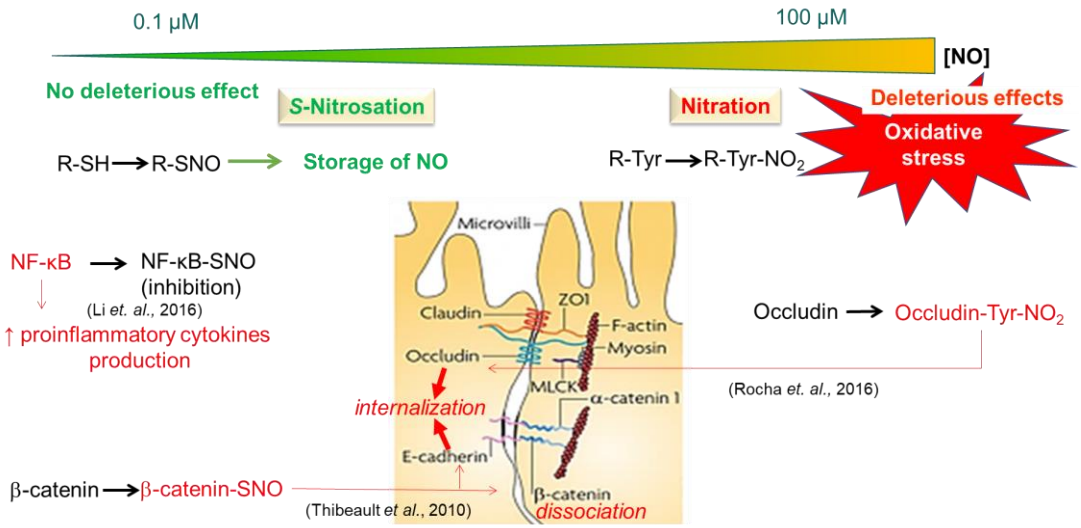

Figure 5 Possible mechanism of intestinal barrier integrity modulation by NO.

NF-κB ability to induce the production of proinflammatory cytokines is reduced after a *S*-nitrosation step and thus this might be associated with the potential protective action in intestinal barrier integrity of NO (Li *et al.*, 2016). Another target of *S*-nitrosation caused by NO could be adherens junction proteins. As reported in literature, *S*-nitrosation of β-catenin leads to changes in microvascular permeability after administration of vascular endothelial growth factor (VEGF) for 15 min (Thibeault *et al.*, 2010): *S*-nitrosation amino acid of β-catenin was Cysteine 619 which is located at the interaction site of β-catenin with VE-cadherin. Its *S*-nitrosation causes dissociation of the complex and an increase in microvascular permeability (Thibeault *et al.*, 2010). p120-catenin was considered as another target of *S*-nitrosation (Marin *et al.*, 2012). Cys 579 as the main *S*-nitrosated- residue was the responsible amino acid in p120-catenin. Cys 579 is also located in the interaction site with VE-cadherin. Thus, *S*-nitrosation regulated protein-protein interactions and promoted the dissociation of the adherens

junction complex. *S*-nitrosation of β-catenin and p120-catenin destabilizes the adherens junction complex, which leads to changes in the localization and interaction between these proteins at the adherens junction, which finally induce the internalization of VE-cadherin. All these actions were well investigated within microvascular. Thus, we hypothesize that similar mechanism could occurs in intestinal mucosa. *S*-nitrosation of β-catenin caused by NO incubation leads to E-cadherin internalization, which finally increased the intestinal permeability.

Occludin was reported that could be nitrated by NO through the tyrosine residue, which may finally lead to the internalization and destroy the tight-junction between epithelial cells (Rocha *et al.*, 2016).

For further study of mechanism exploration, more work need to be done, such as identification of post-translational modifications (*S*-nitrosation or nitration) targets and quantification of the modification level to understand the modulation process of the intestinal barrier integrity in the presence of NO.

To conclude about the present study, different GSNO concentrations (0.1, 10 and 100 μM) were added in the luminal side of intestine to investigate its effect on intestinal barrier integrity in Ussing chamber system by following the intestinal permeability to a paracellular marker (NaFlu). The preliminary mechanism was studied by western blot to follow the expression of tight junction proteins (ZO-1 and occludin) and adherens junction proteins (E-cadherin and β-catenin). Finally, a dose-dependent effect was observed for GSNO effects on intestinal barrier integrity. High concentration of GSNO (100 μM) showed deleterious impact in intestinal barrier while low concentration of GSNO (0.1 μM) preserving intestinal permeability with healthy intestine tissue. Through the current study, we can conclude that the secure concentration of GSNO for an application of IBD prevention should be less than 0.1 μM. In order to confirm the feasibility of luminal GSNO preventing intestinal barrier disruption, further study is necessary to continue with an *ex vivo* inflammation model that can induce the disruption of intestinal barrier (need to be explored, because no existing model in the literatures)

or with a proposal of formulation to oral deliver GSNO in an *in vivo* inflammation model which has been well investigated. Meanwhile, the mechanism of GSNO regulating intestinal barrier integrity will also be studied by following the GSNO metabolism (involved enzymes) in contact with intestine tissue and the functionalization of GSNO by post-translation (nitrosation/nitrosylation/nitration) of proteins. Therefore, an innovative chronic treatment of IBD – in order to prevent relapses of inflammation - may rely on supplementation of small amounts of nitric oxide to preserve the intestinal barrier integrity.

References

Cheadle, G.A., Costantini, T.W., Lopez, N., Bansal, V., Eliceiri, B.P. & Coimbra, R., 2013. Enteric glia cells attenuate cytomix-induced intestinal epithelial barrier breakdown. *PloS one,* 8**,** e69042.

Clarke, L.L., 2009. A guide to Ussing chamber studies of mouse intestine. *Am J Physiol Gastrointest Liver Physiol,* 296**,** G1151-66.

Clère, N., Faure, S. & Guerriaud, M., 2014. *Bases fondamentales en pharmacologie: Sciences du médicament*: Elsevier Masson.

Dattilo, J.B. & Makhoul, R.G., 1997. The role of nitric oxide in vascular biology and pathobiology. *Annals of vascular surgery,* 11**,** 307-314.

Forsgård, R., Korpela, R., Stenman, L., Österlund, P. & Holma, R., 2014. Deoxycholic acid induced changes in electrophysiological parameters and macromolecular permeability in murine small intestine with and without functional enteric nervous system plexuses. *Neurogastroenterology & Motility,* 26**,** 1179-1187.

Fortuna, A., Alves, G., Falcao, A. & Soares-Da-Silva, P., 2012. Evaluation of the permeability and P-glycoprotein efflux of carbamazepine and several derivatives across mouse small intestine by the Ussing chamber technique. *Epilepsia,* 53**,** 529-38.

Hooper, L.V. & Macpherson, A.J., 2010. Immune adaptations that maintain homeostasis with the intestinal microbiota. *Nature reviews. Immunology,* 10**,** 159.

Kim, Y.S. & Ho, S.B., 2010. Intestinal goblet cells and mucins in health and disease: recent insights and progress. *Current gastroenterology reports,* 12**,** 319-330.

Kochar, N.I., Chandewal, A.V., Bakal, R.L. & Kochar, P.N., 2011. Nitric oxide and the gastrointestinal tract. *Int. J. Pharmacol,* 7**,** 31-39.

Kolios, G., Valatas, V. & Ward, S.G., 2004. Nitric oxide in inflammatory bowel disease: a universal messenger in an unsolved puzzle. *Immunology,* 113**,** 427-437.

Li, Z., Zhang, X., Zhou, H., Liu, W. & Li, J., 2016. Exogenous *S*-nitrosoglutathione attenuates inflammatory response and intestinal epithelial barrier injury in endotoxemic rats. *Journal of Trauma and Acute Care Surgery,* 80**,** 977-984.

Marin, N., Zamorano, P., Carrasco, R., Mujica, P., Gonzalez, F.G., Quezada, C., Meininger, C.J., Boric, M.P., Duran, W.N. & Sanchez, F.A., 2012. *S*-Nitrosation of beta-catenin and p120 catenin: a novel regulatory mechanism in endothelial hyperpermeability. *Circ Res,* 111**,** 553-63.

Parent, M., Dahboul, F., Schneider, R., Clarot, I., Maincent, P., Leroy, P. & Boudier, A., 2013a. A complete physicochemical identity card of *S*-nitrosoglutathione. *Current Pharmaceutical Analysis,* 9**,** 31-42.

Parent, M., Dupuis, F., Maincent, P., Vigneron, C., Leroy, P. & Boudier, A., Year. Quel avenir en thérapeutique cardiovasculaire pour le monoxyde d'azote et ses dérivés?ed.^eds. *Annales Pharmaceutiques Françaises*Elsevier, 84-94.

Payros, D., Secher, T., Boury, M., Brehin, C., Ménard, S., Salvador-Cartier, C., Cuevas-Ramos, G., Watrin, C., Marcq, I. & Nougayrède, J.-P., 2014. Maternally

acquired genotoxic Escherichia coli alters offspring's intestinal homeostasis. *Gut Microbes,* 5**,** 313-512.

Potten, C.S., Owen, G. & Booth, D., 2002. Intestinal stem cells protect their genome by selective segregation of template DNA strands. *J Cell Sci,* 115**,** 2381-2388.

Rocha, B.S., Correia, M.G., Fernandes, R.C., Goncalves, J.S. & Laranjinha, J., 2016. Dietary nitrite induces occludin nitration in the stomach. *Free Radical Research,* 50**,** 1257-1264.

Savidge, T.C., Newman, P., Pothoulakis, C., Ruhl, A., Neunlist, M., Bourreille, A., Hurst, R. & Sofroniew, M.V., 2007. Enteric glia regulate intestinal barrier function and inflammation via release of *S*-nitrosoglutathione. *Gastroenterology,* 132**,** 1344-1358.

Srinivasan, B., Kolli, A.R., Esch, M.B., Abaci, H.E., Shuler, M.L. & Hickman, J.J., 2015. TEER measurement techniques for *in vitro* barrier model systems. *Journal of laboratory automation,* 20**,** 107-126.

Stephens, R.H., Tanianis-Hughes, J., Higgs, N.B., Humphrey, M. & Warhurst, G., 2002. Region-dependent modulation of intestinal permeability by drug efflux transporters: *in vitro* studies in mdr1a(-/-) mouse intestine. *J Pharmacol Exp Ther,* 303**,** 1095-101.

Thibeault, S., Rautureau, Y., Oubaha, M., Faubert, D., Wilkes, B.C., Delisle, C. & Gratton, J.-P., 2010. *S*-Nitrosylation of β-catenin by eNOS-derived NO promotes VEGF-induced endothelial cell permeability. *Molecular cell,* 39**,** 468-476.

Turner, J.R., 2000. Show me the pathway!: Regulation of paracellular permeability by Na+-glucose cotransport. *Advanced drug delivery reviews,* 41**,** 265-281.

Turner, J.R., 2009. Intestinal mucosal barrier function in health and disease. *Nature reviews. Immunology,* 9**,** 799.

Woitiski, C.B., Sarmento, B., Carvalho, R.A., Neufeld, R.J. & Veiga, F., 2011. Facilitated nanoscale delivery of insulin across intestinal membrane models. *International journal of pharmaceutics,* 412**,** 123-131.

Chapter 3.
Formulations of GSNO nanocomposites adapted to oral delivery

3.1 Introduction

Concentration of GSNO is crucial for its application in pharmacology, as previously described in chapter 2. Thus, formulations are necessary to control GSNO concentration at target site. As showed in Table 2 from chapter 1, there is not a lot of research about GSNO formulation. Among all the development, they are mostly concentrated on topical treatment for wound healing (Shishido *et al.*, 2003, Seabra *et al.*, 2004a, Seabra and De Oliveira, 2004, Seabra *et al.*, 2004b, Seabra *et al.*, 2005, Simoes and de Oliveira, 2010, Vercelino *et al.*, 2013) or implants for vascular disease treatment (Heikal *et al.*, 2009, Heikal *et al.*, 2011, Acharya *et al.*, 2012, de Mel *et al.*, 2014, Parent *et al.*, 2015a, Parent *et al.*, 2015b). Few publications introduced about GSNO formulations for oral treatment (Wu *et al.*, 2016). In fact, oral administration is the best choice for chronic and incurable disease such as cardiovascular disease and IBD, because of its apparent advantages, such as convenience, cost-effectiveness, good patient compliance, non-injections, and decreased risk of infection (Sarmento *et al.*, 2007). However, the unique article mentioned about GSNO oral delivery was published by our laboratory (Wu *et al.*, 2016). The nanocomposite particles were developed based on natural polymers alginate and chitosan with an enhanced GSNO bioavailability adapted to oral administration for the application of cardiovascular disease (Wu *et al.*, 2016). The encapsulation strategy is based on a double incorporation: GSNO is firstly entrapped in nanoparticles, followed by a second encapsulation in polymer matrix. This double encapsulation provides not only a strong protection of GSNO but also sustained release over 24 h. Therefore, the strategy of polymer nanocomposites is good candidate for GSNO oral delivery.

As described in chapter 1, polymer nanocomposites showed lots of advantages, such as improved drug bioavailability and efficiency, controlled of pharmacokinetics, targeted delivery as well as the overcoming of obstacles arising from low drug solubility, degradation, fast clearance rated, relatively short biological activity and inability to cross biological barriers. All these advantages of polymer nanocomposites make it an

adapted delivery system for fragile molecules, such as GSNO. As delivery vehicles of GSNO, nanoplatforms and polymer matrix are not conflict but complementary. Nanoplatforms were capable of efficient entrapment of drug but quick release within 3 h (Wu *et al.*, 2015a). Whereas, polymer matrix presents prominent sustained release as well as stabilization effect, but are limited by burst release. Application of polymer nanocomposites for GSNO delivery represent a promising strategy to merge the advantages of nanoplatforms and polymer matrix in one system to improve the therapeutic effect.

To develop GSNO formulation adapted to oral administration for IBD application, several requirements need to be followed:

1) Polymer adapted to oral route
2) Size less than 100 μm (adapted to gavage experiment of rat)
3) Efficient GSNO encapsulation
4) Sustained release profile
5) Local delivery in intestine (mucoadhesion)

To answer to the first requirement, different polymers classically used by industry (pharmaceutic or food) and authorized by authorities were preferred.

Eudragit® RL is synthetic cationic copolymers of ethyl acrylate, methyl methacrylate and a low content of methacrylic acid ester with quaternary ammonium groups (Patra *et al.*, 2017). It's a cationic and non-degradable polymer which is not soluble in water (Kadian and Harikumar, 2016). Eudragit® RL characterized with mucoadhesion property is mainly used for sustaining drug release in diverse drug delivery systems like nanoparticles (Gandhi *et al.*, 2014, Wu *et al.*, 2015a), mucoadhesive tablets (Singh and Rana, 2013) and patches (Pandey *et al.*, 2013), solid dispersions (Varshosaz *et al.*, 2006, Dahiya *et al.*, 2008, Sahoo *et al.*, 2009). Singh *et al* investigated the effect of iron oxide in the development of mucoadhesive tablets of cinnarizine utilizing Eudragit®RL (Singh and Rana, 2013). Eudragit®RL and iron oxide showed potential for gastroretentive and mucoadhesive drug delivery systems. Pandey *et al* tried site-

specific drug delivery by formulating bi-layered gastro-retentable and mucoadhesive patch (stomach) (Pandey *et al.*, 2013). Both Eudragit®RS and RL were used for formulation of patch. Patches could achieve sustained drug release up to 12 h, with mucoadhesion. Sahoo *et al* formulated solid dispersion of verapamil utilizing Eudragit®RL or Kollidon SR to control drug release (Sahoo *et al.*, 2009) and prolonged the drug release up to 12 h was obtained based on Eudragit®RL.

Eudragit®E is synthetic cationic copolymer based on dimethylaminoethyl methacrylate, butylmethacrylate and methyl methacrylate (Patra *et al.*, 2017). It is soluble in gastric pH up to 5.0. Eudragit®E has characteristic properties such as low viscosity, high pigment binding capacity, good adhesion and low polymer weight. It has been widely used in oral delivery systems such as nanoparticles (Eerikainen and Kauppinen, 2003, Khan and Schneider, 2014, Chaurasia *et al.*, 2016), microparticles(Shishu *et al.*, 2010), solid dispersions (Chella *et al.*, 2016, Dangre *et al.*, 2016), tablets and films (Shishu *et al.*, 2009, Shams *et al.*, 2010, Brniak *et al.*, 2015), solid complex (Moustafine *et al.*, 2005) and pellets (Avachat and Shinde, 2016). Chaurasia *et al* prepared Eudragit®E nanoparticle by emulsification-diffusion-evaporation method to enhance the bioavailability of curcumin (Chaurasia *et al.*, 2016). Brniak *et al* developed Eudragit®E coated microparticle to obtain an efficient taste masking of a bitter drug substance (Brniak *et al.*, 2015). Avachat *et al* fomulated pellets coated with Eudragit®E 100 and Eudragit®L 100 multi-particulates systems for colon delivery (Avachat and Shinde, 2016).

Alginate is an anionic polysaccharide linear unbranched polymer which contains varying amounts of 1,4'- linked β-D-mannuronic acid and α-L-guluronic acid residues, isolated from brown seaweed (Phaeophyceae) (Tonnesen and Karlsen, 2002). Alginate has several unique properties that have enabled it to be used as a matrix for the entrapment and/or delivery of a variety of bioactive compounds. These properties include: (i) mucoadhesive, biodegradable and low toxicity properties (Sonavane and Devarajan, 2007, Simonoska Crcarevska *et al.*, 2008); (ii) pH-sensitive property (not

soluble in gastric pH less than 3) (Aguero *et al.*, 2017); (iii) a mild room temperature encapsulation process free of organic solvents(Gombotz and Wee, 2012). pH-sensitivity and mucoadhesiveness presented the key properties for oral intestine application.

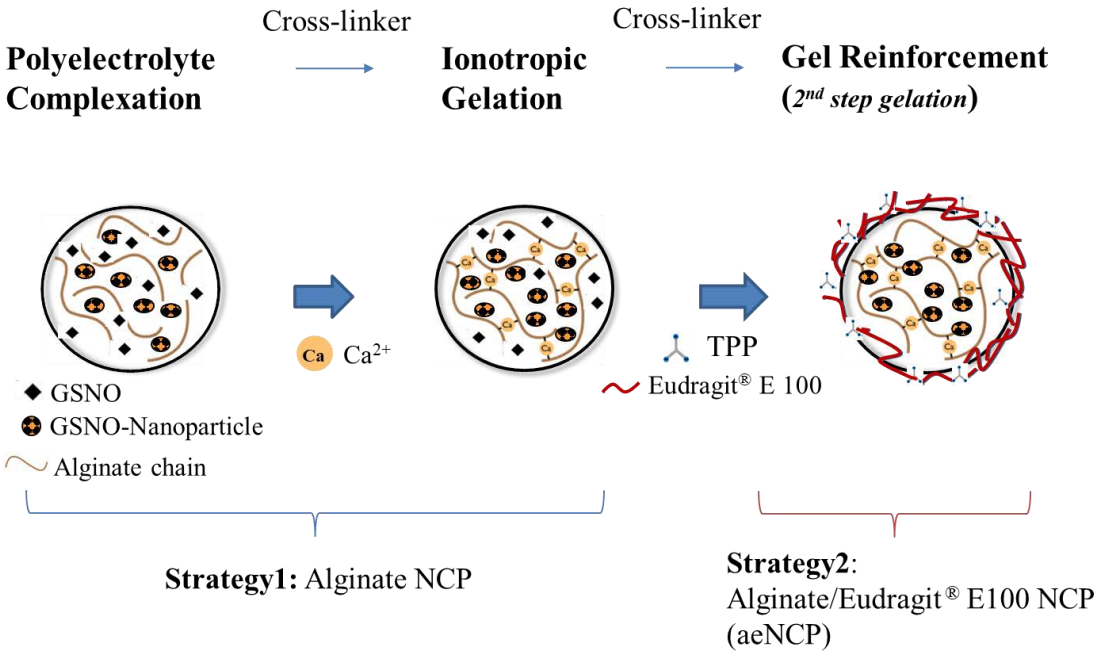

Figure 23 Strategies of polymer matrix

In our project, we purchase the GSNO nanocomposite particles formulation We focused on the polymer matrix composition and behavior of this nanocomposite particles, by two different strategies (Figure 23).

Strategy1: Polyelectrolyte complexation is the first step of this matrix establishment. It consists in electrolyte interactions between positively charged nanoparticles and negatively charged alginate chains. A cross-linker can be added in the following step to reinforce the polymer matrix structure. In our case, it is calcium ions. These divalent ions can act as a bridge between alginate chains, which can result in tighter structure. The ionotropic gelation process is not complicated but required many steps which can lead to GSNO degradation, GSNO leakage and finally decrease the encapsulation efficiency. The proposition of a simpler process based on polyelectrolyte complexation can optimized alginate nanocomposite. A comparison of both process will be presented in the first part of this chapter (article submitted in Journal of Microencapsulation in

September 2017).

Strategy2: In parallel, another strategy was conducted to optimize the polymer matrix of the nanocomposites. In a previous study from our team, a complementary "coating" of Ca-alginate nanocomposite with chitosan was proposed (Wu *et al.*, 2016). This natural well-known polymer, form delivery system by ionotropic gelation process and cross-linking with sodium Tripolyphosphate (TPP) (Yang *et al.*, 2009). Chitosan with positive charge can also interact directly with alginate chain (Simonoska Crcarevska *et al.*, 2008). Chitosan was reported to reduce the transepithelial electrical resistance and to open tight junction between epithelial cells transiently, which resulted in intestinal drug absorption enhancement (Dodane *et al.*, 1999, Thanou *et al.*, 2001, Wu *et al.*, 2016). This tight-junction opening is not desirable in our case because totally opposite to the aim of barrier reinforcement. Fragile intestine in presence of chitosan could be further overrun by commensal bacteria which could finally induce inflammation. Furthermore, the aim of present GSNO delivery is to localize the drug in intestine instead of permeation through intestine. Taking into consideration of above reasons, Eudragit®E 100 which present similar properties and widely used for colon delivery was used to replace chitosan to conserve the gel reinforcement property and achieve GSNO local effect in intestine. Alginate/Eudragit®E 100 nanocomposite formulation will be presented as complementary data in this chapter:

3.2 Alginate nanocomposite particles optimization

The major aims of the first strategy based on alginate nanocomposite particles are: 1) simplify the preparation process; 2) increasing encapsulation efficiency; 3) achieve GSNO local effect in intestine.

3.2.1 Pre-optimization

GSNO-loaded alginate nanocomposite particles (GSNO-aNCP) was formulated as described previously (Wu *et al.*, 2015b). Briefly, GSNO was firstly encapsulate in to Eudragit®RL nanoparticle (NP) by double-emulsion and solvent-evaporation method.

Briefly, an aqueous solution of GSNO (10 mg) in 500 mL of 0.1% (w/w) Pluronic1 F-68 solution was emulsified by sonication for 60s (100% amplitude, Vibra-cell™, France) in ice bath in 5 mL of dichloromethane (DCM) containing 500 mg of Eudragit® RL PO. This primary emulsion was further emulsified in 20 mL of 0.1% (w/w) Pluronic1 F-68 solution by 30 s sonication (30 W, Vibra-cell™, France), in ice bath to form a water–oil–water emulsion. Finally, the GSNO-NP were hardened by solvent evaporation. The second encapsulation was based on ionotropic gelation of alginate with Ca^{2+}. Sodium alginate (20 mg) was completely dissolved in 20 mL GSNO-NP suspension with magnetic agitation at a speed 100. On ice, 1.5 mL of calcium chloride solution ($CaCl_2$, 2 M) was added dropwise into this mixture to cross-link the alginate. During this step, this mixture was homogenized by sonication (40 W, ultrasonic processor, France).

Finally, two consecutive encapsulation steps are performed in this process: GSNO is firstly encapsulated in NP and GSNO-NP are encapsulated in polymer matrix. During the second step of encapsulation (NP into polymer matrix), a part of non-encapsulating GSNO can be entrapped in the matrix, increasing the final GSNO loading. However, in reality, a half percentage of encapsulated GSNO (around 20% in total GSNO) was leaked after the second encapsulation step. We speculated that GSNO was diffused during strong energy intervention to form the polymer matrix such as strong mechanical agitation to dissolve sodium alginate and ultrasonication step during Ca^{2+} cross-linking. GSNO could also diffused in the aqueous environment or could be degraded during the formulation process. Therefore, a simple experiment was conducted to confirm this hypothesis. GSNO encapsulation efficiency (EE) was measured at three stages during the process: 1) after nanoparticles preparation (at the end of the first encapsulation step); 2) after alginate dissolution in NP suspension; 3) after Ca^{2+} cross-linking (at the end of the process). The result showed that around 10% GSNO was diffused at stage “2)-alginate dissolution” and 7% GSNO at stage “3) cross-linking”, respectively. No increase of nitrite ions level was remarked. These results confirm the hypothesis of a GSNO diffusion in the aqueous environment, a leakage outside the delivery system.

Thus, different attempts were performed to optimize EE and avoid the GSNO leakage during the process (Table 3). The EE in the table was calculated by indirect method as below：

$$\mathrm{EE} = \frac{initial\ GSNO\ amount - unencapsulated\ GSNO\ amount}{initial\ GSNO\ amount} \times 100\%$$

The first attempt was to reinforce the gel by increasing alginate concentration. 40 mg alginate was used instead of 20 mg. Finally, no increase GSNO encapsulation efficiency was obtained (around 20% GSNO diffused compared with the EE of NP-43%).

The second attempt was to avoid the leakage during alginate dissolution step. Two strategies were developed. Firstly, sodium alginate was dissolve in only 5 mL nanosuspension (1/4 of final volume). For a homogeneous dissolution of alginate, a strong agitation was performed (magnetic agitation with a speed of 1300 rpm for 10 min). The remaining nanosuspension was added after alginate was totally dissolved with a reduced agitation speed (200 rpm for 5 min). The second one is dissolving sodium alginate in 10 mL ultrapure water instead of nanosuspension, at the same time different concentration of Ca^{2+} was tested (2 M and 0.05 M). Finally, for the first method we got EE of 37.7%, for the second one, for 2 M and 0.05 M Ca^{2+} concentration respectively, which decrease the GSNO diffusion with losing less than 15% of GSNO encapsulation. However, there are apparent drawbacks for these two methods (1. dissolving alginate in only one part of nanosuspension 2. dissolving alginate in water): for the first one, it's not so easy to dissolve alginate in only 5 mL suspension; for the second one, the final particle sizes were more than 100 μm, which is not adapted for gavage experiment.

The third attempt is to avoid leakage during cross-linking step. We continued to optimize the formulation based on the less complicated process (method 2 in first idea) with improved GSNO leakage. A gentle energy intervention, magnetic agitation was used. In order to homogenize the mixture in a better way to obtain adapted particle size

(less than 100 μm) after reducing the intervention energy level, lower concentration but higher volume of Ca^{2+} was introduced, at the same time, the order of mixing was reversed. EE of 35.9% and 37.1% were achieved for 0.1 and 0.05 M Ca^{2+} respectively. Finally, the method not only obtained smaller particle size (86.1 μm and 84.4 μm) but also improved the process by decreasing GSNO leaking around 5%.

The fourth attempt is to remove Ca^{2+} cross-linking step directly. Because as mentioned in chapter 1, divalent ions may induce the breakdown of S-NO bond. In addition, alginate chain with negative charge can interact direct with the positively charged NP surface which was formed by Eudragit®RL PO by polyelectrolyte complexation. Thus, with a direct mixing of alginate solution with NP suspension can be good method to conserve the GSNO encapsulation efficiency in a maximum way. Different energy intervention methods were involved for the development of this attempt: ultrasonication and mild agitation. The result showed that 48.9% of GSNO EE and acceptable size (66 μm) were observed with a mild agitation while only 30.5% of GSNO EE was obtained with ultrasonication.

To conclude, the last trial of alginate nanocomposite particles based on polyelectrolyte complexation with a simple process improves the GSNO encapsulation efficiency in a best way. More details about physical-chemical characterization and *in vitro* evaluation of this formulation is introduced in the following context with a submitted paper. In this paper, alginate nanocomposite particles base on ionotropic gelation was also fully characterize to compare with the optimize method of polyelectrolyte complexation.

Table 3 Optimization of alginate nanocomposite

nanosuspension	Alginate dissolution		$CaCl_2$ cross-linking		mixing order	intervention method	size (μm)	uniformity	EE (%)	n	aim
	weight (mg)	dissolving medium	concentration (M)	volume (mL)							
20 mL nanosuspension	20	20 mL nanosuspension	2	2	$CaCl_2$ / alginate	ultrasonication	23.6 ± 4.7	0.479 ± 0.058	21.6 ± 3.3	3	obtain stronger gel
	40						16.8	0.575	23.2	1	
15mL + 5mL (alginate dissolution)	20	5 mL nanosuspension	2	2	$CaCl_2$ / alginate	ultrasonication	47.5	1.8	37.7	1	Avoid GSNO leakage during alginate dissolution step
20 mL nanosuspension	20	10 mL water	2	2	$CaCl_2$ / alginate	magnetic agitation; 1000 rpm, 3 min	124	2.37	30	1	
			0.05				236 ± 4	0.661 ± 0.051	32.9 ± 1.2	2	
20 mL nanosuspension	20	10 mL water	0.1	20	alginate/ $CaCl_2$	magnetic agitation; 1000 rpm, 3 min	86.1	0.895	35.9	1	Avoid GSNO leakage during cross-linking step
			0.05				84.4	1.06	37.1	1	
20 mL nanosuspension	20	10 mL water	-	-	-	ultrasonication	4.2	0.398	30.5	3	Simpler process
						mild agitation	66 ± 2	0.980 ± 0.043	48.9 ± 7.1	1	

3.2.2 *S*-nitrosoglutathione loaded alginate nanocomposite particles development

Two different preparation methods were introduced to form the outer polymer matrix: ionotropic gelation and polyelectrolyte complexation. The comparison of physical-chemical characterization, *in vitro* release and swelling study, *in cellulo* study of permeability through Caco-2 cells monolayer has been done and presented in the following article (submitted to Journal of Microencapsulation).

Single step alginate nanocomposite formulation for *S*-nitrosoglutathione intestine delivery: an *in vitro* and *in cellulo* characterization

Hui Ming[a], Franck Hansmannel[b], Romain Schmitt[a], Isabelle Raeth-Fries[a], Wen Wu[a,d], Caroline Gaucher[a], Xian-Ming Hu[c], Philippe Maincent[a], Anne Sapin-Minet[a]*

[a] *University of Lorraine, CITHEFOR EA 3452; Faculty of Pharmacy, BP 80403 Nancy Cedex, France.*

[b] *University of Lorraine, NGERE Inserm U954; Faculty of Medicine, Vandoeuvre-lès-Nancy, France.*

[c] *State Key Laboratory of Virology, Ministry of Education Key Laboratory of Combinatorial Biosynthesis and Drug Discovery, Wuhan University, School of Pharmaceutical Sciences, Wuhan, P. R. China.*

d Chongqing Key Laboratory of Natural Product Synthesis and Drug Research, School of Pharmaceutical Sciences, Chongqing University, Chongqing, P.R. China.

*corresponding author: Anne SAPIN-MINET

CITHEFOR EA 3452

Faculté de Pharmacie

5, rue Albert Lebrun - BP 80403

F-54001 Nancy Cedex, France

Tel: +33 (0)3 83 64 73 30

Email: anne.sapin@univ-lorraine.fr

Abstract: *S*-nitrosoglutathione (GSNO) oral administration represents a novel strategy to prevent inflammation bowel diseases (IBD) relapses. In this project, the development of nanocomposite particles (NCP) encapsulating GSNO and adapted to the oral route was proposed with GSNO protection, controlled delivery and local effects in intestine as major requirements. Polymeric (Eudragit®RL) GSNO nanoparticles were included in a polymer (alginate) matrix based on two different methods (ionotropic gelation and polyelectrolyte complexation*). In vitro* GSNO–NCP formulated by single-step polyelectrolyte complexation leaded to a high GSNO loading, but no sustained release. Nevertheless, cytotoxicity and GSNO permeability performed on intestinal Caco-2 cells demonstrated for both processes their potential for GSNO oral delivery, with sustained release and local retention for 4 h. Thus, GSNO formulation by simple step of polyelectrolyte complexation between Eudragit®RL nanoparticles and alginate matrix can be further proposed for GSNO release and IBD prevention.

Keywords: nanocomposite, *S*-nitrosoglutathione, alginate, oral administration, sustained release, local effect.

Introduction

Inflammatory bowel diseases (IBD), in which the most known subtypes are Crohn's disease and ulcerative colitis, are disabling pathologies affecting young patients caused by the conjunction of genetic susceptibility, environment factors, intestinal microbial flora alteration and immune dysfunction. IBD current treatment present the particularity that most of the current agents act by down regulating chronic inflammation in the intestine mucosa but cannot cure the disease (Kirchgesner *et al.*, 2017, Schumacher *et al.*, 2017). Conventional drugs for the treatment of IBD include aminosalicylates, corticosteroids, antibiotics and immunosuppressive agents, which are necessarily long term administrated and consequently lead to adverse effects (Pithadia and Jain, 2011, Neurath, 2017). Novel therapeutic agents like anti-Tumor Necrosis Factor (anti-TNF) have potent anti-inflammatory effects but a loss of response is frequent over time and only one third of patients achieve clinical remission after one year (Pithadia and Jain, 2011, Neurath, 2017). It is therefore a real challenge to develop novel strategies for decreasing relapses frequency and improving the quality of patient's life.

Nitric oxide (NO) is a free-radical gas and one of the smallest endogenous molecules with the ability to function as a chemical messenger. NO plays a critical role in regulating a diverse range of physiological processes. Among those functions, NO was found to be implied into regulation of immunity and inflammation (Kobayashi, 2010). Depending on NO concentrations, this mediator can favour or prevent inflammation. Large amounts of NO generated primarily by inducible NO synthase increase the formation of peroxynitrites ions. In contrast, low concentration produced by constitutive and neuronal NO synthases inhibit adhesion molecule expression, cytokine and chemokine synthesis and leukocyte adhesion and transmigration (Guzik *et al.*, 2003).

Nitric oxide plays an important role in mucosal defense (Wallace and Miller, 2000) which is defective in IBD. For example, NO produced by epithelial cells can increase mucus (Price *et al.*, 1994) and fluid (Dow *et al.*, 1994) secretions in the

gastrointestinal tract, which reduces bacterial adherence to the epithelium. Furthermore, NO secreted by enteric glial cells can also locally enhance intestinal barrier integrity by improving i) the expression and localization of tight-junction proteins (occludin, zonula occludens-1 (ZO-1) protein), ii) the phosphorylation of myosin light chain which are implied in tight-junction structure (Savidge *et al.*, 2007, Cheadle *et al.*, 2013). In addition, NO acts as a homeostatic regulatory molecule designed to attenuate leukocyte-endothelium interaction (Banick *et al.*, 1997, Lefer and Lefer, 1999), immune response (Van Overveld *et al.*, 1993, Huang *et al.*, 1998, Obermeier *et al.*, 1999) and thus limit the local inflammation.

Reduction of NO with a reactive thiol group in cysteine residues in peptides and proteins, leads to the formation of *S*-nitrosothiols (RSNO), such as *S*-nitrosoglutathione (GSNO) and represents an endogenous form of storage and transport of NO in the body (Noble and Swift, 1999). To propose GSNO (and specifically NO) in a therapeutic of IBD requires a strict controlled supplement with low concentrations in a sustained way. Different innovative formulations of GSNO such as polymeric nanoparticles (D. Marcato *et al.*, 2013, Pereira *et al.*, 2015), inorganic nanoparticles (Santos *et al.*, 2016), polymer matrix (Seabra *et al.*, 2004b, Cariello *et al.*, 2013) polymeric stent (Acharya *et al.*, 2012), polymer films (Yoo *et al.*, 2009, Simoes and de Oliveira, 2010, Kim *et al.*, 2015), liposomes (Diab *et al.*, 2016) and polymer nanocomposites (de Mel *et al.*, 2014) were developed to improve the stability of GSNO and to propose sustained release. Among all the GSNO formulations, few are focused on oral delivery. We have already developed alginate/chitosan polymer nanocomposites adapted to oral route and presenting high GSNO encapsulation efficiency, effective drug protection and a sustained drug release, for a systemic action (Wu *et al.*, 2016).

In the present study, we proposed a novel strategy to limit chronic inflammation and prevent of barrier failure in patients by using alginate nanocomposites (alginate matrix embedding Eudragit® RL nanoparticles) as GSNO oral delivery system. Eudragit® RL, is a synthetic cationic copolymer based on ethyl acrylate, methyl methacrylate widely

used as retardant of drug release in sustained released formulation (Apu *et al*., 2009). A low content of methacrylic acid ester with quaternary ammonium groups leads to positively charged nanoparticles by double emulsion process. Alginate is a natural anionic polysaccharide of (1–4)-linked β-D-mannuronic acid (M) and α-L-guluronic acid (G). It was chosen as the external matrix material, because of its well-documented biocompatibility, mucopenetration and mucoadhesion properties (Tonnesen and Karlsen, 2002, Arora *et al.*, 2011). Alginates are natural polysaccharide polymers isolated from brown seaweed (Tonnesen and Karlsen, 2002). The alginate molecule will undergo an almost immediate hydration to create a hydrocolloidal layer of high viscosity, which builds up a diffusion barrier decreasing and delaying the migration of small molecules (Tonnesen and Karlsen, 2002). Ionotropic gelation and polyelectrolyte complexation, two formulation processes classically described for alginate delivery systems (Lopes *et al.*, 2017), are compared in the present study, in terms of GSNO protection, GSNO controlled delivery and GSNO local effect in intestine. Physico-chemical characterization and kinetic release study were performed. GSNO permeability through Caco-2 cells monolayer was tested to preliminarily prove the local and sustained effects of GSNO loaded nanocomposite particles (GSNO-NCP).

Methods

Acrylates / ammonium methacrylate copolymer (Eudragit® RL PO) was a generous gift from Evonik industries (Germany). Alginate sodium (medium viscosity, mannuronic acid/guluronic acid ratio of 1.56), polyoxyethylene-polyoxypropylene block copolymer (Pluronic® F-68), calcium chloride and all other reagents were obtained from Sigma-Aldrich (France). *S*-nitrosoglutathione (GSNO) was synthesized by reaction of reduced glutathione (GSH) and an equimolar ratio of sodium nitrite in acidic medium as a previously described method (Parent *et al.*, 2013a).

Formulation of GSNO loaded alginate nanocomposite particle

Preparation of GSNO-NCP

GSNO-NCP were constituted by inner cores and external polymer matrix (Wu *et al.*,

2015b). GSNO-nanoparticles were prepared by a double emulsion and solvent evaporation method (Wu *et al.*, 2015a). Briefly, 10 mg GSNO were dissolved in 500 µL of 0.1% Pluronic® F-68 solution as the inner aqueous phase. In a separate step, 500 mg of Eudragit® RL PO were dissolved in 5 mL of dichloromethane (DCM) constituting organic phase, and then poured into inner aqueous phase and homogenized by sonication (60 seconds, over an ice bath, 100 % amplitude, probe 3 mm, Vibra-cell™, France). The obtained water-in-oil emulsion was poured into 20 mL of 0.1% Pluronic® F-68 solution and homogenized by sonication (30 seconds, over an ice bath, 30 W, probe 6 mm, Vibra-cell™, France) to obtain the water-in-oil-in-water emulsion. The nanoparticles were hardened by solvent evaporation (100 mbar, 10 min, under vacuum, Evaporator Heidolph, Laborota 4000, Pump CVC 2000, Minichiller Huber). The size (289 ± 14 nm) and zeta-potential (40 ± 6 mV) were controlled by Zetasizer® Nano ZS (Malvern® Instrument, France) (Wu *et al.*, 2015a).

Two strategies were used to formulate the external polymer matrix. For ionotropic gelation process, sodium alginate (20 mg) was dissolved in 20 mL GSNO nanosuspension previously prepared. Over an ice bath, 2 mL calcium chloride solution ($CaCl_2$, 2 M) was added drop wisely (needle 26 G, 0.45 x 10 mm; syringe 2.5 mL) into the mixture to cross-link alginate with homogenization by sonication in ice bath (40% amplitude, 40 W, generator 130 W, Bioblock Scientific 7501D, probe CV18-7 mm, France). For polyelectrolyte complexation process, sodium alginate (20 mg) was dissolved in 10 mL ultrapure water. GSNO nanosuspension was poured in the sodium alginate solution. The mixture was homogenized by gently shaking for 1 min and then 10 mins standing before characterization.

Characterization of GSNO-NCP

Determination of particle size

The volume particle size distribution of GSNO-loaded polymer nanocomposite particles (GSNO-NCP) was determined by laser diffraction method (Mastersizer 2000, Malvern Instruments, France). GSNO-NCP were suspended in ultrapure water. The

particle size of the GSNO-NCP was described by the volume mean diameter performed in triplicate. The uniformity of the GSNO-NCP was expressed by the absolute deviation from the median.

Morphology study

The surface morphology and shape of GSNO-NCP were observed by using the scanning electron microscopy (SEM). Briefly, the diluted suspension of particles was dropped on a SEM stub and dried at room temperature. Then, the images were captured by a Hitachi S-4800 SEM (Hitachi, Japan) at 2 kV (accelerating voltage) and 2 μA (emission current). The working distance was 10 mm.

Determination of GSNO loading

GSNO loading describes the quantity of the GSNO loaded within GSNO-NCP compared with the initial drug quantity plus polymer quantity. It was determined according to the following equation (1), where *meGSNO* represents encapsulated GSNO amount, *miGSNO* means initial GSNO weight and *mipolymer* is initial polymer weight, respectively:

$$\text{GSNO loading (mg GSNO/g polymer)} = \frac{meGSNO\ (mg)}{miGSNO(g) + mipolymer\ (g)} \qquad (1)$$

The encapsulated GSNO within GSNO-NCP was evaluated by a two-step-liquid-liquid extraction. Briefly, the external matrix of GSNO-NCP composed of sodium alginate was disrupted by mechanical stirring for 6 min in sodium citrate solution (0.1 M). The resulting suspension was centrifuged at 15,000 *g* for 20 min at 4 °C, and the GSNO remaining in the supernatant was quantified by the Griess-Saville assay (Sun *et al.*, 2003). Briefly, the sample was incubated in a 0.6% (w/v) sulfanilamide solution supplemented with 0.2% (w/v) of $HgCl_2$ (to cleave the S-NO bond) in 0.4 M HCl. The formed diazonium salt was reacted with a 0.6% (w/v) *N*-(*1*-napthyl) ethylenediamine solution to form a chromophoric azo product that absorbs at 540 nm. Free nitrite ions quantified by Griess assay were subtracted from the resulting concentration calculated above.

The resulting pellet, which corresponds to GSNO Eudragit®RL nanosuspension, was dissolved in 2 mL DCM and GSNO was extracted in 9 mL phosphate buffered saline (PBS, 135 mM NaCl, 2.7 mM KCl, 1.5 mM KH_2PO_4, and 8 mM K_2HPO_4 , pH 7.4). The GSNO amount in the nanoparticles was also determined by the Griess-Saville assay as described above. All the samples were prepared in triplicate.

In vitro study

Kinetic release study

One milliliter GSNO-NCP suspension was placed in cellulose dialysis tubing (average flat width 10 mm (0.4 in), cut-off 14 kDa). The kinetic release study was performed in 200 mL of PBS pH 7.4 at 37°C with protection from light. All studies were conducted in triplicate. The GSNO and nitrite ions released were monitored at t=0, 0.25, 0.5, 1, 1.5, 2, 3, 4, 6, 24 h and immediately quantified with fluorometric method (DAN/DAN-Hg^{2+} Assay) (Misko *et al.*, 1993).

Swelling study

The same condition as used in kinetic release study was selected for swelling study. GSNO-NCP suspension (1 mL) was placed in cellulose dialysis tubing (average flat width 10 mm (0.4 in), cut-off 14 kDa). Then, the dialysis bag was immersed in 200 mL of phosphate buffered saline at pH 7.4 at 37°C with protection from light. The sample in the dialysis bag was harvested from the bag for the size measurement with Mastersizer 2000 (Malvern Instruments, France) at t=0, 2, 4, 6, 24 h. The swelling rate was presented by size change which was calculated to evaluate the swelling of the nanocomposite particles. The fractional size change was converted into percentage using equation (2), where S_t and S_i were the particles size at different time intervals and initial time, respectively:

$$\text{swelling rate } \% = \frac{\text{St}}{Si} \times 100 \qquad (2)$$

In cellulo study

Cytotoxicity study of GSNO-NCP

The cytotoxicity of GSNO-NCPs was evaluated on intestinal Caco-2 cells (ATCC® HTB-37™). The cytotoxicity study was conducted as previously described (Wu *et al.*, 2016). Caco-2 cells were seeded in 96-wells plates at 20,000 cells/well 24 h before experiment. They were then exposed to 0.5, 1.0, 5.0, 10.0 or 50.0 g/L of GSNO-NCP for 24 h at 37°C, complete medium being used as control. Cytotoxicity was checked with the MTT assay and expressed by metabolic activity. Briefly, 0.5 mg/mL of MTT was incubated with the cells for 3 h. DMSO (100 µL) was then added under stirring for 10 min to extract the formazan crystals. The absorbance was measured at 570 nm with a reference at 630 nm (in order to subtract the background) using EL 800-microplate reader (Bio-TEK Instrument, Inc®, France). Metabolic activity at the lowest concentration (0.5 g/L) was considered as 100%.

GSNO permeability in NCP across the Caco-2 cells monolayer

The permeability of GSNO across the Caco-2 monolayer was evaluated in the apical to basolateral direction in Hanks Balanced Salt Solution (HBSS, pH 7.4). Caco-2 cells were seeded at 1.0×10^6 cells/well on polycarbonate membranes (pore size: 0.4 µm). after reaching confluency, differentiated cell monolayers were obtained within 10-15 days after seeding. The transepithelial electrical resistance (TEER) gradually increased and reached a plateau at ($1976 \pm 681\ \Omega\cdot cm^2$) indicating the formation of the cell monolayer. Free GSNO, or GSNO-NCPs (50 µM of GSNO) prepared in HBSS without phenol red were placed in the apical compartment. GSNO, nitrite and nitrate ions were quantified in harvested medium from basolateral compartment by DAN/DAN-Hg^{2+} assay after 1, 4 and 24 h. Then each basolateral compartment was filled with the same volume of fresh HBSS. Finally, after 4 and 24 h of incubation, the remaining quantities of GSNO, nitrite ions in the apical compartment were also quantified by DAN/DAN-Hg^{2+} assay. At the end of the experiment, monolayer integrity was assessed by measuring TEER across the cell monolayer using a Millicell®-Electrical Resistance system (Millipore, USA). Monolayer integrity was also evaluated by the ability of

sodium fluorescein (5 µM), a low permeable marker, to cross the mucosa (Khan and Schneider, 2014). Fluorescein was detected in the basolateral compartment after 2 h by excitation at 490 nm and fluorescence emission at 514 nm.

Statistical analysis

Results are shown as either mean ± standard deviation (SD) or mean ± standard error of mean (SEM). All the statistical comparisons were performed with two-way ANOVA and post-test of Bonferroni's multiple comparisons test. $p < 0.05$ was considered significantly different. Statistical analyses were performed using the GraphPad Prism software (GraphPad Software, San Diego, USA).

Results

Physico-chemical characterization of GSNO-NCP after formulation

Size, uniformity and GSNO loading, are shown in Table 1. GSNO loaded nanocomposites (GSNO-NCP) formulated according to ionotropic gelation method present smaller size and better uniformity than GSNO-NCP prepared by polyelectrolyte complexation method (size: 24 ± 5 µm *vs* 66 ± 2 µm and uniformity: 0.48 ± 0.06 *vs* 0.98 ± 0.04, respectively). Nevertheless, with polyelectrolyte complexation method the GSNO loading is twice higher than ionotropic gelation, leading to 4.4 ± 0.4 mg and 2.7 ± 0.2 mg GSNO/g polymer, respectively.

Table 1 Characterization of GSNO-NCP (mean ± SD, n=3)

Formulation method	Size (µm)	Uniformity	GSNO loading (mg GSNO/g polymer)
Ionotropic gelation	24 ± 5	0.48 ± 0.06	2.7 ± 0.2
Polyelectrolyte complexation	66 ± 2	0.98 ± 0.04	4.4 ± 0.4

The GSNO-NCP were morphologically analysed by SEM as shown in Figure 1. Distinct spherical shape with rough surface was observe for both formulations (Figure A1 and B1). In nanoscale, picture enlarging show that nanoparticles are dispersed homogeneously in the matrix (Figure A2 and B2). No difference with blank particle is

observed.

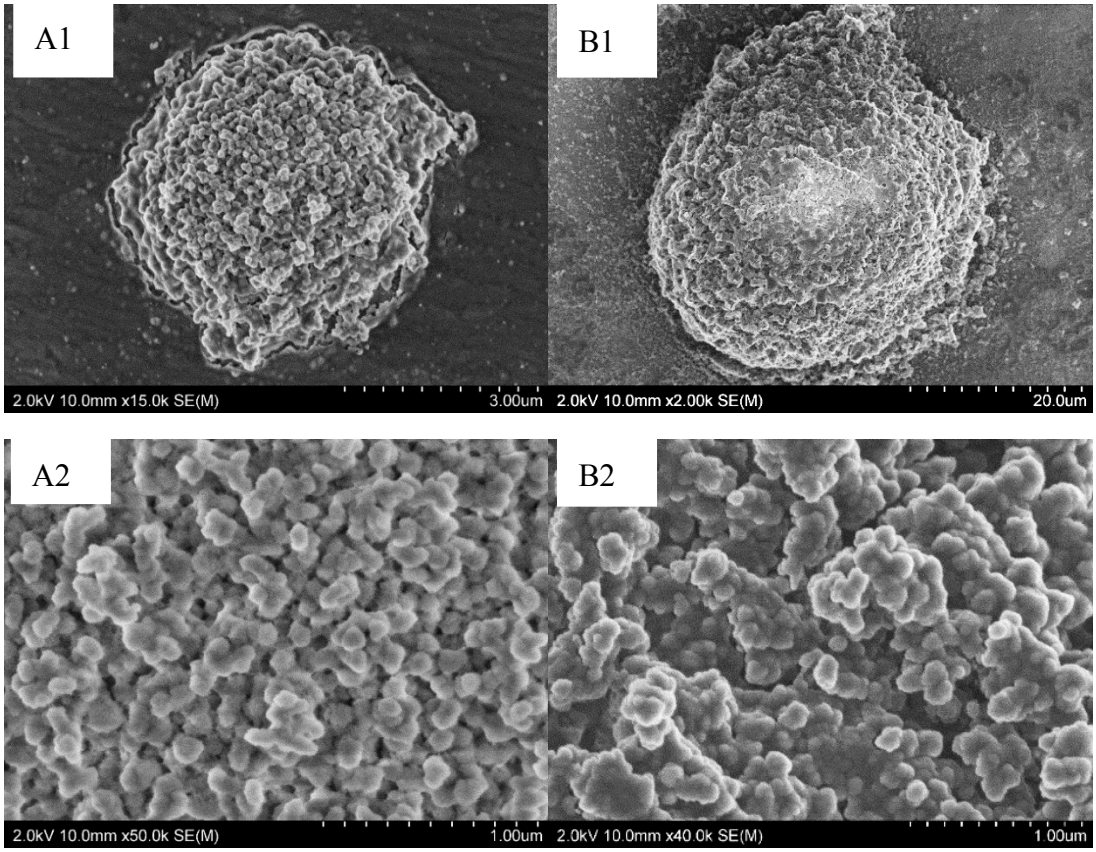

Figure 1 Scanning Electronic Microscopy images of GSNO-NCPs: A, GSNO-NCP prepared by ionotropic gelation method; B, GSNO-NCP prepared by polyelectrolyte complexation.

In vitro study

Kinetic release study

Drug (GSNO and degradation product nitrite ions) release profile from the two formulations prepared by ionotropic gelation and polyelectrolyte complexation is given in Figure 2. A burst release of GSNO reaching around 100% within the first 3 h is observed for GSNO-NCP prepared by polyelectrolyte complexation method (Figure 2). At the opposite, the GSNO-NCP formulated by ionotropic gelation method release only 28% ± 5% GSNO within 3 h and sustaine the release over 24 h (44% ± 9% GSNO and 17% ± 4% nitrite ions). After 24 h, 20% ± 4% GSNO and 20% ± 7% nitrite ions remain in the dialysis bag for this formulation method.

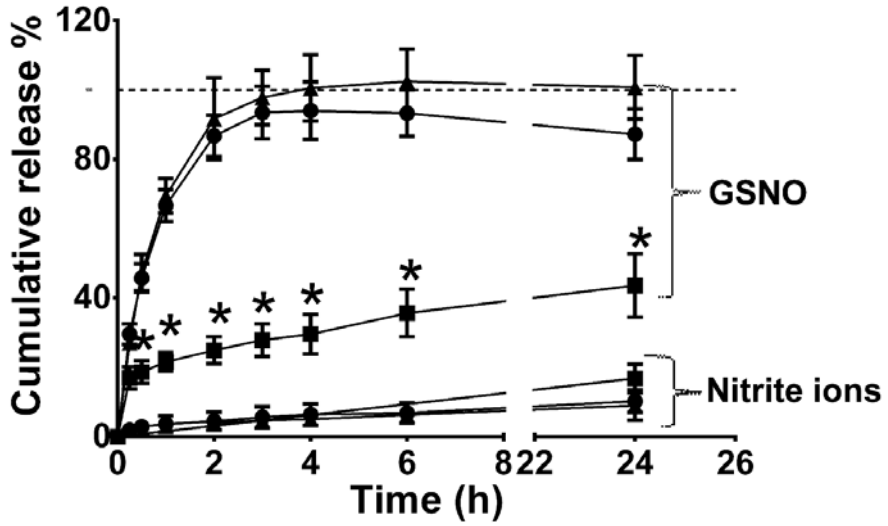

Figure 2 Drug (GSNO and degradation product nitrite ions) release from GSNO-NCP (● free GSNO, ■ ionotropic gelation, ▲ polyelectrolyte complexation) in PBS (0.148 M, pH 7.4, 37 °C). Free GSNO was used as control. Data are shown as mean ± SD (n=3). *$p < 0.05$, ionotropic gelation *vs* free GSNO & polyelectrolyte complexation, two-way ANOVA with post-test of Bonferroni's multiple comparisons test

Swelling study

Drug release rate from the alginate particles is highly dependent on particle swelling. As shown in Figure 3, the particle size decrease during 4 h and stabilized until 24 h for GSNO-NCP prepared by polyelectrolyte complexation method. However, the size of the particles prepared by ionotropic gelation slightly increases from the beginning to 24 h (the end of experiment).

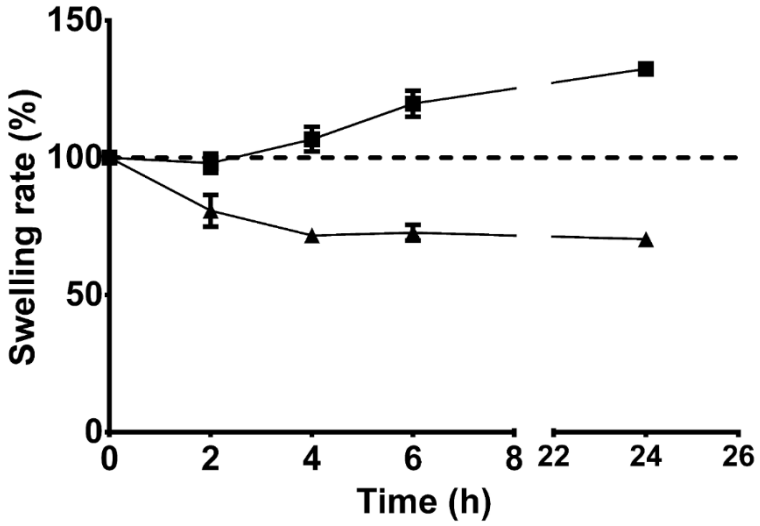

Figure 3 GSNO-NCPs (■ ionotropic gelation, ▲ polyelectrolyte complexation) swell in PBS (0.148 M, pH 7.4, 37 °C). Data are shown as mean ± SD (n=3).

In cellulo study

Cytotoxicity study

In the present study, Caco-2 cells were incubated with GSNO-NCP for 24 h. The results showed in Figure 4 do not fit with a dose-response curve model and a low mortality rate is observed under a polymer concentration less than 1 g/L for both formulations (ionotropic gelation, Figure 4A; polyelectrolyte complexation, Figure 4B). Even for the highest polymer concentration (50 g/L) tested (corresponding to log[polymer concentration] value of 1.5), more than 50% cells were still viable .

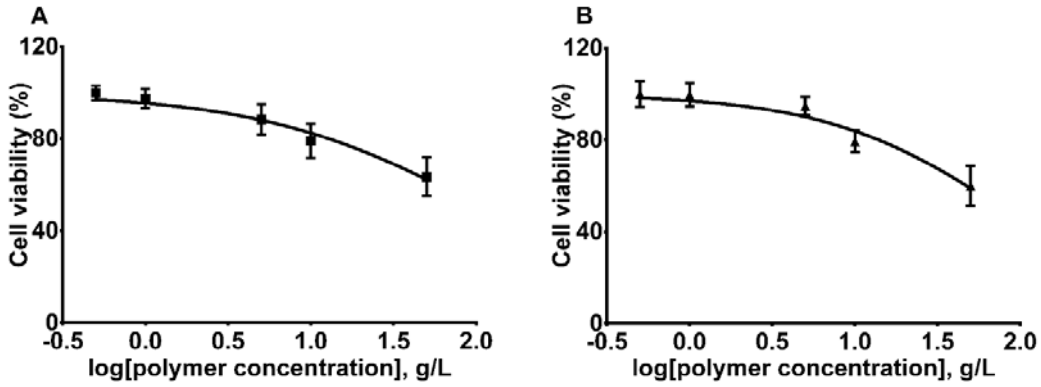

Figure 4 *In vitro* cytotoxicity of GSNO-NCPs (A: ionotropic gelation; B: polyelectrolyte complexation) on Caco-2 cells. Caco-2 cells were treated with indicated concentrations of

GSNO-NCP for 24 h at 37°C. Viability was estimated by MTT assay. Data are expressed as mean ± SEM (n=8).

Permeability of Caco-2 cells monolayer to GSNO delivered by GSNO-NCP

Caco-2 cell monolayers were incubated with 50 µM (25 nmol) free GSNO or GSNO-NCP in apical compartment to investigate the GSNO permeability. An obvious decrease of RSNO permeation in basolateral compartment is observed for both GSNO-NCPs regardless the formulation methods used, after 4 h of incubation (0.50 ± 0.04 nmol for free GSNO and 0.04 ± 0.02 nmol for ionotropic gelation, 0.04 ± 0.02 nmol for polyelectrolyte complexation, respectively) (Figure 5A). With both types of formulation, GSNO degradation forms (nitrite ions and nitrate ions) are much less than with free GSNO within 4 h (Figure 5B and 5C). In the apical compartment, significant less RSNO is observed by formulation groups at 4 h than control group, whereas no difference is seen at 24 h (Figure 5D). Interestingly, GSNO-NCP prepared by ionotropic gelation remain less RSNO in the apical compartment than GSNO-NCP prepared by polyelectrolyte complexation at t=4 h (2.0 ± 0.2 nmol for ionotropic gelation, 7.5 ± 1.6 nmol for polyelectrolyte complexation, respectively, Figure 5D). Meanwhile, the nitrite amount in the apical compartment remain unchanged after 4h and only a slight decrease is observed with polyelectrolyte complexation GSNO-NCP (Figure 5E).

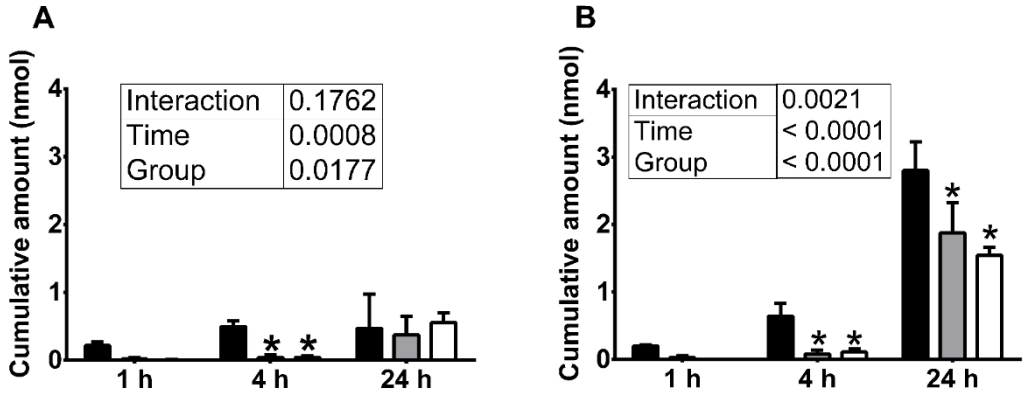

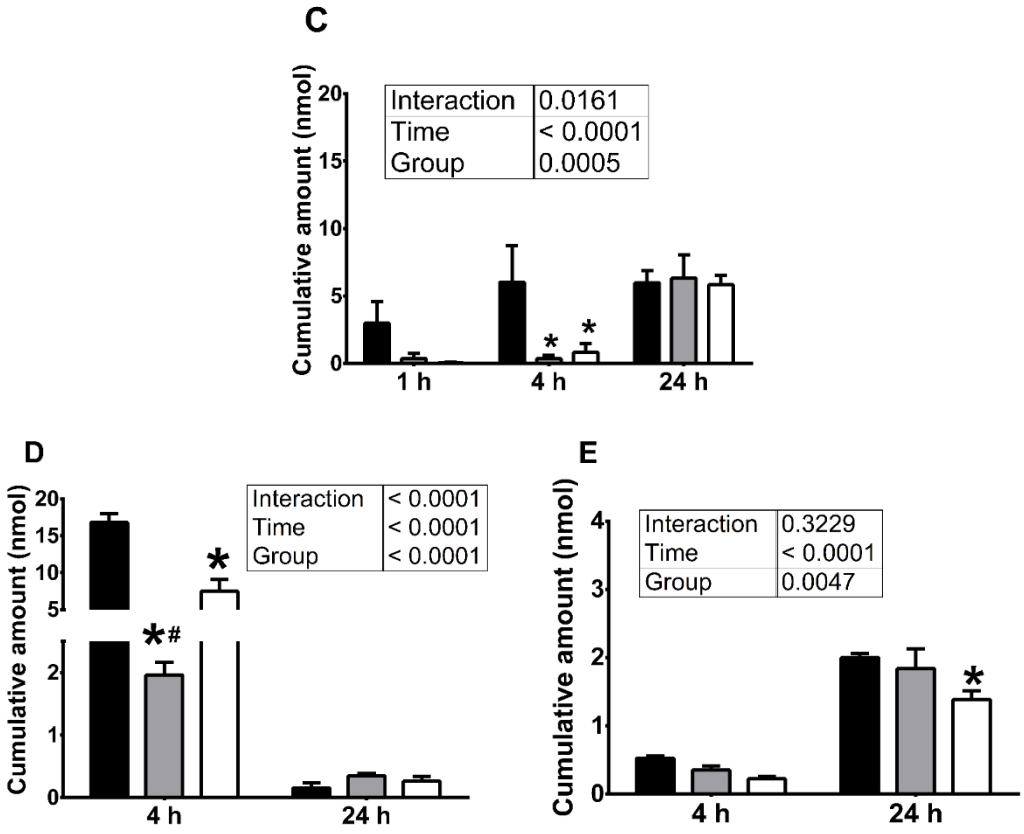

Figure 5: GSNO permeability evaluation of free GSNO (■) and GSNO-NCP (▩ ionotropic gelation, □ polyelectrolyte complexation) in Caco-2 cells monolayers. A, B, C: GSNO, nitrite ions- and nitrate ions permeated from apical to basolateral compartment within 24 h. D, E: GSNO and nitrite ions remained in apical compartment after 4 h and 24 h of incubation. Values presented have been subtracted from control (cells without treatment for free GSNO, NCP without GSNO for GSNO-NCP. Data are shown as mean ± SEM ($n \geq 3$). *$p < 0.05$ *vs* free GSNO, #$p < 0.05$ *vs* polyelectrolyte complexation, two-way ANOVA with post-test of Bonferroni's multiple comparisons test.

Discussion

The role of NO, and related NO donors, in intestinal homeostasis has been clearly demonstrated: maintaining redox balance (Kubes and McCafferty, 2000), helping mucosal healing (Jadeski and Lala, 1999), working on immune cells by inhibiting various immunomodulatory cytokines (Obermeier *et al.*, 1999), protecting intestinal barrier integrity by increasing junction protein expression (Savidge *et al.*, 2007,

Cheadle *et al.*, 2013, Li *et al.*, 2016). *S*-nitrosoglutathione, a naturally produced NO donor, was recently considered as a candidate drug able to prevent intestinal barrier disruption after femoral venous injection (Li *et al.*, 2016) or in *ex vivo* study (Savidge *et al.*, 2007). Oral delivery of GSNO with tune-up concentrations and timing controls necessarily require novel pharmaceutical technologies. With that in mind, different strategies of GSNO formulations were already elaborated, mainly for vascular applications (Heikal *et al.*, 2011, de Mel *et al.*, 2014, Parent *et al.*, 2015b). Nanocomposite particles as proposed in the present study, relay on a double entrapment, which improves GSNO encapsulation and sustains the release of GSNO. Firstly, GSNO was efficiently encapsulated in Eudragit® RL nanoparticles (5.7 mg GSNO/g polymer), which protected GSNO from degradation (Wu *et al.*, 2015a). GSNO loaded nanoparticles were further entrapped by an external matrix to form polymer nanocomposites, which improved the protection of GSNO in gastrointestinal tract, the control of GSNO delivery and the adhesion with intestine tissue. Our previous study demonstrated a systemic NO delivery (establishment of a stock of NO in vascular wall) after oral administration of GSNO loaded nanocomposites (15 mg/kg, rat) composed from Eudragit® RL nanoparticles embedded in an alginate/chitosan polymer matrix formulated by ionotropic gelation process (Wu *et al.*, 2016).

In the present study, alginate nanocomposite particles are proposed for oral GSNO delivery in intestine and adapted to a luminal protective effect. Two formulation processes were compared (ionotropic gelation with $CaCl_2$ as cross-linker and polyelectrolyte complexation) in order to fulfil project requirements and with the objective to limit step number in favour of GSNO encapsulation. To our knowledge, a direct complexation between formulated cationic Eudragit® RL nanoparticles and sodium alginate chains leading to microparticles has never been described before. The literature was focused essentially on tablet coating based on polyelectrolyte complexation film between sodium alginate (anionic) and the cationic Eudragit® RL dispersion. The resulting quaternary polymethacrylate-sodium alginate films have a

strong potential for use in sustained-release tablets (Khuathan and Pongjanyakul, 2014, Pongjanyakul and Khuathan, 2016).

In our case, higher GSNO loading is obtained with polyelectrolyte complexation method than with ionotropic gelation method. Because GSNO is a very small hydrophilic molecule, it can easily diffuse into the aqueous phase. This GSNO leakage might be explained by the intervention of strong mechanical strength during the matrix formation step: indeed, 7% of GSNO leaked from NP during additional step of strong agitation to dissolve sodium alginate in nanosuspension and 10% of GSNO leaked during the last ultrasonication step of adding calcium ions to cross-link alginate chain (data not shown). In contrast, polyelectrolyte complexation method was performed in a single step of gently mixing. Consequently, GSNO encapsulation in Eudragit® RL nanoparticles (5.7 mg GSNO/g polymer was preserved (Wu *et al.*, 2015a)). The difference of the matrix network between both processes was not visible in SEM (figure 1), where the same distribution of nanoparticles was observed.

Nevertheless, as shown in Figure 2, a burst release of GSNO until almost 100% within the first 3 hours was observed for GSNO-NCP formulated with polyelectrolyte complexation method, which is comparable to previous observation with GSNO loaded Eudragit®RL nanoparticles (Wu *et al.*, 2015a). On the contrary, ionotropic gelation led to a sustained release (still > 24 h). This big difference of release kinetics profile between these two methods may be attributed to tight complex structure of the particle prepared by ionotropic gelation method with much smaller particle size (24 ± 15 µm). In this tight complex structure, calcium ions induce alginate chain-chain association leading to the well-known "egg-box model" (Li *et al.*, 2007). With polyelectrolyte complexation method, alginate was only coated on the nanoparticle surface by electrostatic interaction between alginate and Eudragit® RL which led to larger particle size (66 ±2 µm). Eudragit® RL is positively charged because of quaternary ammonium groups of methacrylic acid ester while alginate is negatively charged by carboxyl group existing in the chain (Li *et al.*, 2005b, Vysloužil *et al.*, 2013). However, Eudragit® RL

is insoluble in aqueous phase while alginate is a hydrophilic polymer. Thus, the interaction between alginate and Eudragit® RL is limited because alginate cannot really get into contact very efficiently with Eudragit® RL. The reaction is much more like a coating on the surface of nanoparticle which results in a burst release due to the lack of effective interactions.

The swelling profile was matched with the release study. The swelling characteristics are principally related to the hydration level of hydrophilic groups (Nikoo *et al.*, 2016). The size decrease observed in particles prepared by polyelectrolyte complexation method may be caused by the detachment of alginate chain from nanoparticle. Meanwhile the continuous swelling behaviour of GSNO-NCP prepared from ionotropic gelation method might be explained by the water uptake of calcium alginate in PBS (Bajpai and Sharma, 2004).

The cytotoxicity result of GSNO loaded Eudragit® RL nanoparticles has already been published that a good cytocompatibility was observed a working concentration 3 g/L (containing 50 µM GSNO) (Wu *et al.*, 2015a).. With the nanocomposite particles introduced in the present study, an addition of polymer alginate participated in the formation of particle. Alginate is regarded as generally non-toxic and biocompatible polymer (Tonnesen and Karlsen, 2002). It is widely used in the pharmaceutical, cosmetic, and food industry (Onsoyen, 1996, Skjåk-Bræk and Espevik, 1996). In different cytotoxicity test with alginate microparticles, non-cytotoxic effects were observed on different cell lines (Rossi *et al.*, 2009, D. Marcato *et al.*, 2013, Martins *et al.*, 2015). In the present study, cell viability was studied as metabolic activity by the MTT assay. Therefore, the working concentration 6.2 g/L (ionotropic gelation), 3.8 g/L (polyelectrolyte complexation) delivering 50 µM GSNO, preserved more than 80% cell viability and was used for further investigations on GSNO permeability study through Caco-2 cells monolayer.

Transport experiments were performed from the apical to the basolateral compartment of an insert system. A delay in RSNO and degradation products (nitrite

ions and nitrate ions) permeabilities (basolateral compartment) was observed at least up to 4 h in the case of formulations when compared to free GSNO (figure 5), whatever the formulation process. This sustained release was already mentioned in a previous study, describing a GSNO-NCP formulated by ionotropic gelation process (Wu *et al.*, 2015b). In apical compartment, significant decrease of RSNO amount was observed with both GSNO-NCP formulations. Remaining amount of GSNO in NCP could be progressively released from 4 to 24 h. With alginate matrix /cells interactions, Caco-2 cells monolayer could accumulate RSNO and be considered as RSNO store, consequently participated in the observed delay.

In the case of GSNO-NCP formulated by ionotropic gelation, sustained release was particularly observed: less RSNO were quantified in the apical compartment at 4 h when compared to polyelectrolyte complexation. The tight alginate matrix obtained by ionotropic gelation may retain GSNO and sustain more efficiently the release than complexation process, as observed in *in vitro* release study.

Surprisingly, the clear difference between release profile from ionotropic gelation and polyelectrolyte complexation observed *in vitro* (PBS) disappeared totally in permeability study *in cellulo,* leading to the similar amount of RSNO and degradation ions crossing the barrier (basolateral compartment). We hypothesize that, opposite to *in vitro* experiment in PBS, presence of proteins secreted by Caco-2 and divalent cations in the culture medium may reinforce alginate hydrocolloidal layer. The resulting high viscosity of the matrix may finally delay GSNO release from polyelectrolyte complexation GSNO-NCP. Further experiment should be investigated for the exact mechanism of this alginate matrix modification.

Unlike to other natural polymer such as chitosan, alginate is not known to present a direct action on enterocytes junction (Yeh *et al.*, 2011), but more on mucus organization (Mackie *et al.*, 2016). It could be interesting to further investigate the mucopenetration ability of the GSNO-NCP formulation by the single-step process proposed in this study.

Conclusion

In this study, GSNO, a small, fragile molecule, was successfully encapsulated in alginate-nanocomposite particles based on polyelectrolyte complexation. To our knowledge, it is the first description of a direct complexation between Eudragit® RL nanoparticles (formulated by double emulsion process) and sodium alginate chain leading to NCP. As well as ionotropic gelation process, polyelectrolyte complexation GSNO-NCP formulations achieved the study objectives: GSNO protection, sustained release and retention in apical compartment (for 4 h) in Caco-2 cell experiment. A single step polyelectrolyte complexation leads to higher GSNO loading but a burst release was observed *in vitro*. The drawback of GSNO-NCP with polyelectrolyte complexation method in the *in vitro* environment was overcome when it comes to an *in cellulo* condition (closer to *in vivo* environment). Therefore, GSNO-NCP prepared by polyelectrolyte complexation with high encapsulation and simple formulation process could be a better choice for industrial development and IBD application. Alginate matrix by polyelectrolyte complexation should be further investigated following mucoadhesion/mucopenetration. Local effect of GSNO in intestine thus delivered, NO quantification in intestine should be determined, to definitively make the proof of concept of a new tool preventing IBD relapses.

Acknowledgements:

The authors are grateful to Andreï Lecomte (UMR 7359 GeoRessources - SCMEM) for helpful advice and manipulation in SEM study. The authors acknowledge the program of Chinese Scholarships Council and University of Lorraine for their financial support. The work was co-financed by the European Union with the “Fonds Européen de Développement Régional (FEDER)”.

Declaration of interest:

The funders had no role in study design, data collection and analysis, decision to publish, or preparation of the manuscript. The authors declare no conflict of interest.

Reference:

Acharya, G., Lee, C.H. & Lee, Y., 2012. Optimization of cardiovascular stent against restenosis: factorial design-based statistical analysis of polymer coating conditions. *PLoS One,* 7**,** e43100.

Arora, S., Gupta, S., Narang, R.K. & Budhiraja, R.D., 2011. Amoxicillin loaded chitosan–alginate polyelectrolyte complex nanoparticles as mucopenetrating delivery system for H. pylori. *Scientia pharmaceutica,* 79**,** 673-694.

Bajpai, S. & Sharma, S., 2004. Investigation of swelling/degradation behaviour of alginate beads crosslinked with Ca 2+ and Ba 2+ ions. *Reactive and Functional Polymers,* 59**,** 129-140.

Banick, P.D., Chen, Q., Xu, Y.A. & Thom, S.R., 1997. Nitric oxide inhibits neutrophil β 2 integrin function by inhibiting membrane‐associated cyclic GMP synthesis. *Journal of cellular physiology,* 172**,** 12-24.

Cariello, A.J., De Souza, G.F.P., Lowen, M.S., De Oliveira, M.G. & Hofling-Lima, A.L., 2013. Assessment of ocular surface toxicity after topical instillation of nitric oxide donors. *Arquivos Brasileiros De Oftalmologia,* 76**,** 38-41.

Cheadle, G.A., Costantini, T.W., Lopez, N., Bansal, V., Eliceiri, B.P. & Coimbra, R., 2013. Enteric glia cells attenuate cytomix-induced intestinal epithelial barrier breakdown. *PLoS One,* 8**,** e69042.

D. Marcato, P., F. Adami, L., De Melo Barbosa, R., S. Melo, P., R. Ferreira, I., De Paula, L., Duran, N. & B. Seabra, A., 2013. Development of a Sustained-release System for Nitric Oxide Delivery using Alginate/Chitosan Nanoparticles. *Current Nanoscience,* 9**,** 1-7.

De Mel, A., Naghavi, N., Cousins, B.G., Clatworthy, I., Hamilton, G., Darbyshire, A. & Seifalian, A.M., 2014. Nitric oxide-eluting nanocomposite for cardiovascular implants. *J Mater Sci Mater Med,* 25**,** 917-29.

Diab, R., Virriat, A.-S., Ronzani, C., Fontanay, S., Grandemange, S., Elaïssari, A., Foliguet, B., Maincent, P., Leroy, P. & Duval, R., 2016. Elaboration of sterically stabilized liposomes for *S*-nitrosoglutathione targeting to macrophages. *Journal of biomedical nanotechnology,* 12**,** 217-230.

Dow, J., Maddrell, S., Davies, S.-A., Skaer, N. & Kaiser, K., 1994. A novel role for the nitric oxide-cGMP signaling pathway: the control of epithelial function in Drosophila. *American Journal of Physiology-Regulatory, Integrative and Comparative Physiology,* 266**,** R1716-R1719.

Guzik, T.J., Korbut, R. & Adamek-Guzik, T., 2003. Nitric oxide and superoxide in inflammation and immune regulation. *Journal of Physiology and Pharmacology,* 54**,** 469-487.

Heikal, L., Aaronson, P.I., Ferro, A., Nandi, M., Martin, G.P. & Dailey, L.A., 2011. *S*-nitrosophytochelatins: investigation of the bioactivity of an oligopeptide nitric oxide delivery system. *Biomacromolecules,* 12**,** 2103-13.

Huang, F.-P., Niedbala, W., Wei, X.-Q., Xu, D., Fang, G., Robinson, J.H., Lam, C. &

Liew, F.Y., 1998. Nitric oxide regulates Th1 cell development through the inhibition of IL-12 synthesis by macrophages. *European journal of immunology,* 28**,** 4062-4070.

Jadeski, L.C. & Lala, P.K., 1999. Nitric oxide synthase inhibition by N G-nitro-l-arginine methyl ester inhibits tumor-induced angiogenesis in mammary tumors. *The American journal of pathology,* 155**,** 1381-1390.

Khan, S.A. & Schneider, M., 2014. Stabilization of Gelatin Nanoparticles Without Crosslinking. *Macromolecular Bioscience,* 14**,** 1627-1638.

Khuathan, N. & Pongjanyakul, T., 2014. Modification of quaternary polymethacrylate films using sodium alginate: film characterization and drug permeability. *International journal of pharmaceutics,* 460**,** 63-72.

Kim, J.O., Noh, J.K., Thapa, R.K., Hasan, N., Choi, M., Kim, J.H., Lee, J.H., Ku, S.K. & Yoo, J.W., 2015. Nitric oxide-releasing chitosan film for enhanced antibacterial and *in vivo* wound-healing efficacy. *Int J Biol Macromol,* 79**,** 217-25.

Kirchgesner, J., Beaugerie, L., Carrat, F., Andersen, N.N., Jess, T. & Schwarzinger, M., 2017. Increased risk of acute arterial events in young patients and severely active IBD: a nationwide French cohort study. *Gut***,** gutjnl-2017-314015.

Kobayashi, Y., 2010. The regulatory role of nitric oxide in proinflammatory cytokine expression during the induction and resolution of inflammation. *J Leukoc Biol,* 88**,** 1157-62.

Kubes, P. & Mccafferty, D.-M., 2000. Nitric oxide and intestinal inflammation. *The American journal of medicine,* 109**,** 150-158.

Lefer, A.M. & Lefer, D.J., 1999. II. Nitric oxide protects in intestinal inflammation. *American Journal of Physiology-Gastrointestinal and Liver Physiology,* 276**,** G572-G575.

Li, L., Fang, Y., Vreeker, R., Appelqvist, I. & Mendes, E., 2007. Reexamining the egg-box model in calcium− alginate gels with X-ray diffraction. *Biomacromolecules,* 8**,** 464-468.

Li, Z., Ramay, H.R., Hauch, K.D., Xiao, D. & Zhang, M., 2005. Chitosan–alginate hybrid scaffolds for bone tissue engineering. *Biomaterials,* 26**,** 3919-3928.

Li, Z., Zhang, X., Zhou, H., Liu, W. & Li, J., 2016. Exogenous *S*-nitrosoglutathione attenuates inflammatory response and intestinal epithelial barrier injury in endotoxemic rats. *J Trauma Acute Care Surg,* 80**,** 977-84.

Lopes, M., Abrahim, B., Veiga, F., Seica, R., Cabral, L.M., Arnaud, P., Andrade, J.C. & Ribeiro, A.J., 2017. Preparation methods and applications behind alginate-based particles. *Expert Opin Drug Deliv,* 14**,** 769-782.

Mackie, A.R., Macierzanka, A., Aarak, K., Rigby, N.M., Parker, R., Channell, G.A., Harding, S.E. & Bajka, B.H., 2016. Sodium alginate decreases the permeability of intestinal mucus. *Food hydrocolloids,* 52**,** 749-755.

Martins, A.F., Follmann, H.D., Monteiro, J.P., Bonafe, E.G., Nocchi, S., Silva, C.T., Nakamura, C.V., Girotto, E.M., Rubira, A.F. & Muniz, E.C., 2015.

Polyelectrolyte complex containing silver nanoparticles with antitumor property on Caco-2 colon cancer cells. *Int J Biol Macromol,* 79**,** 748-55.

Misko, T.P., Schilling, R.J., Salvemini, D., Moore, W.M. & Currie, M.G., 1993. A fluorometric assay for the measurement of nitrite in biological samples. *Analytical biochemistry,* 214**,** 11-16.

Neurath, M.F., 2017. Current and emerging therapeutic targets for IBD. *Nat Rev Gastroenterol Hepatol,* 14**,** 269-278.

Nikoo, A.M., Kadkhodaee, R., Ghorani, B., Razzaq, H. & Tucker, N., 2016. Controlling the morphology and material characteristics of electrospray generated calcium alginate microhydrogels. *Journal of Microencapsulation,* 33**,** 605-612.

Noble, D. & Swift, H., 1999. Nitric oxide release from *S*-nitrosoglutathione (GSNO). *Chemical Communications***,** 2317-2318.

Obermeier, F., Gross, V., Schölmerich, J. & Falk, W., 1999. Interleukin-1 production by mouse macrophages is regulated in a feedback fashion by nitric oxide. *Journal of leukocyte biology,* 66**,** 829-836.

Onsoyen, E., 1996. Commercial applications of alginates. *Carbohydr Eur,* 14**,** 26-31.

Parent, M., Boudier, A., Perrin, J., Vigneron, C., Maincent, P., Violle, N., Bisson, J.F., Lartaud, I. & Dupuis, F., 2015. In Situ Microparticles Loaded with *S*-Nitrosoglutathione Protect from Stroke. *PLoS One,* 10**,** e0144659.

Parent, M., Dahboul, F., Schneider, R., Clarot, I., Maincent, P., Leroy, P. & Boudier, A., 2013. A complete physicochemical identity card of *S*-nitrosoglutathione. *Current Pharmaceutical Analysis,* 9**,** 31-42.

Pereira, A.E.S., Narciso, A.M., Seabra, A.B. & Fraceto, L.F., 2015. Evaluation of the effects of nitric oxide-releasing nanoparticles on plants. *Journal of Physics: Conference Series,* 617**,** 012025.

Pithadia, A.B. & Jain, S., 2011. Treatment of inflammatory bowel disease (IBD). *Pharmacological Reports,* 63**,** 629-642.

Pongjanyakul, T. & Khuathan, N., 2016. Quaternary polymethacrylate–sodium alginate films: effect of alginate block structures and use for sustained release tablets. *Pharmaceutical development and technology,* 21**,** 487-498.

Price, K.J., Hanson, P.J. & Whittle, B.J., 1994. Stimulation by carbachol of mucus gel thickness in rat stomach involves nitric oxide. *European journal of pharmacology,* 263**,** 199-202.

Rossi, T., Iannuccelli, V., Coppi, G., Bruni, E. & Baggio, G., 2009. Role of the pharmaceutical excipients in the tamoxifen activity on MCF-7 and vero cell cultures. *Anticancer research,* 29**,** 4529-4533.

Santos, M.C., Seabra, A.B., Pelegrino, M.T. & Haddad, P.S., 2016. Synthesis, characterization and cytotoxicity of glutathione- and PEG-glutathione-superparamagnetic iron oxide nanoparticles for nitric oxide delivery. *Applied Surface Science,* 367**,** 26-35.

Savidge, T.C., Newman, P., Pothoulakis, C., Ruhl, A., Neunlist, M., Bourreille, A., Hurst, R. & Sofroniew, M.V., 2007. Enteric glia regulate intestinal barrier

function and inflammation via release of *S*-nitrosoglutathione. *Gastroenterology,* 132**,** 1344-1358.

Schumacher, M.A., Hedl, M., Abraham, C., Bernard, J.K., Lozano, P.R., Hsieh, J.J., Almohazey, D., Bucar, E.B., Punit, S. & Dempsey, P.J., 2017. ErbB4 signaling stimulates pro-inflammatory macrophage apoptosis and limits colonic inflammation. *Cell death & disease,* 8**,** e2622.

Seabra, A.B., De Souza, G.F.P., Da Rocha, L.L., Eberlin, M.N. & De Oliveira, M.G., 2004. *S*-nitrosoglutathione incorporated in poly (ethylene glycol) matrix: potential use for topical nitric oxide delivery. *Nitric Oxide,* 11**,** 263-272.

Simoes, M.M. & De Oliveira, M.G., 2010. Poly(vinyl alcohol) films for topical delivery of *S*-nitrosoglutathione: effect of freezing-thawing on the diffusion properties. *J Biomed Mater Res B Appl Biomater,* 93**,** 416-24.

Skjåk-Bræk, G. & Espevik, T., 1996. Application of alginate gels in biotechnology and biomedicine. *Carbohydr. Eur,* 14**,** 237-242.

Sun, J., Zhang, X., Broderick, M. & Fein, H., 2003. Measurement of nitric oxide production in biological systems by using Griess reaction assay. *Sensors,* 3**,** 276-284.

Tonnesen, H.H. & Karlsen, J., 2002. Alginate in drug delivery systems. *Drug Dev Ind Pharm,* 28**,** 621-30.

Van Overveld, F., Bult, H., Vermeire, P. & Herman, A., 1993. Nitroprusside, a nitrogen oxide generating drug, inhibits release of histamine and tryptase from human skin mast cells. *Agents and Actions,* 38**,** C237-C238.

Vysloužil, J., Bavoľárová, J., Kejdušová, M., Vetchý, D. & Dvořáčková, K., 2013. Cationic Eudragit® polymers as excipients for microparticles prepared by solvent evaporation method. *Ceska a Slovenska farmacie: casopis Ceske farmaceuticke spolecnosti a Slovenske farmaceuticke spolecnosti,* 62**,** 249-254.

Wallace, J.L. & Miller, M.J.S., 2000. Nitric oxide in mucosal defense: A little goes a long way. *Gastroenterology,* 119**,** 512-520.

Wu, W., Gaucher, C., Diab, R., Fries, I., Xiao, Y.-L., Hu, X.-M., Maincent, P. & Sapin-Minet, A., 2015a. Time lasting *S*-nitrosoglutathione polymeric nanoparticles delay cellular protein *S*-nitrosation. *European Journal of Pharmaceutics and Biopharmaceutics,* 89**,** 1-8.

Wu, W., Gaucher, C., Fries, I., Hu, X.-M., Maincent, P. & Sapin-Minet, A., 2015b. Polymer nanocomposite particles of *S*-nitrosoglutathione: A suitable formulation for protection and sustained oral delivery. *International journal of pharmaceutics,* 495**,** 354-361.

Wu, W., Perrin-Sarrado, C., Ming, H., Lartaud, I., Maincent, P., Hu, X.-M., Sapin-Minet, A. & Gaucher, C., 2016. Polymer nanocomposites enhance *S*-nitrosoglutathione intestinal absorption and promote the formation of releasable nitric oxide stores in rat aorta. *Nanomedicine: Nanotechnology, Biology and Medicine,* 12**,** 1795-1803.

Yeh, T.-H., Hsu, L.-W., Tseng, M.T., Lee, P.-L., Sonjae, K., Ho, Y.-C. & Sung, H.-W.,

2011. Mechanism and consequence of chitosan-mediated reversible epithelial tight junction opening. *Biomaterials,* 32**,** 6164-6173.

Yoo, J.W., Acharya, G. & Lee, C.H., 2009. *In vivo* evaluation of vaginal films for mucosal delivery of nitric oxide. *Biomaterials,* 30**,** 3978-85.

3.2.3 Supplementary study: GSNO alginate nanocomposite particles *in vitro* release in acidic pH

For better understanding of GSNO loaded alginate NCP behavior all along the gastrointestinal tract, the kinetic release study was also performed under an acidic pH which is corresponding to the simulated gastric fluid pH.

3.2.3.1 Method

A similar release study than the previous study performed in PBS at pH 7.4 was proposed. free GSNO solution or GSNO-loaded alginate NCP suspension (1 mL) was placed in cellulose dialysis tubing (average flat width 10 mm (0.4 in), cut-off 14 kDa). The kinetic release study was performed in 200 mL of acidic buffer (1g/L NaCl, 0.7% v/v HCl) at pH 1.2 (simulated gastric fluid pH) at 37°C with protection from light. All studies were conducted in triplicate. The GSNO and nitrite ions released were monitored at t=0, 0.25, 0.5, 1, 1.5, 2, 3, 4, 6, 24 h and immediately quantified with fluorometric method (DAN/DAN-Hg^{2+} Assay) (Misko *et al.*, 1993).

3.2.3.2 Result and discussion

Drug (GSNO and degradation product nitrite ions) release profile from the two formulations prepared by ionotropic gelation and polyelectrolyte complexation is given in Figure 24. As shown in Figure 24, a burst release of GSNO till almost 100% within the first 3 hours was observed for all the formulations. No difference with free GSNO and no sustained release were observed for both formulation. The nitrite ions were not detectable with both nanocomposite particles at pH 1.2 (less than limit of quantification = 0.25 μM). Finally, GSNO loaded alginate NCP prepared by polyelectrolyte complexation method still got the same release profile for both acidic pH (1.2) and neutral pH (7.4). Electrostatic interactions between carboxyl group from alginate chain and quaternary ammonium group from Eudragit® RL on the surface of NP were expected. The structure could be not tight enough to prevent small hydrophilic molecules (GSNO and nitrite ions) diffusion, which leads to a quick release in both

conditions. What is interesting is the totally different release behavior for GSNO loaded alginate NCP prepared by ionotropic gelation method in different pH (sustained release (28% ± 5%) at pH 7.4 and burst release (almost 100%) at pH 1.2 within 3h). It might be explained by that alginate is more stable near neutral pH, since with extreme pH, its degradation increases (Takka and Gürel, 2010). Below pH 5, a proton-catalyzed hydrolysis and alginate gel shrinks lead to in alginate instability (Lopes *et al.*, 2017). As a result, the alginate monomers linkages can be cleaved in this acidic pH environment (pH 1.2), which finally caused as rapid GSNO diffusion as Eudragit® RL NP release profile (Wu *et al.*, 2015a).

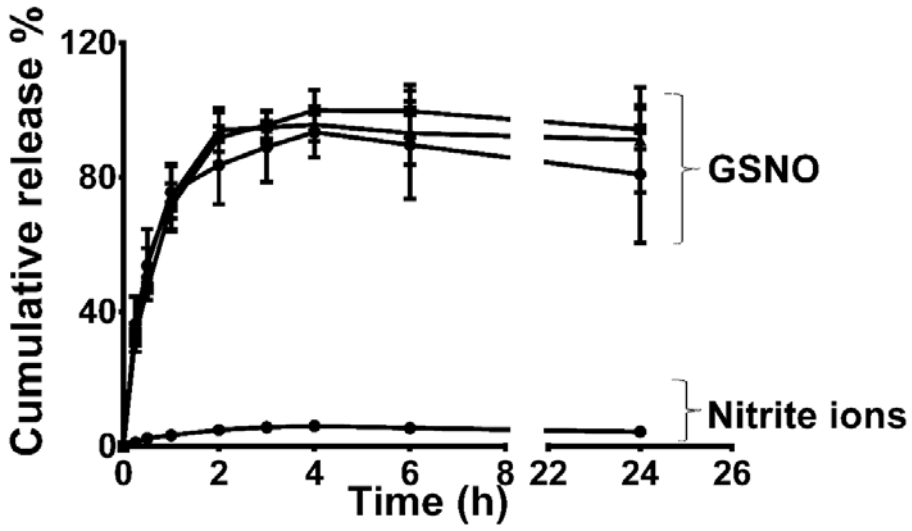

Figure 24 Drug (GSNO and degradation product nitrite ions) release from GSNO-NCP (● free GSNO, ■ ionotropic gelation, ▲ polyelectrolyte complexation) in acidic buffer (pH 1.2, 37 °C). Data are shown as mean ±SD (n=6).

3.2.4 Discussion

For alginate-NCP, we finally obtained 2 different particles through ionotropic gelation method and polyelectrolyte complexation method. The comparison was done between these two formulations through the different experiments introduced in paragraph 3.2.2. With ionotropic gelation method, the final particles have sustained GSNO release *in vitro* but lower GSNO loading and longer preparation process with high energy

intervention (potential to destroy S-NO bond of GSNO). With polyelectrolyte complexation method, the final particles have higher GSNO loading and simpler process but fast GSNO release *in vitro*.

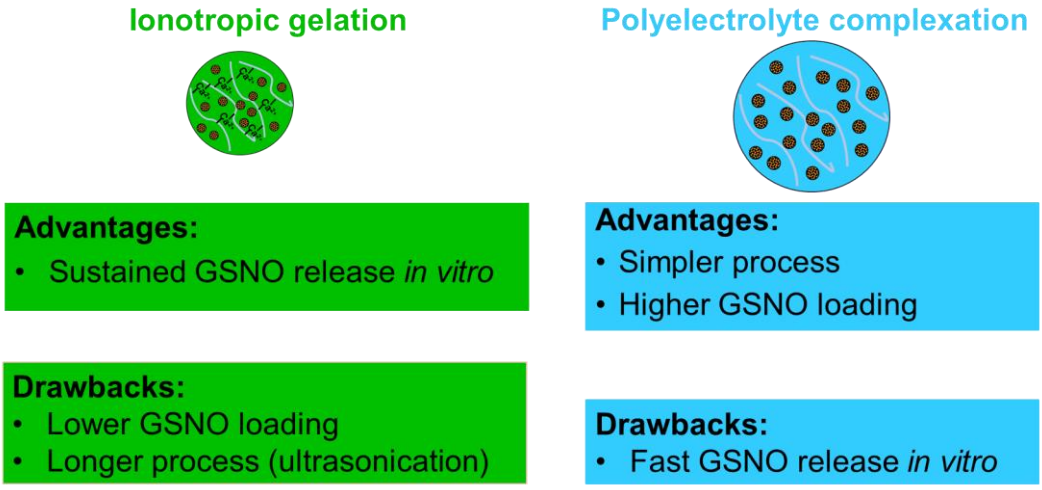

Figure 25 Advantages and drawbacks of two different alginate-NCP.

The possible mechanism of different release behaviors observed in vitro might be explained with different structure characteristics (figure 26). With ionotropic gelation method, the structure of the final particles is very tight. Water uptake of the particles (Nikoo *et al.*, 2016) leads to slow and continuous swelling during release experiment, which can explain the slowly continuous size increasing during 24 h experimental duration. As a result, GSNO can be diffused from the particles sustainably. But with polyelectrolyte complexation method, bigger size is obtained for these particles, which might be explained with the loose network between the nanoparticles and alginate chain. It's not easy to have very tight interaction between the positively charged hydrophobic polymer (Eudragit®RL) on the surface of nanoparticles and negatively charged hydrophilic polymer (alginate) chain. Thus, the risk of detachment of alginate chain from the surface of nanoparticles exists, and this might explain the quick size decreasing within 4 h in the beginning of experiment. GSNO and even GSNO-NP can be diffused easily into the outer aqueous phase from the loose network of these particles. As published in laboratory previously (Wu *et al.*, 2015a), fast release of GSNO-NP was observed. All these reasons might finally explained the fast release of alginate-NCP

prepared by polyelectrolyte complexation in *in vitro* condition.

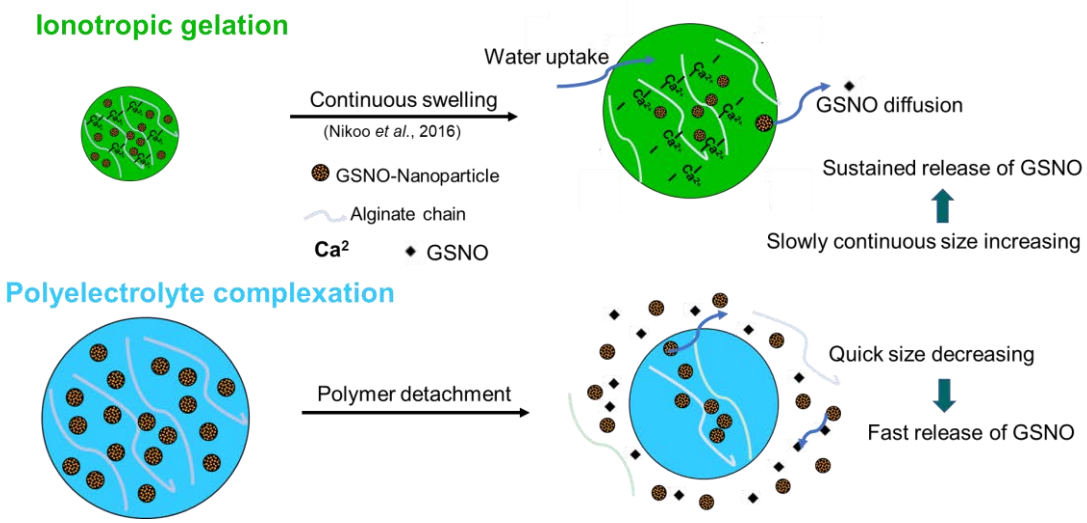

Figure 26 Possible mechanism of GSNO release in different alginate-NCP in in vitro environment.

A following *in cellulo* study was performed to understand the behavior of different alginate-NCPs in contact with cells. The permeability study trough Caco-2 cells monolayer in paragraph 3.2.2 showed that both formulations obtain delayed release in contact with cells for minimum 4 h, but better efficiency for ionotropic gelation. This might be explained by a more complex condition in contact with cells may help particles prepared by polyelectrolyte complexation to retain GSNO. But the exact mechanism need to be further explored.

The following step is to study NO storage into the cells. For this study, two different aspects could be interesting to investigate (figure 27). The first one is the quantification of NO species into the cells. This study will be performed by HPLC-MS (High-performance liquid chromatography-mass spectrometry) with ^{15}N labeled GSNO after derivatization by DAN (2,3-diaminonaphthalene) which just developed in the laboratory. With this method, we can distinguish the endogenous NO produced naturally by cells from the exogenous NO added during the experiment. Thus, the accuracy of the detection is increased. Besides, this method also significantly increased the sensitivity by 20 times through decrease the LOQ (limit of the quantification) to 5 nM compared with the traditional detection method (fluorescence) with the LOQ at 100

nM. The second aspect that has to be studied is to know the duration of NO can localized into the cells. This study will be further investigated by kinetic study between 4 h and 24.

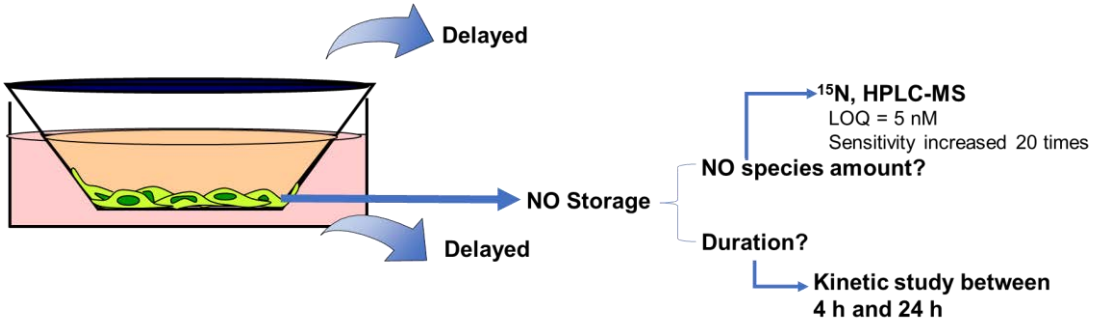

Figure 27 Perspectives of *in cellulo* study to explore the mechanism of NO localization in intestine.

3.3 Alginate/Eudragit®E 100 nanocomposite particles development

As described in the introduction part of this chapter, there are two purposes of this second strategy: 1) reinforce of the polymer matrix to limit GSNO diffusion; 2) achieve GSNO local effects in intestine.

3.3.1 Pre-experiment

Before the formulation step, a pre-experiment is necessary to explore the interaction between Eudragit®E 100 and sodium Tripolyphosphate (TPP) (cross-linker of chitosan). The mechanism of TPP cross-linking with chitosan is the interaction between a positively charged amino group (NH^{3+}) of chitosan and $P_3O_{10}^{5-}$ anions (Figure 28) (Yang *et al.*, 2009).

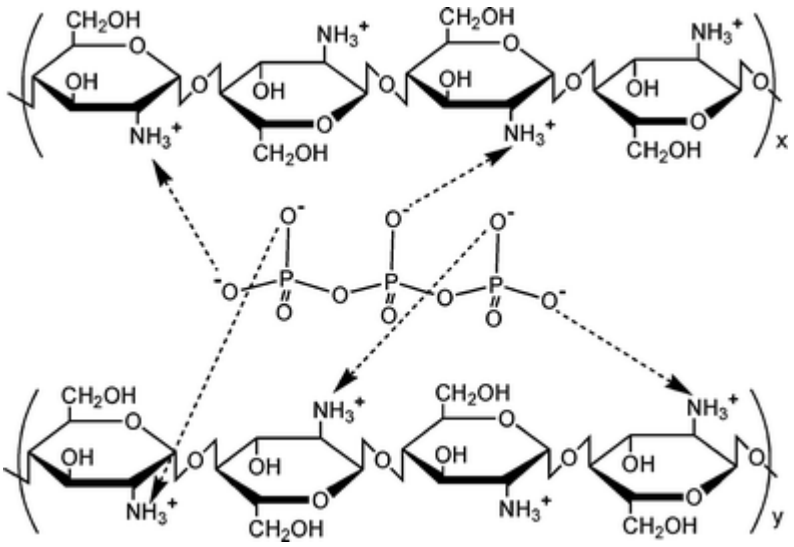

Figure 28 Mechanism of Interaction between TPP and chitosan (Yang et al., 2009)

As described already, Eudragit®E 100 is also a positively charge polymer which consists of dimethylaminoethyl methacrylate, butylmethacrylate and methyl methacrylate (Figure 29). But there is no publication mentioned a 3D matrix based on Eudragit®E 100 and cross linker association. We speculated that the positively charged dimethylamino groups of Eudragit®E 100 can still interact with $P_3O_{10}^{5-}$ anion by electrostatic interaction. The possible mechanism is shown in Figure 26 under acidic pH.

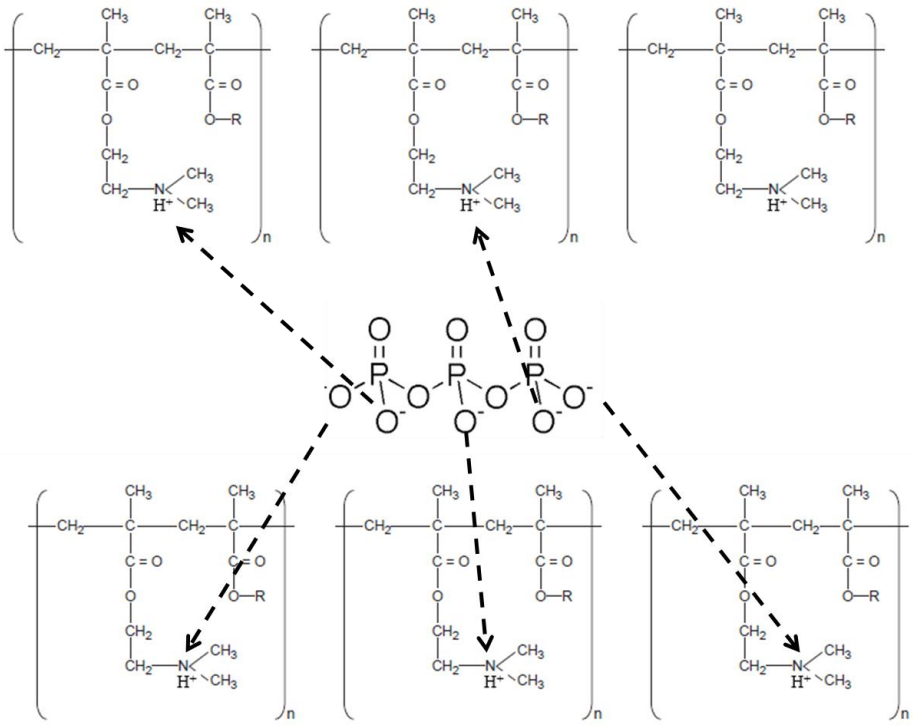

Figure 29 Possible mechanism of Interaction between TPP and Eudragit®E 100 (Moustafine et al., 2005)

Eudragit®E 100-TPP cross-linking and ionotropic gelation process were explored. Briefly, 220 mg TPP was dissolved in 20 mL 0.1% pluronic®F-68, while 20 mg Eudragit®E 100 was dissolved in 20 mL 1% acetic acid. TPP solution was added drop wisely in Eudragit®E 100 under agitation of 1000 rpm. Twenty mL 0.1% pluronic®F-68 without TPP or 1% acetic acid without Eudragit®E 100 was used as controls. During the experiment, pH of each solution before reaction and mixture after reaction was measured, at the same time, the final mixture state was observed visually. The result is given in Table 4.

Table 4 Experiment of interaction between TPP and Eudragit®E 100

TPP/Eudragit®E 100 reaction	TPP in 20 mL 0.1% pluronic®F-68		Eudragit®E 100 in 20 mL 1% acetic acid		final pH	observation
	m (mg)	pH	m (mg)	pH		
Ex1	220	9.5	-	2.9	4.2	transparent
Ex2	-	5.8	20	2.8	3.0	transparent
Ex3	220	9.5	20	3.0	4.3	white precipitation

Ex1: control group without Eudragit®E 100; Ex2: control group without TPP; Ex3: experiment

group.

From Table 4, an interaction between TPP and Eudragit®E 100 existed obviously, proved by white precipitates formation, obtained only if the both presence of TPP and Eudragit®E 100. Without TPP or Eudragit®E 100, the final mixture was still transparent without any opalescence or precipitation. Thus, the hypothesis at the beginning was confirmed. The preparation of GSNO loaded alginate/Eudragit®E 100 nanocomposite particles can be prepared in the same way as described for GSNO loaded alginate/chitosan nanocomposite particles (Wu *et al.*, 2016).

3.3.2 Methods

3.3.2.1 Preparation of GSNO loaded alginate/Eudragit®E 100 nanocomposite particles

GSNO-aeNCP were constituted by inner cores and external polymer matrix (Wu *et al.*, 2015b). GSNO-nanoparticles (GSNO-NP) were prepared by a double emulsion and solvent evaporation method as previously described (Wu *et al.*, 2015a). Then, alginate sodium (20 mg) and sodium tripolyphosphate (TPP, 220 mg) was fully dissolved in 20 mL GSNO-NP suspension. Over an ice bath, 2 mL calcium chloride solution (CaCl2, 2 M) was added dropwisely into this mixture to cross-link sodium alginate and homogenized by sonication (40 W, ultrasonic processor, France). Meanwhile, 20 mg Eudragit®E 100 was dissolved in 20 mL 1% (v/v) acetic acid. GSNO-loaded alginate Eudragit®E 100 nanocomposites (GSNO-aeNCP) were formed by dropwise addition of GSNO-nanoparticle-alginate mixture into chitosan solution under mechanical stirring (1000 rpm) over ice bath.

3.3.2.2 Characterization of GSNO-aeNCP

3.3.2.2.1 Determination of particle size

The volume particle size distribution of GSNO-aeNCP was determined by laser diffraction method (Mastersizer 2000, Malvern Instruments, France). The GSNO-acNCP were suspended in ultrapure water. The size of GSNO-acNCP was described by

the volume mean diameter performed in triplicate.

3.3.2.2.2 Morphology study

The surface morphology and shape of GSNO-aeNCP were carried out by using the scanning electron microscopy (SEM) as previously mentioned in article 3 of chapter 3.

3.3.2.2.3 Determination of GSNO loading

GSNO loading is calculated in the same way as described in article 2.

The encapsulated GSNO within GSNO-NCP was evaluated by a two-step-liquid-liquid extraction. Briefly, the external matrix of GSNO-NCP composed of sodium alginate and Eudragit®E 100 were disrupted by vortex for 5 min in sodium citrate/HCl solution. The resulting suspension was centrifuged at 15,000 g for 20 min at 4 °C, and the GSNO remaining in the supernatant was quantified by the Griess-Saville assay as previously described (Sun et al., 2003).

The resulting pellet, which corresponds to GSNO-NP, was dissolved in 1 mL DCM and GSNO was extracted in 9 mL of pH 7.4 phosphate buffered saline (PBS, 135 mM NaCl, 2.7 mM KCl, 1.5 mM KH_2PO4, and 8 mM K_2HPO4). The amount of GSNO in the nanoparticles was also determined by the Griess-Saville assay as previously described. All the samples were prepared in triplicate.

3.3.2.3 Cytotoxicity study

The cytotoxicity of GSNO-aeNCP was evaluated on intestinal Caco-2 cells ATCC® HTB-37™ as previously described in article 3 of chapter 3.

3.3.3 Result and discussion:

3.3.3.1 Physical-chemical characterization of GSNO-aeNCP

The size measured by Mastersizer and GSNO loading was shown in table 5. Smaller size (12 ± 1 µm) but similar loading (2.7 ± 0.2 mg GSNO/g polymer) was obtained after one more step of gelation with Eudragit®E 100 compared with only alginate gelation (23.6 ± 4.7 µm for size and 2.5 ± 0.6 mg GSNO/g polymer for loading). The smaller size can be involved in tighter-network of polymer matrix. Calcium ions cross-

linked alginate and TPP cross-linked Eudragit®E 100, beyond that Eudragit®E 100 chain can be bonded directly with alginate chain by polyelectrostatic interaction. These multiple interactions between different polymers resulted in tighter structure of polymer matrix, which might limit GSNO diffusion.

Table 5 Characterization of GSNO-aeNCP (mean ± SD, n=3)

Formulation	Size (µm)	Uniformity	GSNO loading (mg GSNO/g polymer)
GSNO-aeNCP	12 ± 1	0.63 ± 0.06	2.5 ± 0.6

The GSNO-aeNCPs are morphologically analyzed by SEM as shown in Figure 30. The images showed distinct spherical shape with smooth surface, which further confirmed of the tighter network. In nano-scale, it was observed by zooming the picture that nanoparticles were dispersed homogeneously in the matrix. Through figure 30 b), the polymer matrix formation was observed within the mark of red circle. The particles sizes are found to be smaller than those obtained from Mastersizer analysis. This may be explained by hydrodynamic diameter of freshly prepared particles are generally measured by Mastersizer, whereas SEM images can nullify the swelling effects with dry samples (Mukhopadhyay *et al.*, 2015).

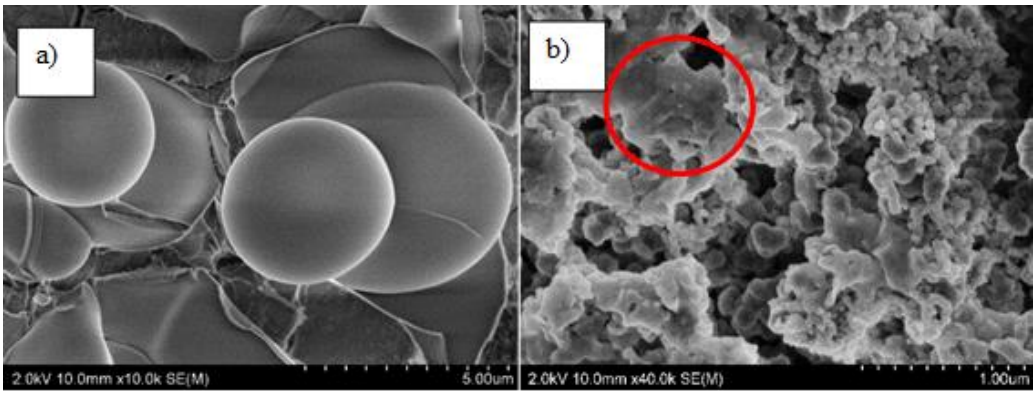

Figure 30 SEM images of GSNO-aeNCPs: a) surface morphology and b) zoomed in nano-scale

3.3.3.2 Cytotoxicity result

The concentration-response curve built from the MTT metabolic activity assay (Figure 31) gave an IC_{50} at 20.39 g/L for GSNO-aeNCP. Therefore, a concentration of 6.7 g/L (containing 50 µM GSNO) that maintained more than 80% of cell viability can be

envisaged for Caco-2 permeability studies.

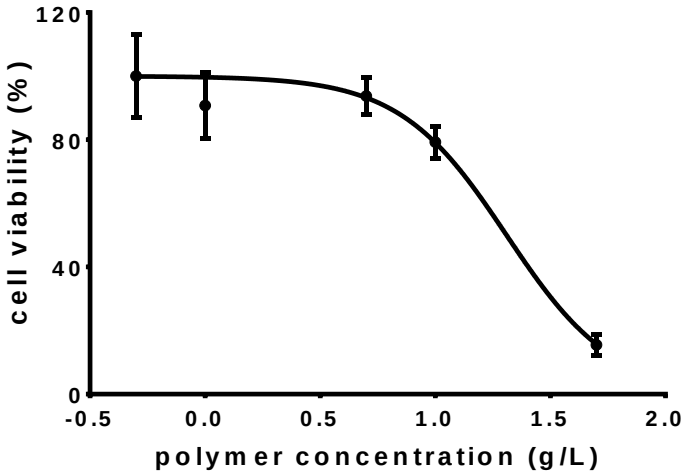

Figure 31 *In vitro* cytotoxicity of GSNO-aeNCP on Caco-2 cells. Caco-2 cells were treated with indicated polymer concentrations of GSNO-aeNCP for 24 h at 37◦C. viability was estimated by MTT assay. Data are expressed as mean ± SEM (n=4).

3.3.4 Conclusion

The GSNO potential in oral chronic treatment in IBD relapses prevention is limited by its poor stability and high hydrophilicity. In the second strategy, the polymer nanocomposite particles based on alginate/ Eudragit®E 100 blend polymers approved by the pharmaceutical authorities as suitable for oral delivery has been developed. This GSNO-aeNCP showed efficient encapsulation efficiency related to application (effective concentration for intestinal barrier protection).

3.4 Conclusion and perspectives:

To develop GSNO formulation adapted to oral administration for IBD application, we fixed several requirements in the beginning of this chapter:

1) Polymer adapted to oral route
2) Size less than 100 μm (adapted to gavage experiment of rat)
3) Efficient GSNO encapsulation
4) Sustained release profile
5) Local delivery in intestine (mucoadhesion)

During the study, all the attempts are made to answer these requirements. In conclusion, three formulations based on two strategies adapted to oral administration for IBD application have been developed: alginate nanocomposite particles based on ionotropic gelation method and alginate nanocomposite particles based on polyelectrolyte complexation method; alginate/Eudragit®E 100 blend nanocomposite particles.

1) All the formulations are prepared with polymers approved by the pharmaceutical authorities as suitable for oral delivery, which has been defined in the beginning of this chapter.
2) The size of all the formulations (24±5 μm, 66±2 μm and 12±1 μm respectively) is less than 100 μm which is adapted to further investigation.
3) From the chapter 2, we know that the effective concentration of GSNO for intestinal barrier protection is 0.1 μM. According to this result, a calculation related to effective concentration per cm^2 surface area of intestine to transfer the *ex vivo* dose to *in vivo* dose. The final theoretical calculated dose of oral administration for preclinical experiment is 0.91 mg GSNO/kg rat weight. One formulation containing 1.4 mg GSNO to 2.3 mg GSNO depending on formulations, which cover finally what could be needed in preclinical study.
4) The sustained release till 24 h has been achieved with alginate nanocomposite particles based on ionotropic gelation method and polyelectrolyte complexation method when contacted to Caco-2 cells. With alginate nanocomposite particles,

polyelectrolyte complexation method has revealed process simplification adapted to industry application, which will be further standardized. Release profile of alginate/Eudragit®E 100 blend nanocomposite particles need to be performed.

5) Finally, the mucoadhesion ability of these GSNO delivery system should be further investigated to complete the requirement we fixed at the beginning of this project. The mucoadhesion study can be carried out by measurement of the mucosal residence time of particles with excised intestine tissue according the published methods (Mukhopadhyay *et al.*, 2015, Menzel *et al.*, 2016).

Chapter 4.
General discussion and perspectives

4.1 Discussion

S-nitrosoglutathion (GSNO), the main endogenous low-molecular-weight *S*-nitrosothiol, plays a dual role in the inflammation modulation depending on the its concentration (Savidge *et al.*, 2007, Flamant *et al.*, 2011, Cheadle *et al.*, 2013, Goncalves *et al.*, 2015, Li *et al.*, 2016). The physiological levels of GSNO may promote beneficial action, whereas higher concentration exacerbate pathological condition. Low "physiological" GSNO concentrations (< 10 μM) were found to promote NF-κB activation and IL-6 expression in human peripheral blood mononuclear cells. Conversely, higher GSNO concentrations (> 100 μM) exhibited opposite effect (Siednienko *et al.*, 2011). A biphasic effect was also observed in epithelial cell, at low micromolar concentrations GSNO (10 μM) promotes tight-junction–associated proteins (ZO-1) to associate with cytoskeletal components, whereas at higher and potentially pathogenic doses (250 μM) it directly disrupts this cytoskeletal F-actin network (Savidge *et al.*, 2007). Similarly, low concentration of GSNO (0.05 μM) inhibited the iNOS expression, improved morphological bowel changes in gastroschisis while higher concentration (5 μM) was not as effective in the treatment of bowel morphology changes (Goncalves *et al.*, 2015). Furthermore, 100 μM GSNO was reported to be able to decrease $CoCl_2$-induced hypoxia-inducible factor-1α stabilization while 1 mM GSNO was ineffective (Sandau *et al.*, 2001). Low concentrations of GSNO (<10 μM) promoted Sp3 and inhibited Sp1 binding to 'housekeeping' genes. On the other hand, nitrosative stress-associated high concentration of GSNO (10 μM-100 μM) resulted in a complete reversal of the observed effects (Zaman *et al.*, 2004). Altogether, if GSNO is produced in small amounts, it generally exerts physiological functions, whereas production of high amounts of GSNO can result in a number of pathophysiological processes. In this context, the delivery of controlled low amount of GSNO is crucial to promote beneficial action of GSNO in intestine.

4.1.1 Impact of luminal GSNO on the integrity of the intestinal mucosa

Our study is in accordance with these results as we showed a dual and dose dependent

effect on the maintenance of the integrity of the mucosal barrier: As expected, high concentration of GSNO accelerated the loss of integrity of the mucosal barrier when we studied the permeability of the intestinal mucosa to a paracellular marker in the Ussing chamber system. This result indicates that the cell junctions might be disrupt in the presence of a such a high concentration of NO and it was confirmed by the decrease of the amount of occludin. Although low concentration of GSNO (0.1 μM) do not change the amount of cell junction proteins in the intestinal mucosa, it delayed the loss of integrity of the intestinal barrier during the permeability study.

Therefore, this low concentration of NO on the luminal side of the mucosa preserved the integrity of the intestinal barrier. That is the reason why we proposed NO donor administrated by oral route as a good methodology to prevent relapses in IBD patients. The mechanism of this protective action of NO was not investigated yet. Nevertheless, it might be involved in post-translational or proteolytic processing or regulation of protein kinase A (PKA) pathway, which can modulate occludin redistribution or degradation (Feldman *et al.*, 2005, Tai *et al.*, 2006, Runswick *et al.*, 2007, Kawedia *et al.*, 2008) or post-translation of adherens junction proteins as mentioned in the discussion part of article 2 in chapter 2.

4.1.2 Oral administration of GSNO

According to the result of chapter 2, to control the GSNO concentration is crucial in the application in IBD treatment. In addition, GSNO is a very fragile molecule which is easily degraded by many factors, such as light, pH, temperature, enzymes… Therefore, the development of GSNO delivery system for the chronic treatment in IBD is necessary. Oral administration is a better choice for chronic treatment because of good patient compliance and convenience. However, the drastic environment, such as various pH, temperature and enzymes, exists in gastrointestinal tract is the first obstacle to be overcome for GSNO oral administration. The second challenge is to control and sustain GSNO release in small amount and achieve GSNO local effect in intestine. As a small hydrophilic molecule, GSNO can be easily diffused, which cause low

encapsulation efficiency and rapid penetration to external aqueous phase in encapsulation process. Besides, the sensitivity of GSNO to light, pH, temperature, metal ions and mechanical agitation leads to greater challenge in GSNO encapsulation. Double emulsion technique is commonly used for encapsulation of hydrophilic molecules. In our study, GSNO is firstly encapsulated in Eudragit®RL nanoparticle by double emulsion-solvent evaporation method, which presented favorable encapsulation efficiency, increased stability and preserved bioavailability of GSNO (intracellular protein *S*-nitrosation) (Wu *et al.*, 2015a). However, no sustained release was observed *in vitro*. It might be caused by rapid diffusion in aqueous phase. Therefore, a second barrier to capture GSNO from penetration was developed by an extra entrapment in polymer matrix. This double encapsulation structure was called polymer nanocomposites. As described in chapter 1, with one more encapsulation layer, which may also promote the encapsulation efficiency by re-entrapment of GSNO with the polymer matrix. In the previous study in our laboratory, nanocomposite particles (NCP) based on alginate/chitosan blend polymers was developed to increase GSNO bioavailability for the application of cardiovascular disease. As chitosan was identified to open tight-junction between intestinal epithelial cells, it was finally characterized as a pro-inflammatory polymer (Thanou *et al.*, 2001, Wu *et al.*, 2016). The main idea of our study is to optimize this developed formulation for the application of IBD. Two strategies were carried out in parallel:

Firstly, chitosan was avoided in the construction of the polymer matrix. Two methods were utilized to form this alginate NCP: polyelectrolyte complexation and ionotropic gelation. With polyelectrolyte complexation method, the alginate NCP exhibited bigger size and simpler preparation process with higher GSNO loading capacity, but burst release in an *in vitro* artificial environment (pH 7.4 PBS at 37°C) was observed. Meanwhile, with ionotropic gelation method, the alginate NCP showed smaller size with better uniformity, less GSNO loading capacity but sustained release for at least 24 hours in *in vitro*. The smaller size and better uniformity were caused by stronger energy

intervention (ultrasonication instead of mechanical agitation) and stronger network after calcium ions cross-linking with ionotropic gelation method. Burst release of polyelectrolyte complexation might be caused by the loose structure of polymer matrix layer which was formed by a simple electrostatic interaction between negatively charged alginate chain and positively charged Eudragit® RL. Furthermore, Eudragit® RL is a hydrophobic polymer, which leads to only parts of the polymer existed on the surface of NP can contact with alginate. Thus, the interaction is not tight enough to capture GSNO diffusion in a good way. But with ionotropic gelation, alginate not only react with Eudragit® RL on the surface of NP but also interact with calcium ions to form an "egg-box" structure, which result in stronger structure. Calcium ion is small and divalent ion. It can be diffused to anywhere of the alginate chain and replace sodium ions, act as a bridge between two chains. There exists lots of binding sites for calcium ions in alginate chain. Thus, the interaction in the alginate NCP based on ionotropic gelation is much stronger and tighter, which leads to better capacity of GSNO capture. However, the GSNO permeability study in Caco-2 cells monolayer showed that similar apparent delayed release and same behavior were obtained for both NCPs. One possible reason could be the calcium ions existed in the medium and cells may enhance the structure of alginate NCP based on polyelectrolyte complexation method. Because calcium ions can penetrate into the polymer matrix, then replace sodium ions and connect those alginate chains which finally preventing GSNO penetration. Therefore, we hypothesis that the only shortcoming of alginate nanocomposites particles based on polyelectrolyte complexation can be overcome when it will be applied in *in vivo* study.

The second strategy is to replace chitosan with another positively charged polymer Eudragit® E which is often used in formulation for targeting inflamed colon sites (Avachat and Shinde, 2016). It is widely used in oral delivery system for film coating, odour and taste masking, moisture and light protection (Patra *et al.*, 2017). The resulting alginate/Eudragit® E NCP showed smaller size than alginate/chitosan NCP. The

polymer molecular weight and viscosity are the key factors influencing the particle size, higher molecular weight and higher viscosity resulting in bigger particle size. Thus, the smaller size might be explained by lower polymer weight (47 kDa for Eudragit® E and 50-190 kDa for chitosan) and lower viscosity.

With the optimization of NCP polymer matrix, not really increased GSNO encapsulation efficiency was achieved compared with NP. As mentioned before, GSNO, as a small hydrophilic molecule, can be easily diffused into aqueous phase. During the second entrapment, one more preparation step in aqueous medium with strong mixing method (ultrasonication) leads to rapid diffusion of GSNO, which finally leaded to less GSNO encapsulation efficiency than NP. Nevertheless, the burst release of the particle was improved. The application of NCP for GSNO delivery emerged the merits of both nanoparticles (considerable GSNO encapsulation efficiency) and polymer matrix (controlled and sustained release) and overcome the shortcomings of each other (burst release for NP and low GSNO capture ability) in one system.

4.2 Conclusion and Perspectives

4.2.1 Formulations

In conclusion, Four formulations have been developed for oral delivery of GSNO:

1. Eudragit®RL nanoparticle
2. Alginate NCPs based on ionotropic gelation;
3. Alginate NCPs based on polyelectrolyte complexation;
4. Alginate/ Eudragit®E blend NCP.

For the alginate/ Eudragit®E blend NCP, *in vitro* release study and permeability study through Caco-2 cells monolayer need to be completed. Cytotoxicity evaluation is not enough. As the ability of Eudragit®E to open tight junction is not yet reported, it is important to compare this new formulation we proposed with the alginate/ chitosan blend NCP. Caco-2 cells monolayer is really adapted to this exploration with a high

expression of cell junctions in differentiated status (Sun *et al.*, 2008). Following TEER, marker permeability and by visualization of junction protein by immunostaining during and after the permeability study through Caco-2 cells monolayer, the definitive utility of this formulation will be demonstrated.

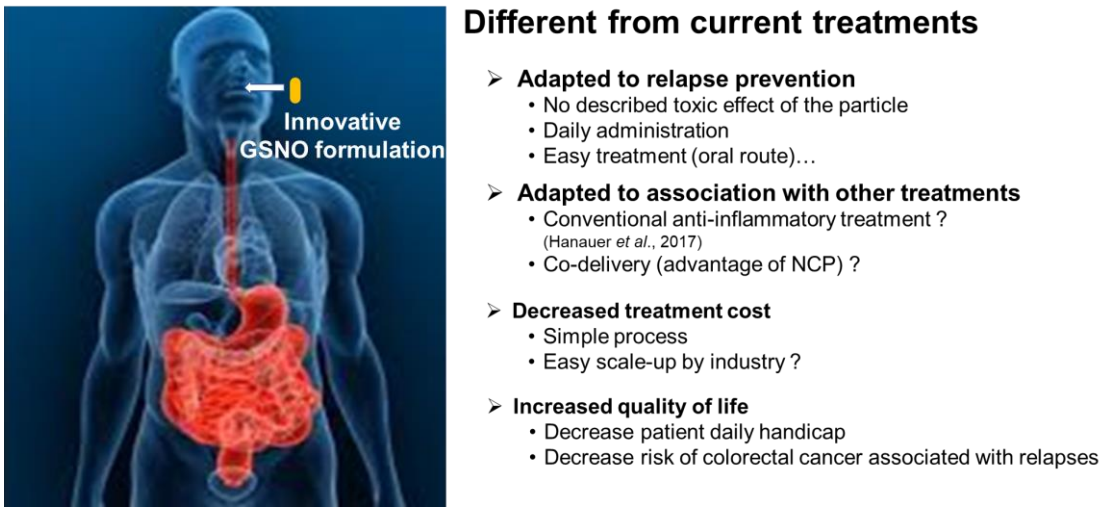

Figure 32 A crucial goal for the patients: Inflammation prevention.

The aim of our study was to find an innovative treatment to prevent intestinal inflammation relpases in IBD patients (figure 32). We developed formulations with no described toxic effect of the particle and good patient compliance achieved by daily administration with easy treatment (oral route).

We have also the possibility to associated our treatment with other treatments. Combination therapy has been published as a novel strategy of IBD treatment (Hanauer, 2017). It was shown that combination therapy with infliximab (anti-TNF agent) and azathioprine (immunosuppressive drug) is superior to induce corticosteroid-free clinical remission than monotherapy with either agent in both Crohn's disease and ulcerative colitis (Colombel *et al.*, 2010, Panaccione *et al.*, 2014). Therefore, drugs synergistic effect is promising strategy in IBD treatment. Our formulation strategy can be a good candidate to improve this combination therapy by co-delivery GSNO with drug that can induce remission, such as corticosteroids. Corticosteroids was reported to inhibit endogenous growth factors, thus preventing angiogenesis at the local tissue

(Patil *et al.*, 2007) while GSNO can promote angiogenesis through mediating induction of vascular endothelial growth factor (Khan *et al.*, 2015). Corticosteroids and GSNO can act as supplementary treatment for each other. Corticosteroids can reinforce the anti-inflammation function while GSNO can accelerate the therapeutic effect by helping mucosa healing. Furthermore, local effect can be achieved to reduce the side effect and enhance the therapeutic function with the developed nanocomposite delivery strategy. A co-delivery of dexamethasone (a type of corticosteroid medication) and VEGF using PLGA microsphere/PVA hydrogel composites has already been developed for localized inflammation control and angiogenesis (Patil *et al.*, 2007). In the present study, the strategy could be GSNO and corticosteroids firstly encapsulated in NPs separately, followed by a further encapsulation of polymer matrix. Thus, GSNO co-delivered with anti-inflammation drugs in polymer NCP can be a promising strategy in IBD treatment. With our NCP strategy, it gives us potential to co-delivery the two different drugs. As previously mentioned in the conclusion part of chapter 3, main requirements of the formulations have already been achieved. But the main advantages of the NCP have not been explored yet: co-encapsulation of two drugs in the same delivery system. Different strategies could be proposed: a). different drug-loaded-NP, prepared separately, entrapped in the same matrix system; b). one drug loaded in NP and a second one included into the matrix system. The choice of strategies a) or b) may induce modification of physical-chemical characterization and drug release profile. The strategy will be selected according to the drug.

However, for a further application in clinical trial for human, more investigations of the formulation part need to be done. Additional “difficulties” will rise when theses formulations will be tested in clinical trial for human. Stable conservation form like powder need to be developed for longer and convenient storage. For the further economic consideration, we still have to optimize the formulation to increase encapsulation efficiency. The strategy could be increasing the interaction between

GSNO and polymer by electrostatic interaction or covalently bonding. For example, *S*-nitrosoglutathione-alginate (SNA) which has been developed in the laboratory can be used to replace sodium alginate in the present study. SNA is a novel NO-donor by cross-linking alginate with *S*-nitroglutathione, which can deliver NO in a sustained manner (Shah *et al.*, 2016). With the chemical bonding, GSNO loading capacity can be absolutely increased without worrying about GSNO diffusion. In addition, we expect that the release behavior will be further controlled and sustained by replace alginate with SNA. Because, the remaining GSH in the SNA can react with NO released by GSNO and there might be transnitrosation reaction between GSNO and SNA to retain GSNO in a better way.

The final goals of our study are to decrease the treatment cost and to increase quality of patients' life. With our proposed simple preparation process, it could be easy to scale-up in industry, which can finally improve the low cost-benefits ratio of current treatments. Meanwhile, to decrease patient daily handicap and decrease the risk of colorectal cancer associated with relapses could finally increase quality of patients' life.

4.2.2 Effects of released GSNO in inflammation

For the application part, we have confirmed our concept that luminal GSNO (oral administration) also showed a dose-dependent effects on intestinal barrier integrity as published mucosal source GSNO. However, the limitation of our study is the absence of *ex vivo* inflammation model. The application of our study is to prevent the inflammation in IBD patient. To assess the luminal GSNO ability of preventing inflammation, we used the healthy intestine tissue in Ussing Chamber as a stress model with loss of TJ expression (occludin and beta-catenin) compared with wild-type rat intestine tissue. But the mechanism was not deeply investigated yet. This investigation should be performed with a model closer to the pathophysiological context of inflammation *in vivo*. There are lots of *in vivo* inflammation models described in the

literature that trigger inflammation process similar to what is observed in IBD patients. No similar model has been developed in Ussing chamber as an *ex vivo* model for better mimicking the therapy process as *in vivo* process. We tried to induce inflammation in the Ussing chamber with addition of colitogenic agent (such as Dextran Sodium Salt) and LPS (Emmanuel *et al.*, 2007)) in the luminal compartment in order to study the intestinal permeability to the paracellular marker, the expression of cell junction proteins and of inflammation markers (data not shown). Unfortunately, no differences were observed between colitogenic and control conditions. The time limitation of this *ex vivo* study probably explain this negative result. Because, it is probably not suitable for a study of inflammation process involving transcription, translation, post-translational modification, protein transportation and mediator releasing and so on…

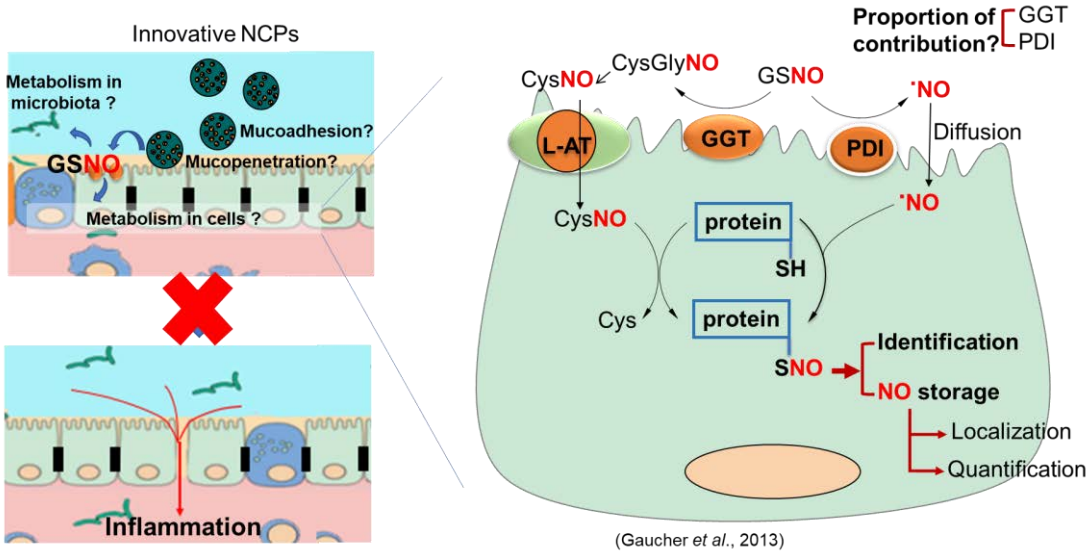

Figure 33 Perspectives of NO action with intestine. (GGT: γ-Glutamyltransferase; PDI: Protein disulfide isomerase; L-AT: the L-amino acid transporter system)

When the developed formulations reach the target-intestine, the interaction between formulation and mucus is essential and it would be important to further investigate mucoadhesion and mucopenetration.

Another question that has to be considered is the bioavalability of GSNO in the intestine *in vivo*. After GSNO release, it can be used by cells and bacteria as well. The proportion of bacterial and cells contribute in the GSNO metabolism is interesting to be known the

effective GSNO bioavailability. GSNO cannot be transported directly into cells. But different enzyme presenting in the cells can help the transportation of NO. Firstly, GSNO can be catalyzed to CysGlyNO by GGT. But CysGlyNO is not stable, which will finally be transnitrosated to CysNO. CysNO can be transported into cells by the L-amino acid transporter system (L-AT) to participate the transnitrosation of target proteins. A second transportation way is conducted by PDI, GSNO can be catalyzed to NO radical with PDI. Then this radical can be easily diffused into the cells, which may finally contribute in the *S*-nitrosation of target proteins. Thus, the proportion of GGT and PDI participate in the GSNO metabolism can be further studied for GSNO metabolism mechanism exploration in intestine *in vivo*. The identification of target proteins and NO storage into intestine are also necessary to completed the mechanism study. The identification of target proteins can be performed by Biotin Switch method. The investigation will start with the possible target proteins, such as NF-κB, β-catenin and occludin, which are mentioned in chapter 2. NO storage will be studied by DAF-2 DA (5,6-Diaminofluorescein diacetate) assay to check the localization of NO in intestine and NO amount quantification by HPLC-MS with ^{15}N labeled GSNO after DAN derivatization which mentioned in paragraph 3.3.4 of chapter 3.

The goal of our study is to check if oral administrated GSNO can prevent IBD relapses or not. The *ex vivo* experiments in order to mimic inflamed condition in the intestinal mucosa seems to be not adapted, which finally impose to use *in vivo* models. Now that we have developed three formulations that could be adapted to oral administration, we are able to plan *in vivo* studies in order to check that the protection of the integrity of the mucosa is conserved in physiological conditions, and to check if in inflamed condition, it can prevent, delay or protect from the inflammation. DSS inflammation model will be used. Alginate nanocomposite particles based on polyelectrolyte complexation method will be firstly tested in this DSS model rat because of higher GSNO encapsulation efficiency but simpler preparation process. The experiment schedule is shown in Figure 34.

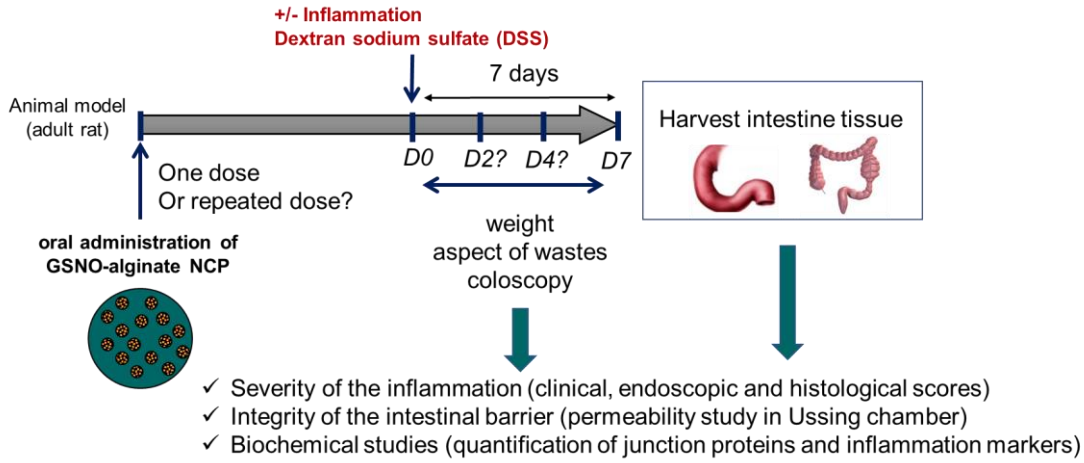

Figure 34 *In vivo* evaluation of GSNO loaded formulations in inflammation model

The *in vivo* model is used to determine the formulation efficiency and GSNO therapeutic potential as a chronic oral treatment of IBD prevention. GSNO loaded NCP, free GSNO, and corresponding blank- NCP or PBS as controls will be administrated by gavage to rats before inflammation induction. Dextran sodium sulfate (5%) in drinking water will be used to induce colitis (Melhem *et al.*, 2015). The treatment of GSNO, such as duration and repetition times, should be further confirmed to maximize the efficiency. Meanwhile, the exact duration of inflammation induction should be defined according to the severity of inflammation. Seven days of DSS induction was known to finally result in severe inflammation in rat intestine (Melhem *et al.*, 2015). In order to make sure we can see difference between GSNO treatment group and control group. We need to adapt the inflammation severity to our study in advance, maybe 2 days, or 4 days... The inflammation severity will be visually determined by clinical scoring changes in weight, hemoccult positivity or gross bleeding, and stool consistency during the induction (Murthy *et al.*, 1993) and endoscopic, histological scores at the end of the induction (Melhem *et al.*, 2016, Kökten *et al.*, 2017). The integrity of intestinal barrier will be followed by permeability study to paracellular marker in Ussing Chamber system after DSS induction. The biochemical studies containing quantification of junction proteins and inflammation markers will be fulfilled by western blot and ELISA as well.

GSNO loaded NCPs adapted to oral administration has been developed, presenting a promising methodology for the care of patients, that could be proposed in parallel or as an alternative of classical treatment in order to ameliorates the quality of life of patients.

Reference

Abbott, W.A., Griffith, O.W. & Meister, A., 1986. Gamma-glutamyl-glutathione. Natural occurrence and enzymology. *Journal of Biological Chemistry,* 261**,** 13657-13661.

Acharya, G., Lee, C.H. & Lee, Y., 2012. Optimization of cardiovascular stent against restenosis: factorial design-based statistical analysis of polymer coating conditions. *PLoS One,* 7**,** e43100.

Adachi, M., Inoko, A., Hata, M., Furuse, K., Umeda, K., Itoh, M. & Tsukita, S., 2006. Normal establishment of epithelial tight junctions in mice and cultured cells lacking expression of ZO-3, a tight-junction MAGUK protein. *Molecular and cellular biology,* 26**,** 9003-9015.

Aguero, L., Zaldivar-Silva, D., Pena, L. & Dias, M.L., 2017. Alginate microparticles as oral colon drug delivery device: A review. *Carbohydr Polym,* 168**,** 32-43.

Ahmad, Z., Shah, A., Siddiq, M. & Kraatz, H.-B., 2014. Polymeric micelles as drug delivery vehicles. *RSC Advances,* 4**,** 17028.

Ahnfelt-Rønne, I., Nielsen, O.H., Christensen, A., Langholz, E., Binder, V. & Riis, P., 1990. Clinical evidence supporting the radical scavenger mechanism of 5-aminosalicylic acid. *Gastroenterology,* 98**,** 1162-1169.

Akbarzadeh, A., Rezaei-Sadabady, R., Davaran, S., Joo, S.W., Zarghami, N., Hanifehpour, Y., Samiei, M., Kouhi, M. & Nejati-Koshki, K., 2013. Liposome: classification, preparation, and applications. *Nanoscale research letters,* 8**,** 1.

Al-Sadi, R., Khatib, K., Guo, S., Ye, D., Youssef, M. & Ma, T., 2011. Occludin regulates macromolecule flux across the intestinal epithelial tight junction barrier. *American Journal of Physiology-Gastrointestinal and Liver Physiology,* 300**,** G1054-G1064.

Alberts, B., Johnson, A., Lewis, J., Raff, M., Roberts, K. & Walter, P., 2002. Cell junctions.

Ananthakrishnan, A.N., 2013. Environmental Triggers for Inflammatory Bowel Disease. *Current gastroenterology reports,* 15**,** 302-302.

Ananthakrishnan, A.N., 2015. Epidemiology and risk factors for IBD. *Nature reviews Gastroenterology & hepatology,* 12**,** 205-217.

Ananthakrishnan, A.N., Khalili, H., Konijeti, G.G., Higuchi, L.M., De Silva, P., Fuchs, C.S., Willett, W.C., Richter, J.M. & Chan, A.T., 2014. Long-term intake of dietary fat and risk of ulcerative colitis and Crohn's disease. *Gut,* 63**,** 776-784.

Aoki, N., Johnson, G. & Lefer, A.M., 1990. Beneficial effects of two forms of NO administration in feline splanchnic artery occlusion shock. *American Journal of Physiology-Gastrointestinal and Liver Physiology,* 258**,** G275-G281.

Arnér, E.S. & Holmgren, A., 2000. Physiological functions of thioredoxin and thioredoxin reductase. *European Journal of Biochemistry,* 267**,** 6102-6109.

Arora, S., Gupta, S., Narang, R.K. & Budhiraja, R.D., 2011. Amoxicillin loaded chitosan–alginate polyelectrolyte complex nanoparticles as mucopenetrating delivery system for H. pylori. *Scientia pharmaceutica,* 79**,** 673-694.

Artis, D., Wang, M.L., Keilbaugh, S.A., He, W., Brenes, M., Swain, G.P., Knight, P.A.,

Donaldson, D.D., Lazar, M.A. & Miller, H.R., 2004. RELMβ/FIZZ2 is a goblet cell-specific immune-effector molecule in the gastrointestinal tract. *Proceedings of the National Academy of Sciences of the United States of America,* 101**,** 13596-13600.

Atuma, C., Strugala, V., Allen, A. & Holm, L., 2001. The adherent gastrointestinal mucus gel layer: thickness and physical state in vivo. *American Journal of Physiology-Gastrointestinal and Liver Physiology,* 280**,** G922-G929.

Avachat, A.M. & Shinde, A.S., 2016. Feasibility studies of concomitant administration of optimized formulation of probiotic-loaded Vancomycin hydrochloride pellets for colon delivery. *Drug Dev Ind Pharm,* 42**,** 80-90.

Awad, E., Khan, S., Sokolikova, B., Brunner, P., Olcaydu, D., Wojta, J., Breuss, J. & Uhrin, P., 2013. Cold induces reactive oxygen species production and activation of the NF‐kappa B response in endothelial cells and inflammation in vivo. *Journal of Thrombosis and Haemostasis,* 11**,** 1716-1726.

Babinska, A., Kedees, M.H., Athar, H., Sobocki, T., Sobocka, M.B., Ahmed, T., Ehrlich, Y.H., Hussain, M.M. & Kornecki, E., 2002. Two regions of the human platelet F11-receptor (F11R) are critical for platelet aggregation, potentiation and adhesion. *Thrombosis and haemostasis,* 87**,** 712-721.

Baj-Krzyworzeka, M., Szatanek, R., Węglarczyk, K., Baran, J., Urbanowicz, B., Brański, P., Ratajczak, M.Z. & Zembala, M., 2006. Tumour-derived microvesicles carry several surface determinants and mRNA of tumour cells and transfer some of these determinants to monocytes. *Cancer Immunology, Immunotherapy,* 55**,** 808-818.

Bajpai, S. & Sharma, S., 2004. Investigation of swelling/degradation behaviour of alginate beads crosslinked with Ca 2+ and Ba 2+ ions. *Reactive and Functional Polymers,* 59**,** 129-140.

Balda, M.S., Flores-Maldonado, C., Cereijido, M. & Matter, K., 2000. Multiple domains of occludin are involved in the regulation of paracellular permeability. *Journal of cellular biochemistry,* 78**,** 85-96.

Banick, P.D., Chen, Q., Xu, Y.A. & Thom, S.R., 1997. Nitric oxide inhibits neutrophil β 2 integrin function by inhibiting membrane‐associated cyclic GMP synthesis. *Journal of cellular physiology,* 172**,** 12-24.

Bannaga, A.S. & Selinger, C.P., 2015. Inflammatory bowel disease and anxiety: links, risks, and challenges faced. *Clinical and experimental gastroenterology,* 8**,** 111.

Barglow, K.T., Knutson, C.G., Wishnok, J.S., Tannenbaum, S.R. & Marletta, M.A., 2011. Site-specific and redox-controlled S-nitrosation of thioredoxin. *Proceedings of the National Academy of Sciences,* 108**,** E600-E606.

Barker, N., Van De Wetering, M. & Clevers, H., 2008. The intestinal stem cell. *Genes & development,* 22**,** 1856-1864.

Barrett, J.C., Lee, J.C., Lees, C.W., Prescott, N.J., Anderson, C.A., Phillips, A., Wesley, E., Parnell, K., Zhang, H. & Drummond, H., 2009. Genome-wide association study of ulcerative colitis identifies three new susceptibility loci, including the

HNF4A region. *Nature genetics,* 41**,** 1330-1334.

Bazzoni, G., 2003. The JAM family of junctional adhesion molecules. *Current opinion in cell biology,* 15**,** 525-530.

Bazzoni, G., MartìNez-Estrada, O.M., Mueller, F., Nelboeck, P., Schmid, G., Bartfai, T., Dejana, E. & Brockhaus, M., 2000. Homophilic interaction of junctional adhesion molecule. *Journal of Biological Chemistry,* 275**,** 30970-30976.

Berg, D.J., Zhang, J., Weinstock, J.V., Ismail, H.F., Earle, K.A., Alila, H., Pamukcu, R., Moore, S. & Lynch, R.G., 2002. Rapid development of colitis in NSAID-treated IL-10–deficient mice. *Gastroenterology,* 123**,** 1527-1542.

Bhattacharya, S., Gupta, R. & Kamal, M., 2008. *Polymeric nanocomposites theory and practice*: Carl Hanser Publishers.

Bhavsar, M.D. & Amiji, M.M., 2007. Gastrointestinal distribution and in vivo gene transfection studies with nanoparticles-in-microsphere oral system (NiMOS). *J Control Release,* 119**,** 339-48.

Bhavsar, M.D. & Amiji, M.M., 2008. Development of novel biodegradable polymeric nanoparticles-in-microsphere formulation for local plasmid DNA delivery in the gastrointestinal tract. *AAPS PharmSciTech,* 9**,** 288-94.

Bhavsar, M.D., Tiwari, S.B. & Amiji, M.M., 2006. Formulation optimization for the nanoparticles-in-microsphere hybrid oral delivery system using factorial design. *Journal of controlled release,* 110**,** 422-430.

Billat, P.-A., Roger, E., Faure, S. & Lagarce, F., 2017. Models for drug absorption from the small intestine: where are we and where are we going? *Drug discovery today*.

Birrenbach, T. & Böcker, U., 2004. Inflammatory bowel disease and smoking. A review of epidemiology, pathophysiology, and therapeutic implications. *Inflammatory bowel diseases,* 10**,** 848-859.

Bischoff, S.C., Barbara, G., Buurman, W., Ockhuizen, T., Schulzke, J.-D., Serino, M., Tilg, H., Watson, A. & Wells, J.M., 2014. Intestinal permeability–a new target for disease prevention and therapy. *BMC gastroenterology,* 14**,** 189.

Bissonnette, E.Y., Hogaboam, C.M., Wallace, J.L. & Befus, A.D., 1991. Potentiation of tumor necrosis factor-alpha-mediated cytotoxicity of mast cells by their production of nitric oxide. *The Journal of Immunology,* 147**,** 3060-3065.

Bitton, A., Dobkin, P., Edwardes, M.D., Sewitch, M., Meddings, J., Rawal, S., Cohen, A., Vermeire, S., Dufresne, L. & Franchimont, D., 2008. Predicting relapse in Crohn's disease: a biopsychosocial model. *Gut,* 57**,** 1386-1392.

Bornslaeger, E.A., Corcoran, C.M., Stappenbeck, T.S. & Green, K.J., 1996. Breaking the connection: displacement of the desmosomal plaque protein desmoplakin from cell-cell interfaces disrupts anchorage of intermediate filament bundles and alters intercellular junction assembly. *The Journal of cell biology,* 134**,** 985-1001.

Bouma, G. & Strober, W., 2003. The immunological and genetic basis of inflammatory bowel disease. *Nature Reviews Immunology,* 3**,** 521-533.

Brniak, W., Maslak, E. & Jachowicz, R., 2015. Orodispersible films and tablets with

prednisolone microparticles. *European Journal of Pharmaceutical Sciences,* 75**,** 81-90.

Broniowska, K.A., Diers, A.R. & Hogg, N., 2013. S-nitrosoglutathione. *Biochimica et Biophysica Acta (BBA)-General Subjects,* 1830**,** 3173-3181.

Cámara, R.J., Schoepfer, A.M., Pittet, V., Begré, S. & Von Känel, R., 2011. Mood and nonmood components of perceived stress and exacerbation of Crohn's disease. *Inflammatory bowel diseases,* 17**,** 2358-2365.

Carding, S., Verbeke, K., Vipond, D.T., Corfe, B.M. & Owen, L.J., 2015. Dysbiosis of the gut microbiota in disease. *Microbial Ecology in Health and Disease,* 26**,** 10.3402/mehd.v26.26191.

Cariello, A.J., De Souza, G.F.P., Lowen, M.S., De Oliveira, M.G. & Hofling-Lima, A.L., 2013. Assessment of ocular surface toxicity after topical instillation of nitric oxide donors. *Arquivos Brasileiros De Oftalmologia,* 76**,** 38-41.

Carnahan, R.H., Rokas, A., Gaucher, E.A. & Reynolds, A.B., 2010. The molecular evolution of the p120-catenin subfamily and its functional associations. *PLoS One,* 5**,** e15747.

Chaurasia, S., Chaubey, P., Patel, R.R., Kumar, N. & Mishra, B., 2016. Curcumin-polymeric nanoparticles against colon-26 tumor-bearing mice: cytotoxicity, pharmacokinetic and anticancer efficacy studies. *Drug Development and Industrial Pharmacy,* 42**,** 694-700.

Cheadle, G.A., Costantini, T.W., Lopez, N., Bansal, V., Eliceiri, B.P. & Coimbra, R., 2013. Enteric glia cells attenuate cytomix-induced intestinal epithelial barrier breakdown. *PLoS One,* 8**,** e69042.

Chella, N., Daravath, B., Kumar, D. & Tadikonda, R.R., 2016. Formulation and Pharmacokinetic Evaluation of Polymeric Dispersions Containing Valsartan. *European Journal of Drug Metabolism and Pharmacokinetics,* 41**,** 517-526.

Cho, J.H., 2008. The genetics and immunopathogenesis of inflammatory bowel disease. *Nature Reviews Immunology,* 8**,** 458-466.

Chourasia, M. & Jain, S., 2003. Pharmaceutical approaches to colon targeted drug delivery systems. *J Pharm Pharm Sci,* 6**,** 33-66.

Chu, H. & Mazmanian, S.K., 2013. Innate immune recognition of the microbiota promotes host-microbial symbiosis. *Nature immunology,* 14**,** 668-675.

Ćirković Veličković, T. & Gavrović-Jankulović, M., 2014. Intestinal Permeability and Transport of Food Antigens. 29-56.

Clarke, H., Soler, A.P. & Mullin, J.M., 2000. Protein kinase C activation leads to dephosphorylation of occludin and tight junction permeability increase in LLC-PK1 epithelial cell sheets. *Journal of Cell Science,* 113**,** 3187-3196.

Clarke, L.L., 2009. A guide to Ussing chamber studies of mouse intestine. *American Journal of Physiology-Gastrointestinal and Liver Physiology,* 296**,** G1151-G1166.

Colombel, J.F., Sandborn, W.J., Reinisch, W., Mantzaris, G.J., Kornbluth, A., Rachmilewitz, D., Lichtiger, S., D'haens, G., Diamond, R.H. & Broussard, D.L.,

2010. Infliximab, azathioprine, or combination therapy for Crohn's disease. *New England Journal of Medicine,* 362**,** 1383-1395.

Colucci, F., Caligiuri, M.A. & Di Santo, J.P., 2003. What does it take to make a natural killer? *Nature Reviews Immunology,* 3**,** 413-425.

Conner, S.D. & Schmid, S.L., 2003. Regulated portals of entry into the cell. *Nature,* 422**,** 37-44.

Cosnes, J., 2004. Tobacco and IBD: relevance in the understanding of disease mechanisms and clinical practice. *Best practice & research Clinical gastroenterology,* 18**,** 481-496.

Cosnes, J., Gower–Rousseau, C., Seksik, P. & Cortot, A., 2011. Epidemiology and natural history of inflammatory bowel diseases. *Gastroenterology,* 140**,** 1785-1794. e4.

Cronstein, B.N., Naime, D. & Ostad, E., 1993. The antiinflammatory mechanism of methotrexate. Increased adenosine release at inflamed sites diminishes leukocyte accumulation in an in vivo model of inflammation. *Journal of Clinical Investigation,* 92**,** 2675.

Cunningham, S.A., Arrate, M.P., Rodriguez, J.M., Bjercke, R.J., Vanderslice, P., Morris, A.P. & Brock, T.A., 2000. A Novel Protein with Homology to the Junctional Adhesion Molecule CHARACTERIZATION OF LEUKOCYTE INTERACTIONS. *Journal of Biological Chemistry,* 275**,** 34750-34756.

D'souza, T., Agarwal, R. & Morin, P.J., 2005. Phosphorylation of claudin-3 at threonine 192 by cAMP-dependent protein kinase regulates tight junction barrier function in ovarian cancer cells. *Journal of Biological Chemistry,* 280**,** 26233-26240.

D'souza, T., Indig, F.E. & Morin, P.J., 2007. Phosphorylation of claudin-4 by PKCε regulates tight junction barrier function in ovarian cancer cells. *Experimental cell research,* 313**,** 3364-3375.

D. Marcato, P., F. Adami, L., De Melo Barbosa, R., S. Melo, P., R. Ferreira, I., De Paula, L., Duran, N. & B. Seabra, A., 2013. Development of a Sustained-release System for Nitric Oxide Delivery using Alginate/Chitosan Nanoparticles. *Current Nanoscience,* 9**,** 1-7.

Dahboul, F., Perrin-Sarrado, C., Boudier, A., Lartaud, I., Schneider, R. & Leroy, P., 2014. S, S′ -dinitrosobucillamine, a new nitric oxide donor, induces a better vasorelaxation than other S-nitrosothiols. *European journal of pharmacology,* 730**,** 171-179.

Dahiya, S., Pathak, K. & Sharma, R., 2008. Development of extended release coevaporates and coprecipitates of promethazine HCl with acrylic polymers: formulation considerations. *Chemical and Pharmaceutical Bulletin,* 56**,** 504-508.

Dangre, P.V., Godbole, M.D., Ingale, P.V. & Mahapatra, D.K., 2016. Improved Dissolution and Bioavailability of Eprosartan Mesylate Formulated as Solid Dispersions using Conventional Methods. *Indian Journal of Pharmaceutical Education and Research,* 50**,** S209-S217.

Darfeuille-Michaud, A., Boudeau, J., Bulois, P., Neut, C., Glasser, A.-L., Barnich, N., Bringer, M.-A., Swidsinski, A., Beaugerie, L. & Colombel, J.-F., 2004. High prevalence of adherent-invasive Escherichia coli associated with ileal mucosa in Crohn's disease. *Gastroenterology,* 127**,** 412-421.

Dattilo, J.B. & Makhoul, R.G., 1997. The role of nitric oxide in vascular biology and pathobiology. *Annals of vascular surgery,* 11**,** 307-314.

Davenpeck, K.L., Gauthier, T.W. & Lefer, A.M., 1994. Inhibition of endothelial-derived nitric oxide promotes P-selectin expression and actions in the rat microcirculation. *Gastroenterology,* 107**,** 1050-1050.

De Mel, A., Naghavi, N., Cousins, B.G., Clatworthy, I., Hamilton, G., Darbyshire, A. & Seifalian, A.M., 2014. Nitric oxide-eluting nanocomposite for cardiovascular implants. *J Mater Sci Mater Med,* 25**,** 917-29.

De Rosa, G., Iommelli, R., La Rotonda, M.I., Miro, A. & Quaglia, F., 2000. Influence of the co-encapsulation of different non-ionic surfactants on the properties of PLGA insulin-loaded microspheres. *Journal of Controlled Release,* 69**,** 283-295.

Delmar, K. & Bianco-Peled, H., 2016. Composite chitosan hydrogels for extended release of hydrophobic drugs. *Carbohydr Polym,* 136**,** 570-80.

Diab, R., Virriat, A.-S., Ronzani, C., Fontanay, S., Grandemange, S., Elaïssari, A., Foliguet, B., Maincent, P., Leroy, P. & Duval, R., 2016. Elaboration of sterically stabilized liposomes for S-nitrosoglutathione targeting to macrophages. *Journal of biomedical nanotechnology,* 12**,** 217-230.

Dignass, A., Lynch-Devaney, K., Kindon, H., Thim, L. & Podolsky, D.K., 1994. Trefoil peptides promote epithelial migration through a transforming growth factor beta-independent pathway. *Journal of Clinical Investigation,* 94**,** 376.

Dodane, V., Khan, M.A. & Merwin, J.R., 1999. Effect of chitosan on epithelial permeability and structure. *International journal of pharmaceutics,* 182**,** 21-32.

Dow, J., Maddrell, S., Davies, S.-A., Skaer, N. & Kaiser, K., 1994. A novel role for the nitric oxide-cGMP signaling pathway: the control of epithelial function in Drosophila. *American Journal of Physiology-Regulatory, Integrative and Comparative Physiology,* 266**,** R1716-R1719.

Drakes, M.L., Blanchard, T.G. & Czinn, S.J., 2005. Colon lamina propria dendritic cells induce a proinflammatory cytokine response in lamina propria T cells in the SCID mouse model of colitis. *Journal of leukocyte biology,* 78**,** 1291-1300.

Dringen, R., Gutterer, J.M. & Hirrlinger, J., 2000. Glutathione metabolism in brain - Metabolic interaction between astrocytes and neurons in the defense against reactive oxygen species. *European Journal of Biochemistry,* 267**,** 4912-4916.

Dubuquoy, L., Rousseaux, C., Thuru, X., Peyrin-Biroulet, L., Romano, O., Chavatte, P., Chamaillard, M. & Desreumaux, P., 2006. PPARγ as a new therapeutic target in inflammatory bowel diseases. *Gut,* 55**,** 1341-1349.

Duerkop, B.A., Vaishnava, S. & Hooper, L.V., 2009. Immune responses to the microbiota at the intestinal mucosal surface. *Immunity,* 31**,** 368-376.

Duong, H.T., Dong, Z., Su, L., Boyer, C., George, J., Davis, T.P. & Wang, J., 2015. The

use of nanoparticles to deliver nitric oxide to hepatic stellate cells for treating liver fibrosis and portal hypertension. *Small,* 11**,** 2291-304.

Duong, H.T., Kamarudin, Z.M., Erlich, R.B., Li, Y., Jones, M.W., Kavallaris, M., Boyer, C. & Davis, T.P., 2013. Intracellular nitric oxide delivery from stable NO-polymeric nanoparticle carriers. *Chem Commun (Camb),* 49**,** 4190-2.

Ebnet, K., 2008. Organization of multiprotein complexes at cell–cell junctions. *Histochemistry and cell biology,* 130**,** 1-20.

Ebnet, K., Suzuki, A., Ohno, S. & Vestweber, D., 2004. Junctional adhesion molecules (JAMs): more molecules with dual functions? *Journal of Cell Science,* 117**,** 19-29.

Eerikainen, H. & Kauppinen, E.I., 2003. Preparation of polymeric nanoparticles containing corticosteroid by a novel aerosol flow reactor method. *International Journal of Pharmaceutics,* 263**,** 69-83.

Emmanuel, D.G., Madsen, K.L., Churchill, T.A., Dunn, S.M. & Ametaj, B.N., 2007. Acidosis and lipopolysaccharide from Escherichia coli B:055 cause hyperpermeability of rumen and colon tissues. *J Dairy Sci,* 90**,** 5552-7.

Fang, F.C., 1997. Perspectives series: host/pathogen interactions. Mechanisms of nitric oxide-related antimicrobial activity. *Journal of Clinical Investigation,* 99**,** 2818.

Fanning, A.S., Ma, T.Y. & Anderson, J.M., 2002. Isolation and functional characterization of the actin binding region in the tight junction protein ZO-1. *The FASEB Journal,* 16**,** 1835-1837.

Feldman, G.J., Mullin, J.M. & Ryan, M.P., 2005. Occludin: structure, function and regulation. *Adv Drug Deliv Rev,* 57**,** 883-917.

Fiocchi, C., 2008. What is "physiological" intestinal inflammation and how does it differ from "pathological" inflammation? *Inflammatory bowel diseases,* 14**,** S77-S78.

Flamant, M., Aubert, P., Rolli-Derkinderen, M., Bourreille, A., Neunlist, M.R., Mahe, M.M., Meurette, G., Marteyn, B., Savidge, T., Galmiche, J.P., Sansonetti, P.J. & Neunlist, M., 2011. Enteric glia protect against Shigella flexneri invasion in intestinal epithelial cells: a role for S-nitrosoglutathione. *Gut,* 60**,** 473-84.

Forsgård, R., Korpela, R., Stenman, L., Österlund, P. & Holma, R., 2014. Deoxycholic acid induced changes in electrophysiological parameters and macromolecular permeability in murine small intestine with and without functional enteric nervous system plexuses. *Neurogastroenterology & Motility,* 26**,** 1179-1187.

Fortuna, A., Alves, G., Falcao, A. & Soares-Da-Silva, P., 2012. Evaluation of the permeability and P-glycoprotein efflux of carbamazepine and several derivatives across mouse small intestine by the Ussing chamber technique. *Epilepsia,* 53**,** 529-38.

Francis, S.H., Busch, J.L. & Corbin, J.D., 2010. cGMP-dependent protein kinases and cGMP phosphodiesterases in nitric oxide and cGMP action. *Pharmacological reviews,* 62**,** 525-563.

Furchgott, R.F. & Zawadzki, J.V., 1980. The obligatory role of endothelial cells in the

relaxation of arterial smooth muscle by acetylcholine. *Nature,* 288**,** 373-376.

Furuse, M., Itoh, M., Hirase, T., Nagafuchi, A., Yonemura, S., Tsukita, S. & Tsukita, S., 1994. Direct association of occludin with ZO-1 and its possible involvement in the localization of occludin at tight junctions. *Journal of Cell Biology,* 127**,** 1617-1626.

Galipeau, H.J. & Verdu, E.F., 2016. The complex task of measuring intestinal permeability in basic and clinical science. *Neurogastroenterol Motil,* 28**,** 957-65.

Gallicano, G.I., Kouklis, P., Bauer, C., Yin, M., Vasioukhin, V., Degenstein, L. & Fuchs, E., 1998. Desmoplakin is required early in development for assembly of desmosomes and cytoskeletal linkage. *J Cell Biol,* 143**,** 2009-2022.

Gallo, R.L. & Hooper, L.V., 2012. Epithelial antimicrobial defence of the skin and intestine. *Nature reviews. Immunology,* 12**,** 503-516.

Gandhi, A., Jana, S. & Sen, K.K., 2014. In-vitro release of acyclovir loaded Eudragit RLPO® nanoparticles for sustained drug delivery. *International journal of biological macromolecules,* 67**,** 478-482.

Garcıa-Fuentes, M., Torres, D. & Alonso, M., 2003. Design of lipid nanoparticles for the oral delivery of hydrophilic macromolecules. *Colloids and Surfaces B: Biointerfaces,* 27**,** 159-168.

Garrait, G., Beyssac, E. & Subirade, M., 2014. Development of a novel drug delivery system: chitosan nanoparticles entrapped in alginate microparticles. *J Microencapsul,* 31**,** 363-72.

Garthwaite, J., 2008. Concepts of neural nitric oxide‐mediated transmission. *European Journal of Neuroscience,* 27**,** 2783-2802.

Gassler, N., Rohr, C., Schneider, A., Kartenbeck, J., Bach, A., Obermüller, N., Otto, H.F. & Autschbach, F., 2001. Inflammatory bowel disease is associated with changes of enterocytic junctions. *American Journal of Physiology-Gastrointestinal and Liver Physiology,* 281**,** G216-G228.

Gaston, B., Reilly, J., Drazen, J.M., Fackler, J., Ramdev, P., Arnelle, D., Mullins, M.E., Sugarbaker, D.J., Chee, C. & Singel, D.J., 1993. Endogenous nitrogen oxides and bronchodilator S-nitrosothiols in human airways. *Proceedings of the National Academy of Sciences of the United States of America,* 90**,** 10957-10961.

Gaucher, C., Boudier, A., Dahboul, F., Parent, M. & Leroy, P., 2013. S-nitrosation/denitrosation in cardiovascular pathologies: facts and concepts for the rational design of S-nitrosothiols. *Current pharmaceutical design,* 19**,** 458-472.

George, M. & Abraham, T.E., 2006. Polyionic hydrocolloids for the intestinal delivery of protein drugs: alginate and chitosan—a review. *Journal of controlled release,* 114**,** 1-14.

Georgii, J.L., Amadeu, T.P., Seabra, A.B., De Oliveira, M.G. & Monte-Alto-Costa, A., 2011. Topical S-nitrosoglutathione-releasing hydrogel improves healing of rat ischaemic wounds. *J Tissue Eng Regen Med,* 5**,** 612-9.

Gerald A. Cheadle, T.W.C., Nicole Lopez, Vishal Bansal, Brian P. Eliceiri, Raul Coimbra, 2012. Enteric glia cells attenuate cytomix-induced intestinal epithelial barrier breakdown. *Plos One,* 8**,** e69042.

Gersemann, M., Wehkamp, J., Fellermann, K. & Stange, E.F., 2008. Crohn's disease–defect in innate defence. *World J Gastroenterol,* 14**,** 5499-5503.

Gombotz, W.R. & Wee, S.F., 2012. Protein release from alginate matrices. *Advanced drug delivery reviews,* 64**,** 194-205.

Goncalves, F.L., Bueno, M.P., Schmidt, A.F., Figueira, R.L. & Sbragia, L., 2015. Treatment of bowel in experimental gastroschisis with a nitric oxide donor. *Am J Obstet Gynecol,* 212**,** 383 e1-7.

Gonzalez, D.R., Treuer, A., Sun, Q.-A., Stamler, J.S. & Hare, J.M., 2009. S-Nitrosylation of cardiac ion channels. *Journal of cardiovascular pharmacology,* 54**,** 188.

Grès, M.-C., Julian, B., Bourrié, M., Meunier, V., Roques, C., Berger, M., Boulenc, X., Berger, Y. & Fabre, G., 1998. Correlation between oral drug absorption in humans, and apparent drug permeability in TC-7 cells, a human epithelial intestinal cell line: comparison with the parental Caco-2 cell line. *Pharmaceutical research,* 15**,** 726-733.

Groschwitz, K.R. & Hogan, S.P., 2009. Intestinal barrier function: molecular regulation and disease pathogenesis. *J Allergy Clin Immunol,* 124**,** 3-20; quiz 21-2.

Gulsun, T., Gursoy, R. & Levent, O., 2009. Nanocrystal technology for oral delivery of poorly water-soluble drugs. *FARAD Journal of Pharmaceutical Sciences,* 34**,** 55-65.

Guzik, T.J., Korbut, R. & Adamek-Guzik, T., 2003. Nitric oxide and superoxide in inflammation and immune regulation. *Journal of Physiology and Pharmacology,* 54**,** 469-487.

Haendeler, J., Hoffmann, J., Tischler, V., Berk, B.C., Zeiher, A.M. & Dimmeler, S., 2002. Redox regulatory and anti-apoptotic functions of thioredoxin depend on S-nitrosylation at cysteine 69. *Nature cell biology,* 4**,** 743-749.

Han, Y., Tian, H., He, P., Chen, X. & Jing, X., 2009. Insulin nanoparticle preparation and encapsulation into poly (lactic-co-glycolic acid) microspheres by using an anhydrous system. *International journal of pharmaceutics,* 378**,** 159-166.

Hanauer, S.B., 2017. Combination Therapy for Inflammatory Bowel Disease. *Gastroenterology & Hepatology,* 13.

Harhaj, N.S. & Antonetti, D.A., 2004. Regulation of tight junctions and loss of barrier function in pathophysiology. *The international journal of biochemistry & cell biology,* 36**,** 1206-1237.

Hart, T.W., 1985. Some observations concerning the S-nitroso and S-phenylsulphonyl derivatives of L-cysteine and glutathione. *Tetrahedron Letters,* 26**,** 2013-2016.

Hartmann, F. & Stein, J., 2010. Clinical trial: controlled, open, randomized multicentre study comparing the effects of treatment on quality of life, safety and efficacy of budesonide or mesalazine enemas in active left‐sided ulcerative colitis.

Alimentary pharmacology & therapeutics, 32**,** 368-376.

Hartsock, A. & Nelson, W.J., 2008. Adherens and tight junctions: structure, function and connections to the actin cytoskeleton. *Biochimica et Biophysica Acta (BBA)-Biomembranes,* 1778**,** 660-669.

Hasan, A.S., Socha, M., Lamprecht, A., Ghazouani, F.E., Sapin, A., Hoffman, M., Maincent, P. & Ubrich, N., 2007. Effect of the microencapsulation of nanoparticles on the reduction of burst release. *Int J Pharm,* 344**,** 53-61.

Haskins, J., Gu, L., Wittchen, E.S., Hibbard, J. & Stevenson, B.R., 1998. ZO-3, a novel member of the MAGUK protein family found at the tight junction, interacts with ZO-1 and occludin. *The Journal of cell biology,* 141**,** 199-208.

Hassan, A.S., Sapin, A., Lamprecht, A., Emond, E., El Ghazouani, F. & Maincent, P., 2009. Composite microparticles with in vivo reduction of the burst release effect. *European Journal of Pharmaceutics and Biopharmaceutics,* 73**,** 337-344.

Hatzfeld, M., 2007. Plakophilins: Multifunctional proteins or just regulators of desmosomal adhesion? *Biochimica et Biophysica Acta (BBA)-Molecular Cell Research,* 1773**,** 69-77.

Heanue, T.A. & Pachnis, V., 2007. Enteric nervous system development and Hirschsprung's disease: advances in genetic and stem cell studies. *Nature reviews. Neuroscience,* 8**,** 466.

Heikal, L., Aaronson, P.I., Ferro, A., Nandi, M., Martin, G.P. & Dailey, L.A., 2011. S-nitrosophytochelatins: investigation of the bioactivity of an oligopeptide nitric oxide delivery system. *Biomacromolecules,* 12**,** 2103-13.

Heikal, L., Martin, G.P. & Dailey, L.A., 2009. Characterisation of the decomposition behaviour of S-nitrosoglutathione and a new class of analogues: S-Nitrosophytochelatins. *Nitric Oxide,* 20**,** 157-165.

Hermiston, M.L. & Gordon, J.I., 1995. In vivo analysis of cadherin function in the mouse intestinal epithelium: essential roles in adhesion, maintenance of differentiation, and regulation of programmed cell death. *Journal of Cell Biology,* 129**,** 489-506.

Hewlett, L.J., Prescott, A.R. & Watts, C., 1994. The coated pit and macropinocytic pathways serve distinct endosome populations. *Journal of Cell Biology,* 124**,** 689-689.

Hindorf, U., Johansson, M., Eriksson, A., Kvifors, E. & Almer, S., 2009. Mercaptopurine treatment should be considered in azathioprine intolerant patients with inflammatory bowel disease. *Alimentary pharmacology & therapeutics,* 29**,** 654-661.

Hinds, K.D., Campbell, K.M., Holland, K.M., Lewis, D.H., Piché, C.A. & Schmidt, P.G., 2005. PEGylated insulin in PLGA microparticles. In vivo and in vitro analysis. *Journal of controlled release,* 104**,** 447-460.

Hoffman, B.D. & Yap, A.S., 2015. Towards a Dynamic Understanding of Cadherin-Based Mechanobiology. *Trends Cell Biol,* 25**,** 803-14.

Hogaboam, C.M., Befus, A.D. & Wallace, J.L., 1993. Modulation of rat mast cell

reactivity by IL-1 beta. Divergent effects on nitric oxide and platelet-activating factor release. *The Journal of Immunology,* 151**,** 3767-3774.

Hogg, N., 2000. Biological chemistry and clinical potential of S-nitrosothiols. *Free Radical Biology and Medicine,* 28**,** 1478-1486.

Höög, J.-O. & Östberg, L.J., 2011. Mammalian alcohol dehydrogenases–a comparative investigation at gene and protein levels. *Chemico-biological interactions,* 191**,** 2-7.

Hooper, L.V., 2009. Do symbiotic bacteria subvert host immunity? *Nature reviews microbiology,* 7**,** 367-374.

Hooper, L.V. & Macpherson, A.J., 2010. Immune adaptations that maintain homeostasis with the intestinal microbiota. *Nature reviews. Immunology,* 10**,** 159.

Hu, J., Johnston, K.P. & Williams Iii, R.O., 2004. Nanoparticle engineering processes for enhancing the dissolution rates of poorly water soluble drugs. *Drug development and industrial pharmacy,* 30**,** 233-245.

Huang, C., Haritunians, T., Okou, D.T., Cutler, D.J., Zwick, M.E., Taylor, K.D., Datta, L.W., Maranville, J.C., Liu, Z. & Ellis, S., 2015. Characterization of genetic loci that affect susceptibility to inflammatory bowel diseases in African Americans. *Gastroenterology,* 149**,** 1575-1586.

Huang, F.-P., Niedbala, W., Wei, X.-Q., Xu, D., Fang, G., Robinson, J.H., Lam, C. & Liew, F.Y., 1998. Nitric oxide regulates Th1 cell development through the inhibition of IL-12 synthesis by macrophages. *European journal of immunology,* 28**,** 4062-4070.

Huang, X., Xiao, Y. & Lang, M., 2012. Micelles/sodium-alginate composite gel beads: A new matrix for oral drug delivery of indomethacin. *Carbohydrate polymers,* 87**,** 790-798.

Huang, Y. & Chen, Z., 2016. Inflammatory bowel disease related innate immunity and adaptive immunity. *American Journal of Translational Research,* 8**,** 2490-2497.

Ignarro, L.J., 2000. *Nitric oxide: biology and pathobiology*: Academic press.

Ignarro, L.J., Lippton, H., Edwards, J.C., Baricos, W.H., Hyman, A.L., Kadowitz, P.J. & Gruetter, C.A., 1981. Mechanism of vascular smooth muscle relaxation by organic nitrates, nitrites, nitroprusside and nitric oxide: evidence for the involvement of S-nitrosothiols as active intermediates. *Journal of Pharmacology and Experimental Therapeutics,* 218**,** 739-749.

Itoh, M., Furuse, M., Morita, K., Kubota, K., Saitou, M. & Tsukita, S., 1999. Direct binding of three tight junction-associated MAGUKs, ZO-1, ZO-2, and ZO-3, with the COOH termini of claudins. *The Journal of cell biology,* 147**,** 1351-1363.

Jadeski, L.C. & Lala, P.K., 1999. Nitric oxide synthase inhibition by N G-nitro-l-arginine methyl ester inhibits tumor-induced angiogenesis in mammary tumors. *The American journal of pathology,* 155**,** 1381-1390.

Jaffrey, S.R., Erdjument-Bromage, H., Ferris, C.D., Tempst, P. & Snyder, S.H., 2001.

Protein S-nitrosylation: a physiological signal for neuronal nitric oxide. *Nat Cell Biol,* 3**,** 193-197.

Jain, S., Suzuki, T., Seth, A., Samak, G. & Rao, R., 2011. Protein kinase Cζ phosphorylates occludin and promotes assembly of epithelial tight junctions. *Biochemical Journal,* 437**,** 289-299.

Jandhyala, S.M., Talukdar, R., Subramanyam, C., Vuyyuru, H., Sasikala, M. & Reddy, D.N., 2015. Role of the normal gut microbiota. *World Journal of Gastroenterology : WJG,* 21**,** 8787-8803.

Jensen, D.E., Belka, G.K. & Du Bois, G.C., 1998. S-Nitrosoglutathione is a substrate for rat alcohol dehydrogenase class III isoenzyme. *Biochemical Journal,* 331**,** 659-668.

Jess, T., Rungoe, C. & Peyrin–Biroulet, L., 2012. Risk of colorectal cancer in patients with ulcerative colitis: a meta-analysis of population-based cohort studies. *Clinical Gastroenterology and Hepatology,* 10**,** 639-645.

Johansson, M.E., Phillipson, M., Petersson, J., Velcich, A., Holm, L. & Hansson, G.C., 2008. The inner of the two Muc2 mucin-dependent mucus layers in colon is devoid of bacteria. *Proceedings of the national academy of sciences,* 105**,** 15064-15069.

Joshi, A., Keerthiprasad, R., Jayant, R.D. & Srivastava, R., 2010. Nano-in-micro alginate based hybrid particles. *Carbohydrate Polymers,* 81**,** 790-798.

Jostins, L., Ripke, S., Weersma, R.K., Duerr, R.H., Mcgovern, D.P., Hui, K.Y., Lee, J.C., Schumm, L.P., Sharma, Y. & Anderson, C.A., 2012. Host-microbe interactions have shaped the genetic architecture of inflammatory bowel disease. *Nature,* 491**,** 119-124.

Kadian, S.S. & Harikumar, S., 2016. Eudragit and its pharmaceutical significance.

Kaiser, G.C., Yan, F. & Polk, D.B., 1999. Mesalamine blocks tumor necrosis factor growth inhibition and nuclear factor κB activation in mouse colonocytes. *Gastroenterology,* 116**,** 602-609.

Kakizawa, Y., Nishio, R., Hirano, T., Koshi, Y., Nukiwa, M., Koiwa, M., Michizoe, J. & Ida, N., 2010. Controlled release of protein drugs from newly developed amphiphilic polymer-based microparticles composed of nanoparticles. *Journal of Controlled Release,* 142**,** 8-13.

Kanai, T., Kawamura, T., Dohi, T., Makita, S., Nemoto, Y., Totsuka, T. & Watanabe, M., 2006. TH1/TH2 - mediated colitis induced by adoptive transfer of CD4+ CD45RBhigh T lymphocytes into nude mice. *Inflammatory bowel diseases,* 12**,** 89-99.

Kang, J.H. & Ko, Y.T., 2015. Lipid-coated gold nanocomposites for enhanced cancer therapy. *Int J Nanomedicine,* 10 Spec Iss**,** 33-45.

Katsuno, T., Umeda, K., Matsui, T., Hata, M., Tamura, A., Itoh, M., Takeuchi, K., Fujimori, T., Nabeshima, Y.-I. & Noda, T., 2008. Deficiency of zonula occludens-1 causes embryonic lethal phenotype associated with defected yolk sac angiogenesis and apoptosis of embryonic cells. *Molecular biology of the*

cell, 19**,** 2465-2475.

Kawedia, J.D., Jiang, M., Kulkarni, A., Waechter, H.E., Matlin, K.S., Pauletti, G.M. & Menon, A.G., 2008. The protein kinase A pathway contributes to Hg2+-induced alterations in phosphorylation and subcellular distribution of occludin associated with increased tight junction permeability of salivary epithelial cell monolayers. *J Pharmacol Exp Ther,* 326**,** 829-37.

Keck, C.M. & Müller, R.H., 2006. Drug nanocrystals of poorly soluble drugs produced by high pressure homogenisation. *European Journal of Pharmaceutics and Biopharmaceutics,* 62**,** 3-16.

Kesarwani, P., Rastogi, S., Bhalla, V. & Arora, V., 2014. Solubility Enhancement of Poorly Water Soluble Drugs: A Review. *International Journal of Pharmaceutical Sciences and Research,* 5**,** 3123.

Kettenhofen, N.J., Broniowska, K.A., Keszler, A., Zhang, Y. & Hogg, N., 2007. Proteomic methods for analysis of S-nitrosation. *Journal of Chromatography B,* 851**,** 152-159.

Khan, M., Dhammu, T.S., Matsuda, F., Baarine, M., Dhindsa, T.S., Singh, I. & Singh, A.K., 2015. Promoting endothelial function by S-nitrosoglutathione through the HIF-1alpha/VEGF pathway stimulates neurorepair and functional recovery following experimental stroke in rats. *Drug Des Devel Ther,* 9**,** 2233-47.

Khan, S.A. & Schneider, M., 2014. Stabilization of Gelatin Nanoparticles Without Crosslinking. *Macromolecular Bioscience,* 14**,** 1627-1638.

Khuathan, N. & Pongjanyakul, T., 2014. Modification of quaternary polymethacrylate films using sodium alginate: film characterization and drug permeability. *International journal of pharmaceutics,* 460**,** 63-72.

Kim, J.O., Noh, J.K., Thapa, R.K., Hasan, N., Choi, M., Kim, J.H., Lee, J.H., Ku, S.K. & Yoo, J.W., 2015. Nitric oxide-releasing chitosan film for enhanced antibacterial and in vivo wound-healing efficacy. *Int J Biol Macromol,* 79**,** 217-25.

Kim, Y.S. & Ho, S.B., 2010. Intestinal goblet cells and mucins in health and disease: recent insights and progress. *Current gastroenterology reports,* 12**,** 319-330.

Kirchgesner, J., Beaugerie, L., Carrat, F., Andersen, N.N., Jess, T. & Schwarzinger, M., 2017. Increased risk of acute arterial events in young patients and severely active IBD: a nationwide French cohort study. *Gut***,** gutjnl-2017-314015.

Klingler, C., Müller, B.W. & Steckel, H., 2009. Insulin-micro-and nanoparticles for pulmonary delivery. *International journal of pharmaceutics,* 377**,** 173-179.

Knowles, R.G. & Moncada, S., 1994. Nitric oxide synthases in mammals. *Biochemical Journal,* 298**,** 249.

Kobayashi, Y., 2010. The regulatory role of nitric oxide in proinflammatory cytokine expression during the induction and resolution of inflammation. *J Leukoc Biol,* 88**,** 1157-62.

Kochar, N.I., Chandewal, A.V., Bakal, R.L. & Kochar, P.N., 2011. Nitric oxide and the gastrointestinal tract. *Int. J. Pharmacol,* 7**,** 31-39.

Koivusalo, M., Baumann, M. & Uotila, L., 1989. Evidence for the identity of glutathione-dependent formaldehyde dehydrogenase and class III alcohol dehydrogenase. *FEBS letters,* 257**,** 105-109.

Kökten, T., Gibot, S., Lepage, P., D'alessio, S., Hablot, J., Ndiaye, N.-C., Busby-Venner, H., Monot, C., Garnier, B. & Moulin, D., 2017. TREM-1 inhibition restores impaired autophagy activity and reduces colitis in mice. *Journal of Crohn's and Colitis*.

Kolios, G., Valatas, V. & Ward, S.G., 2004. Nitric oxide in inflammatory bowel disease: a universal messenger in an unsolved puzzle. *Immunology,* 113**,** 427-437.

Konturek, P., Haziri, D., Brzozowski, T., Hess, T., Heyman, S., Kwiecien, S., Konturek, S. & Koziel, J., 2015. Emerging role of fecal microbiota therapy in the treatment of gastrointestinal and extra-gastrointestinal diseases. *J Physiol Pharmacol,* 66**,** 483-491.

Koukaras, E.N., Papadimitriou, S.A., Bikiaris, D.N. & Froudakis, G.E., 2012. Insight on the formation of chitosan nanoparticles through ionotropic gelation with tripolyphosphate. *Molecular pharmaceutics,* 9**,** 2856-2862.

Kowalczyk, A.P. & Green, K.J., 2013. Structure, Function and Regulation of Desmosomes. *Progress in molecular biology and translational science,* 116**,** 95-118.

Krishnaiah, Y.S., 2012. Pharmaceutical technologies for enhancing oral bioavailability of poorly soluble drugs. *Journal of Bioequivalence & Bioavailability,* 2010.

Krug, S.M., Amasheh, S., Richter, J.F., Milatz, S., Günzel, D., Westphal, J.K., Huber, O., Schulzke, J.D. & Fromm, M., 2009. Tricellulin forms a barrier to macromolecules in tricellular tight junctions without affecting ion permeability. *Molecular biology of the cell,* 20**,** 3713-3724.

Kubes, P. & Mccafferty, D.-M., 2000. Nitric oxide and intestinal inflammation. *The American journal of medicine,* 109**,** 150-158.

Kumar, H., Kawai, T. & Akira, S., 2011. Pathogen recognition by the innate immune system. *Int Rev Immunol,* 30**,** 16-34.

Kumar, K., Dhawan, N., Sharma, H., Vaidya, S. & Vaidya, B., 2014. Bioadhesive polymers: Novel tool for drug delivery. *Artificial cells, nanomedicine, and biotechnology,* 42**,** 274-283.

Kushare, S.S. & Gattani, S.G., 2013. Microwave‐generated bionanocomposites for solubility and dissolution enhancement of poorly water‐soluble drug glipizide: in‐vitro and in‐vivo studies. *Journal of pharmacy and pharmacology,* 65**,** 79-93.

Laffleur, F. & Bernkop-Schnürch, A., 2013. Strategies for improving mucosal drug delivery. *Nanomedicine,* 8**,** 2061-2075.

Lapaquette, P., Glasser, A.L., Huett, A., Xavier, R.J. & Darfeuille‐Michaud, A., 2010. Crohn's disease‐associated adherent‐invasive E. coli are selectively favoured by impaired autophagy to replicate intracellularly. *Cellular microbiology,* 12**,** 99-113.

Laukoetter, M.G., Nava, P., Lee, W.Y., Severson, E.A., Capaldo, C.T., Babbin, B.A., Williams, I.R., Koval, M., Peatman, E. & Campbell, J.A., 2007. JAM-A regulates permeability and inflammation in the intestine in vivo. *Journal of Experimental Medicine,* 204**,** 3067-3076.

Leach, W.T., Simpson, D.T., Val, T.N., Anuta, E.C., Yu, Z., Williams, R.O. & Johnston, K.P., 2005. Uniform encapsulation of stable protein nanoparticles produced by spray freezing for the reduction of burst release. *Journal of pharmaceutical sciences,* 94**,** 56-69.

Lee, S.H., 2015. Intestinal Permeability Regulation by Tight Junction: Implication on Inflammatory Bowel Diseases. *Intestinal Research,* 13**,** 11-18.

Lefer, A.M. & Lefer, D.J., 1999. II. Nitric oxide protects in intestinal inflammation. *American Journal of Physiology-Gastrointestinal and Liver Physiology,* 276**,** G572-G575.

Li, J.K., Wang, N. & Wu, X.S., 1997. A novel biodegradable system based on gelatin nanoparticles and poly (lactic‐co‐glycolic acid) microspheres for protein and peptide drug delivery. *Journal of pharmaceutical sciences,* 86**,** 891-895.

Li, L., Fang, Y., Vreeker, R., Appelqvist, I. & Mendes, E., 2007. Reexamining the egg-box model in calcium− alginate gels with X-ray diffraction. *Biomacromolecules,* 8**,** 464-468.

Li, Y., Fanning, A.S., Anderson, J.M. & Lavie, A., 2005a. Structure of the conserved cytoplasmic C-terminal domain of occludin: identification of the ZO-1 binding surface. *Journal of molecular biology,* 352**,** 151-164.

Li, Z., Ramay, H.R., Hauch, K.D., Xiao, D. & Zhang, M., 2005b. Chitosan–alginate hybrid scaffolds for bone tissue engineering. *Biomaterials,* 26**,** 3919-3928.

Li, Z., Zhang, X., Zhou, H., Liu, W. & Li, J., 2016. Exogenous S-nitrosoglutathione attenuates inflammatory response and intestinal epithelial barrier injury in endotoxemic rats. *J Trauma Acute Care Surg,* 80**,** 977-84.

Liu, J., Walker, N.M., Ootani, A., Strubberg, A.M. & Clarke, L.L., 2015a. Defective goblet cell exocytosis contributes to murine cystic fibrosis–associated intestinal disease. *The Journal of Clinical Investigation,* 125**,** 1056-1068.

Liu, J.Z., Van Sommeren, S., Huang, H., Ng, S.C., Alberts, R., Takahashi, A., Ripke, S., Lee, J.C., Jostins, L. & Shah, T., 2015b. Association analyses identify 38 susceptibility loci for inflammatory bowel disease and highlight shared genetic risk across populations. *Nature genetics,* 47**,** 979-986.

Liu, W., Liu, W., Ye, A., Peng, S., Wei, F., Liu, C. & Han, J., 2016. Environmental stress stability of microencapsules based on liposomes decorated with chitosan and sodium alginate. *Food Chem,* 196**,** 396-404.

Liu, Y., Nusrat, A., Schnell, F.J., Reaves, T.A., Walsh, S., Pochet, M. & Parkos, C.A., 2000. Human junction adhesion molecule regulates tight junction resealing in epithelia. *J Cell Sci,* 113**,** 2363-2374.

Löbenberg, R. & Amidon, G.L., 2000. Modern bioavailability, bioequivalence and biopharmaceutics classification system. New scientific approaches to

international regulatory standards. *European Journal of Pharmaceutics and Biopharmaceutics,* 50**,** 3-12.

Loftsson, T. & Brewster, M.E., 2010. Pharmaceutical applications of cyclodextrins: basic science and product development. *Journal of pharmacy and pharmacology,* 62**,** 1607-1621.

Lopes, M., Abrahim, B., Veiga, F., Seica, R., Cabral, L.M., Arnaud, P., Andrade, J.C. & Ribeiro, A.J., 2017. Preparation methods and applications behind alginate-based particles. *Expert Opin Drug Deliv,* 14**,** 769-782.

Luissint, A.-C., Nusrat, A. & Parkos, C.A., Year. JAM-related proteins in mucosal homeostasis and inflammationed.^eds. *Seminars in immunopathology*Springer, 211-226.

Lund, J.N. & Scholefield, J.H., 1997. A randomised, prospective, double-blind, placebo-controlled trial of glyceryl trinitrate ointment in treatment of anal fissure. *The Lancet,* 349**,** 11-14.

Lutgendorff, F., Akkermans, L. & Soderholm, J.D., 2008. The role of microbiota and probiotics in stress-induced gastrointestinal damage. *Current molecular medicine,* 8**,** 282-298.

Macfarlane, S. & Macfarlane, G.T., 2003. Regulation of short-chain fatty acid production. *Proceedings of the Nutrition Society,* 62**,** 67-72.

Mackie, A.R., Macierzanka, A., Aarak, K., Rigby, N.M., Parker, R., Channell, G.A., Harding, S.E. & Bajka, B.H., 2016. Sodium alginate decreases the permeability of intestinal mucus. *Food hydrocolloids,* 52**,** 749-755.

Macpherson, A.J. & Harris, N.L., 2004. Interactions between commensal intestinal bacteria and the immune system. *Nature Reviews Immunology,* 4**,** 478-485.

Magierowski, M., Magierowska, K., Kwiecien, S. & Brzozowski, T., 2015. Gaseous mediators nitric oxide and hydrogen sulfide in the mechanism of gastrointestinal integrity, protection and ulcer healing. *Molecules,* 20**,** 9099-9123.

Mahid, S.S., Minor, K.S., Soto, R.E., Hornung, C.A. & Galandiuk, S., Year. Smoking and inflammatory bowel disease: a meta-analysised.^eds. *Mayo Clinic Proceedings*Elsevier, 1462-1471.

Mahida, Y., Lamming, C., Gallagher, A., Hawthorne, A. & Hawkey, C., 1991. 5-Aminosalicylic acid is a potent inhibitor of interleukin 1 beta production in organ culture of colonic biopsy specimens from patients with inflammatory bowel disease. *Gut,* 32**,** 50-54.

Mansuri, S., Kesharwani, P., Tekade, R.K. & Jain, N.K., 2016. Lyophilized mucoadhesive-dendrimer enclosed matrix tablet for extended oral delivery of albendazole. *Eur J Pharm Biopharm,* 102**,** 202-13.

Marcato, P.D., Adami, L.F., Melo, P.S., De Paula, L., Durán, N. & Seabra, A., Year. Glutathione and S-nitrosoglutathione in alginate/chitosan nanoparticles: Cytotoxicityed.^eds. *Journal of Physics: Conference Series*IOP Publishing, 012045.

Marchiando, A.M., Shen, L., Graham, W.V., Weber, C.R., Schwarz, B.T., Austin, J.R., Raleigh, D.R., Guan, Y., Watson, A.J. & Montrose, M.H., 2010. Caveolin-1–dependent occludin endocytosis is required for TNF-induced tight junction regulation in vivo. *The Journal of cell biology,* 189**,** 111-126.

Mariette, X., Matucci-Cerinic, M., Pavelka, K., Taylor, P., Van Vollenhoven, R., Heatley, R., Walsh, C., Lawson, R., Reynolds, A. & Emery, P., 2011. Malignancies associated with tumour necrosis factor inhibitors in registries and prospective observational studies: a systematic review and meta-analysis. *Annals of the rheumatic diseases,* 70**,** 1895-1904.

Marin, N., Zamorano, P., Carrasco, R., Mujica, P., Gonzalez, F.G., Quezada, C., Meininger, C.J., Boric, M.P., Duran, W.N. & Sanchez, F.A., 2012. S-Nitrosation of beta-catenin and p120 catenin: a novel regulatory mechanism in endothelial hyperpermeability. *Circ Res,* 111**,** 553-63.

Markowitz, J., Grancher, K., Kohn, N., Lesser, M., Daum, F. & Pediatric, T., 2000. A multicenter trial of 6-mercaptopurine and prednisone in children with newly diagnosed Crohn's disease. *Gastroenterology,* 119**,** 895-902.

Marshall, H.E., Hess, D.T. & Stamler, J.S., 2004. S-nitrosylation: Physiological regulation of NF-κB. *Proceedings of the National Academy of Sciences of the United States of America,* 101**,** 8841-8842.

Martins, A.F., Follmann, H.D., Monteiro, J.P., Bonafe, E.G., Nocchi, S., Silva, C.T., Nakamura, C.V., Girotto, E.M., Rubira, A.F. & Muniz, E.C., 2015. Polyelectrolyte complex containing silver nanoparticles with antitumor property on Caco-2 colon cancer cells. *Int J Biol Macromol,* 79**,** 748-55.

Masini, E., Salvemini, D., Pistelli, A., Mannaioni, P. & Vane, J., 1991. Rat mast cells synthesize a nitric oxide like-factor which modulates the release of histamine. *Agents and actions,* 33**,** 61-63.

Matsuoka, K. & Kanai, T., 2015. The gut microbiota and inflammatory bowel disease. *Seminars in Immunopathology,* 37**,** 47-55.

Mawdsley, J.E. & Rampton, D.S., 2007. The role of psychological stress in inflammatory bowel disease. *Neuroimmunomodulation,* 13**,** 327-336.

May, G., Crook, P., Moore, P. & Page, C., 1991. The role of nitric oxide as an endogenous regulator of platelet and neutrophil activation within the pulmonary circulation of the rabbit. *British journal of pharmacology,* 102**,** 759-763.

Maynard, C.L., Elson, C.O., Hatton, R.D. & Weaver, C.T., 2012. Reciprocal interactions of the intestinal microbiota and immune system. *Nature,* 489**,** 231-241.

Mcgovern, D.P., Kugathasan, S. & Cho, J.H., 2015. Genetics of inflammatory bowel diseases. *Gastroenterology,* 149**,** 1163-1176. e2.

Mclean, L.P. & Cross, R.K., 2014. Adverse events in IBD: to stop or continue immune suppressant and biologic treatment. *Expert review of gastroenterology & hepatology,* 8**,** 223-240.

Mcneil, E., Capaldo, C.T. & Macara, I.G., 2006. Zonula occludens-1 function in the

assembly of tight junctions in Madin-Darby canine kidney epithelial cells. *Molecular biology of the cell,* 17**,** 1922-1932.

Mehta, S., Nijhuis, A., Kumagai, T., Lindsay, J. & Silver, A., 2015. Defects in the adherens junction complex (E-cadherin/ beta-catenin) in inflammatory bowel disease. *Cell Tissue Res,* 360**,** 749-60.

Meissner, Y. & Lamprecht, A., 2008. Alternative drug delivery approaches for the therapy of inflammatory bowel disease. *Journal of pharmaceutical sciences,* 97**,** 2878-2891.

Melhem, H., Hansmannel, F., Bressenot, A., Battaglia-Hsu, S.-F., Billioud, V., Alberto, J.M., Gueant, J.L. & Peyrin-Biroulet, L., 2015. Methyl-deficient diet promotes colitis and SIRT1-mediated endoplasmic reticulum stress. *Gut***,** gutjnl-2014-307030.

Melhem, H., Hansmannel, F., Bressenot, A., Battaglia-Hsu, S.F., Billioud, V., Alberto, J.M., Gueant, J.L. & Peyrin-Biroulet, L., 2016. Methyl-deficient diet promotes colitis and SIRT1-mediated endoplasmic reticulum stress. *Gut,* 65**,** 595-606.

Menzel, C., Bonengel, S., Pereira De Sousa, I., Laffleur, F., Prufert, F. & Bernkop-Schnurch, A., 2016. Preactivated thiolated nanoparticles: A novel mucoadhesive dosage form. *Int J Pharm,* 497**,** 123-8.

Meunier, V., Bourrie, M., Berger, Y. & Fabre, G., 1995. The human intestinal epithelial cell line Caco-2; pharmacological and pharmacokinetic applications. *Cell biology and toxicology,* 11**,** 187-194.

Misko, T.P., Schilling, R.J., Salvemini, D., Moore, W.M. & Currie, M.G., 1993. A fluorometric assay for the measurement of nitrite in biological samples. *Analytical biochemistry,* 214**,** 11-16.

Mitchell, D.A. & Marletta, M.A., 2005. Thioredoxin catalyzes the S-nitrosation of the caspase-3 active site cysteine. *Nature chemical biology,* 1**,** 154-158.

Mitic, L.L. & Van Itallie, C.M., 2001. Occludin and claudins: transmembrane proteins of the tight junction. *Tight junctions***,** 213-230.

Molina, M.M., Seabra, A.B., De Oliveira, M.G., Itri, R. & Haddad, P.S., 2013. Nitric oxide donor superparamagnetic iron oxide nanoparticles. *Materials Science and Engineering: C,* 33**,** 746-751.

Moller, F.T., Andersen, V., Wohlfahrt, J. & Jess, T., 2015. Familial risk of inflammatory bowel disease: a population-based cohort study 1977–2011. *The American journal of gastroenterology,* 110**,** 564-571.

Molodecky, N.A., Soon, S., Rabi, D.M., Ghali, W.A., Ferris, M., Chernoff, G., Benchimol, E.I., Panaccione, R., Ghosh, S. & Barkema, H.W., 2012. Increasing incidence and prevalence of the inflammatory bowel diseases with time, based on systematic review. *Gastroenterology,* 142**,** 46-54. e42.

Monteiro, H.P., Oliveira, C.J.R., Curcio, M.F., Moraes, M.S. & Arai, R.J., 2005. Tyrosine Phosphorylation in Nitric Oxide–Mediated Signaling Events. *Methods in enzymology,* 396**,** 350-358.

Morita, K., Furuse, M., Fujimoto, K. & Tsukita, S., 1999. Claudin multigene family

encoding four-transmembrane domain protein components of tight junction strands. *Proceedings of the National Academy of Sciences,* 96**,** 511-516.

Moustafine, R.I., Kemenova, V.A. & Van Den Mooter, G., 2005. Characteristics of interpolyelectrolyte complexes of Eudragit E 100 with sodium alginate. *International Journal of Pharmaceutics,* 294**,** 113-120.

Mukherjee, S., Ghosh, R.N. & Maxfield, F.R., 1997. Endocytosis. *Physiological reviews,* 77**,** 759-803.

Mukherjee, S., Ray, S. & Thakur, R., 2009. Solid lipid nanoparticles: a modern formulation approach in drug delivery system. *Indian journal of pharmaceutical sciences,* 71**,** 349.

Mukherjee, S., Zheng, H., Derebe, M.G., Callenberg, K.M., Partch, C.L., Rollins, D., Propheter, D.C., Rizo, J., Grabe, M. & Jiang, Q.-X., 2014. Antibacterial membrane attack by a pore-forming intestinal C-type lectin. *Nature,* 505**,** 103-107.

Mukhopadhyay, P., Chakraborty, S., Bhattacharya, S., Mishra, R. & Kundu, P.P., 2015. pH-sensitive chitosan/alginate core-shell nanoparticles for efficient and safe oral insulin delivery. *Int J Biol Macromol,* 72**,** 640-8.

Mulder, C.J., Fockens, P., Meijer, J.W., Van Der Heide, H., Wiltink, H. & Tytgat, G.N., 1996. Beclomethasone dipropionate (3mg) versus 5-aminosalicylic acid (2g) versus the combination of both (3mg/2g) as retention enemas in active ulcerative proctitis. *European journal of gastroenterology & hepatology,* 8**,** 549-554.

Murthy, S., Cooper, H.S., Shim, H., Shah, R.S., Ibrahim, S.A. & Sedergran, D.J., 1993. Treatment of dextran sulfate sodium-induced murine colitis by intracolonic cyclosporin. *Digestive diseases and sciences,* 38**,** 1722-1734.

Muscará, M.N., Mcknight, W., Del Soldato, P. & Wallace, J.L., 1998. Effect of a nitric oxide-releasing naproxen derivative on hypertension and gastric damage induced by chronic nitric oxide inhibition in the rat. *Life sciences,* 62**,** PL235-PL240.

Nair, M.G., Guild, K.J., Du, Y., Zaph, C., Yancopoulos, G.D., Valenzuela, D.M., Murphy, A., Stevens, S., Karow, M. & Artis, D., 2008. Goblet cell-derived resistin-like molecule β augments CD4+ T cell production of IFN-γ and infection-induced intestinal inflammation. *The Journal of Immunology,* 181**,** 4709-4715.

Nasti, A., Zaki, N.M., De Leonardis, P., Ungphaiboon, S., Sansongsak, P., Rimoli, M.G. & Tirelli, N., 2009. Chitosan/TPP and chitosan/TPP-hyaluronic acid nanoparticles: systematic optimisation of the preparative process and preliminary biological evaluation. *Pharmaceutical research,* 26**,** 1918-1930.

Neil, H., Singh, R.J., Konorev, E., Joseph, J. & Kalyanaraman, B., 1997. S-Nitrosoglutathione as a substrate for γ-glutamyl transpeptidase. *Biochemical Journal,* 323**,** 477-481.

Neurath, M.F., 2017. Current and emerging therapeutic targets for IBD. *Nat Rev*

Gastroenterol Hepatol, 14**,** 269-278.

Ng, S.C., Tang, W., Ching, J.Y., Wong, M., Chow, C.M., Hui, A., Wong, T., Leung, V.K., Tsang, S.W. & Yu, H.H., 2013. Incidence and phenotype of inflammatory bowel disease based on results from the Asia-pacific Crohn's and colitis epidemiology study. *Gastroenterology,* 145**,** 158-165. e2.

Ng, W.K., Wong, S.H. & Ng, S.C., 2016. Changing epidemiological trends of inflammatory bowel disease in Asia. *Intestinal Research,* 14**,** 111-119.

Nielsen, O., Verspaget, H. & Elmgreen, J., 1988. Inhibition of intestinal macrophage chemotaxis to leukotriene B4 by sulphasalazine, olsalazine, and 5‐aminosalicylic acid. *Alimentary pharmacology & therapeutics,* 2**,** 203-211.

Nikitovic, D. & Holmgren, A., 1996. S-nitrosoglutathione is cleaved by the thioredoxin system with liberation of glutathione and redox regulating nitric oxide. *Journal of Biological Chemistry,* 271**,** 19180-19185.

Nikoo, A.M., Kadkhodaee, R., Ghorani, B., Razzaq, H. & Tucker, N., 2016. Controlling the morphology and material characteristics of electrospray generated calcium alginate microhydrogels. *Journal of Microencapsulation,* 33**,** 605-612.

Nishiyama, A., Masutani, H., Nakamura, H., Nishinaka, Y. & Yodoi, J., 2001. Redox Regulation by Thioredoxin and Thioredoxin‐Binding Proteins. *IUBMB life,* 52**,** 29-33.

Noble, D. & Swift, H., 1999. Nitric oxide release from S-nitrosoglutathione (GSNO). *Chemical Communications***,** 2317-2318.

Obermeier, F., Gross, V., Schölmerich, J. & Falk, W., 1999. Interleukin-1 production by mouse macrophages is regulated in a feedback fashion by nitric oxide. *Journal of leukocyte biology,* 66**,** 829-836.

Odenwald, M.A. & Turner, J.R., 2017. The intestinal epithelial barrier: a therapeutic target? *Nat Rev Gastroenterol Hepatol,* 14**,** 9-21.

Onsoyen, E., 1996. Commercial applications of alginates. *Carbohydr Eur,* 14**,** 26-31.

Owen, R.L., Pierce, N.F., Apple, R. & Cray, W.C., 1986. M Cell Transport of Vibrio cholerae from the Intestinal. Lumen into Peyer's Patches: A Mechanism for Antigen Sampling and for Microbial Transepithelial Migration. *Journal of Infectious Diseases,* 153**,** 1108-1118.

Palmer, R.M., Ferrige, A. & Moncada, S., 1987. Nitric oxide release accounts for the biological activity of endothelium-derived relaxing factor. *Nature,* 327**,** 524-526.

Panaccione, R., Ghosh, S., Middleton, S., Márquez, J.R., Scott, B.B., Flint, L., Van Hoogstraten, H.J., Chen, A.C., Zheng, H. & Danese, S., 2014. Combination therapy with infliximab and azathioprine is superior to monotherapy with either agent in ulcerative colitis. *Gastroenterology,* 146**,** 392-400. e3.

Pandey, S., Jirwankar, P., Mehta, S., Pandit, S., Tripathi, P. & Patil, A., 2013. Formulation and evaluation of bilayered gastroretentable mucoadhesive patch for stomach-specific drug delivery. *Current drug delivery,* 10**,** 374-383.

Parent, M., Boudier, A., Fries, I., Gostynska, A., Rychter, M., Lulek, J., Leroy, P. & Gaucher, C., 2015a. Nitric oxide-eluting scaffolds and their interaction with

smooth muscle cells in vitro. *J Biomed Mater Res A,* 103**,** 3303-11.

Parent, M., Boudier, A., Perrin, J., Vigneron, C., Maincent, P., Violle, N., Bisson, J.F., Lartaud, I. & Dupuis, F., 2015b. In Situ Microparticles Loaded with S-Nitrosoglutathione Protect from Stroke. *PLoS One,* 10**,** e0144659.

Parent, M., Dahboul, F., Schneider, R., Clarot, I., Maincent, P., Leroy, P. & Boudier, A., 2013a. A complete physicochemical identity card of S-nitrosoglutathione. *Current Pharmaceutical Analysis,* 9**,** 31-42.

Parent, M., Dupuis, F., Maincent, P., Vigneron, C., Leroy, P. & Boudier, A., Year. Quel avenir en thérapeutique cardiovasculaire pour le monoxyde d'azote et ses dérivés?ed.^eds. *Annales Pharmaceutiques Françaises*Elsevier, 84-94.

Parent, M., Nouvel, C., Koerber, M., Sapin, A., Maincent, P. & Boudier, A., 2013c. PLGA in situ implants formed by phase inversion: Critical physicochemical parameters to modulate drug release. *Journal of controlled release,* 172**,** 292-304.

Patil, S.D., Papadmitrakopoulos, F. & Burgess, D.J., 2007. Concurrent delivery of dexamethasone and VEGF for localized inflammation control and angiogenesis. *Journal of Controlled Release,* 117**,** 68-79.

Patra, C.N., Priya, R., Swain, S., Kumar Jena, G., Panigrahi, K.C. & Ghose, D., 2017. Pharmaceutical significance of Eudragit: A review. *Future Journal of Pharmaceutical Sciences,* 3**,** 33-45.

Pavelka, M., Roth, J., Pavelka, M. & Roth, J., 2010. Junctional Complex. *Functional Ultrastructure: Atlas of Tissue Biology and Pathology***,** 166-167.

Payros, D., Secher, T., Boury, M., Brehin, C., Ménard, S., Salvador-Cartier, C., Cuevas-Ramos, G., Watrin, C., Marcq, I. & Nougayrède, J.-P., 2014. Maternally acquired genotoxic Escherichia coli alters offspring's intestinal homeostasis. *Gut Microbes,* 5**,** 313-512.

Pereira, A.E.S., Narciso, A.M., Seabra, A.B. & Fraceto, L.F., 2015. Evaluation of the effects of nitric oxide-releasing nanoparticles on plants. *Journal of Physics: Conference Series,* 617**,** 012025.

Perez-Moreno, M. & Fuchs, E., 2006. Catenins: keeping cells from getting their signals crossed. *Developmental cell,* 11**,** 601-612.

Perez-Moreno, M., Jamora, C. & Fuchs, E., 2003. Sticky business: orchestrating cellular signals at adherens junctions. *Cell,* 112**,** 535-548.

Peterson, L.W. & Artis, D., 2014. Intestinal epithelial cells: regulators of barrier function and immune homeostasis. *Nat Rev Immunol,* 14**,** 141-53.

Petschow, B., Doré, J., Hibberd, P., Dinan, T., Reid, G., Blaser, M., Cani, P.D., Degnan, F.H., Foster, J. & Gibson, G., 2013. Probiotics, prebiotics, and the host microbiome: the science of translation. *Annals of the New York Academy of Sciences,* 1306**,** 1-17.

Pithadia, A.B. & Jain, S., 2011. Treatment of inflammatory bowel disease (IBD). *Pharmacological Reports,* 63**,** 629-642.

Ponder, A. & Long, M.D., 2013. A clinical review of recent findings in the

epidemiology of inflammatory bowel disease. *Clin Epidemiol,* 5**,** 237-247.

Pongjanyakul, T. & Khuathan, N., 2016. Quaternary polymethacrylate–sodium alginate films: effect of alginate block structures and use for sustained release tablets. *Pharmaceutical development and technology,* 21**,** 487-498.

Potten, C.S., Owen, G. & Booth, D., 2002. Intestinal stem cells protect their genome by selective segregation of template DNA strands. *J Cell Sci,* 115**,** 2381-2388.

Prasad, K., Badarinath, A., Anilkumar, P., Reddy, B.R., Naveen, N., Nirosha, M. & Hyndavi, M., 2011. Colon targeted drug delivery systems: A review. *Journal of Global Trends in Pharmaceutical Sciences,* 2**,** 459-475.

Press, B. & Di Grandi, D., 2008. Permeability for intestinal absorption: Caco-2 assay and related issues. *Current drug metabolism,* 9**,** 893-900.

Price, K.J., Hanson, P.J. & Whittle, B.J., 1994. Stimulation by carbachol of mucus gel thickness in rat stomach involves nitric oxide. *European journal of pharmacology,* 263**,** 199-202.

Qi, R., Li, Y.Z., Chen, C., Cao, Y.N., Yu, M.M., Xu, L., He, B., Jie, X., Shen, W.W., Wang, Y.N., Van Dongen, M.A., Liu, G.Q., Banaszak Holl, M.M., Zhang, Q. & Ke, X., 2015. G5-PEG PAMAM dendrimer incorporating nanostructured lipid carriers enhance oral bioavailability and plasma lipid-lowering effect of probucol. *J Control Release,* 210**,** 160-8.

Quigley, E.M., 2016. Leaky gut–concept or clinical entity? *Current opinion in gastroenterology,* 32**,** 74-79.

Ramachandran, N., Jacob, S., Zielinski, B., Curatola, G., Mazzanti, L. & Mutus, B., 1999. N-Dansyl-S-nitrosohomocysteine a fluorescent probe for intracellular thiols and S-nitrosothiols. *Biochimica et Biophysica Acta (BBA)-Protein Structure and Molecular Enzymology,* 1430**,** 149-154.

Ramachandran, N., Root, P., Jiang, X.-M., Hogg, P.J. & Mutus, B., 2001. Mechanism of transfer of NO from extracellular S-nitrosothiols into the cytosol by cell-surface protein disulfide isomerase. *Proceedings of the National Academy of Sciences,* 98**,** 9539-9544.

Rassaf, T., Bryan, N.S., Maloney, R.E., Specian, V., Kelm, M., Kalyanaraman, B., Rodriguez, J. & Feelisch, M., 2003. NO adducts in mammalian red blood cells: too much or too little? *Nature medicine,* 9**,** 481-482.

Reis, C.P., Neufeld, R.J., Ribeiro, A.J. & Veiga, F., 2006. Nanoencapsulation I. Methods for preparation of drug-loaded polymeric nanoparticles. *Nanomedicine: Nanotechnology, Biology and Medicine,* 2**,** 8-21.

Reynaert, N.L., Ckless, K., Korn, S.H., Vos, N., Guala, A.S., Wouters, E.F.M., Van Der Vliet, A. & Janssen-Heininger, Y.M.W., 2004. Nitric oxide represses inhibitory κB kinase through S-nitrosylation. *Proceedings of the National Academy of Sciences of the United States of America,* 101**,** 8945-8950.

Richardson, G. & Benjamin, N., 2002. Potential therapeutic uses for S-nitrosothiols. *Clinical science,* 102**,** 99-105.

Robinson, K., Deng, Z., Hou, Y. & Zhang, G., 2014. Regulation of the Intestinal Barrier

Function by Host Defense Peptides. *Frontiers in Veterinary Science,* 2**,** 57-57.

Rossi, T., Iannuccelli, V., Coppi, G., Bruni, E. & Baggio, G., 2009. Role of the pharmaceutical excipients in the tamoxifen activity on MCF-7 and vero cell cultures. *Anticancer research,* 29**,** 4529-4533.

Rousseaux, C., Lefebvre, B., Dubuquoy, L., Lefebvre, P., Romano, O., Auwerx, J., Metzger, D., Wahli, W., Desvergne, B. & Naccari, G.C., 2005. Intestinal antiinflammatory effect of 5-aminosalicylic acid is dependent on peroxisome proliferator–activated receptor-γ. *Journal of Experimental Medicine,* 201**,** 1205-1215.

Rubin, D.C. & Langer, J.C., 2009. Small intestine: anatomy and structural anomalies. *Yamada's Atlas of Gastroenterology***,** 19-23.

Runswick, S., Mitchell, T., Davies, P., Robinson, C. & Garrod, D.R., 2007. Pollen proteolytic enzymes degrade tight junctions. *Respirology,* 12**,** 834-42.

Sabath, E., Negoro, H., Beaudry, S., Paniagua, M., Angelow, S., Shah, J., Grammatikakis, N., Alan, S. & Denker, B.M., 2008. Gα12 regulates protein interactions within the MDCK cell tight junction and inhibits tight-junction assembly. *J Cell Sci,* 121**,** 814-824.

Sahoo, J., Murthy, P. & Biswal, S., 2009. Formulation of sustained-release dosage form of verapamil hydrochloride by solid dispersion technique using eudragit RLPO or Kollidon® SR. *AAPS PharmSciTech,* 10**,** 27-33.

Saito, M., Tucker, D.K., Kohlhorst, D., Niessen, C.M. & Kowalczyk, A.P., 2012. Classical and desmosomal cadherins at a glance. *J Cell Sci,* 125**,** 2547-2552.

Saitoh, Y., Suzuki, H., Tani, K., Nishikawa, K., Irie, K., Ogura, Y., Tamura, A., Tsukita, S. & Fujiyoshi, Y., 2015. Structural insight into tight junction disassembly by Clostridium perfringens enterotoxin. *Science,* 347**,** 775-778.

Sakakibara, A., Furuse, M., Saitou, M., Ando-Akatsuka, Y. & Tsukita, S., 1997. Possible involvement of phosphorylation of occludin in tight junction formation. *The Journal of cell biology,* 137**,** 1393-1401.

Sales-Campos, H., Basso, P.J., Alves, V.B., Fonseca, M.T., Bonfa, G., Nardini, V. & Cardoso, C.R., 2015. Classical and recent advances in the treatment of inflammatory bowel diseases. *Braz J Med Biol Res,* 48**,** 96-107.

Salim, S.Y. & Soderholm, J.D., 2011. Importance of disrupted intestinal barrier in inflammatory bowel diseases. *Inflamm Bowel Dis,* 17**,** 362-81.

Salvemini, D., Masini, E., Anggard, E., Mannaioni, P.F. & Vane, J., 1990. Synthesis of a nitric oxide-like factor from L-arginine by rat serosal mast cells: stimulation of guanylate cyclase and inhibition of platelet aggregation. *Biochemical and biophysical research communications,* 169**,** 596-601.

Salzman, N.H., Underwood, M.A. & Bevins, C.L., Year. Paneth cells, defensins, and the commensal microbiota: a hypothesis on intimate interplay at the intestinal mucosaed.^eds. *Seminars in immunology*Elsevier, 70-83.

Sandau, K.B., Fandrey, J. & Brüne, B., 2001. Accumulation of HIF-1α under the influence of nitric oxide. *Blood,* 97**,** 1009-1015.

Sandborn, W.J. & Hanauer, S.B., 1999. Antitumor necrosis factor therapy for inflammatory bowel disease: a review of agents, pharmacology, clinical results, and safety. *Inflammatory bowel diseases,* 5**,** 119-133.

Sands, B.E., 2000. Therapy of inflammatory bowel disease. *Gastroenterology,* 118**,** S68-S82.

Sangwai, M. & Vavia, P., 2013. Amorphous ternary cyclodextrin nanocomposites of telmisartan for oral drug delivery: Improved solubility and reduced pharmacokinetic variability. *International journal of pharmaceutics,* 453**,** 423-432.

Santos, M.C., Seabra, A.B., Pelegrino, M.T. & Haddad, P.S., 2016. Synthesis, characterization and cytotoxicity of glutathione- and PEG-glutathione-superparamagnetic iron oxide nanoparticles for nitric oxide delivery. *Applied Surface Science,* 367**,** 26-35.

Sarmento, B., Ribeiro, A., Veiga, F., Sampaio, P., Neufeld, R. & Ferreira, D., 2007. Alginate/chitosan nanoparticles are effective for oral insulin delivery. *Pharm Res,* 24**,** 2198-206.

Sarr, M., Lobysheva, I., Diallo, A.S., Stoclet, J.-C., Schini-Kerth, V.B. & Muller, B., 2005. Formation of releasable NO stores by S-nitrosoglutathione in arteries exhibiting tolerance to glyceryl-trinitrate. *European journal of pharmacology,* 513**,** 119-123.

Sartor, R.B., 2008. Microbial influences in inflammatory bowel diseases. *Gastroenterology,* 134**,** 577-594.

Savidge, T.C., Newman, P., Pothoulakis, C., Ruhl, A., Neunlist, M., Bourreille, A., Hurst, R. & Sofroniew, M.V., 2007. Enteric glia regulate intestinal barrier function and inflammation via release of S-nitrosoglutathione. *Gastroenterology,* 132**,** 1344-1358.

Schäffer, M., Efron, P.A., Thornton, F.J., Klingel, K., Gross, S.S. & Barbul, A., 1997. Nitric oxide, an autocrine regulator of wound fibroblast synthetic function. *The Journal of Immunology,* 158**,** 2375-2381.

Schäffer, M.R., Tantry, U., Gross, S.S., Wasserkrug, H.L. & Barbul, A., 1996. Nitric oxide regulates wound healing. *Journal of Surgical Research,* 63**,** 237-240.

Schneeberger, E.E. & Lynch, R.D., 2004. The tight junction: a multifunctional complex. *American Journal of Physiology-Cell Physiology,* 286**,** C1213-C1228.

Schoubben, A., Blasi, P., Giovagnoli, S., Perioli, L., Rossi, C. & Ricci, M., 2009. Novel composite microparticles for protein stabilization and delivery. *Eur J Pharm Sci,* 36**,** 226-34.

Schubert, S., Delaney, J.J.T. & Schubert, U.S., 2011. Nanoprecipitation and nanoformulation of polymers: from history to powerful possibilities beyond poly(lactic acid). *Soft Matter,* 7**,** 1581-1588.

Schumacher, M.A., Hedl, M., Abraham, C., Bernard, J.K., Lozano, P.R., Hsieh, J.J., Almohazey, D., Bucar, E.B., Punit, S. & Dempsey, P.J., 2017. ErbB4 signaling stimulates pro-inflammatory macrophage apoptosis and limits colonic

inflammation. *Cell death & disease,* 8**,** e2622.

Schwartz, A.L., 1995. Receptor cell biology: receptor-mediated endocytosis. *Pediatric research,* 38**,** 835-843.

Seabra, A., Fitzpatrick, A., Paul, J., De Oliveira, M. & Weller, R., 2004a. Topically applied S‐nitrosothiol‐containing hydrogels as experimental and pharmacological nitric oxide donors in human skin. *British Journal of Dermatology,* 151**,** 977-983.

Seabra, A.B., Da Rocha, L.L., Eberlin, M.N. & De Oliveira, M.G., 2005. Solid films of blended poly (vinyl alcohol)/poly (vinyl pyrrolidone) for topical S‐nitrosoglutathione and nitric oxide release. *Journal of pharmaceutical sciences,* 94**,** 994-1003.

Seabra, A.B. & De Oliveira, M.G., 2004. Poly(vinyl alcohol) and poly(vinyl pyrrolidone) blended films for local nitric oxide release. *Biomaterials,* 25**,** 3773-82.

Seabra, A.B., De Souza, G.F.P., Da Rocha, L.L., Eberlin, M.N. & De Oliveira, M.G., 2004b. S-nitrosoglutathione incorporated in poly (ethylene glycol) matrix: potential use for topical nitric oxide delivery. *Nitric Oxide,* 11**,** 263-272.

Sengupta, R. & Holmgren, A., 2013. Thioredoxin and thioredoxin reductase in relation to reversible S-nitrosylation. *Antioxidants & redox signaling,* 18**,** 259-269.

Sengupta, R., Ryter, S.W., Zuckerbraun, B.S., Tzeng, E., Billiar, T.R. & Stoyanovsky, D.A., 2007. Thioredoxin catalyzes the denitrosation of low-molecular mass and protein S-nitrosothiols. *Biochemistry,* 46**,** 8472-8483.

Seth, A., Sheth, P., Elias, B.C. & Rao, R., 2007. Protein phosphatases 2A and 1 interact with occludin and negatively regulate the assembly of tight junctions in the CACO-2 cell monolayer. *Journal of Biological Chemistry,* 282**,** 11487-11498.

Sezgin, Z., Yuksel, N. & Baykara, T., 2006. Preparation and characterization of polymeric micelles for solubilization of poorly soluble anticancer drugs. *Eur J Pharm Biopharm,* 64**,** 261-8.

Shah, S.U., Martinho, N., Socha, M., Pinto Reis, C. & Gibaud, S., 2015. Synthesis and characterization of S-nitrosoglutathione-oligosaccharide-chitosan as a nitric oxide donor. *Expert opinion on drug delivery,* 12**,** 1209-1223.

Shah, S.U., Socha, M., Fries, I. & Gibaud, S., 2016. Synthesis of S-nitrosoglutathione-alginate for prolonged delivery of nitric oxide in intestines. *Drug delivery,* 23**,** 2927-2935.

Shams, M.S., Alam, M.I., Ali, A., Sultana, Y., Aqil, M. & Shakeel, F., 2010. Pharmacokinetics of a losartan potassium released from a transdermal therapeutic system for the treatment of hypertension. *Pharmazie,* 65**,** 679-682.

Sheikh Hassan, A., Sapin, A., Lamprecht, A., Emond, E., El Ghazouani, F. & Maincent, P., 2009. Composite microparticles with in vivo reduction of the burst release effect. *Eur J Pharm Biopharm,* 73**,** 337-44.

Shen, L., Weber, C.R., Raleigh, D.R., Yu, D. & Turner, J.R., 2011. Tight junction pore and leak pathways: a dynamic duo. *Annu Rev Physiol,* 73**,** 283-309.

Shishido, S.L.M., Seabra, A.B., Loh, W. & Ganzarolli De Oliveira, M., 2003. Thermal and photochemical nitric oxide release from S-nitrosothiols incorporated in Pluronic F127 gel: potential uses for local and controlled nitric oxide release. *Biomaterials,* 24**,** 3543-3553.

Shishu, Kamalpreet & Kapoor, V.R., 2010. Development of Taste Masked Oral Formulation of Ornidazole. *Indian Journal of Pharmaceutical Sciences,* 72**,** 211-215.

Shishu, Kapoor, V.R. & Kamalpreet, 2009. Taste Masking and Formulation of Ofloxacin Rapid Disintegrating Tablets and Oral Suspension. *Indian Journal of Pharmaceutical Education and Research,* 43**,** 150-155.

Siednienko, J., Nowak, J., Moynagh, P.N. & Gorczyca, W.A., 2011. Nitric oxide affects IL-6 expression in human peripheral blood mononuclear cells involving cGMP-dependent modulation of NF-κB activity. *Cytokine,* 54**,** 282-288.

Simoes, M.M. & De Oliveira, M.G., 2010. Poly(vinyl alcohol) films for topical delivery of S-nitrosoglutathione: effect of freezing-thawing on the diffusion properties. *J Biomed Mater Res B Appl Biomater,* 93**,** 416-24.

Simonoska Crcarevska, M., Glavas Dodov, M. & Goracinova, K., 2008. Chitosan coated Ca-alginate microparticles loaded with budesonide for delivery to the inflamed colonic mucosa. *Eur J Pharm Biopharm,* 68**,** 565-78.

Simonovic, I., Arpin, M., Koutsouris, A., Falk-Krzesinski, H.J. & Hecht, G., 2001. Enteropathogenic Escherichia coli activates ezrin, which participates in disruption of tight junction barrier function. *Infection and immunity,* 69**,** 5679-5688.

Singh, A., Worku, Z.A. & Van Den Mooter, G., 2011. Oral formulation strategies to improve solubility of poorly water-soluble drugs. *Expert opinion on drug delivery,* 8**,** 1361-1378.

Singh, I. & Rana, V., 2013. Iron oxide induced enhancement of mucoadhesive potential of Eudragit RLPO: formulation, evaluation and optimization of mucoadhesive drug delivery system. *Expert opinion on drug delivery,* 10**,** 1179-1191.

Singh, S. & Dikshit, M., 2007. Apoptotic neuronal death in Parkinson's disease: involvement of nitric oxide. *Brain research reviews,* 54**,** 233-250.

Skjåk-Bræk, G. & Espevik, T., 1996. Application of alginate gels in biotechnology and biomedicine. *Carbohydr. Eur,* 14**,** 237-242.

Sliskovic, I., Raturi, A. & Mutus, B., 2005. Characterization of the S-denitrosation activity of protein disulfide isomerase. *Journal of Biological Chemistry,* 280**,** 8733-8741.

Sluzky, V., Tamada, J.A., Klibanov, A.M. & Langer, R., 1991. Kinetics of insulin aggregation in aqueous solutions upon agitation in the presence of hydrophobic surfaces. *Proceedings of the National Academy of Sciences,* 88**,** 9377-9381.

Snoeck, V., Goddeeris, B. & Cox, E., 2005. The role of enterocytes in the intestinal barrier function and antigen uptake. *Microbes Infect,* 7**,** 997-1004.

Snyder, A.H., Mcpherson, M.E., Hunt, J.F., Johnson, M., Stamler, J.S. & Gaston, B.,

2002. Acute effects of aerosolized S-nitrosoglutathione in cystic fibrosis. *American journal of respiratory and critical care medicine,* 165**,** 922-926.

Snyder, S.H., 1992. Nitric oxide and neurons. *Current opinion in neurobiology,* 2**,** 323-327.

Sonavane, G.S. & Devarajan, P.V., 2007. Preparation of Alginate Nanoparticles Using Eudragit E100 as a New Complexing Agent: Development, <I>In-Vitro</I>, and <I>In-Vivo</I> Evaluation. *Journal of Biomedical Nanotechnology,* 3**,** 160-169.

Sonnenberg, A. & Liem, R.K., 2007. Plakins in development and disease. *Experimental cell research,* 313**,** 2189-2203.

Srinivasan, B., Kolli, A.R., Esch, M.B., Abaci, H.E., Shuler, M.L. & Hickman, J.J., 2015. TEER measurement techniques for in vitro barrier model systems. *Journal of laboratory automation,* 20**,** 107-126.

Staab, C.A., Ålander, J., Brandt, M., Lengqvist, J., Morgenstern, R., Grafström, R.C. & Höög, J.-O., 2008. Reduction of S-nitrosoglutathione by alcohol dehydrogenase 3 is facilitated by substrate alcohols via direct cofactor recycling and leads to GSH-controlled formation of glutathione transferase inhibitors. *Biochemical Journal,* 413**,** 493-504.

Staab, C.A., Hartmanová, T., El-Hawari, Y., Ebert, B., Kisiela, M., Wsol, V., Martin, H.-J. & Maser, E., 2011. Studies on reduction of S-nitrosoglutathione by human carbonyl reductases 1 and 3. *Chemico-biological interactions,* 191**,** 95-103.

Stappenbeck, T.S., Hooper, L.V. & Gordon, J.I., 2002. Developmental regulation of intestinal angiogenesis by indigenous microbes via Paneth cells. *Proceedings of the National Academy of Sciences,* 99**,** 15451-15455.

Stephens, R.H., Tanianis-Hughes, J., Higgs, N.B., Humphrey, M. & Warhurst, G., 2002. Region-dependent modulation of intestinal permeability by drug efflux transporters: in vitro studies in mdr1a(-/-) mouse intestine. *J Pharmacol Exp Ther,* 303**,** 1095-101.

Sterin‐Borda, L., Echagüe, A.V., Leiros, C.P., Genaro, A. & Borda, E., 1995. Endogenous nitric oxide signalling system and the cardiac muscarinic acetylcholine receptor‐inotropic response. *British journal of pharmacology,* 115**,** 1525-1531.

Suares, N., Hamlin, P., Greer, D., Warren, L., Clark, T. & Ford, A., 2012. Efficacy and tolerability of methotrexate therapy for refractory Crohn’s disease: a large single‐centre experience. *Alimentary pharmacology & therapeutics,* 35**,** 284-291.

Sun, H., Chow, E.C., Liu, S., Du, Y. & Pang, K.S., 2008. The Caco-2 cell monolayer: usefulness and limitations. *Expert opinion on drug metabolism & toxicology,* 4**,** 395-411.

Sun, J. & Chang, E.B., 2014. Exploring gut microbes in human health and disease: pushing the envelope. *Genes & Diseases,* 1**,** 132-139.

Sun, J., Zhang, X., Broderick, M. & Fein, H., 2003. Measurement of nitric oxide

production in biological systems by using Griess reaction assay. *Sensors,* 3**,** 276-284.

Sun, S., Liang, N., Yamamoto, H., Kawashima, Y., Cui, F. & Yan, P., 2015. pH-sensitive poly(lactide-co-glycolide) nanoparticle composite microcapsules for oral delivery of insulin. *Int J Nanomedicine,* 10**,** 3489-98.

Suzuki, T., Elias, B.C., Seth, A., Shen, L., Turner, J.R., Giorgianni, F., Desiderio, D., Guntaka, R. & Rao, R., 2009. PKCη regulates occludin phosphorylation and epithelial tight junction integrity. *Proceedings of the National Academy of Sciences,* 106**,** 61-66.

Tai, H.Y., Tam, M.F., Chou, H., Peng, H.J., Su, S.N., Perng, D.W. & Shen, H.D., 2006. Pen ch 13 allergen induces secretion of mediators and degradation of occludin protein of human lung epithelial cells. *Allergy,* 61**,** 382-8.

Takka, S. & Gürel, A., 2010. Evaluation of chitosan/alginate beads using experimental design: formulation and in vitro characterization. *Aaps Pharmscitech,* 11**,** 460-466.

Tamura, A., Hayashi, H., Imasato, M., Yamazaki, Y., Hagiwara, A., Wada, M., Noda, T., Watanabe, M., Suzuki, Y. & Tsukita, S., 2011. Loss of claudin-15, but not claudin-2, causes Na+ deficiency and glucose malabsorption in mouse small intestine. *Gastroenterology,* 140**,** 913-923.

Tan, C., Zhang, Y., Abbas, S., Feng, B., Zhang, X., Xia, W. & Xia, S., 2015. Biopolymer-Lipid Bilayer Interaction Modulates the Physical Properties of Liposomes: Mechanism and Structure. *J Agric Food Chem,* 63**,** 7277-85.

Taupin, D., Kinoshita, K. & Podolsky, D., 2000. Intestinal trefoil factor confers colonic epithelial resistance to apoptosis. *Proceedings of the National Academy of Sciences,* 97**,** 799-804.

Thanou, M., Verhoef, J. & Junginger, H., 2001. Oral drug absorption enhancement by chitosan and its derivatives. *Advanced drug delivery reviews,* 52**,** 117-126.

Thibeault, S., Rautureau, Y., Oubaha, M., Faubert, D., Wilkes, B.C., Delisle, C. & Gratton, J.-P., 2010. S-Nitrosylation of β-catenin by eNOS-derived NO promotes VEGF-induced endothelial cell permeability. *Molecular cell,* 39**,** 468-476.

Thomas, D.D., Ridnour, L.A., Espey, M.G., Donzelli, S., Ambs, S., Hussain, S.P., Harris, C.C., Degraff, W., Roberts, D.D. & Mitchell, J.B., 2006. Superoxide fluxes limit nitric oxide-induced signaling. *Journal of Biological Chemistry,* 281**,** 25984-25993.

Thomas, D.D., Ridnour, L.A., Isenberg, J.S., Flores-Santana, W., Switzer, C.H., Donzelli, S., Hussain, P., Vecoli, C., Paolocci, N. & Ambs, S., 2008. The chemical biology of nitric oxide: implications in cellular signaling. *Free Radical Biology and Medicine,* 45**,** 18-31.

Thomason, H.A., Scothern, A., Mcharg, S. & Garrod, D.R., 2010. Desmosomes: adhesive strength and signalling in health and disease. *Biochemical Journal,* 429**,** 419-433.

Tomasello, E. & Bedoui, S., 2013. Intestinal innate immune cells in gut homeostasis and immunosurveillance. *Immunol Cell Biol,* 91**,** 201-3.

Tong, M., Li, X., Parfrey, L.W., Roth, B., Ippoliti, A., Wei, B., Borneman, J., Mcgovern, D.P., Frank, D.N. & Li, E., 2013. A modular organization of the human intestinal mucosal microbiota and its association with inflammatory bowel disease. *PloS one,* 8**,** e80702.

Tonnesen, H.H. & Karlsen, J., 2002. Alginate in drug delivery systems. *Drug Dev Ind Pharm,* 28**,** 621-30.

Torres, J., Mehandru, S., Colombel, J.-F. & Peyrin-Biroulet, L., 2016. Crohn's disease. *The Lancet*.

Traweger, A., Toepfer, S., Wagner, R.N., Zweimueller-Mayer, J., Gehwolf, R., Lehner, C., Tempfer, H., Krizbai, I., Wilhelm, I., Bauer, H.C. & Bauer, H., 2013. Beyond cell-cell adhesion: Emerging roles of the tight junction scaffold ZO-2. *Tissue Barriers,* 1**,** e25039.

Tsukita, S., Furuse, M. & Itoh, M., 2001. Multifunctional strands in tight junctions. *Nature reviews Molecular cell biology,* 2**,** 285-293.

Tsukita, S., Katsuno, T., Yamazaki, Y., Umeda, K., Tamura, A. & Tsukita, S., 2009. Roles of ZO‐1 and ZO‐2 in Establishment of the Belt‐like Adherens and Tight Junctions with Paracellular Permselective Barrier Function. *Annals of the New York Academy of Sciences,* 1165**,** 44-52.

Turksen, K. & Troy, T.-C., 2004. Barriers built on claudins. *Journal of cell science,* 117**,** 2435-2447.

Turner, J.R., 2000. Show me the pathway!: Regulation of paracellular permeability by Na+-glucose cotransport. *Advanced drug delivery reviews,* 41**,** 265-281.

Turner, J.R., 2009. Intestinal mucosal barrier function in health and disease. *Nat Rev Immunol,* 9**,** 799-809.

Ungaro, R., Chang, H.L., Cote-Daigneaut, J., Mehandru, S., Atreja, A. & Colombel, J.-F., 2016a. Statins associated with decreased risk of new onset inflammatory bowel disease. *The American journal of gastroenterology*.

Ungaro, R., Mehandru, S., Allen, P.B., Peyrin-Biroulet, L. & Colombel, J.-F., 2016b. Ulcerative colitis. *The Lancet*.

Vaishnava, S., Behrendt, C.L., Ismail, A.S., Eckmann, L. & Hooper, L.V., 2008. Paneth cells directly sense gut commensals and maintain homeostasis at the intestinal host-microbial interface. *Proceedings of the National Academy of Sciences,* 105**,** 20858-20863.

Van Der Sluis, M., De Koning, B.A., De Bruijn, A.C., Velcich, A., Meijerink, J.P., Van Goudoever, J.B., Büller, H.A., Dekker, J., Van Seuningen, I. & Renes, I.B., 2006. Muc2-deficient mice spontaneously develop colitis, indicating that MUC2 is critical for colonic protection. *Gastroenterology,* 131**,** 117-129.

Van Itallie, C.M. & Anderson, J.M., 2006. Claudins and epithelial paracellular transport. *Annu. Rev. Physiol.,* 68**,** 403-429.

Van Itallie, C.M., Fanning, A.S., Bridges, A. & Anderson, J.M., 2009. ZO-1 stabilizes

the tight junction solute barrier through coupling to the perijunctional cytoskeleton. *Molecular biology of the cell,* 20**,** 3930-3940.

Van Overveld, F., Bult, H., Vermeire, P. & Herman, A., 1993. Nitroprusside, a nitrogen oxide generating drug, inhibits release of histamine and tryptase from human skin mast cells. *Agents and Actions,* 38**,** C237-C238.

Varshosaz, J., Faghihian, H. & Rastgoo, K., 2006. Preparation and characterization of metoprolol controlled-release solid dispersions. *Drug Delivery,* 13**,** 295-302.

Vercelino, R., Cunha, T.M., Ferreira, E.S., Cunha, F.Q., Ferreira, S.H. & De Oliveira, M.G., 2013. Skin vasodilation and analgesic effect of a topical nitric oxide-releasing hydrogel. *Journal of Materials Science: Materials in Medicine,* 24**,** 2157-2169.

Vrignaud, S., Benoit, J.-P. & Saulnier, P., 2011. Strategies for the nanoencapsulation of hydrophilic molecules in polymer-based nanoparticles. *Biomaterials,* 32**,** 8593-8604.

Vysloužil, J., Bavoľárová, J., Kejdušová, M., Vetchý, D. & Dvořáčková, K., 2013. Cationic Eudragit® polymers as excipients for microparticles prepared by solvent evaporation method. *Ceska a Slovenska farmacie: casopis Ceske farmaceuticke spolecnosti a Slovenske farmaceuticke spolecnosti,* 62**,** 249-254.

Wallace, B.D., Wang, H., Lane, K.T., Scott, J.E., Orans, J., Koo, J.S., Venkatesh, M., Jobin, C., Yeh, L.-A. & Mani, S., 2010. Alleviating cancer drug toxicity by inhibiting a bacterial enzyme. *Science,* 330**,** 831-835.

Wallace, J.L. & Miller, M.J.S., 2000. Nitric oxide in mucosal defense: A little goes a long way. *Gastroenterology,* 119**,** 512-520.

Wallace, J.L., Vergnolle, N., Muscará, M.N., Asfaha, S., Chapman, K., Mcknight, W., Del Soldato, P., Morelli, A. & Fiorucci, S., 1999. Enhanced anti-inflammatory effects of a nitric oxide–releasing derivative of mesalamine in rats. *Gastroenterology,* 117**,** 557-566.

Wang, Y., Chen, L., Tan, L., Zhao, Q., Luo, F., Wei, Y. & Qian, Z., 2014. PEG-PCL based micelle hydrogels as oral docetaxel delivery systems for breast cancer therapy. *Biomaterials,* 35**,** 6972-85.

Watson, C., Rowland, M. & Warhurst, G., 2001. Functional modeling of tight junctions in intestinal cell monolayers using polyethylene glycol oligomers. *American Journal of Physiology-Cell Physiology,* 281**,** C388-C397.

Weber, C.R., Raleigh, D.R., Su, L., Shen, L., Sullivan, E.A., Wang, Y. & Turner, J.R., 2010. Epithelial myosin light chain kinase activation induces mucosal interleukin-13 expression to alter tight junction ion selectivity. *Journal of Biological Chemistry,* 285**,** 12037-12046.

Wehkamp, J., Fellermann, K. & Stange, E.F., 2005. Human defensins in Crohn's disease. *Mechanisms of Epithelial Defense.* Karger Publishers, 42-54.

Woitiski, C.B., Sarmento, B., Carvalho, R.A., Neufeld, R.J. & Veiga, F., 2011. Facilitated nanoscale delivery of insulin across intestinal membrane models. *International journal of pharmaceutics,* 412**,** 123-131.

Woo, B.H., Jiang, G., Jo, Y.W. & Deluca, P.P., 2001. Preparation and characterization of a composite PLGA and poly (acryloyl hydroxyethyl starch) microsphere system for protein delivery. *Pharmaceutical research,* 18**,** 1600-1606.

Wu, W., Gaucher, C., Diab, R., Fries, I., Xiao, Y.-L., Hu, X.-M., Maincent, P. & Sapin-Minet, A., 2015a. Time lasting S-nitrosoglutathione polymeric nanoparticles delay cellular protein S-nitrosation. *European Journal of Pharmaceutics and Biopharmaceutics,* 89**,** 1-8.

Wu, W., Gaucher, C., Fries, I., Hu, X.-M., Maincent, P. & Sapin-Minet, A., 2015b. Polymer nanocomposite particles of S-nitrosoglutathione: A suitable formulation for protection and sustained oral delivery. *International journal of pharmaceutics,* 495**,** 354-361.

Wu, W., Perrin-Sarrado, C., Ming, H., Lartaud, I., Maincent, P., Hu, X.-M., Sapin-Minet, A. & Gaucher, C., 2016. Polymer nanocomposites enhance S-nitrosoglutathione intestinal absorption and promote the formation of releasable nitric oxide stores in rat aorta. *Nanomedicine: Nanotechnology, Biology and Medicine,* 12**,** 1795-1803.

Xu, J., Kausalya, P.J., Phua, D.C., Ali, S.M., Hossain, Z. & Hunziker, W., 2008. Early embryonic lethality of mice lacking ZO-2, but Not ZO-3, reveals critical and nonredundant roles for individual zonula occludens proteins in mammalian development. *Molecular and cellular biology,* 28**,** 1669-1678.

Yan, F., Cao, H., Cover, T.L., Washington, M.K., Shi, Y., Liu, L., Chaturvedi, R., Peek, R.M., Wilson, K.T. & Polk, D.B., 2011. Colon-specific delivery of a probiotic-derived soluble protein ameliorates intestinal inflammation in mice through an EGFR-dependent mechanism. *The Journal of clinical investigation,* 121**,** 2242-2253.

Yang, C.-H., Lin, Y.-S., Huang, K.-S., Huang, Y.-C., Wang, E.-C., Jhong, J.-Y. & Kuo, C.-Y., 2009. Microfluidic emulsification and sorting assisted preparation of monodisperse chitosan microparticles. *Lab on a Chip,* 9**,** 145-150.

Yap, L.-P., Sancheti, H., Ybanez, M.D., Garcia, J., Cadenas, E. & Han, D., 2010. Determination of GSH, GSSG, and GSNO Using HPLC with Electrochemical Detection. 473**,** 137-147.

Yeh, T.-H., Hsu, L.-W., Tseng, M.T., Lee, P.-L., Sonjae, K., Ho, Y.-C. & Sung, H.-W., 2011. Mechanism and consequence of chitosan-mediated reversible epithelial tight junction opening. *Biomaterials,* 32**,** 6164-6173.

Yeo, Y., Baek, N. & Park, K., 2001. Microencapsulation methods for delivery of protein drugs. *Biotechnology and Bioprocess Engineering,* 6**,** 213-230.

Yoo, J.W., Acharya, G. & Lee, C.H., 2009. In vivo evaluation of vaginal films for mucosal delivery of nitric oxide. *Biomaterials,* 30**,** 3978-85.

Yu, H., Wang, Q., Sun, Y., Shen, M., Li, H. & Duan, Y., 2015. A new PAMPA model proposed on the basis of a synthetic phospholipid membrane. *PloS one,* 10**,** e0116502.

Yu, Y.B. & Li, Y.Q., 2014. Enteric glial cells and their role in the intestinal epithelial

barrier. *World J Gastroenterol,* 20**,** 11273-80.

Yu, Z., Rogers, T.L., Hu, J., Johnston, K.P. & Williams, R.O., 2002. Preparation and characterization of microparticles containing peptide produced by a novel process: spray freezing into liquid. *European journal of pharmaceutics and biopharmaceutics,* 54**,** 221-228.

Zai, A., Rudd, M.A., Scribner, A.W. & Loscalzo, J., 1999. Cell-surface protein disulfide isomerase catalyzes transnitrosation and regulates intracellular transfer of nitric oxide. *The Journal of clinical investigation,* 103**,** 393-399.

Zaman, K., Palmer, L.A., Doctor, A. & Gaston, B., 2004. Concentration-dependent effects of endogenous S-nitrosoglutathione on gene regulation by specificity proteins Sp3 and Sp1. *Biochemical Journal,* 380**,** 67-74.

Zenewicz, L.A., Yancopoulos, G.D., Valenzuela, D.M., Murphy, A.J., Stevens, S. & Flavell, R.A., 2008. Innate and adaptive interleukin-22 protects mice from inflammatory bowel disease. *Immunity,* 29**,** 947-957.

Zeng, H., Spencer, N.Y. & Hogg, N., 2001. Metabolism of S-nitrosoglutathione by endothelial cells. *American journal of physiology. Heart and circulatory physiology,* 281**,** H432-9.

Zhang, Y. & Hogg, N., 2004. The mechanism of transmembrane S-nitrosothiol transport. *Proceedings of the National Academy of Sciences of the United States of America,* 101**,** 7891-7896.

Ziegler, T.R., Smith, R.J., O'dwyer, S.T., Demling, R.H. & Wilmore, D.W., 1988. Increased intestinal permeability associated with infection in burn patients. *Archives of Surgery,* 123**,** 1313-1319.

Attachments

Attachment 1: Article-Polymer nanocomposites enhance *S*-nitrosoglutathione intestinal absorption and promote the formation of releasable nitric oxide stores in rat aorta

BASIC SCIENCE

Nanomedicine: Nanotechnology, Biology, and Medicine
12 (2016) 1795–1803

nanomedicine
Nanotechnology, Biology, and Medicine

ELSEVIER

Original Article

nanomedjournal.com

Polymer nanocomposites enhance *S*-nitrosoglutathione intestinal absorption and promote the formation of releasable nitric oxide stores in rat aorta

Wen Wu, PharmD, PhD[a], Caroline Perrin-Sarrado, PharmD, PhD[a], Hui Ming, PharmD[a], Isabelle Lartaud, PharmD, PhD[a], Philippe Maincent, PharmD, PhD[a], Xian-Ming Hu, PhD[b], Anne Sapin-Minet, PhD[a], Caroline Gaucher, PhD[a,*]

[a]*CITHEFOR EA3452 "Drug targets, formulation and preclinical assessment", Faculté de Pharmacie, Université de Lorraine, Nancy, France*
[b]*State Key Laboratory of Virology, Ministry of Education Key Laboratory of Combinatorial Biosynthesis and Drug Discovery, Wuhan University School of Pharmaceutical Sciences, Wuhan, China*

Received 16 October 2015; accepted 5 May 2016

Abstract

Alginate/chitosan nanocomposite particles (GSNO-acNCPs), *i.e.* *S*-nitrosoglutathione (GSNO) loaded polymeric nanoparticles incorporated into an alginate and chitosan matrix, were developed to increase the effective GSNO loading capacity, a nitric oxide (NO) donor, and to sustain its release from the intestine following oral administration. Compared with free GSNO and GSNO loaded nanoparticles, GSNO-acNCPs promoted 2.7-fold GSNO permeation through a model of intestinal barrier (Caco-2 cells). After oral administration to Wistar rats, GSNO-acNCPs promoted NO storage into the aorta during at least 17 h, as highlighted by (i) a long-lasting hyporeactivity to phenylephrine (decrease in maximum vasoconstrictive effect of aortic rings) and (ii) *N*-acetylcysteine (a thiol which can displace NO from tissues)-induced vasodilation of aorxxtic rings preconstricted with phenylephrine. In conclusion, GSNO-acNCPs enhance GSNO intestinal absorption and promote the formation of releasable NO stores into the rat aorta. GSNO-acNCPs are promising carriers for chronic oral application devoted to the treatment of cardiovascular diseases.

Key words: NO-donor; Polymer nanocomposites; Oral delivery; Isolated aorta vasoreactivity

In the cardiovascular system, deficiency of endogenous nitric oxide (NO) is the consequence of either insufficient synthesis (endothelium dysfunction)[1,2] or excessive NO degradation[3,4] (increased oxidative or nitrosative stresses, decreased antioxidant enzyme activity). NO depletion is one of the key factors in the initiation and progress of many diseases, such as atherosclerosis,[5] pulmonary hypertension,[6] thrombosis,[7] ischemia[8] and cardiac arrhythmia.[9] To maintain an appropriate level of NO and treat NO deficiency, several NO-related therapeutics have been developed such as nitrosamines, organic nitrates, metal–NO complexes, *N*-diazeniumdiolates. However, all act at very short term and lead to tolerance phenomena. *S*-nitrosothiols (RSNOs) present the advantage of a longer half-life, with no tolerance nor oxidative stress induction. Under physiological conditions, *S*-nitrosoglutathione (GSNO), a major endogenous RSNO, is one of the main storage forms of NO in tissues.[10] GSNO has been investigated for its powerful antiplatelet activity,[11,12] arterio/venous selective vasodilator effects,[13,14] antimicrobial[15] and antithrombotic effects.[16]

Despite such therapeutic potencies, GSNO pharmaceutical forms are still lacking. This may be related to the fast and often unpredictable rate of decomposition of GSNO. *In vitro*, because of pH-, light- and temperature-dependent sensitivities, GSNO is susceptible to many degradation processes

Funding and conflicts of interest: This work was supported by the 'Université de Lorraine and Région Lorraine'. W. Wu and H. Ming acknowledge Chinese Scholarships Council for their doctoral fellowships. X.-M. Hu was a guest professor at the Université de Lorraine, CITHEFOR EA 3452, for three months between 2014 and 2015.

The funders had no role in study design, data collection and analysis, decision to publish, or preparation of the manuscript.

*Corresponding author.

E-mail address: caroline.gaucher@univ-lorraine.f (C. Gaucher).

http://dx.doi.org/10.1016/j.nano.2016.05.006
1549-9634/

Please cite this article as: Wu W, et al, Polymer nanocomposites enhance *S*-nitrosoglutathione intestinal absorption and promote the formation of releasable nitric oxide stores in rat aorta. *Nanomedicine: NBM* 2016;12:1795-1803, http://dx.doi.org/10.1016/j.nano.2016.05.006

including *S*-NO bond homolysis, metal ion-catalyzed decomposition, and hydrolysis. *In vivo*, it is subjected to enzymes-induced decomposition such as GSNO reductase[17] and carbonyl reductase 1.[18] For this reason, the bioavailability of GSNO when administrated orally is limited. Two main strategies were described to overcome such limitations, through either inhibiting GSNO reductases activity[19] or improving the stability of GSNO. In respect to the latter, many researchers focused on the protection of GSNO – during storage and in biological media – through the combination with delivery systems to promote pharmaceutical and medical applications. For instance, Seabra and co-workers dispersed GSNO into polyethylene glycol (PEG)[20] or solid poly(vinyl alcohol)/poly(vinyl pyrrolidone) film[21] to achieve the controlled release of NO adapted to topical application. de Mel and co-workers passively incorporated GSNO into a polyhedral oligomeric silsesquioxane poly(carbonate-urea)urethane (POSS-PCU) composite to produce a NO realizing implant for cardiovascular diseases treatment.[22] Encapsulation followed by *S*-nitrosation of glutathione (GSH, the GSNO precursor) into mucoadhesive polymeric nanoparticles produced GSNO loaded nanoparticles, which slowed down GSNO decomposition at physiological temperature.[23,24] Similarly, Shah et al described another way to prolong the release of NO by conjugating GSH on chitosan backbone and *S*-nitrosating the GSH thiol group.[25] In our previous work, polymeric nanoparticles based on poly(methyl)methacrylate were developed to load GSNO through direct encapsulation (GSNO-NP), which protect GSNO and preserve its availability during interaction with smooth muscle cells.[26] However, the release profile we obtained was not long enough for chronic *in vivo* therapeutic applications. In our following work,[27] we developed polymer nanocomposite particles (NCP), which refer to nanoparticles of nanometric size embedded in a polymer matrix forming a composite particle of micrometric size, as defined by Bhattacharya and coworkers.[28] Microparticles were composed in our case of an alginate or a chitosan matrix including our previously described GSNO-NP.[26] These GSNO-NPs embedded into chitosan or alginate nanocomposites increased the encapsulation efficiency of GSNO compared to GSNO-NPs (from 54% to 69% or 76%, respectively) and sustained the *in vitro* release of GSNO until 24 h.[27]

From these promising results, in the present study, our aims were to further improve GSNO oral bioavailability, to control its delivery at the absorption site and to prolong the residence time into the gastrointestinal tract, by combining both alginate plus chitosan in the matrix. Alginate and chitosan were chosen as mucoadhesive polymers increasing the residence time on the intestine mucus layer.[29-32] As alginate has the capacity to penetrate the mucus layer,[30] this will bring the drug closer to the intestinal cells, while chitosan exerts the property to open cells tight junction.[31,32] Therefore, their combination will lead to increase drug permeability through the intestine. To broke new ground in the field of nanocomposite particles and merge mucopenetration and mucoadhesion properties in one system, we therefore developed GSNO-loaded alginate/chitosan nanocomposite particles (GSNO-acNCPs) formed through the incorporation of GSNO-NPs into a mix of alginate/chitosan matrix. The efficient encapsulation capacity and the sustained release profile of GSNO encouraged us to further investigate GSNO permeability through an intestinal cell barrier model (Caco-2). Finally, for the first time, we administrated GSNO-acNCPs to Wistar rats by gavage in order to evaluate their vascular effects, more particularly their capacity to increase the NO-storage inside the vascular wall.

Methods

Materials

All reagents were of analytical grade and all solutions prepared with ultrapure deionized water (> 18.2 mΩ.cm at 25 °C). Sodium nitrite was purchased from Merck (Germany). Acrylates/ammonium methacrylate copolymer (Eudragit® RL PO) was a generous gift from Evonik industries (Germany). Alginate sodium, chitosan (4-6 kDa), polyoxyethylene-polyoxypropylene block copolymer (Pluronic® F-68), mucin from porcine stomach, HBSS with Ca^{2+} and $Mg^{2+}$and all other reagents were obtained from Sigma-Aldrich (France). All experiments and assays involving GSNO were conducted under conditions of subdued light and at +4 °C in order to minimize light- and temperature-induced GSNO degradation.

Methods

GSNO synthesis

GSNO was synthesized according to a previously described method.[33] Briefly, reduced GSH was incubated with an equivalent of sodium nitrite under acidic condition (0.626 M HCl); after precipitation, the solid form of GSNO was obtained. The purity of GSNO was assessed by HPLC and UV spectrophotometry using the specific molar absorbance of the *S*-NO bond at 334 nm (ε = 922 $M^{-1}cm^{-1}$).

Preparation of GSNO-loaded alginate/chitosan nanocomposite particles

GSNO-loaded alginate/chitosan nanocomposite particles (GSNO-acNCPs) were constituted by inner cores and external polymer matrix. The inner cores were GSNO-loaded nanoparticles (GSNO-NP) prepared by a double emulsion (water–oil–water) and solvent evaporation method as described in previous work.[26] Briefly, an aqueous solution containing GSNO in 0.1% (w/w) Pluronic® F-68 was emulsified by sonication with an organic phase containing Eudragit® RL PO (100 mg/mL in dichloromethane). Then, sodium alginate and sodium tripolyphosphate (TPP, 220 mg) were fully dissolved in the resulting GSNO-NP suspension. Over an ice bath, calcium chloride solution ($CaCl_2$, 2 M) was added dropwise into this mixture to cross-link alginate homogenized by sonication (40 W, ultrasonic processor, France). GSNO-loaded alginate/chitosan nanocomposites particles (GSNO-acNCPs) were finally formed by dropwise addition of GSNO-NP-alginate mixture into the chitosan solution (1 mg/mL in 1% (v/v) acetic acid), under mechanical stirring (1300 rpm) over ice bath.

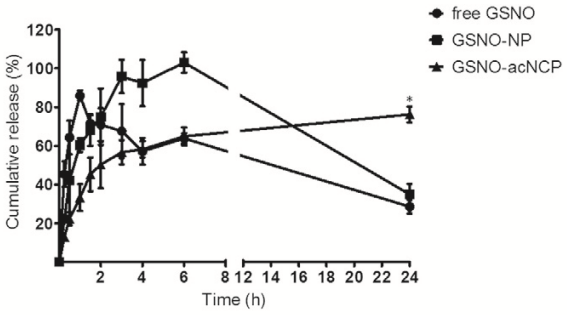

Figure 1. Release kinetic of the payload (GSNO and nitrite ions) from polymer nanocomposite particles in phosphate buffered saline (0.148 M) at 37 °C. Data are shown as mean ± sd, $n = 3$. *: $P < 0.05$ *vs* free GSNO and GSNO-NP (two-way ANOVA). GSNO-NP: GSNO-loaded nanoparticles, GSNO-acNCPs: GSNO-loaded alginate/chitosan nanocomposite particles.

Characterization of GSNO-loaded alginate/chitosan nanocomposite particles

Determination of size. The volume particle size distribution of GSNO-acNCPs was determined by the laser diffraction method (Mastersizer 2000, Malvern Instruments, France). The GSNO-acNCPs were suspended in ultrapure water. The size of GSNO-acNCPs was described by the volume mean diameter measured in triplicate.

Evaluation of GSNO encapsulation efficiency. Encapsulation efficiency (EE) describes the quantity of the drug entrapped within GSNO-acNCPs compared with the initial drug amount. It was determined according to the following equation:

$$EE = m_e/m_i \times 100$$

where EE is the encapsulation efficiency in percent (%), m_e is the mass of drug entrapped in particles, and m_i is the initial mass of drug. The entrapped drug within particles was evaluated by a two-step-liquid–liquid extraction. The external matrix of particles composed of sodium alginate and chitosan was disrupted by mechanical stirring followed by centrifugation and the amount of GSNO remaining in the supernatant, subtracted by the free nitrite ions quantified by the Griess assay,[34] was quantified by the Griess–Saville assay using sulfanilamide and $HgCl_2$ in acidic conditions to cleave the *S*-NO bond, and *N*-(1-napthyl)ethylenediamine to form a chromophoric azo product that absorbs at 540 nm.[34]

The resulting pellet, which corresponds to GSNO-NPs, was dissolved in 2 mL dichloromethane and the amount of GSNO in the nanoparticles was extracted in phosphate buffered saline (PBS) at pH 7.4 and determined by the Griess–Saville assay as described above. All the samples were prepared in triplicate.

Core loading expressed in mg of GSNO/g of polymer was estimated from initial GSNO, Eudragit® RL PO, sodium alginate and chitosan amounts.

In vitro release kinetic. GSNO-acNCPs were suspended in 1 mL of PBS and were placed in cellulose dialysis tubing (average flat width 10 mm (0.4 in), cut-off 14 kDa). Release kinetic was measured as previously described[27] in 200 mL of PBS at 37 °C protected from light. The GSNO and nitrite ions released were monitored every 30 min during two hours, every hour from two to six hours, then at 24 h, and immediately quantified with a fluorometric method[35] using diaminonaphthalene (added or not with $HgCl_2$ to cleave the *S*-NO bond) producing naphthotriazole (emission 415 nm/excitation 375 nm, JASCO FP-8300, France).

Stability of GSNO in GSNO-loaded alginate/chitosan nanocomposite particles. The GSNO-acNCP or GSNO-NP suspensions were centrifuged (15,000 *g*, 20 min, 4 °C) and the resulting pellets were kept in a freezer at −20 °C, in a fridge at +4 °C or at +37 °C in a humidified incubator. At predetermined time intervals over 15 days (D) (1D, 2D, 3D, 4D, 5D and 15D), the GSNO was extracted and analyzed by the Griess–Saville assay as above to determine the remaining intact and decomposed GSNO. All the samples were prepared in triplicate.

Mucins binding assay

Changes in size and zeta potential of GSNO-NPs in contact with a mucin dispersion were examined.[36] After centrifugation (42,000 *g*, 30 min, 4 °C; Heraeus Instruments, France), nanoparticles were resuspended in a mucin dispersion at a concentration of 5 mg/mL polymer in 1 mg/mL mucin (ratio 5:1). The volume particle size distribution of GSNO-NPs was determined by the laser diffraction method (Mastersizer 2000, Malvern Instruments, France) and zeta potential was estimated by electrophoretic mobility (ZetaSizer NanoZS, Malvern Instruments, France).

Cytocompatibility

The cytocompatibility of GSNO-acNCPs was evaluated on intestinal Caco-2 cells ATCC® HTB-37™. Caco-2 cells were grown in complete medium consisting of Eagle's Minimum Essential Medium EMEM supplemented with 20% (v/v) fetal bovine serum, 4 mM of glutamine, 100 U/mL of penicillin, 100 U/mL of streptomycin, 1% (v/v) of non-essential amino acids. Cells were cultivated at 37 °C under 5% CO_2 (v/v) in a humidified incubator. Caco-2 cells were seeded in 96-wells plates at 20,000 cells/well 24 h before experiment. They were then exposed to 0.5, 1.0, 5.0, 10.0 or 50.0 mg/mL of GSNO-acNCP for 24 h at 37 °C, complete medium being used as control. Cytocompatibility expressed by metabolic activity was checked with the 3(4,5-dimethylthiazol-2-yl)-2,5-diphenyltetrazolium bromide (MTT) assay. The absorbance of extracted formazan crystals was read at 570 nm with a reference at 630 nm (EL 800 microplate reader, Bio-TEK Instrument, Inc®, France). Metabolic activity in control condition was considered as 100%.

In vitro cell permeability

The permeability of GSNO across the Caco-2 monolayer was evaluated in the apical-to-basolateral direction in Hank's Balanced Salt Solution (HBSS, pH 6.5). After seeding 10^6 cells on cell culture inserts (Transwell®, Corning, USA) with 0.4 μm pore size disposed in a 12-wells plate, the medium was replaced every two days during the first week and every day during the lasting days until the differentiated cell monolayer was formed (14-18 days, 588 ± 44 Ω/cm^2). For

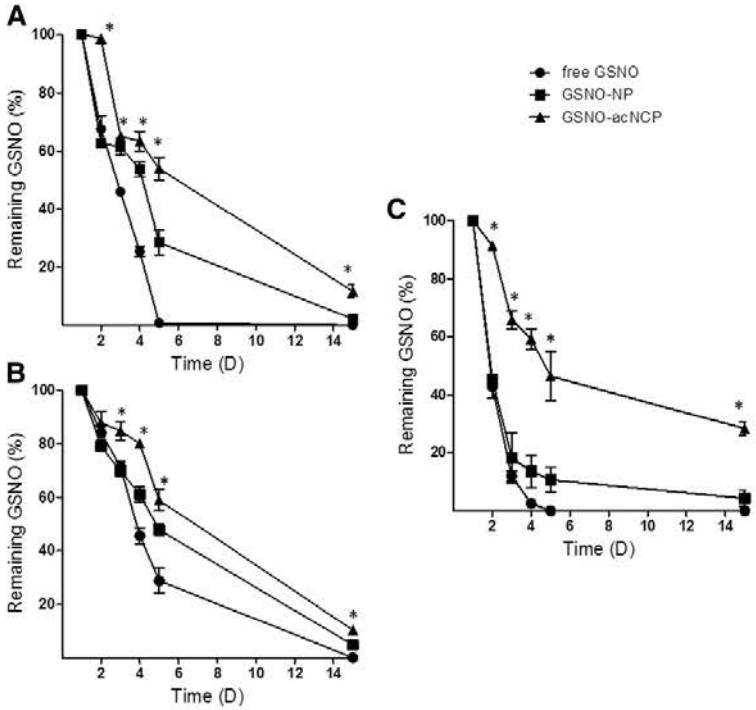

Figure 2. Stability of GSNO in polymer particles. GSNO-loaded alginate/chitosan nanocomposite particles (GSNO-acNCPs) or GSNO-loaded nanoparticles (GSNO-NP) suspensions were centrifuged and the resulting pellets were stored at −20 °C **(A)**, +4 °C **(B)** and +37 °C **(C)** for 15 days. At regular intervals, the remaining intact GSNO was determined by the Griess–Saville assay. Data are expressed as mean ± sd (n = 3). *: $P < 0.05$ *vs* free GSNO (two-way ANOVA).

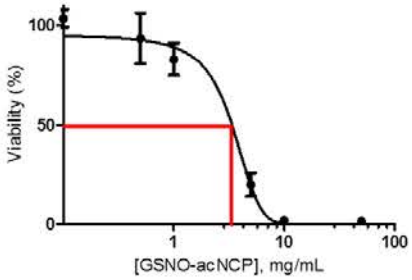

Figure 3. *In vitro* cytotoxicity of polymer nanocomposite particles on Caco-2 cells. Caco-2 cells were treated with the indicated concentrations of GSNO-loaded alginate/chitosan nanocomposite particles (GSNO-acNCPs) for 24 h at 37 °C. Viability was estimated through mitochondrial activity by the MTT assay. Data are expressed as mean ± sem (n = 3).

the permeation experiments, polymer nanocomposite particles containing 50 μM of GSNO were suspended in 500 μL of HBSS and introduced in the apical (donor) compartment, whereas, 1.5 mL of HBSS was placed in basolateral (receptor) compartment. After 1, 4 and 24 h, each basolateral compartment was withdrawn and replaced with the same volume of fresh HBSS. The GSNO, nitrite and nitrate ions permeated and presented in basolateral (for each time) and apical (after 24 h only) compartments were detected using the fluorometric method.[26]

The integrity of the cell monolayer was checked before the permeability studies by measuring the transepithelial electrical resistance (TEER) using a Millicell®-Electrical Resistance system (Millipore, USA). In addition, the permeation of fluorescein sodium (5 μM) was also used to verify the integrity of monolayer.

The cumulative amounts of GSNO crossing the Caco-2 monolayer were calculated from the concentrations measured in basolateral compartments. The apparent permeability coefficient (Papp) values were calculated using the following equation:

$$\text{Papp} = \frac{dQ}{dt} \times \frac{1}{A \times C_0}$$

dQ/dt (mol/s) refers to the permeability rate (mol) of RSNO in the basolateral compartment at the time of quantification, A (cm^2) refers to membrane diffusion area, and C_0 (mol/mL) refers to the initial concentration in the apical compartment.

The enhancement ratio (R) was calculated through the following equation:

$$R = \text{Papp1}/\text{Papp2}$$

Papp1 refers to the apparent permeability coefficient of each treatment, and Papp2 corresponds to the apparent permeability coefficient of free GSNO.

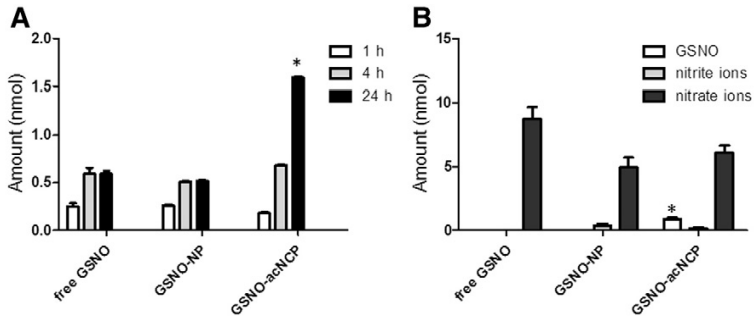

Figure 4. Caco-2 cell permeability of GSNO from polymer particles. Twenty five nmol of free GSNO or equivalent amount of GSNO-loaded nanoparticles (GSNO-NP) or GSNO-loaded alginate/chitosan nanocomposite particles (GSNO-acNCPs) were loaded in the apical compartment of a transwell® system seeded with Caco-2 cells 15 days before. **(A)** Amount of GSNO permeated from the apical to the basolateral compartment after 1 h, 4 h or 24 h. **(B)** Amount of the different nitric oxide species remained in the apical compartment after 24 h. Values presented have been corrected from control (cells without treatment for free GSNO, blank formulations for GSNO loaded formulations). Data are shown as mean ± sem ($n = 3$). *: $P < 0.05$ *vs* free GSNO and GSNO-NP (two-way ANOVA).

Ex vivo pharmacological evaluation

Animals used and ethical statement. Vasorelaxation was evaluated on endothelium-removed aortic rings isolated from 12 week-old, male, normotensive, Wistar rats (Janvier Laboratories, Le Genest-St-Isle, France; 400-500 g). All experiments were performed in accordance with the European Community guidelines (2010/63/EU) for the use of experimental animals in the respect of the 3 Rs' requirements for Animal Welfare (C. Perrin-Sarrado permit number n°54-72, I. Lartaud n° 54-5; the project untitled "Nitro-Vivo" was positively evaluated the19th of December 2014 by the CELMEA (regional ethical committee for animal experiments) and approved by the French Ministry of Research n°APAFIS1614-2015090216575422v2). Animals were kept under standard conditions (temperature: 21 ± 1 °C, hygrometry 60 ± 10%, light on from 6 am to 6 pm) and had free access to standard diet (A04, Safe, Villemoisson-sur-Orge, France) and water (reverse osmosis system, Culligan, Brussells, Belgium).

Treatment schedule. GSNO-acNCPs (15 mg of GSNO/kg body weight), free GSNO (15 mg of GSNO/kg body weight), blank-acNCPs or PBS as controls were administrated by gavage (10 mL/kg of rat) to Wistar rats (fasted 8 h before gavage). Seventeen hours after gavage, rats were sacrificed by exsanguination after anesthesia (sodium pentobarbitone 60 mg/kg, intraperitoneal, Sanofi Santé Nutrition Animale, Libourne, France) and intravenous administration of heparin (500 U, Heparine Choay). A segment (around 3 cm) of the descending thoracic aorta was removed and immediately placed in cold Krebs' solution. Vessels were cleaned from surrounding connective tissues and cut into 2-mm long rings (8 rings per rat). The endothelium was removed by rubbing the intimal surface of the rings with forceps and immediately used for *ex vivo* vasoactivity studies.

Measurement of vasoactivity. Aortic vasoactivity was measured using an isometric tension recording system in 10 mL organ chambers (EMKABATH, Emka Technology, France). Baths were filled with Krebs' solution (10 mL, 37 °C, pH 7.4) and continuously bubbled with 95% O_2 and 5% CO_2. Following 60-min equilibration with a basal resting tension determined at 2 g, viability of aortic rings was assessed with potassium chloride (KCl, 6×10^{-2} M) added in the baths. The contraction rapidly reached a steady state and was expressed, after 15 min exposure, as the developed tension from the basal resting tension of 2 g. Arteries showing less than 2.5 g of developed tension were excluded. After viability test and a 30 min wash-out period so that tension returns to baseline, aortic rings were tested with two protocols: i) vasoconstriction of aortic rings (n = 10-12 per group, from 4 different rats in each group) was measured with increasing concentrations of phenylephrine (PHE) (10^{-10} M to 3×10^{-5} M); ii) NO storage in the aorta was evaluated with *N*-acetylcysteine (NAC) used to displace NO from cysteine-NO residue. Rings (n = 10-12 per group, from 4 different rats in each group) preconstricted with 10^{-6} M PHE, were added with NAC (10^{-5} M and 10^{-4} M). Contractile effects were expressed as induced developed tension (Delta T, g) and relaxant ones in percentage of contraction (100% being the stable tension caused by 10^{-6} M PHE).

The absence of functional endothelium was confirmed by the ability of carbachol 10^{-5} M, a muscarinic receptors agonist, to induce less than 10 % of relaxation on 10^{-6} M PHE-preconstricted aortic rings.

Statistical analysis

Results are shown as either mean ± standard deviation (sd) or mean ± standard error of the mean (sem) values. The half maximal effective concentration (EC_{50}) and maximal response (E_{max}) were calculated by fitting each concentration response curve using the Hill logistic equation. For the comparison of Papp, and that of E_{max} and EC_{50} for PHE, statistical comparisons were performed using the one-way ANOVA ($P < 0.05$). Other analyses were performed using the two-way ANOVA ($P_{treatment} < 0.05$; $P_{time} < 0.05$). Statistical analyses were performed using the GraphPad Prism software (GraphPad Software version 5.0, San Diego, USA).

Table 1
Apparent permeability coefficient (Papp) and enhancement ratio (R) of GSNO permeation across Caco-2 monolayers.

Group	Papp (10^{-8} cm/s)	R
Free GSNO	8.3 ± 0.3	1.0
GSNO-NP	7.7 ± 3.1	0.9
GSNO-acNCPs	34.1 ± 1.5*	4.1

Data are shown as mean ±sem, $n = 3$. All data sets were compared to free GSNO. *: $P < 0.05$ *vs* free GSNO (one-way ANOVA). GSNO-NP: GSNO-loaded nanoparticles, GSNO-acNCPs: GSNO-loaded alginate/chitosan nanocomposite particles.

Results

Physico-chemical characterization of GSNO-loaded alginate/chitosan nanocomposite particles

The average size of the developed nanocomposite particles was 56 ± 15 μm (mean ± sd; $n = 3$). GSNO was entrapped within the nanocomposite particles with a high encapsulation efficiency (76 ± 10%), corresponding to an estimated core loading of 15.0 ± 1.9 mg of GSNO/g of polymer. The inner core of GSNO loaded nanoparticles presented an estimated core loading of 5.7 mg of GSNO/g of polymer with a zeta potential of +40 ± 6 mV and a mean diameter of 0.289 ± 0.014 μm.[26] As shown in Figure 1, 75 ± 3% of free GSNO was released from the dialysis bag during the first hour. Similarly, GSNO-NPs showed a release profile with a burst release of 95 ± 2% of the initially loaded GSNO within the first 3 h. On the other hand, only 57 ± 6% of GSNO was released from GSNO-acNCPs within 3 h and the remaining amount was released in a sustained way over the next 21 h.

Stability of GSNO in GSNO-loaded alginate/chitosan nanocomposite particles

The stability of GSNO within the polymer nanocomposite particles was evaluated at −20 °C, +4 °C and +37 °C. After 5 days of storage at −20 °C or +4 °C, 100 ± 1% or 70 ± 5% of free GSNO respectively, was decomposed (Figure 2, *A*, *B*). When incorporated into the polymer nanocomposite particles, 16 ± 5% (−20 °C) and 12 ± 4% (+4 °C) of intact GSNO was preserved for 15 days, showing improvement of GSNO stability. At +37 °C, GSNO degraded faster (Figure 2, *C*): 57 ± 4% of free GSNO had decomposed within two days and 98 ± 1% after 4 days. Polymer nanocomposite particles increased the life-time of GSNO as 46 ± 9% and 12 ± 4% of intact GSNO were detected on the 4th and 15th days respectively.

Mucin binding assay

The mucoadhesion property of the polymeric GSNO-NPs was also evaluated. The diameter of GSNO-NPs in contact with mucin dispersion immediately increased from 0.2 ± 0.0 μm to 18.2 ± 3.2 μm (100 times more) and estimated zeta potential value was divided per 3 (from +54 ± 4 mV to +18 ± 5 mV, (mean ± sd; $n = 3$)).

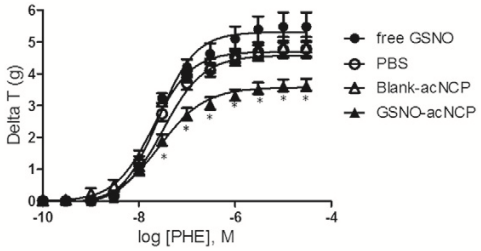

Figure 5. Contractile effect of phenylephrine (PHE) on aortic rings isolated from rats orally treated with free GSNO or GSNO-loaded polymer nanocomposite particles (GSNO-acNCPs) at 15 mg of GSNO/kg of body weight, 17 h before. Blank alginate/chitosan nanocomposite particles (Blank-acNCPs) and phosphate buffered saline (PBS) have been used as controls. Results are expressed as mean ± sem (n = 10-12 per group, from 4 different rats in each group). *: $P < 0.05$ *vs* PBS (two-way ANOVA).

Cytocompatibility and cell permeability

The concentration-response curve built from the MTT metabolic activity assay (Figure 3) gave an IC_{50} at 3.24 ± 0.38 mg/mL for GSNO-acNCPs. Therefore, a concentration of 1 mg/mL (containing 50 μM GSNO) that maintained 83 ± 1% of cell viability was chosen for Caco-2 permeability studies.

Caco-2 cell monolayers were incubated with 50 μM (representing 25 nmol of GSNO in 0.5 mL) free or nanoparticle-associated GSNO in the apical compartment to investigate GSNO permeability. After 1 h of incubation, a similar concentration of GSNO was detected in the basolateral compartment for all formulations (Figure 4, *A*). The permeation kinetics of the RSNO were similar for GSNO and GSNO-NPs: the amount transported rose rapidly to 0.59 ± 0.07 nmol and 0.51 ± 0.01 nmol, respectively, over the first 4 h, and then remained at a plateau up to 24 h. GSNO-acNCPs showed a steady penetration rate over the whole 24 h, and promoted 2.7-fold more GSNO crossing the cell monolayer than free GSNO or GSNO-NP (Figure 4, *A*). The Papp value of GSNO (showing the ability of NPs and acNCPs to help the transport of GSNO across Caco-2 cell monolayer) did not change with NP, but significantly increased after GSNO-NPs incorporation into nanocomposite particles, showing an enhancement ratio of 4.1 (Table 1). In contrast to free GSNO and GSNO-NPs, GSNO-acNCPs retained 0.9 ± 0.1 nmol of intact GSNO in the apical compartment after 24 h of incubation (Figure 4, *B*) showing that GSNO-acNCPs could have an even longer release profile.

At the end of experiments, the test using the low molecular weight hydrophilic tracer sodium fluorescein, showed that the permeation of sodium fluorescein in the treated groups (18 ± 5%) was higher than the positive control (6.1 ± 0.5%) and less than negative control (32 ± 9%), in which cells were treated with HBSS without Ca^{2+} and Mg^{2+}. Taken together, these results confirmed the integrity of cells monolayer after incubation with the GSNO-acNCPs with a slight opening of tight junction due to chitosan.

GSNO-NPs[26] showed a core loading two times under the GSNO-acNCPs core loading (5.7 mg of GSNO/g of polymer

Table 2
Half maximum effective concentration (EC_{50}) and maximum effect (E_{max}) of phenylephrine measured in isolated aortic rings.

Group	EC_{50} (10^{-8} M)	E_{max} (g)
PBS	3.1 ± 0.1	4.8 ± 0.1
Blank-acNCPs	1.9 ± 0.2	4.8 ± 0.3
Free GSNO	3.1 ± 0.1	4.9 ± 0.1
GSNO-acNCPs	3.1 ± 0.1	3.7 ± 0.1*

Data are shown as mean ±sem, (n = 10-12 per group, from 4 different rats in each group). *: $P < 0.05$ *vs* PBS (one-way ANOVA). PBS: phosphate buffered saline. Blank-acNCPs: blank alginate/chitosan nanocomposite particles, GSNO-acNCPs: GSNO-loaded alginate/chitosan nanocomposite particles.

and 15.0 ± 1.9 mg of GSNO/g of polymer, respectively). Furthermore, the permeability studies failed in showing a higher and long lasting absorption of GSNO for the GSNO-NPs through intestinal cells compared to free GSNO. For these two reasons, the GSNO-NPs were moved aside from the *in vivo* studies

Pharmacological vascular effects

The dose–response curves to PHE were similar in aortic rings from Wistar rats orally treated 17 h earlier with free GSNO, blank-acNCP or PBS (Figure 5). In aortic rings from rats treated with GSNO-acNCP (15 mg/kg body weight), the contractile maximal effect (E_{max}) of PHE significantly decreased (from 4.8 g in control groups to 3.7 g in the GSNO-acNCP group, −25%, $P < 0.05$) with no change in EC_{50} (Table 2).

In all the control groups, NAC failed to relax the vessels. However, in the group treated with GSNO-acNCP, NAC induced significant relaxation (11 ± 1% at 10^{-5} M and 24 ± 3% at 10^{-4} M, $P < 0.05$ compared to controls, Figure 6).

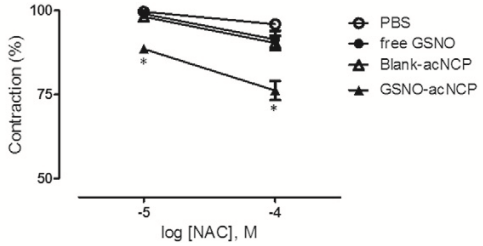

Figure 6. Vascular effect of 10^{-5} M and 10^{-4} M *N*-acetylcysteine (NAC) on precontracted (10^{-6} M phenylephrine) aortic rings isolated from rats orally treated with free GSNO or GSNO-loaded polymer nanocomposite particles (GSNO-acNCPs) at 15 mg of GSNO/kg of body weight, 17 h before. Blank alginate/chitosan nanocomposite particles (Blank-acNCPs) and phosphate buffered saline (PBS) have been used as controls. Results are expressed as mean ± sem (n = 10-12 per group, from 4 different rats in each group). *: $P < 0.05$ *vs* PBS (two-way ANOVA).

Discussion

The encapsulation of the fragile molecule GSNO within drug delivery systems is still challenging. Different approaches, either through *S*-nitrosation of free or conjugated GSH[23,25] or direct encapsulation of GSNO[21,37] are described in the literature. In the present study, we adopted the second approach with gentle formulation process to develop polymer nanocomposite particles loaded with GSNO. The polymer nanocomposites were obtained by incorporation of GSNO loaded Eudragit® RL nanoparticles (GSNO-NP)[26] into a polymer matrix prepared from a mixture of alginate and chitosan by ionic gelation. The challenge was to control the loading of GSNO within the nanocomposite particles in order to get potential pharmacological efficiency. We based our calculations on the minimal concentration of NO required to stimulate the synthesis of cyclic GMP by soluble guanylate cyclase in vascular smooth muscle (approximately 10 nmol/L[38]), and the dose of GSNO that significantly decreases mean arterial blood pressure (*i.e.* 3 mg; 100 μg/min for 30 min, intravenous, in human[39]).

Compared to our previous published results on GSNO-NP,[26] the newly formulated composite particles improved the loading capacity of GSNO by 2.6-fold (from 5.7 to 15.0 mg of GSNO/g of polymer). This improvement can probably be attributed to the use of alginate and chitosan, which are hydrophilic and have good affinity for GSNO thus allowing the entrapment not only of GSNO-NP but also of the free GSNO remaining outside the nanoparticles. This is consistent with our previously reported polymer nanocomposites based on chitosan or alginate separately.[27]

Our results on *in vitro* release demonstrate that the polymer nanocomposite particles prevented the burst release of hydrophilic GSNO observed with GSNO-NP alone. This is in agreement with the results of Hasan et al[40] showing that composite particles were able to reduce the burst release. GSNO-acNCPs present two polymer barriers to the diffusion of GSNO: the first being formed by the hydrophobic Eudragit® RL polymer and the second by the outer hydrophilic matrix composed of chitosan and alginate. The combination of both leads the diffusion distance to increase and the release rate to slow down. Furthermore, as reported by de Seabra et al[20,41,42] increased microviscosity of the solvent improve the stability of RSNO. The presence of alginate and chitosan, which build a hydrophilic matrix for the particles, increases the viscosity thereby protecting GSNO from thermal decomposition and improved GSNO stability. Moreover, the increased stability we obtained at +37 °C for GSNO-acNCPs was in accordance with our previous observations using alginate or chitosan in polymer nanocomposite particles.[27]

GSNO-acNCPs also improved the permeability of GSNO through the Caco-2 cells model, and increased the Papp value, a marker of drug absorption. This permeation enhancement may be attributed to three major factors: i) the positive charge of GSNO-acNCPs (zeta potential approximately equal to +18.5 ± 0.8 mV), which allows electrostatic attraction with the negatively charged cell membrane; ii) the composition of nanocomposite particles based on chitosan and alginate, which have mucoadhesive properties and reinforce the interaction with cells; iii) the high level of protection of GSNO afforded by the nanocomposite particles. While we did not directly measure GSNO crossing through intestinal tissue, our results augur a promising oral delivery, for which intestinal absorption is one of the key factors determining drug bioavailability. The mechanisms involved in intestinal crossing remain to be evaluated. However, the glycosidic bonds of chitosan were shown to be rapidly hydrolyzed under gastric conditions,[43] so only a portion

of this polymer and the alginate of the complex matrix will be able to adhere on the mucus layer and to open tight junctions in the intestinal compartment.[44] Moreover, alginate will help the inner core made of GSNO-NPs to penetrate the mucus layer. GSNO-NPs will no longer stay at the nanometer size: as we showed they adsorb proteins like mucins or albumin[26] to reach a final size around 20 μm. Others also showed that the mucus layer strongly increase particle size and modify absorption of particles through the intestine.[45] Indeed, Bajka et al demonstrated that a particle diameter higher than 500 nm largely decreased particles diffusion.[45] Therefore, it is probable that only GSNO or other NO species will diffuse within the intestinal tight junctions, already opened by chitosan, and reach the vascular compartment.

Whatever the mechanisms involved in intestinal crossing, oral administration of GSNO-acNCPs to Wistar rats reveals NO-related vascular effects attesting that NO effectively reaches the blood stream. The decreased contractile response of aorta to PHE is the proof that the absorbed GSNO is transported from the intestine to the aortic wall by itself or through transnitrosation process of albumin or hemoglobin in the blood stream. Then, close to the vascular wall, transnitrosation processes occur again to generate a NO store inside the vascular wall. The final storage of NO in vascular smooth muscle cells was highlighted by aortic hyporeactivity to PHE and vasorelaxation in response to NAC. Indeed, in the absence of NO storage, NAC is not able to relax aortic rings, whereas, in presence of NO stores (*S*-nitrosation of proteins/peptides cysteine residues) within the vessel wall, NAC after entering into the cells displaces NO from vascular stores, which finally activates the guanylate cyclase/GMPc pathway inducing relaxation. Finally, the transnitrosation reactions with *S*-nitrosated proteins/peptides,[46] leading to the formation of unstable *S*-nitrosothiols may be involved, both in the storage processes during the 17 hours following gavage, and in the release of NO induced by NAC.[47] Similar results were obtained *ex vivo* in previous experiments where NO donors applied directly on the aortic rings, sustained hyporeactivity to vasoconstrictors from 1 to 4 hours.[47-50] Oral administrations of PBS or blank-acNCPs, as that of free GSNO – due to its limited stability – were unable to form a reservoir of NO in vascular tissue, and NAC has no vasorelaxant effect.

Another hypothesis for the decreased response to PHE may relate to the *S*-nitrosation of the alpha1–adrenergic receptor leading to its decreased affinity for sympathetic ligands.[51] This is unlikely in the present study as EC_{50} remained similar in all groups of treatment.

In conclusion, we demonstrated the therapeutic potential of polymer nanocomposite particles based on poly(methyl)methacrylate inside an alginate plus chitosan matrix for oral delivery of GSNO. The efficient loading, protection and sustained release of GSNO provided by these formulations promote GSNO absorption through the intestinal barrier, allow GSNO to reach the blood stream and contribute to form a reservoir of NO by transnitrosation inside the vascular wall. Seventeen hours following oral administration, vascular hyporeactivity to the vasoconstrictor remained. These new drug delivery systems of NO donors may be particularly adapted for oral treatment of cardiovascular diseases.

Acknowledgments

The authors are grateful to Dr. François Dupuis, Patrick Liminana and Isabelle Fries (EA 3452, CITHEFOR, Lorraine University) for the helpful advices and technical support to experimental studies, Pr Gillian Barratt (UMR CNRS 861, Paris-Sud University) for manuscript spelling corrections.

References

1. `Versari D, Daghini E, Virdis A, Ghiadoni L, Taddei S. Endothelium-dependent contractions and endothelial dysfunction in human hypertension. *Pharmacol* 2009;**157**:527-36, http://dx.doi.org/10.1111/j.1476-5381.2009.00240.x.
2. `Davignon J, Ganz P. Role of endothelial dysfunction in atherosclerosis. *Circulation* 2004;**109**:27-32, http://dx.doi.org/10.1161/01.CIR.0000131515.03336.f8.
3. Moncada S, Palmer RM, Higgs EA. Nitric oxide: Physiology, pathophysiology, and pharmacology. *Pharmacol Rev* 1991;**43**:109-42 [doi:0031-6997/91/4302-0109$03.00/0].
4. `Cai H, Harrison DG. Endothelial dysfunction in cardiovascular diseases: The role of oxidant stress. *Circ Res* 2000;**87**:840-4, http://dx.doi.org/10.1161/01.RES.87.10.840.
5. Napoli C, de Nigris F, Williams-Ignarro S, Pignalosa O, Sica V, Ignarro LJ. Nitric oxide and atherosclerosis: An update. *Nitric Oxide* 2006;**15**:265-79.
6. `Sim Ji-Yeon. Nitric oxide and pulmonary hypertension. *Anesthesiol* 2010;**58**:4-14, http://dx.doi.org/10.4097/kjae.2010.58.1.4.
7. `Loscalzo J. Nitric oxide insufficiency, platelet activation, and arterial thrombosis. *Circ Res* 2001;**88**:756-62, http://dx.doi.org/10.1161/hh0801.089861.
8. `Bolaños JP, Almeida A. Roles of nitric oxide in brain hypoxia-ischemia. *Biochim Biophys Acta* 1999;**1411**:415-36, http://dx.doi.org/10.1016/S0005-2728(99)00030-4.
9. `Tamargo J, Caballero R, Gómez R, Delpón E. Cardiac electrophysiological effects of nitric oxide. *Cardiovasc Res* 2010;**87**:593-600, http://dx.doi.org/10.1093/cvr/cvq214.
10. `Hogg N, Singh RJ, Kalyanaraman B. The role of glutathione in the transport and catabolism of nitric oxide. *FEBS Lett* 1996;**382**:223-8, http://dx.doi.org/10.1016/0014-5793(96)00086-5.
11. `Riccio DA, Dobmeier KP, Hetrick EM, Privett BJ, Paul HS, Schoenfisch MH. Nitric oxide-releasing *S*-nitrosothiol-modified xerogels. *Biomaterials* 2009;**30**:4494-502, http://dx.doi.org/10.1016/j.biomaterials.2009.05.006.
12. `Langford EJ, Brown AS, Wainwright RJ, de Belder AJ, Thomas MR, Smith RE, et al. Inhibition of platelet activity by *S*-nitrosoglutathione during coronary angioplasty. *Lancet* 1994;**344**:1458-60, http://dx.doi.org/10.1016/S0140-6736(94)90287-9.
13. MacAllister RJ, Calver AL, Riezebos J, Collier J, Vallance P. Relative potency and arteriovenous selectivity of nitrovasodilators on human blood vessels: An insight into the targeting of nitric oxide delivery. *J Pharmacol Exp Ther* 1995;**273**:154-60.
14. `Rassaf T, Kleinbongard P, Preik M, Dejam A, Gharini P, Lauer T, et al. Plasma nitrosothiols contribute to the systemic vasodilator effects of intravenously applied NO: Experimental and clinical study on the fate of NO in human blood. *Circ Res* 2002;**91**:470-7, http://dx.doi.org/10.1161/01.RES.0000035038.41739.CB.
15. `Friedman AJ, Blecher K, Schairer D, Tuckman-Vernon C, Nacharaju P, Sanchez D, et al. Improved antimicrobial efficacy with nitric oxide releasing nanoparticle generated *S*-nitrosoglutathione. *Nitric Oxide* 2011;**25**:381-6, http://dx.doi.org/10.1016/j.niox.2011.09.001.
16. `Sorragi Cde L, Shishido SM, Lemos ME, Marcondes S, Antunes E, Krieger MH. *In vitro* evaluation of the safe margin, antithrombotic and antiproliferative actions for the treatment of restenosis: Nitric oxide

donor and polymers. *Cell Biochem Funct* 2011;**29**:207-14, http://dx.doi.org/10.1002/cbf.1738.
17. Jensen DE, Belka GK, Du Bois GC. *S*-Nitrosoglutathione is a substrate for rat alcohol dehydrogenase class III isoenzyme. *Biochem J* 1998;**331**(Pt 2):659-68.
18. `Bateman RL, Rauh D, Tavshanjian B, Shokat KM. Human carbonyl reductase 1 is an *S*-nitrosoglutathione reductase. *J Biol Chem* 2008;**283**:35756-62, http://dx.doi.org/10.1074/jbc.M807125200.
19. `Chen Q, Sievers RE, Varga M, Kharait S, Haddad DJ, Patton AK, et al. Pharmacological inhibition of *S*-nitrosoglutathione reductase improves endothelial vasodilatory function in rats *in vivo*. *J Appl Physiol* 2013;**114**:752-60, http://dx.doi.org/10.1152/japplphysiol.01302.2012.
20. `Seabra AB, de Souza GF, da Rocha LL, Eberlin MN, de Oliveira MG. *S*-Nitrosoglutathione incorporated in poly(ethylene glycol) matrix: Potential use for topical nitric oxide delivery. *Nitric Oxide* 2004;**11**:263-72, http://dx.doi.org/10.1016/j.niox.2004.09.005.
21. `Seabra AB, da Rocha LL, Eberlin MN, de Oliveira MG. Solid films of blended poly(vinyl alcohol)/poly(vinyl pyrrolidone) for topical *S*-nitrosoglutathione and nitric oxide release. *J Pharm Sci* 2005;**94**:994-1003, http://dx.doi.org/10.1002/jps.20314.
22. `de Mel A, Naghavi N, Cousins BG, Clatworthy I, Hamilton G, Darbyshire A, et al. Nitric oxide-eluting nanocomposite for cardiovascular implants. *J Mater Sci Mater Med* 2014;**25**:917-29, http://dx.doi.org/10.1007/s10856-013-5103-2.
23. `Marcato PD, Adami LF, de Melo Barbosa R, Melo PS, Ferreira IR, de Paula L, et al. Development of a sustained-release system for nitric oxide delivery using alginate/chitosan nanoparticles. *Curr Nanosci* 2013;**9**:1-7, http://dx.doi.org/10.2174/15734131380511784 8.
24. `Marcato PD, Adami LF, Melo PS, de Paula L, Durán N, Seabra AB. Glutathione and *S*-nitrosoglutathione in alginate/chitosan nanoparticles: Cytotoxicity. *JPCS* 2011;**304**:012045, http://dx.doi.org/10.1088/1742-6596/304/1/012045.
25. `Shah SU, Martinho N, Socha M, Pinto Reis C, Gibaud S. Synthesis and characterization of *S*-nitrosoglutathione-oligosaccharide-chitosan as a nitric oxide donor. *Expert Opin Drug Deliv* 2015;**12**:1-15, http://dx.doi.org/10.1517/17425247.2015.1028916.
26. `Wu W, Gaucher C, Diab R, Fries I, Xiao YL, Hu XM, et al. Time lasting *S*-nitrosoglutathione polymeric nanoparticles delay cellular protein *S*-nitrosation. *Pharm Biopharm* 2015;**89**:1-8, http://dx.doi.org/10.1016/j.ejpb.2014.11.005.
27. `Wu W, Gaucher C, Fries I, Hu XM, Maincent P, Sapin-Minet A. Polymer nanocomposite particles of *S*-nitrosoglutathione: A suitable formulation for protection and sustained oral delivery. *Pharm* 2015;**495**:354-61, http://dx.doi.org/10.1016/j.ijpharm.2015.08.074.
28. Bhattacharya SN, Kamal MR, Gupta RK. *Polymeric Nanocomposites: Theory and Practice*. Carl Hanser Verlag GmbH & Co. KG978-3-446-40270-6; 20071-13.
29. `Gomez-Orellana I. Strategies to improve oral drug bioavailability. *Expert Opin Drug Deliv* 2005;**2**:419-33, http://dx.doi.org/10.1517/17425247.2.3.419.
30. `Zhang H, Zhang J, Streisand JB. Oral mucosal drug delivery: Clinical pharmacokinetics and therapeutic applications. *Clin Pharmacokinet* 2002;**41**:661-80, http://dx.doi.org/10.2165/00003088-200241090-00003.
31. Dodane V, Amin Khan M, Merwin JR. Effect of chitosan on epithelial permeability and structure. *Pharm* 1999;**182**:21-32.
32. `Thanou M, Verhoef JC, Junginger HE. Oral drug absorption enhancement by chitosan and its derivatives. *Adv Drug Deliv Rev* 2001;**52**:117-26, http://dx.doi.org/10.1016/S0169-409X(01)00231-9.
33. Parent M, Dahboul F, Schneider R, Clarot I, Maincent P, Lerroy P, et al. A complete physicochemical identity card of *S*-nitrosoglutathione. *Curr Pharm Anal* 2013;**9**:31-42.
34. `Sun J, Zhang X, Broderick M, Fein H. Measurement of nitric oxide production in biological systems by using griess reaction assay. *Sensors* 2003;**3**:276-84, http://dx.doi.org/10.3390/s30800276.
35. `Liu CY, Zhao M, Ren CY, YANG GP, Li PF, Han Y. Direct measurement of nitric oxide in seawater medium by fluorometric method. *Anal Chem* 2009;**37**:1463-7, http://dx.doi.org/10.1016/S1872-2040(08)60136-X.
36. `Lim JH, You SK, Baek JS, Hwang CJ, Na YG, Shin SC, et al. Preparation and evaluation of polymeric microparticulates for improving cellular uptake of gemcitabine. *Nanomedicine* 2012;**7**:2307-14, http://dx.doi.org/10.2147/IJN.S30465.
37. `Parent M, Boudier A, Fries I, Gostyńska A, Rychter M, Lulek J. Nitric oxide-eluting scaffolds and their interaction with smooth muscle cells *in vitro*. *J Biomed Mater Res A* 2015;**103**:3303-11, http://dx.doi.org/10.1002/jbm.a.35464.
38. `Hutchinson PJ, Palmer RM, Moncada S. Comparative pharmacology of EDRF and nitric oxide on vascular strips. *Pharmacol* 1987;**141**:445-51, http://dx.doi.org/10.1016/0014-2999(87)90563-2.
39. `Everett TR, Wilkinson IB, Mahendru AA, McEniery CM, Garner SF, Goodall AH, et al. *S*-Nitrosoglutathione improves haemodynamics in early-onset pre-eclampsia. *Clin Pharmacol* 2014;**78**:660-9, http://dx.doi.org/10.1111/bcp.12379.
40. `Hasan AS, Socha M, Lamprecht A, Ghazouani FE, Sapin A, Hoffman M, et al. Effect of the microencapsulation of nanoparticles on the reduction of burst release. *Pharm* 2007;**344**:53-61, http://dx.doi.org/10.1016/j.ijpharm.2007.05.066.
41. `Seabra AB, De Oliveira MG. Poly(vinyl alcohol) and poly(vinyl pyrrolidone) blended films for local nitric oxide release. *Biomaterials* 2004;**25**:3773-82, http://dx.doi.org/10.1016/j.biomaterials.2003.10.035.
42. `Seabra AB, Fitzpatrick A, Paul J, De Oliveira MG, Weller R. Topically applied *S*-nitrosothiol-containing hydrogels as experimental and pharmacological nitric oxide donors in human skin. *Dermatol* 2004;**151**:977-83, http://dx.doi.org/10.1111/j.1365-2133.2004.06213.x.
43. `George M, Abraham TE. Polyionic hydrocolloids for the intestinal delivery of protein drugs: Alginate and chitosan – a review. *J Control Release* 2006;**114**:1-14, http://dx.doi.org/10.1016/j.jconrel.2006.04.017.
44. `Garrait G, Beyssac E, Subirade M. Development of a novel drug delivery system: Chitosan nanoparticles entrapped in alginate microparticles. *J Microencapsul* 2014;**31**:363-72, http://dx.doi.org/10.3109/02652048.2013.858792.
45. `Bajka BH, Rigby NM, Cross KL, Macierzanka A, Mackie AR. The influence of small intestinal mucus structure on particle transport *ex vivo*. *Colloids Surf B: Biointerfaces* 2015;**135**:73-80, http://dx.doi.org/10.1016/j.colsurfb.2015.07.038.
46. Gaucher C, Boudier A, Dahboul F, Parent M, Leroy P. *S*-nitrosation/denitrosation in cardiovascular pathologies: Facts and concepts for the rational design of *S*-nitrosothiols. *Curr Pharm Des* 2013;**19**:458-72.
47. Alencar JL, Lobysheva I, Geffard M, Sarr M, Schott C, Schini-Kerth VB, et al. Role of *S*-nitrosation of cysteine residues in long-lasting inhibitory effect of nitric oxide on arterial tone. *Mol Pharmacol* 2003;**63**:1148-58.
48. `Khan SI, Abourashed EA, Khan IA, Walker LA. Transport of harman alkaloids across Caco-2 cell monolayers. *Chem Pharm Bull* 2004;**52**:394-7, http://dx.doi.org/10.1248/cpb.52.394.
49. `Megson IL, Greig IR, Gray GA, Webb DJ, Butler AR. Prolonged effect of a novel S-nitrosated glyco-amino acid in endothelium-denuded rat femoral arteries: Potential as a slow release nitric oxide donor drug. *Pharmacol* 1997;**122**:1617-24, http://dx.doi.org/10.1038/sj.bjp.0701557.
50. `Megson IL, Morton S, Greig IR, Mazzei FA, Field RA, Butler AR. N-Substituted analogues of S-nitroso-N-acetyl-D, L-penicillamine: Chemical stability and prolonged nitric oxide mediated vasodilatation in isolated rat femoral arteries. *Pharmacol* 1999;**126**:639-48, http://dx.doi.org/10.1038/sj.bjp.0702346.
51. `Nozik-Grayck E, Whalen EJ, Stamler JS, McMahon TJ, Chitano P, Piantadosi CA. S-nitrosoglutathione inhibits alpha1-adrenergic receptor-mediated vasoconstriction and ligand binding in pulmonary artery. *Physiol Lung Cell Mol Physiol* 2006;**290**:L136-43, http://dx.doi.org/10.1152/ajplung.00230.2005.

Attachment 2: Protocols

Preparation of polymer nanocomposite particles loaded with *S*-nitrosoglutathione

Principle

Nanoparticles are prepared with the double emulsion / solvent evaporation process. Formulation of nanocomposites is based on ionotropic gelation (cross-linker of alginate and Eudragit® E100 are $CaCl_2$, and tripolyphosphate respectively) and polyelectrolyte complexation (negatively charged alginate chain attached to the positively charged Eudragit® RL from the nanoparticle by electrostatic interaction).

During all the formulation process, it is necessary to protect GSNO from degradation (using **fresh ultrapure water from the day**, aluminum-foil paper, under ice bath).

When using glass pipettes, be sure that they are of category A, A^+ or AS.

1. Preparation of GSNO loaded nanoparticles based on Eudragit® RL PO

Reagents

Eudragit® RL PO (EVONIK REF: G111236245)

Alginic acid sodium salt from brown algae (Sigma-Aldrich REF: A2033)

$CaCl_2$ dihydrate (Sigma-Aldrich REF: 223506)

Dichloromethane (DCM) (Carlo Erba REF: 463001) – ***work beneath a fume hood with appropriate gloves***

Materials

Magnetic stirrer: Heidolph MR 3000D

Ultrasonic probe 1: generator 50 kW Vibra-Cell 72434, block CV18 4076, tip S&M 0103 (7 mm)

Ultrasonic probe 2: generator 130 kW Vibra-Cell 75022, block CV18 6299, S&M 0703 (13 mm)

Ultrasonic probe 3: generator 130 W, Bioblock Scientific 7501D, block CV18 (7 mm)

Evaporator Heidolph, Laborota 4000, Pump CVC 2000, Minichiller Huber

Centrifuge: Biofuge Stratos Heraeus Instrument

30 ml and 5 mL brown bottles

	30 mL	5 mL

	bottle	bottle
Height (cm)	6.2	4.0
$Ø_{bottom}$ (cm)	3.0	2.0
$Ø_{up}$ (cm)	2.6	1.9

1.1 **Prepare the organic phase**:

In a 30 mL brown bottle, weight 500 mg Eudragit® RL PO and dissolve in 5,0 mL (glass pipette) of DCM (magnetic stirring 500 rpm,~ 10 min with parafilm over the cap to avoid DCM evaporation).

NB: Add the magnetic stirrer after the DCM to avoid stickiness of the polymer.

1.2 **Prepare the outer aqueous phase**:

In a 30 mL brown bottle, weight 20 mg of Eudragit® RL PO and dissolve in 20,0 mL (glass pipette 20 mL) of ultrapure water (magnetic stirring 500 rpm,~ 5 min).

Remove the stirrer and keep the bottle on ice before using.

1.3 **Prepare the inner aqueous phase**:

In a 5 mL brown bottle, weight 10 mg of GSNO and dissolve in 500 µL (automatic pipette P1000) of the Eudragit® RL PO solution (taken from the outer aqueous phase) at room temperature.

If in winter it's not so easy to dissolve, it can be held in hand to warm a bit to accelerate the dissolution. If it's totally dissolved, usually in~ 5-10 min, the solution should be transparent.

Do not pause between the following steps 1.4 to 1.6, so check that everything is available and ready before starting*: a chronometer, the two ultrasonic probes, the three phases, the balloon for evaporation, and the evaporator (water-bath 25 °C, chiller 10 °C, end of the exhaust gas tube outside).*

For emulsification steps, the tip of the ultrasonic probe should be introduced halfway of the liquid height. Experimenter(s) must wear the ear protections provided.

1.4 **Primary emulsion**:

Retaining the magnetic stirrer with a bigger one, pour the organic phase into the inner aqueous phase and continue immediately by ultrasonication (ultrasonic **system 1**; **100 % amplitude, 60 s**, over ice bath, with horizontal movement for homogenization).

1.5 Secondary emulsion:

Pour immediately the primary emulsion into the outer aqueous phase (if necessary use glass pipette to transfer the totality), followed by ultrasonication (ultrasonic **system 2**, **amplitude maximum**, corresponding to 30 W displayed on the screen, **30 s**, over ice bath, with horizontal movement for homogenization). Transfer immediately in a 1 L brown balloon. The suspension should be milky, without aggregates.

1.6 <u>Nanoparticle hardening:</u>

Immediately evaporate the secondary emulsion (100 mbar, 10 min; water-bath 25°C, chiller 10 °C, 60 rpm). When the pump reaches 100 mbar, press immediately the "Mode" button to set this as target value (NB: if the pump has been previously used the same day and not switched off, there is no need to press "Mode" button).

In the case of composite particles preparation, prepare the chitosan solution during evaporation: in a 50 mL brown bottle, weight 20 mg of low molecular weight chitosan and dissolve in 20,0 mL (18,0 mL of ultrapure water and 2,0 mL of acetic acid, glass pipettes) under magnetic stirring at 1000 rpm. Keep on ice before using.

After evaporation, measure the volume of suspension in a cylinder (usually~ 18 mL). For preparation of nanocomposites particles, adjust the volume at 20 mL with ultrapure water (this volume is necessary to ensure a correct dissolution of alginate).

The protocol for preparation of GSNO-NP is schematized in the following Figure.

Preparation of *S*-Nitrosoglutathione Nanoparticle Protocol

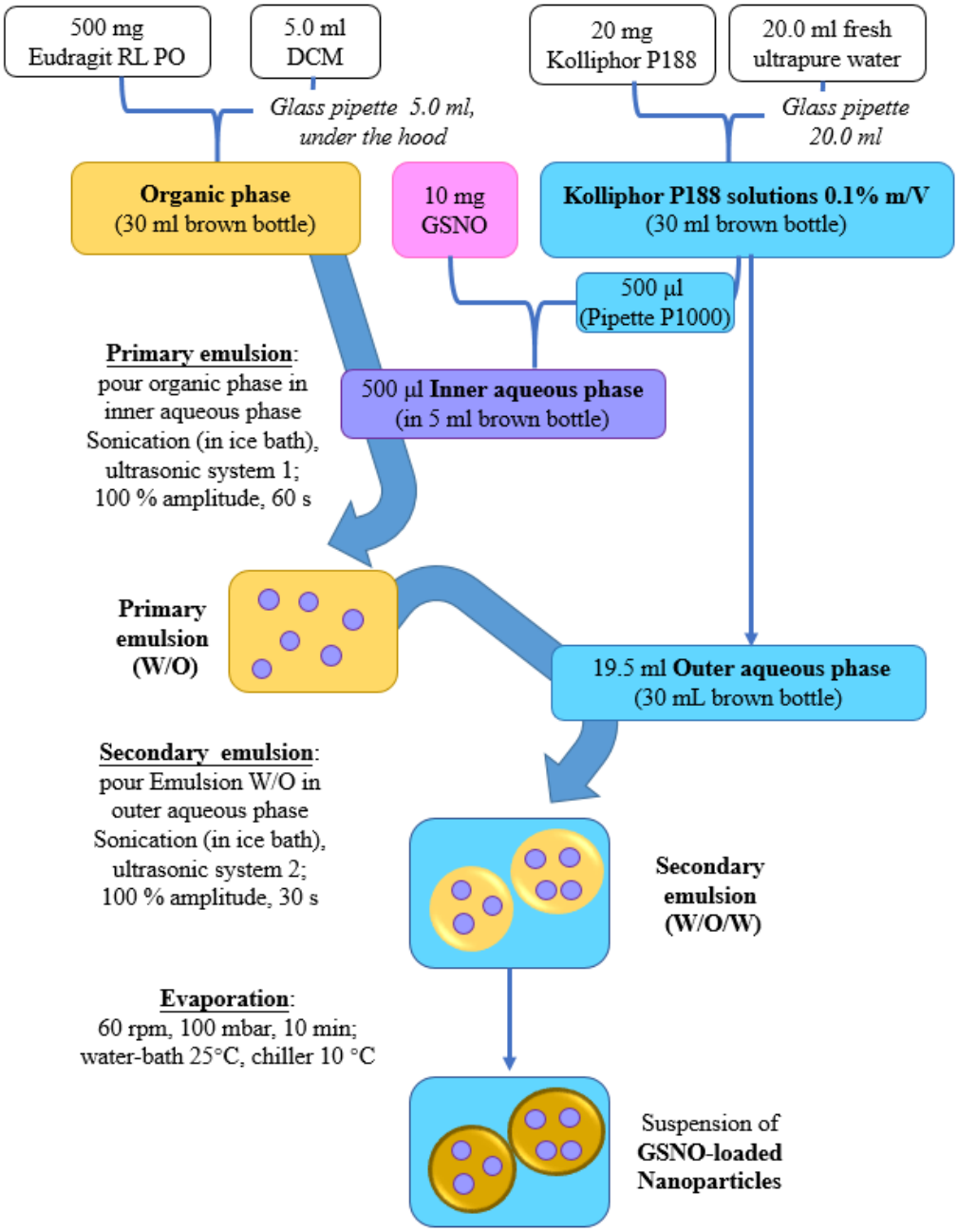

2. Preparation of alginate nanocomposite particles loaded with *S*-nitrosoglutathione (two methods: ionotropic gelation and polyelectrolyte complexation)

2.1 Ionotropic gelation (IG):

2.1.1 Reagent preparation

$CaCl_2$ solution: dissolve 2.9 g $CaCl_2$ in 10 mL water to obtain 2 M.

2.1.2 Sodium alginate dissolving

20 mg sodium alginate were dispersed on the surface of nanosuspension for 5 min (formation of a transparent gel, on the surface), then keep agitation (magnetic stirrer, 1000 rpm, Heidolph MR 3000D),) for 10 min (total dissolution of alginate) at room temperature (to avoid the solubility decrease of alginate at low temperature)

2.1.3 Cross-linking with calcium ions

2 mL $CaCl_2$ (2M) are added drop-wisely (23 G) into the mixture of nanoparticles and sodium alginate under ultrasonication (ultrasonic **system 1**; **30 % amplitude, 40 W,** over ice bath, with horizontal movement for homogenization, about 2 min 30s.

The protocol for preparation of GSNO-alginate NCP based on IG method is schematized in the following Figure.

Preparation of Alginate Nanocomposites loaded with *S*-nitrosoglutathione with Ionotropic Gelation Method

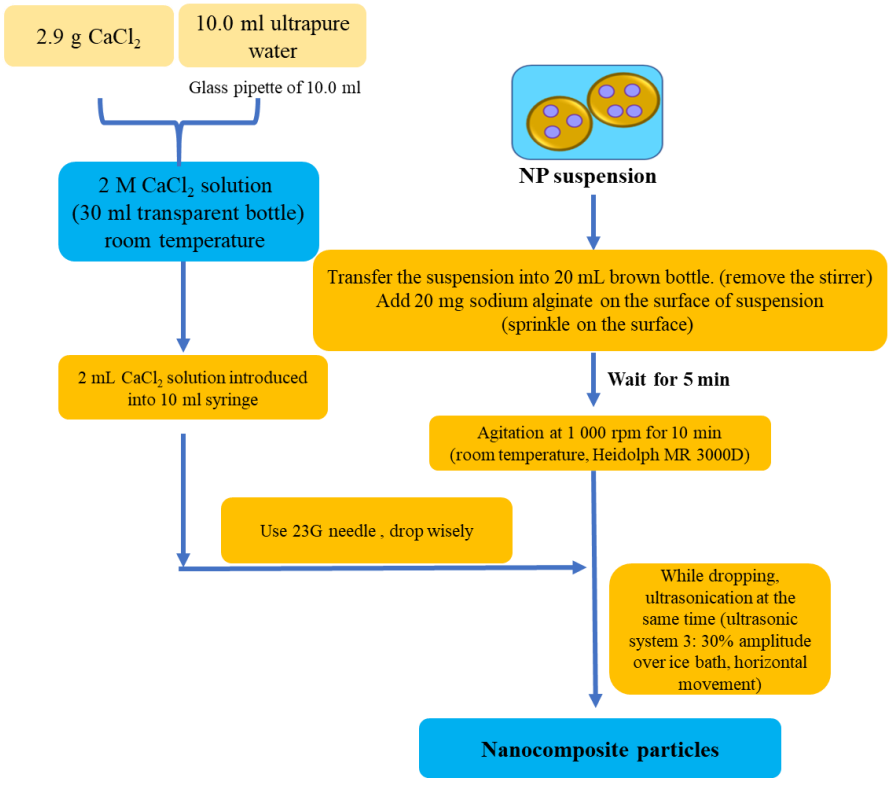

2.2 Polyelectrolyte complexation (PEC)

2.2.1 Reagent preparation

Sodium alginate solution: dissolve 20 mg sodium alginate in 10 mL ultrapure water.

2.2.2 Reaction with NP

GSNO nanosuspension was poured in the sodium alginate solution. The mixture was homogenized by gently shaking with hand through one direction for 1 minute and then 10 minutes standing before characterization.

The protocol for preparation of GSNO-alginate NCP based on PEC method is schematized in the following Figure.

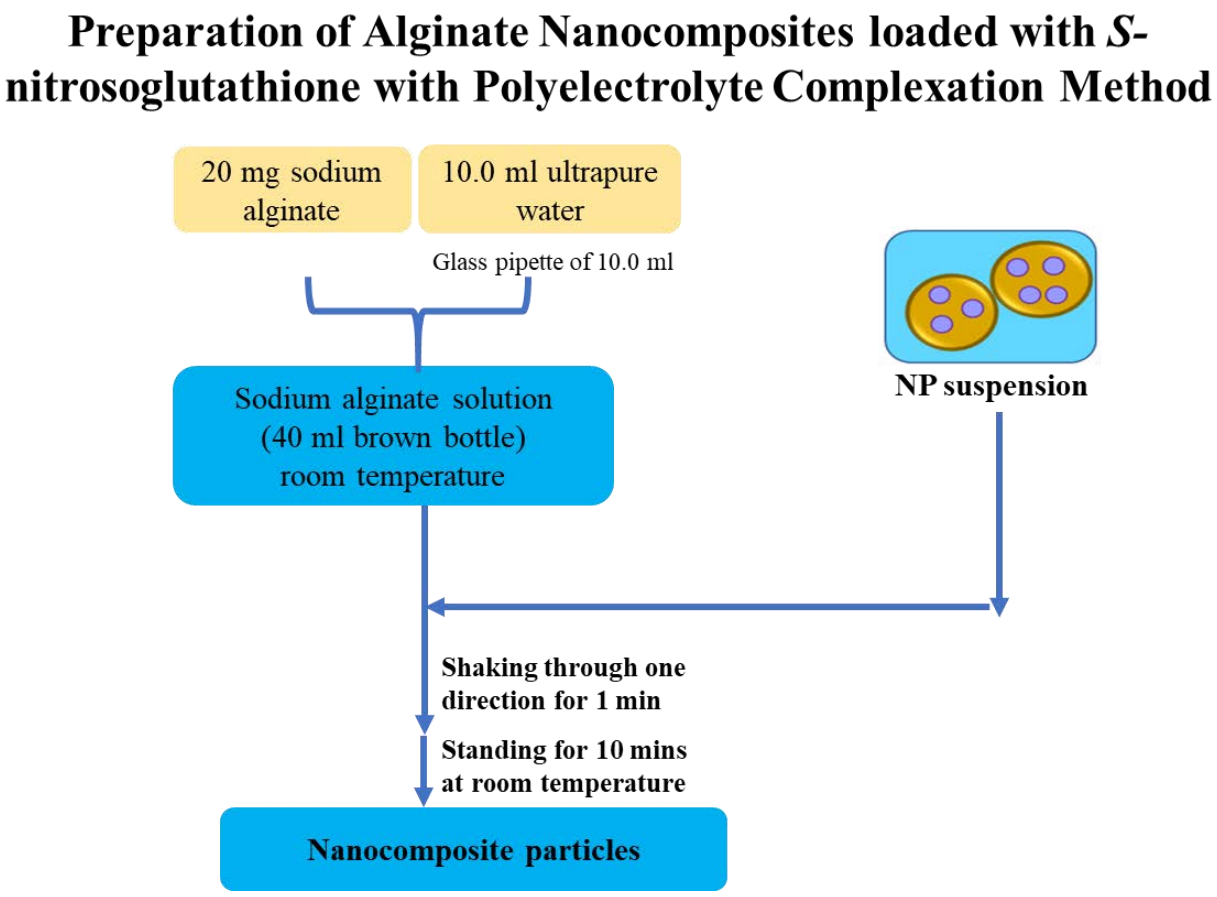

3. Preparation of alginate/Eudragit® E100 blend nanocomposite particles loaded with *S*-nitrosoglutathione)

3.1 Reagent preparation

$CaCl_2$ solution: dissolve 2.9 g $CaCl_2$ in 10 mL water to obtain 2 M.

Eudragit® E100: dissolve 20 mg Eudragit® E100 in 20 mL water.

3.2 Alginate dissolution

20 mg sodium alginate were dispersed on the surface of nanosuspension for 5 min (formation of a transparent gel, on the surface), then keep agitation (magnetic stirrer, 1000 rpm, Heidolph MR 3000D),) for 10 min (total dissolution of alginate) at room temperature (to avoid the solubility decrease of alginate at low temperature).

3.3 Cross-linker of Eudragit® E100 dissolution

220 of Sodium tripolyphosphate pentabasic (TPP) were added, agitation for another 5 min.

3.4 Interaction between alginate and calcium ions

2 mL $CaCl_2$ (2M) are added drop-wisely (23 G) into the mixture of nanoparticles and sodium alginate under ultrasonication (ultrasonic **system 1**; **30 % amplitude, 40 W,** over ice bath, with horizontal movement for homogenization, about 2 min 30s.

3.5 Interaction between Eudragit® E100 and TPP

With agitation, the obtained emulsion was added into chitosan solution using syringe (18 G) drop-wisely. In ice bath, keep agitation at 1000 rpm for 30 min.

*The protocol for preparation of GSNO-*alginate/Eudragit® E100 *NCP is schematized in the following Figure.*

Preparation of Alginate/Eudragit® E100 Nanocomposites loaded with *S*-nitrosoglutathione Protocol

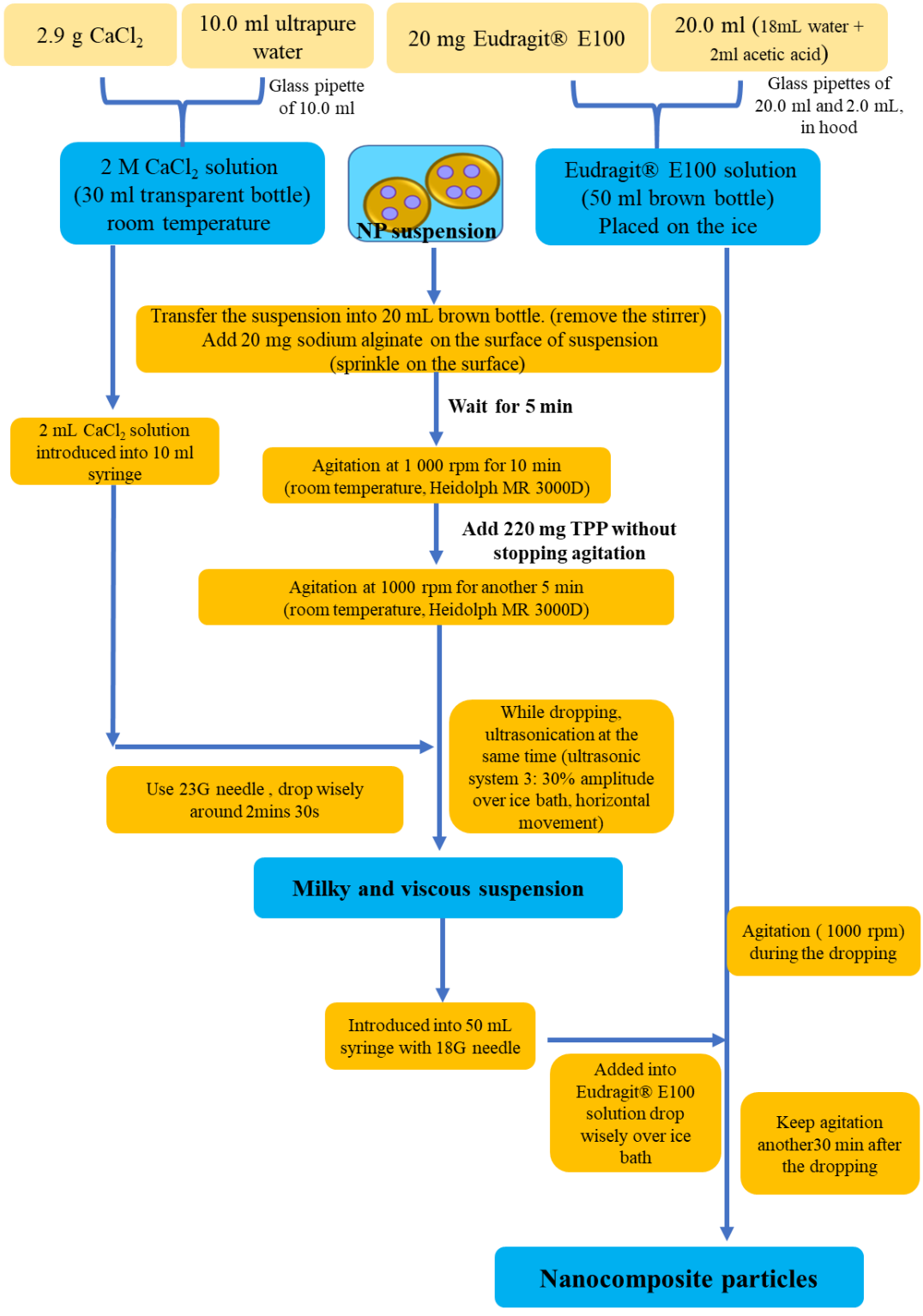

Protein extraction from intestine

Principal

Maximal extraction and solubilization of protein from tissue is important to make the whole protein complement available for proteomic analysis. It also helps to maximize reproducibility and to minimize waste. Minimal degradation of the protein amino acid backbone or dephosphorylation is essential to preserve the analytical utility of the extract.

RIPA buffer is the lysis buffer. PMSF (phenylmethanesulfonylfluoride or phenylmethylsulfonyl fluoride) is a serine protease inhibitor. Na_3VO_4 (sodium orthovanadate) is a phosphatase inhibitor. As to protease inhibitor cocktail, just as the name suggests, it's used to inhibite protease. So all the components we use here is to obtain maximal extraction and solubilization of protein and minimal degradation of he protein amino acid backbone or dephosphorylation.

Material

RIPA buffer

NaCl	**Sigma**	**ref S-9888**	**FW=58,44**	
Na_2HPO_4	**Sigma**	**ref S-0876**	**FW=142,0**	
KH_2PO_4	**Merck**	**ref 646A148973**	**FW=136,09**	
NP40	**Euromedex**	**ref UN3500-A**	**FW=603**	
DOC	**Sigma**	**ref D 6750**		
SDS	**Sigma**	**ref L-4509**	**FW=288,4**	
Just before the manipulation				
PMSF	**Sigma**	**ref P 7626**	**FW=174,2**	10µl/ml RIPA
Na_3VO_4	**Sigma**	**ref S 6508**	**FW=183,9**	10µl/ml RIPA
PIC	**Roche**	**ref**		10µl/mLRIPA

NaCl:*sodium chloride;* **Na_2HPO_4:** *sodium phosphate anhydrous dibasic;* **KH_2PO_4***: potassium dihydrogen phosphate;* **NP40:** *Nonidet P40;* **DOC:** *Deoxycholate de sodium;* **SDS:** *Lauryl sulfate ou sodium dodecyl sulfate;* **PMSF:** *phenylmethanesulfonyl fluoride ;* **Na_3VO_4***: sodium orthovanadate* **PIC:** *Cocktail antiprotease*

Stock Solutions

RIPA buffer	NaCl	8 g/l
	Na_2HPO_4	1,44 g/l
	KH_2PO_4	0,24 g/l
	NP40	1 %
	DOC	0,5 %
	SDS	0,1 %

in ultrapure water (conserve the aliquots in -20°C)

PMSF 10 mg/ml d'éthanol (sensible a la lumière)
conserve the aliquots in -20°C

Na_3VO_4 à 100mM 18,39 mg/ml of ultrapure H_2O
Adjust pH to 9
Boil the solution till colorless
Cool to room temperature
Adjust pH to 9
Boil the solution till colorless
Cool to room temperature
Repeat the above steps till pH to 9 after boiling and cooling
Adjust volume with water
conserve the aliquots in -20°C

PIC 10µL/mL de RIPA
conserve the aliquots in -20°C

Tools and apparatus

Liquid nitrogen
Eppendorf tube 1.5 mL (the quantity number depends on your sample)
Mortar-pestle
Centrifuge machine (Heraeus instruments)

Protein extraction :

- Mush the tissue with mortar-pestle in liquid nitrogen.
- Weight the mass of the tissue.
- Calculate the volume of lysis buffer needed to extract the protein from tissue(1mg tissue/ 4µL buffer)
- Defreeze all the components of lysis buffer: RIPA, PMSF, Na_3VO_4 and cocktail anti-protease in a flowing water bath
- Prepare the lysis buffer:
  PMSF 10µL/mL RIPA
  Na_3VO_4 10µL/mL RIPA
  Protease inhibitor cocktail 10µL/mL RIPA
- Add the corresponding volume of lysis buffer into the tissue.
- Incubate 10 min on the ice.
- Homogenize the mixture by a 1 mL syringe and blue needle. Pull and push the syringe 10 times.
- Freeze and defreeze the mixture 3 times by liquid nitrogen and 37 °C water bath.
- Balance the tube and then centrifuge at 12000 rpm for 30 min at 4 °C.
- Transfer the supernatant and divide into different aliquots.
- Quantify the protein amount with BCA assay according to protocol

Western Blot protocol

Principle:

Western blotting uses specific antibodies to identify proteins that have been separated based on size by gel electrophoresis. The immunoassay uses a membrane made of nitrocellulose or PVDF (polyvinylidene fluoride). The gel is placed next to the membrane and application of an electrical current induces the proteins to migrate from the gel to the membrane. The membrane can then be further processed with antibodies specific for the target of interest, and visualized using secondary antibodies and detection reagents.

Solutions preparation:

Material

Reagent information

Reagents	Company	Reference	MW
Trizma@Base (Tris-HCl)	Sigma	T-6066	121.1
Lauryl sulfate (SDS)	Sigma	L-4509	288.4
Ammonium persulfate (APS)	Sigma	A-3678	228.2
Temed	Carlo Erba	600461	
2-mercaptoethanol	Merck	12006	78.13
Sample buffer laemmli x2	Sigma	S-3401	
Glycine	Sigma	G-7126	75.07
Sodium chloride (NaCl)	Sigma	S-9888	58.44
Ethanol			
Tween 20	Sigma	P-1379	
Isopropanol	Sigma	I-9516	60.10
ImmobilonTM-P(PVDF)	Millipore	IPVH00010	
Mini Trans-Blot filter paper	Bio-Rad	1703932	
Ponceau S (rouge Ponceau)	Sigma	P-3504	760.6
Albumine Bovine, fractionV	Eruomedex	04-100-810C	
Acetic acid 100%	Prlabo	20-104.323	
ECLTM Werstern blotting detection reagent	Amersham Bioscience	RPN2106	
Kodak LX24(revelateur)	Merck Eurolab	5070933	
Kodak AL4(fixteur)	Merck Eurolab	5071071	
HyperfilmTM MP(film photo graphique)	Amersham Bioscience	RPN1675K	

All Solutions are prepared with ultrapure water (18,2 MΩ•cm).

Solutions for gel preparation:

Tris-HCl 1.5 M pH 8.8
18.165 g of Tris/100 mL ultrapure water, adjust pH to 8.8 with HCl (37%), filter through 0.22 µm and conserve at 4 °C

Tris-HCl 0.5 M pH 6.8
6.055 g of Tris/100 mL ultrapure water, adjust pH to 6.8 with HCl (37%), filter through 0.22 µm and conserve at 4 °C

SDS 10%
10 g of SDS/100 mL ultrapure water, agitate gently to dissolve the SDS to avoid bubble, conserve at room temperature.

APS (ammonium persulfate) 10%
1 g APS/100 mL ultrapure water, then aliquot in 400-µL tubes, conserve at –20°C.

Laemmli 2X sample buffer
2-mercaptoethanol 50 µL + 950 µL Laemmli 2X sample buffer , freshly prepared.

Migration buffer:
for 1 L 10X stock solution

Reagents	Concentration	Amount
Tris	10 mM	30 g
Glycine	1.92 M	144 g
SDS	1% (m/V)	10 g

Fill the 1 L volumetric flask with ultrapure water. Conserve at 4 °C.
1X working solution (extemporaneously prepared): dilute 100 mL of 10X stock solution to 1 L with ultrapure water. Use at room temperature.
pH ≈ 8.3, don't need to adjust pH.

Transfer buffer:
for 1 L 10X stock solution

Reagents	Concentration	Amount
Tris	480 mM	58.1 g
Glycine	390 mM	29.3 g
SDS	0.375 % (m/V) (13 mM)	3.75 g

Fill the 1 L volumetric flask with ultrapure water. Conserve at 4 °C.
1X working solution (extemporaneously prepared): 100 mL of 10X stock solution +

200 mL ethanol, fill to 1 L with ultrapure water. Conserve at 4 °C and use cold solution. pH ≈ 9.2, don't need to adjust pH.

Washing buffer:

for 1 L 10X stock solution

Reagents	Concentration	Amount
Tris	200 mM	24.2 g
NaCl	1.5 M	87.5 g

Fill the 1 L volumetric flask with ultrapure water. Conserve at 4 °C.
Adjust pH to 7.4 with HCl (37%).
1X working solution: 100 mL of 10X stock solution, fill to 1 L with ultrapure water, add 1 mL of Tween 20. Conserve at 4 °C.

Gel preparation:

10 mL separating gel solution and 4 mL stacking solution/1 gel

- Different concentration of acrylamide in the separating gel solution can be used for different molecule weight of protein. The less amount of acrylamide is used; the bigger molecule weight of protein can be separated. 10% is mostly usually used concentration.
- Place the gel plate holder on a table. Adjust the position to horizontal.
- Check the leakage of the glass plate with distilled water
- Prepare the gel solution according to the table of gel preparation which is in the last page.
- 10% APS and TEMED are used for solidifying the solution, so both gels solution can be prepared at the same time. Just pay attention that TEMED is added at the end just before pouring in the plates.
- Pour separating gel solution into the plate till 2-3 cm away the top of thr shorter glass. Add 500 µL isopropanol to separate the media from air. Wait for 15-30 min till the gel is solidified.
- Remove the isopropanol and rinse with distilled water.
- Overlay the separating gel with stacking gel till the plate is full
- Insert the comb. Ensure that there is not bubble
- Wait till the gel is solidified.

Sample preparation:

- Set the temperature of heating plate to 100 °C and switch on it.
- Add the same volume of Laemmli 2X sample buffer into each sample
- Heat the sample with heating plate for 5 min at 100 °C
- Make aliquots for samples and conserve them at -80°C.

Electrophoresis

- Place gel inside the electroporator. (attention: bigger glass plate is face to outside)
- Pour the migration buffer into the electroporator, firstly inside, then outside. Ensure that the buffer covers the gel completely. Remove the comb carefully
- Add sample and marker carefully to each well (according to the volume calculated before, to get 20-30 µg proteins in each well). Connect to a power supply (attention: red to red, black to black)
- Run the stacking gel with low voltage (80V) for 15 min to 20 min till the loading buffer was concentrated in one line. Then turn up to higher voltage (110 V) for separating gel for around 1 h 30 min till the dye front runs off the bottom of the gel.

Transfer:

- Cut 6 filter paper sheets to fit the measurement of gel (6 cm * 8.5 cm minimum) and one membrane of 0.2 µm (nitrocellulose or PVDF) (or 0.45 µm for bigger protein) with the same dimension.

If PVDF membrane is chosen, it should be immersed in methanol at least 30 sec to activate the positively charged groups on the membrane, in order to enhance reacting with negatively charged protein.

- Wet two sponges, the 6 filter papers and the membrane (5 min maximum) in pre-cold transfer buffer in a plate with transfer buffer, conserve at 4°C
- Take out the glass plate from the electroporator, separate the plate and cut the stacking gel. Cut a corner of the gel to remember the sides.
- Put the gel in transfer buffer (5 min maximum)
- Prepare a transfer sandwich as follow: place the white side down and black side up

✧ 1 x sponge
✧ x filter papers
✧ 1 x membrane
✧ 1 x gel
✧ 3 x filter papers
✧ 1 x sponge

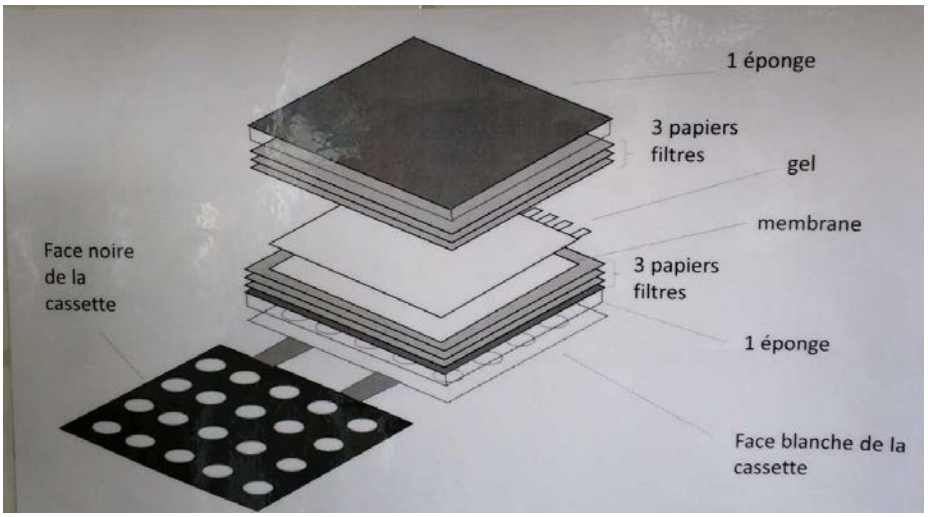

Ensure there is no bubbles between the gel and membrane, exclude the bubbles by finger slowly, squeeze out the extra liquid by a rotor

- Relocate the sandwich to transfer apparatus, which should be placed in ice to avoid del deformation because of heating produce by high electric current. Put a magnetic stirrer inside the apparatus. Add transfer buffer into the apparatus and ensure that the sandwich is covered by the buffer. Place the electrodes on the top of the apparatus.
- Begin the transfer at 350 mA for 45 min.
- After the transfer, take out the sandwich from the apparatus, open it carefully and take out the membrane. Use different color pens (red, blue, green) to mark clearly all the bands: this is to avoid missing during the next steps.
- Verification of transfer **(in option):** color of the membrane with a solution (rouge Ponceau S) for 5 min on a shaker with speed of 15 rpm, then remove the color with 5-6 distilled water till the membrane back to white color.

Blocking:

- Block the membrane with 25 mL TBST/5 % non-fat milk (or BSA) under agitation at room temperature for 1 hour.

Primary antibody incubation:

- Cut the redundant part of the membrane (to minimize the dosage of the antibody)
- Prepare a plastic bag which is bigger than the membrane and write antibody information, dilution times, dilution medium date and experimentor's name on the bag.
- Dilute the first antibody solution in TBST/5 % non-fat milk (or BSA) (normally is 1:1000, but check the recommended dilution from the company and check in the literature which has the same sample and same antibody; the final volume for one membrane is around 5 mL in total)

β-catenin, MA1-2001, PIERCE, 1:800 5% non-fat milk/TBST;
E-cadherin, SC-7870, Santa Cruz, 1:700 5% BSA/TBST;
Occludin, 71-1500, Invitrogen, 1:600 5% non-fat milk/TBST;
Claudin-1, 37-4900, Invitrogen, 1:600 5% non-fat milk/TBST;
IL-1β, ab9722, abcam, 1:1000 5% non-fat milk/TBST;
TNF-α, ab6671, abcam, 1:1000 5% BSA/TBST
Reference proteins:
If the reference protein is conjugated with Horseradish Peroxidase (HRP), it is not necessary to incubate with another second antibody. Then, use the dilution which is recommended by the company and follow the same protocol above.
β-actin, ab197277, abcam, 1:10,000 5% BSA/TBST; room temperature, 1h

- Place the membrane in the plastic bag
- Pour the first antibody solution carefully inside the bag, remove all the bubbles inside the bag and seal it.
- Incubate at 4 °C overnight in a tray, use adhesive tape to fix all the bags, switch on the agitator at a speed 15 rpm.
- Conserve the antibody solution at -20 °C for repeated use (normally 3 times maximum).

Washing:

- Take out the membrane from the plastic bag. Then put it in a small tray.
- Conserve the remaining antibody solution in the plastic bag at -20 °C. It can be reused for 2-3 times.
- Rinse it rapidly with TBST firstly to remove most of the residual liquid. Then rinse the membrane 10 min, 4 times, on a shaker with a speed of 70 rpm at room temperature.

Reference protein:
For reference proteins which is conjugated with HRP, the membranes can go directly revelation ECL step.

Secondary antibody incubation:

- Prepare a plastic bag which is bigger than the membrane and write antibody information, dilution times, dilution medium date and experimentor's name on the bag.
- Dilute the second antibody solution in TBST/5 % non-fat milk (or BSA) (recommend 1:10,000)
- Incubate it on a shaker with a speed of 15 rpm at room temperature for 1 hour

Washing:

- Same process with the first antibody washing.

- Take out the membrane from the plastic bag. Then put it in a small tray.
- Rinse it rapidly with TBST firstly to remove most of the residual liquid. Then rinse the membrane 10 min, 4 times, on a shaker with a speed of 70 rpm at room temperature.

Revelation ECL:

Principal: Enhanced chemiluminescence (ECL) is a method which provides highly precise detection of proteins from Western blots. In the chemiluminescence reaction horseradish peroxidase (HRP) catalyzes the oxidation of luminol into a reagent which emits light when it decays. Since the oxidation of luminol is catalyzed by horseradish peroxidase, and the HRP is complexed with the protein of interest on the membrane, the amount and location of light that HRP catalyzes the emission of, is directly correlated with the location and amount of protein on the membrane.

- Mix the ECL western blot substrats 500 µL + 500 Ml
- Dry the membrane with tissue. Place it on a flat plastic membrane
- Cover the membrane with 1 mL ECL solution
- Incubate in dark for 5 min.
- Dry the membrane with tissue, put it on a plastic membrane.
- Expose the membranes by following the instructions of "FUSION" software.
- Put the membrane back into the tray
- Conserve the membranes at -20 °C after exposure in a plastic bag without medium (not necessary to dry it)

Gel preparation (SDS-PAGE Tris/Glycine)

Acrylamide 40%

Acrylamide	Components	5 mL	10 mL	15 mL	20 mL	25 mL	30 mL	40 mL	50 mL
6% (~150 kDa)	MQ water	2.8	5.6	8.6	11.6	14.4	17.4	23.2	29.0
	Acrylamide	0.8	1,5	2.3	3	3.8	4.5	6.0	7.5
	Tris 1.5M	1.3	2,5	3.8	5	6.3	7.5	10	12.5
	SDS 10%	0.05	0.1	0.15	0.2	0.25	0.3	0.4	0.5
	APS 10%	0.05	0.1	0.15	0.2	0.25	0.3	0.4	0.5
	TEMED	0.004	0.008	0.012	0.016	0.02	0.024	0.032	0.04
8% (70 kDa -150 kDa)	MQ water	2.6	5.3	7.9	10.6	13.2	15.9	21.2	26.5
	Acrylamide	1.0	2.0	3.0	4.0	5.0	6.0	8.0	10.0
	Tris 1.5M	1.3	2,5	3.8	5	6.3	7.5	10	12.5
	SDS 10%	0.05	0.1	0.15	0.2	0.25	0.3	0.4	0.5
	APS 10%	0.05	0.1	0.15	0.2	0.25	0.3	0.4	0.5
	TEMED	0.003	0.006	0.009	0.012	0.015	0.018	0.024	0.03
10% (50 kDa -70 kDa)	MQ water	2.3	4.8	7.1	9.6	11.9	14.4	19.2	24.0
	Acrylamide	1.3	2,5	3.8	5	6.3	7.5	10	12.5
	Tris 1.5M	1.3	2,5	3.8	5	6.3	7.5	10	12.5
	SDS 10%	0.05	0.1	0.15	0.2	0.25	0.3	0.4	0.5
	APS 10%	0.05	0.1	0.15	0.2	0.25	0.3	0.4	0.5
	TEMED	0.002	0.004	0.006	0.008	0.01	0.012	0.016	0.02
12% (35 kDa - 50 kDa)	MQ water	2.1	4.3	6.4	8.6	10.7	12.9	17.2	21.5
	Acrylamide	1.5	3.0	4.5	6.0	7.5	9.0	12.0	15.0
	Tris 1.5M	1.3	2,5	3.8	5	6.3	7.5	10	12.5
	SDS 10%	0.05	0.1	0.15	0.2	0.25	0.3	0.4	0.5
	APS 10%	0.05	0.1	0.15	0.2	0.25	0.3	0.4	0.5
	TEMED	0.002	0.004	0.006	0.008	0.01	0.012	0.016	0.02
15% (~35 kDa)	MQ water	1.7	3.5	5.3	7.1	8.8	10.6	14.2	17.7
	Acrylamide	1.9	3.8	5.6	7.5	9.4	11.3	15.0	18.8
	Tris 1.5M	1.3	2,5	3.8	5	6.3	7.5	10	12.5
	SDS 10%	0.05	0.1	0.15	0.2	0.25	0.3	0.4	0.5
	APS 10%	0.05	0.1	0.15	0.2	0.25	0.3	0.4	0.5
	TEMED	0.002	0.004	0.006	0.008	0.01	0.012	0.016	0.02

Acrylamide	Components	1 mL	4 mL	8 mL	16 mL	24 mL	6 mL	8 mL	10 mL
Stacking	MQ water	0.72	2.92	5.83	11.66	17.49	4.37	5.83	7,29
	Acrylamide	0.13	0.50	1.00	2.00	3.00	0.75	1.00	1.25
	Tris o.5M	0.13	0.50	1.00	2.00	3.00	0.75	1.00	1.25
	SDS 10%	0.01	0.04	0.08	0.16	0.24	0.06	0.08	0.10
	APS 10%	0.01	0.04	0.08	0.16	0.24	0.06	0.08	0.10
	TEMED	0.001	0.004	0.008	0.016	0.024	0.006	0.008	0.01

Développement de formulations polymériques de *S*-nitrosoglutathion comme traitement *per os* pour prévenir les maladies inflammatoires chroniques de l'intestin

Les maladies inflammatoires chroniques de l'intestin (MICI) représentent un problème de santé publique majeur touchant de jeunes patients. Aux récidives inflammatoires, à la mauvaise qualité de vie et à l'espérance de vie réduite des patients viennent s'ajouter la durée, l'efficacité parfois limitée et le coût des traitements actuellement proposés. La recherche de nouvelles stratégies permettant de prévenir les récidives inflammatoires est primordiale. Ainsi, le rôle du *S*-nitrosoglutathion (GSNO, donneur et forme de stockage naturelle de NO) dans le maintien de l'intégrité de la barrière intestinale est étudié dans cette thèse, en décrivant : i) l'effet concentration-dépendante du GSNO sur la perméabilité intestinale (modèle de chambre de Ussing, expression des protéines de jonctions cellulaires…), ii) des formulations innovantes de GSNO (nanoparticules composites) à base de nanoparticules d'Eudragit®RL, elles-mêmes encapsulées dans une matrice polymérique à base d'alginate. Différents procédés de formulation ont été testés. Une caractérisation physicochimique des objets développés et des études de perméabilité sur des modèles cellulaires (Caco-2) ont conduit à l'obtention de trois formulations, adaptées à la voie orale et permettant de délivrer de façon prolongée le GSNO. Cependant, la prise en charge du GSNO libre ou formulé, l'identification des cibles du NO au niveau intestinal, mais aussi les doses et durées du traitement *in vivo* restent encore à définir avant de proposer ce donneur de NO comme candidat pour un traitement préventif des MICI.

Mot clefs : *S*-nitrosoglutathion, nanoparticules composites, prévention, barrière intestinale.

Development of *S*-nitrosoglutathione loaded particles adapted to oral administration for preventing Inflammatory Bowel Disease relapses

Inflammatory bowel diseases (IBD) (Crohn's disease, ulcerative colitis…), are disabling pathologies affecting young patients and presenting the particularity that most of the current agents act by down regulating chronic inflammation in the intestine mucosa and cannot cure the disease. As the pivotal role of *S*-nitrosoglutathione (GSNO) in preventing intestinal inflammation and gut barrier failure has been clearly pointed out, therapies based on pharmaceutical technology to limit chronic inflammation and prevent relapses of barrier failure by an optimized dosage form of GSNO appears as an interesting challenge. The objective of this project relies on i) studying GSNO concentration/response functions in intestine by using Ussing chamber *ex vivo* model and following protein cell junction expression, ii) developing polymer nanocomposite particles encapsulating GSNO and adapted to the oral route, with GSNO protection, controlled delivery and local effect in intestine as major requirements. GSNO loaded polymeric (Eudragit® RL) nanoparticles were included in polymer matrix based on alginate; different processes were tested and particles were characterized: high GSNO loading, GSNO sustained release and local retention for 4 h *in cellulo* study (Caco-2) were obtained. Thus, therapies based on GSNO administration should represent a novel strategy to limit chronic inflammation and prevent relapses of barrier failure in IBD patients.

Key words: *S*-nitrosoglutathione, intestinal barrier, oral administration, nanocomposites